

Alma Mater Studiorum – Università di Bologna
Chemistry Department - “Giacomo Ciamician”

PhD in Chemistry – XXX cycle

**Development of new protocols
for Organocatalysis**

Phd Student

Marco Giuseppe Emma

Supervisor

Chiar.mo Prof. Marco Lombardo

Co-Supervisor

Chiar.mo Prof. Claudio Trombini

TABLE OF CONTENTS

Abstract

1. Introduction to Organocatalysis.....	10
2. New Sustainable Protocol for the direct asymmetric Proline-catalised aldol reaction.....	15
2.1 Organocatalysis in industrial application.....	15
2.2 Asymmetric aldol reaction catalysed by L-Proline.....	19
2.3 Aim of the work.....	25
2.4 Results and Discussion.....	25
2.5 Conclusion.....	35
2.6 General Procedures and Products Characterization.....	35
3. Study of the α-Fluorination of Chiral γ-Nitroaldehydes.....	39
3.1 Organocatalysis in the synthesis of biologically active compounds.....	39
3.2 Fluorine in medicinal chemistry.....	41
3.3 The Organocatalytic α -fluorination of aldehydes.....	43
3.4 Aim of the work.....	47
3.5 Result and discussion.....	48
3.6 Conclusion.....	61
3.7 General Procedures and Products Characterization.....	61
4. Organocatalysis with carbon-based nanomaterials.....	78
4.1 Organocatalysis on different supported materials.....	78
4.2 Fullerene.....	81
4.3 Carbon Nanotubes.....	84
4.4 Fullerene and Carbon Nanotubes in catalysis.....	90
4.5 Aim of the work.....	94
4.6 Results and discussion.....	96
4.7 Conclusion.....	119
4.8 General Procedures and Products Characterization.....	120

Abstract

In this thesis are reported the main research activities done during the period of my PhD studies, working under the supervision of Prof. Marco Lombardo and Prof. Claudio Trombini. My research has been focused in particular on the study of organocatalysis, and its possible application in different fields.

After a brief introduction on organocatalysis, and in particular enamine and iminium ion activation modes, in Chapter two is reported the study of a new efficient protocol for Proline-catalysed aldol reaction, involving the use of simple Methanol and Water as additives, that can be interesting as a scalable process in industrial applications. The protocol has been optimized for the reaction of several aromatic aldehydes and some ketones, giving good to excellent results if compared to the ones reported for other protocols involving simple proline. Moreover, the reaction has been successfully scaled up to medium scale, showing the possibility in future to produce aldol products in large quantities in a green, sustainable way.

In Chapter three, the study of the α -Fluorination of Chiral γ -Nitroaldehydes is reported, with the construction of fluorinated fully substituted stereocenters. Selective incorporation of fluorine atoms inside biologically active molecules is a trend topic in medicinal organic chemistry, and not many protocols for the fluorination of α,α -dialkyl aldehydes are reported. This study showed how, with commercially available Jorgensen-Hayashi organocatalyst, and the use of trifluoroacetic acid as additive, is possible to obtain fluorinated products with good yields and selectivity, and the scope has been successfully expanded to several differently substituted aldehydes. At the same time, the mechanism of the reaction has been studied, together with the determination of the absolute configuration of products, all done by NMR spectroscopy.

Lastly, in Chapter four, the study of Fullerene and Carbon Nanotube as solid support for organocatalysis is reported. This work has been conducted together with Prof. Maurizio Prato and co-workers, from the university of Trieste. After many preliminary studies, we synthesized a derivative of Maruoka trityl pyrrolidine and covalently supported it on fullerene. Then, we used this new organocatalyst in the classic Michael addition reaction of Malonate to aldehydes, with results comparable to literature. Moreover, this is the first application of trityl pyrrolidine in iminium ion activation. Finally, we tried to recover and reuse the catalyst, recycling it for 3 cycles.

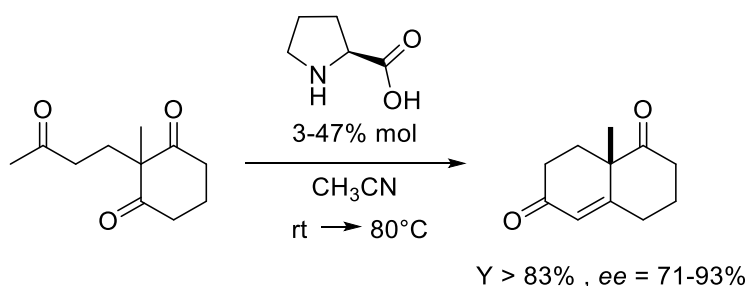
Chapter 1. Introduction to Organocatalysis

Catalysis plays a key-role for the well-being of humanity and is very important enabling technology that supports the global economy. Many industrial fields, including chemical, petroleum, agriculture, polymer, electronics and pharmaceuticals, rely heavily on catalysis. Over 90% of chemicals are produced with catalytic processes. The products generated through catalysis have reached a market value of about 900 billion dollars per annum. The use of catalysis provides an incredible number of benefits for businesses, the principal being cost reduction, time savings and less waste generation. The increasing focus on the development of environmentally sustainable manufacturing processes places catalysis as the principal technology for the green chemistry movement. Catalysis is one of the twelve principles of green chemistry. Compared to stoichiometric, non-selective reactions, catalytic transformations prevent waste from the source and increase the yield of the useful product in less time using less energy. Catalysis also enables smart synthetic design, allowing shorter routes to high-value products. The importance of catalysis in science can be readily appreciated by a survey of Nobel Prizes for Chemistry in the past 40 years. Many of these are about catalysis, the most important being the pioneering work of Ziegler and the Italian Natta on catalysis in polymer synthesis (1963), the fundamental work of Wilkinson and Fischer on organometallic compounds (1973), the asymmetric hydrogenation and oxidation methodologies of Knowles, Noyori and Sharpless (2001), the award for metathesis given to Chauvin, Grubbs, Schrock (2005), and the recent recognition of Heck, Negishi and Suzuki for cross-coupling reactions (2010). This is just the simpler outcome of how the scientific advances in catalysis have proved to be incredibly efficient in solving problems of considerable importance.¹ The catalyst should also be able in most case to transfer also stereochemical information to the products, opening the route for stereoselective synthetic way, obtaining products with high level of stereochemical purity. In fact, the development of efficient methods to provide enantiomerically enriched products is of great current interest to both academia and industry. The occurrence of only one enantiomer of a molecule in nature is connected to the evidence that enantiomers have different biological activity and, in general, they have a different behaviour in a chiral environment.² Over the past few decades, intense research in this field has greatly expanded the scope of catalytic reactions that can be performed with high enantioselectivity and efficiency. Consequently, thousands of chiral ligands and their transition metal complexes have been developed for the homogeneous asymmetric catalysis of various organic transformations.

¹ C. A. Busacca, D. R. Fandrick, J. J. Song, C. H. Senanayake, *Advanced Synthesis and Catalysis*, **2011**, 353, 1825–1864.

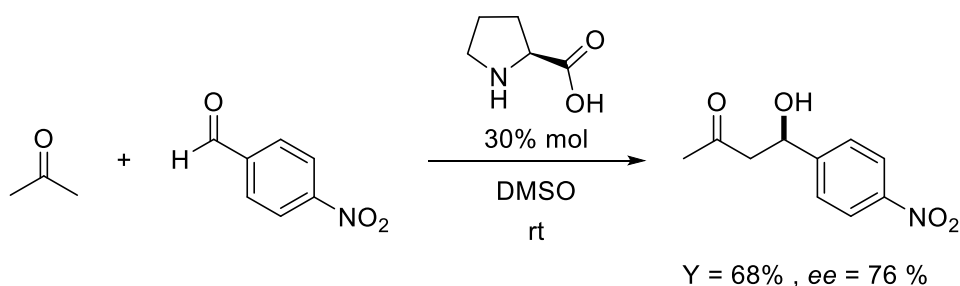
² C. Palumbo, M. Guidotti, *ScienceOpen Research*, **2015**.

In particular, in the last twenty years a new area of research was born, different from the classic metallocatalysis, based on the use of small organic molecules as catalyst for transformations, and the field was named organocatalysis.³ Even if sporadic studies on the use of small organic molecules as asymmetric catalyst were reported between 1968 and 1997, it is now widely accepted that the field of organocatalysis started to grow up from the late 1990s. Probably the first and most important example of this first unaware use of organocatalytic application was the work published by two different research groups, guided by Hajos and Wiechert, in 1971, about the use of natural (S)-Proline for promoting an intramolecular enantioselective aldol reaction giving as a product a bicyclic precursor in steroid synthesis⁴:



Scheme 1: Hajos-Parrish Eder-Sauer-Wiechert's reaction

This and other previous studies were viewed more as unique chemical reactions than as small part of a greater research field. Furthermore, there was no emphasis on the potential benefit of using organocatalysts, but these works were focused only about the single transformation accomplished. The situation changed radically with the publication of two works that are now widely accepted as two cornerstones in organocatalysis. The first one is from Barbas, Lerner and List, who performed the first Proline catalysed aldol reaction between acetone and aromatic aldehydes⁵:



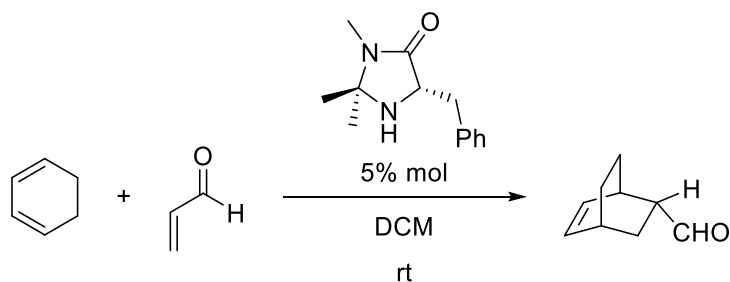
Scheme 2: Proline-catalysed direct asymmetric aldol reaction

³ Reviews on organocatalysis: a) MacMillan D. W. C., *Nature* **2008**, 455, 304-308; b) M. J. Gaunt, C. C. C. Johansson, A. McNally, N. T. Vo, *Drug Discovery Today* **2007**, 12, 8-27; c) J. Seayad, B. List, *Org. Biomol. Chem.* **2005**, 3, 719-724; d) P. I. Dalko, L. Moisan, *Angew. Chem. Int. Ed.* **2004**, 43, 5138-5175; e) P. Melchiorre, M. Marigo, A. Carlone, G. Bartoli, *Angew. Chem. Int. Ed.*, 2008, **47**, 6138.

⁴ a) Z. G. Hajos, D. R. Parrish, *J. Org. Chem.* 1974, 39, 1615; b) U. Eder, G. Sauer, R. Wiechert, *Angew. Chem.* **1971**, 83, 492; *Angew. Chem. Int. Ed. Engl.* **1971**, 10, 496.

⁵ B. List, R. a Lerner, C. F. Barbas III, *J. Am. Chem. Soc.* **2000**, 122, 2395-2396.

The impact of this paper has been unquestionably relevant: It showed that the mechanism of the Hajos-Parrish reaction could be extended and applied for different transformations with a broader applicability; moreover, it was clear that some small organic molecules (such as Proline) are able to catalyse transformations of enzymes using the same mechanism. The second paper from Macmillan and co-workers was about the use of imidazolidinone as organocatalyst for asymmetric Diels-Alder reactions⁶:



Scheme 3: Asymmetric Diels-Alder cycloaddition reaction

In this case Macmillan conceptualized Organocatalysis, underlining how this activation modes can give impressive economic, environmental and scientific benefits, also introducing for the first time the term “Organocatalysis” in the literature. But both this paper were the bases for the generalization of their activation modes, the enamine catalysis and the iminium catalysis, that will be applied to a broad range of reaction classes. Going on, the field of organocatalysis became soon an important area of research, and the growing interest is explained in **Table 1**, which shows the exponential growth of publications in organocatalysis.

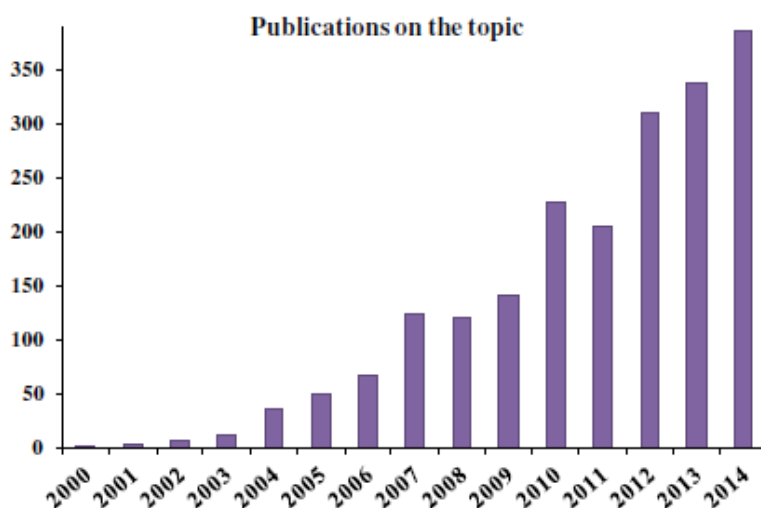


Table 1: The number of publications on organocatalysis, obtained by searching ‘organocatalysis’ in Scifinder. For the year 2014, the number has been calculated until December 15th (see reference 2)

⁶ K. A. Ahrendt, C. J. Borths, D. W. C. MacMillan, *J. Am. Chem. Soc.* **2000**, *122*, 4243-4244

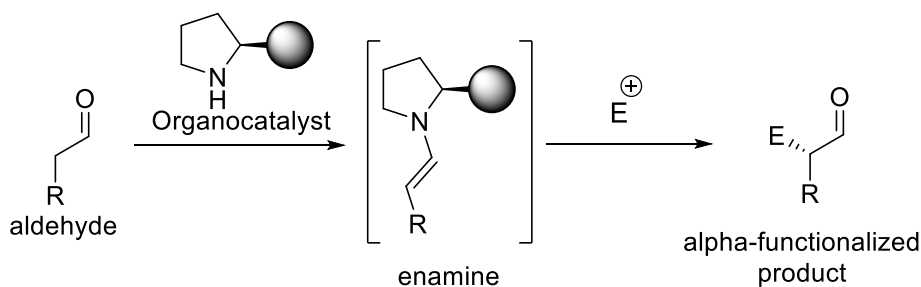
This because of the real advantages offered by this new branch, first of all the development of easy and cheap methods in carrying out such reactions. Compared to organometallic catalyst, that in most cases can be expensive, toxic and very sensible to air and moisture, organic molecules are most of the time cheap, easy-available in a single enantiomer from nature, nontoxic, stable and environmentally friendly. Because of the absence of transition metals, organocatalytic methods seem to be especially attractive for the preparation of compounds that do not tolerate metal contamination, e.g. pharmaceutical products. On the other side, common limitation of organocatalysis are the need for high catalyst loading, usually between 5 and 30 mol%, long reaction times, often more than 24 hours, caused by the poor reactivity of substrates and activated intermediate, and the low tolerance on different substrates. Despite of this, organocatalysis has become a trend topic in research in the last 17 years.

One of the key point for the success of organocatalysis has been the invention or identification of generic modes of catalyst activation, induction and reactivity. A generic activation mode describes a reactive species, whose formation allow the reaction to proceed. This reactive species can participate in many reaction types providing, in many instances, high enantioselectivity. Such reactive species arise from the interaction of the substrate with a single chiral catalyst, owning a determined functional group, in a highly organized and predictable manner. The value of generic activation modes is that, after they have been established, it is relatively straightforward to use them as a platform for designing new enantioselective reactions.

Among the various organocatalytic methodologies, there are different types of activation and two main areas can be identified on the mechanistic basis: *covalent organocatalysis* and *non-covalent organocatalysis*. In the former case, within the catalytic cycle, the catalyst covalently binds the substrate, in the latter case only non-covalent interactions, such as hydrogen bonding or the formation of ion pairs, activate the molecule towards the asymmetric transformation. Between the various types of organocatalysis belonging to this category, the most widespread and best known is without any doubt the aminocatalysis, so the use of primary and in particular secondary amine as catalyst. The two most important types of covalent activation with secondary amine and aldehyde is the enamine and iminium ion, depending on the presence or not of alpha protons. Recently aminocatalysis evolved to the use of primary amines as catalysts too.

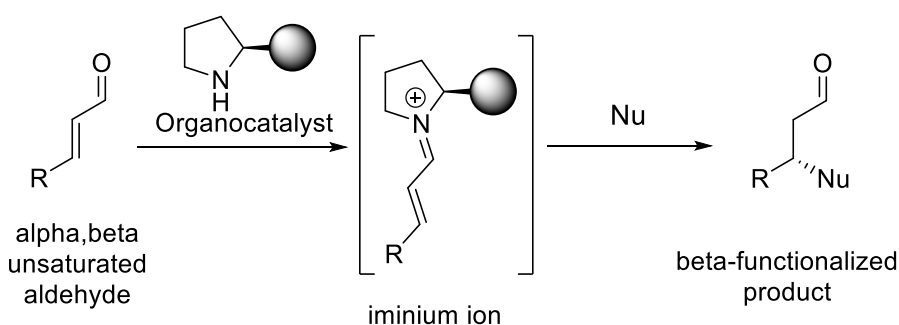
Enamine catalysis is based on the HOMO (Highest Occupied Molecular Orbital) activation of carbonyl compounds with the corresponding increase of electron density at the reaction centre allowing their α -functionalization. The reaction can take place with a diverse array of

electrophiles making possible reactions like aldol, Mannich and conjugate additions, α -oxygenation, amination, chlorination, fluorination, etc.



Scheme 4: α -functionalization of aldehyde via enamine catalysis

Meanwhile MacMillan's group presented the concept of asymmetric iminium catalysis. It is based on the capacity of chiral amines to work as enantioselective catalysts for several transformations that traditionally use Lewis acid catalysts. The reversible formation of iminium ions from α,β -unsaturated aldehydes or ketones and chiral amines might emulate the equilibrium dynamics and π -orbital electronics involved in Lewis acid catalysis. This LUMO (Lowest Unoccupied Molecular Orbital) lowering activates the intermediate toward the attack from a wide variety of nucleophiles to afford β -substituted carbonyl compounds or toward pericyclic reactions.



Scheme 5: β -functionalization of aldehyde via iminium ion activation

During my PhD research work I have focused the attention on these two activation modes, but other are present, like *Hydrogen-bond activation* or more recently *SOMO catalysis*, and are not going to be discussed in this work.

Chapter 2: New Sustainable Protocol for the direct asymmetric Proline-catalysed aldol reaction

This chapter is based on the work done principally during my first year of PhD, and treats about the development of a new protocol for the asymmetric Proline-catalysed aldol reaction. These results will be soon submitted for publication.

2.1 Organocatalysis in industrial application

As reported in the introduction, organocatalysis has attracted the interest of a great part of academia in the last two decades, studying new activation modes and developing new straightforward protocols for organic synthesis. In the last years, there has been a consistent increase in the number of chiral, non-racemic pharmaceuticals available in the market. To overcome the issue, the use of new enantioselective technologies to minimize the losses provoked from making racemic mixtures is becoming more and more important. Due to the operational and economic advantages of asymmetric organocatalysis, this methodology represents one of the possible proposal. Moreover, several groups have made a remarkable effort to show the great applicability of organocatalysis to the total synthesis of drugs currently available in the market such as oseltamivir, warfarin, paroxetine, baclofen and maraviroc. (**Figure 1**).

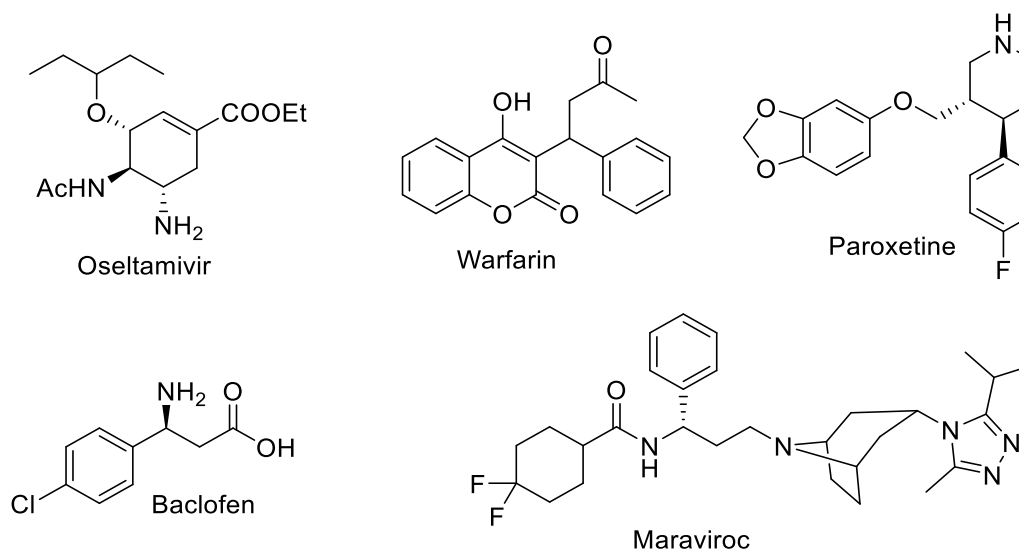
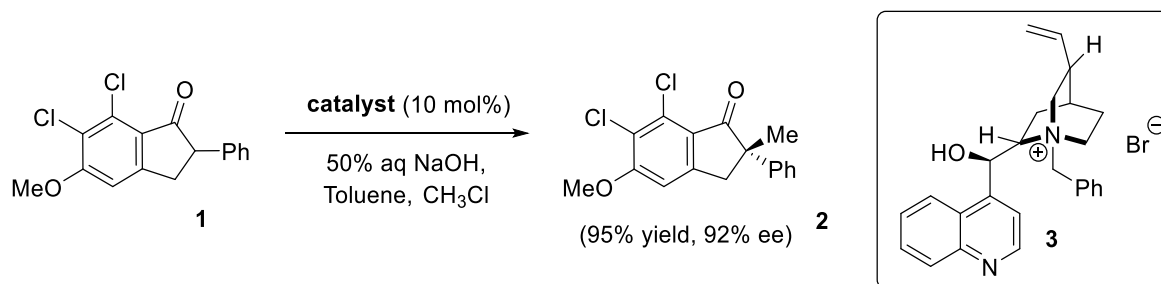


Figure 1: Drugs synthesized using organocatalysis

These efforts have captured the attention of the companies, that have begun to incorporate organocatalysis as a synthetic tool in some industrial scale processes, and in this paragraph some important examples will be reported.⁷

⁷ J. Aleman S. Cabrera, *Chem. Soc. Rev.*, **2013**, 42, 774--793

One of the first example was developed by Merck in 1984 for the synthesis of a uricosuric drug ((+)-indacrinone)).⁸ This development represents the first truly catalytic asymmetric alkylation using phase-transfer catalysts during the 80's. In this work, the alkylation of the starting compound **1** was achieved using cinchona alkaloid derivatives **3** (by N-alkylation of the quinuclidine core), NaOH as base, and CH₃Cl as the alkylating reagent (Scheme 24). This process allowed the access to both enantiomers of intermediate **2**, used for the synthesis of the indacrinone, in high yield and enantiomeric purity on a pilot plant scale (B75 kg).

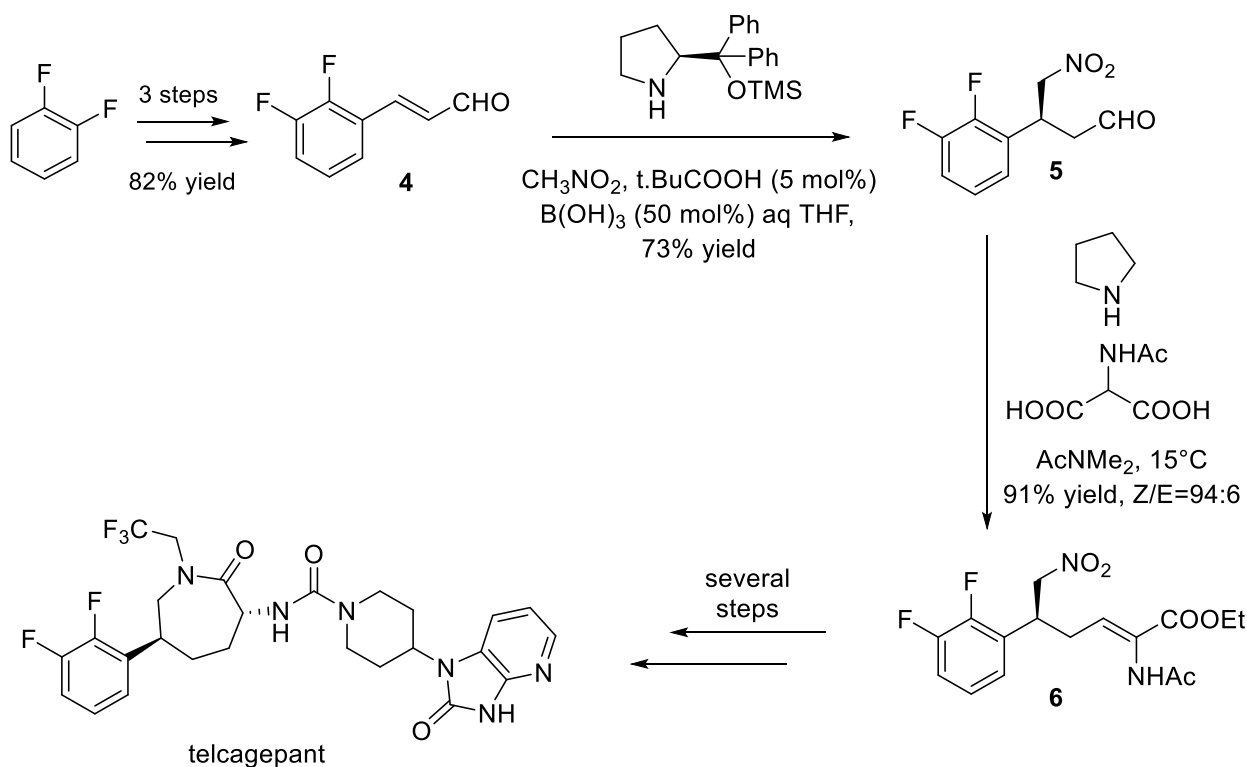


Scheme 6: Synthesis of the enantioenriched intermediate for the synthesis of indacrinone developed by Merck.

its first industrial scale application for a medicinal compound did not appear until 2010. Therefore, Xu and co-workers reported the synthesis of a drug for the treatment of migraine (**Scheme 7**).⁹ Starting from 1,2-difluorobenzene (4.80 kg, 42.1 mol), with a 3 steps procedure, they synthesized aldehyde **4** in 82% yield. The known Hayashi catalyst was chosen as catalyst and was prepared in situ from the alcohol in classic conditions (1.3 equiv. of TMSCl and 1.7 equiv. of imidazole in THF at 50°C) and used after aqueous workup for an organocatalysed addition of Nitromethane to give product **5**. This compound was converted into compound **6** with a formal Doebner-Knoevenagel reaction, using pyrrolidine as catalyst and acylated amino-malonic acid as the reagent. Afterwards, several transformations, including a reduction and cyclization, allowed the preparation of the final product. This synthesis is environmentally friendly, with only three isolated intermediates and a brilliant overall yield of 27%.

⁸ U. H. Dolling, P. Davis and E. J. J. Grabowski, *J. Am. Chem. Soc.*, **1984**, *106*, 446–447.

⁹ F. Xu, M. Zacuto, N. Yoshikawa, R. Desmond, S. Hoerrner, T. Itoh, M. Journet, G. R. Humphrey, C. Cowden, N. Strotman, P. Devine, *J. Org. Chem.*, **2010**, *75*, 7829–7841



Scheme 7: Asymmetric synthesis of telcagepant by Merck.

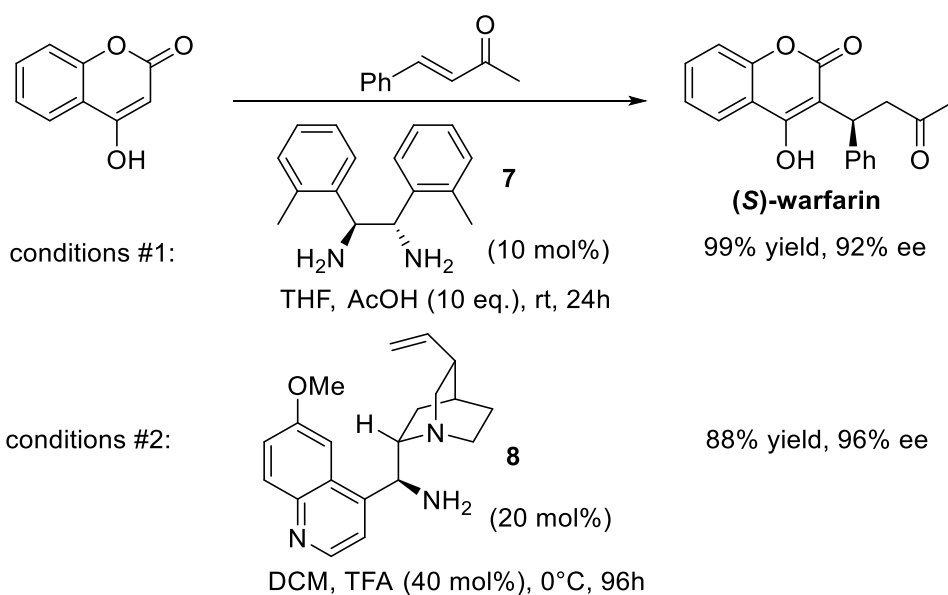
Amine catalysis was used also for the asymmetric synthesis of warfarin, an anti-coagulant frequently prescribed in the United States of America.¹⁰ Racemic warfarin was synthesized in 48% yield via a conjugate addition reaction between 4-hydroxycoumarin and benzalacetone¹¹, but it was known that the (*S*)-warfarin is five times more active than the (*R*)- isomer, and a chemical resolution of the racemic mixture using quinine afforded the (*S*)-warfarin in only 19% yield. To improve the synthetic efficiency, chiral organocatalysts were exploited to perform an enantioselective conjugate addition reaction between hydroxycoumarin and benzalacetone, described by Chin group using primary amine catalysts. Warfarin was formed in 99% yield and 92% ee through the catalysis of 10 mol% of di- amine **7**.¹² In another report, Chen and co-workers developed another asymmetric synthesis of (*S*)-warfarin using a Cinchona alkaloid-derived catalyst **8** (**Scheme 8**).¹³

¹⁰ E. Bush, W. F. Trager, *J. Pharm. Sci.*, **1983**, *72*, 830.

¹¹ M. Ikawa, M. A. Stahmann, K. Paul, *J. Am. Chem. Soc.* **1944**, *66*, 902.

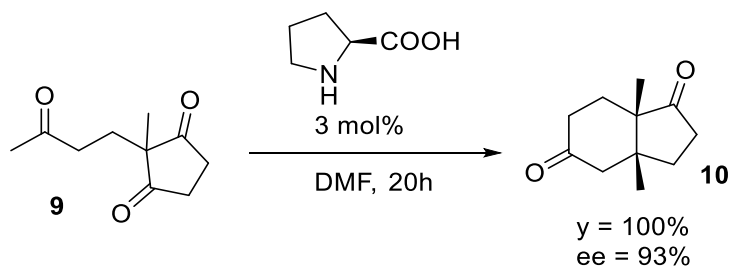
¹² H. Kim, C. Yen, P. Preston, J. Chin, *Org. Lett.* **2006**, *8*, 5239.

¹³ J.-W. Xie, L. Yue, W. Chen, W. Du, J. Zhu, J.-G. Deng, Y.-C. Chen, *Org. Lett.*, **2007**, *9*, 413.



Scheme 8: Organocatalysed synthesis of (S)-warfarin

Talking about chiral amine catalysis, the most important industrial example was implemented even more than 40 years ago, and has been already reported in the introduction. Two industrial groups at Schering and Hoffmann-La Roche discovered in 1971 that *L*-Proline was able to catalyse the asymmetric intramolecular aldol reactions of triketone **9** to afford compound **10** with up to 93% ee which was used to manufacture steroids on multi-kilogram scales¹⁴ (**Scheme 9**). This intramolecular transformation is now famously known as the Hajos–Eder–Sauer–Wiechert reaction.



Scheme 9: The Hajos, Parrish, Eder, Sauer and Wiechert reaction

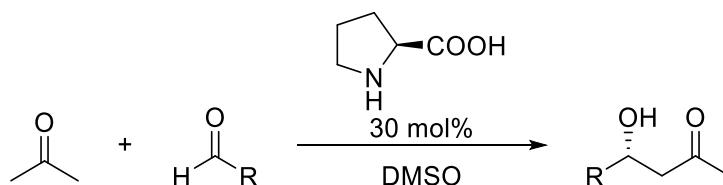
This transformation also showed how simple naturally available amino acids like Proline, thanks to the easy availability, the low supply costs, the mostly absent toxicity and the poor waste production, can be seen as ideal catalyst for industrial application in the synthesis of enantiomerically enriched drugs and fine chemicals. Furthermore, the use of Proline as catalyst has been extensively studied along the golden age of organocatalysis, principally concerning aldol reaction.

¹⁴ C. Agami, N. Platzer, H. Sevestre, *Bull. Soc. Chim. Fr.* **1987**, 2, 358

2.2 Asymmetric aldol reaction catalysed by L-Proline

The aldol reaction, first discovered by Wurtz in 1872,¹⁵ is one of the most powerful transformations in organic chemistry. This process consists in the reaction of two carbonyl partners to give β -hydroxyketones, forming up to two new stereocenters.¹⁶ This transformation presents numerous challenges, including issues of chemo-, regio-, diastereo-, and enantioselectivity to the synthetic chemist, and many powerful stoichiometric processes have been proposed to address these issues. Development of catalytic methods that avoid the production of stoichiometric by-products while maintaining the high levels of control available from stoichiometric processes provides an atom economical alternative. Indeed, numerous catalysts for the aldol reaction have been reported in recent years, including enzymes, catalytic antibodies and small molecules. The focus of this part of the work will be on the use of organocatalysts, in particular simple Proline as catalyst.

As seen previously, the first works that demonstrates the possibility to use L-Proline as catalyst in the asymmetric aldol reaction, were two independent works published in 1971 by Hajos, Parrish, Eder, Sauer and Wiechert, but the first example of an organocatalysed intermolecular direct asymmetric aldol reaction was described only in 2000 by List, Lerner and Barbas, and is reproposed in **Scheme 10**. This work clearly showed how simple could have been the use of chiral secondary amine to catalyse the functionalization of carbonyl compounds. They reported the use of a catalytic amount of proline to promote the direct enantioselective aldol reaction between a ketone, like acetone, and a series of aldehydes.



Scheme 10: The List's approach to aldol reaction

Of course, the aldehydes which gives the best yields resulted to be the non enolizable ones, which can avoid the formation of by-products due to autocondensation. The reaction conditions are quite severe with the use of 30% catalyst and DMSO as solvent. The catalytic cycle is reported in **Figure 2** and follows the mechanism of type I aldolase:

¹⁵ A. Wurtz, *Bull. Soc. Chim. Fr.*, **1872**, *17*, 436.

¹⁶ For reviews on asymmetric aldol addition, see: a) B. List, *Tetrahedron*, 2002, **58**, 5573; b) C. F. Barbas III, *Angew. Chem. Int. Ed.*, 2008, **47**, 42; c) C. Palomo, M. Oiarbide, J. M. García, *Chem. Soc. Rev.*, 2004, **33**, 65; d) H. Wennemers, *Chimia*, 2007, **61**, 276; e) W. Notz, F. Tanaka, C. F. Barbas III, *Acc. Chem. Res.*, 2004, **37**, 580; f) S. Mukherjee, J. W. Yang, S. Hoffmann, B. List, *Chem. Rev.*, 2007, **107**, 5471; g) B. Alcaide, P. Almendros, *Angew. Chem. Int. Ed.*, 2003, **42**, 858; h) B. Alcaide, P. Almendros, *Eur. J. Org. Chem.*, 2002, 1595; i) G. Guillena, C. Nájera, D. J. Ramón, *Tetrahedron: Asymm.*, 2007, **18**, 2249; j) L. M. Geary, P. G. Hultin, *Tetrahedron: Asymm.*, 2009, **20**, 131; k) B. Schetter, R. Mahrwald, *Angew. Chem. Int. Ed.*, 2006, **45**, 7506; l) R. Mestres, *Green Chem.*, 2004, **6**, 583.

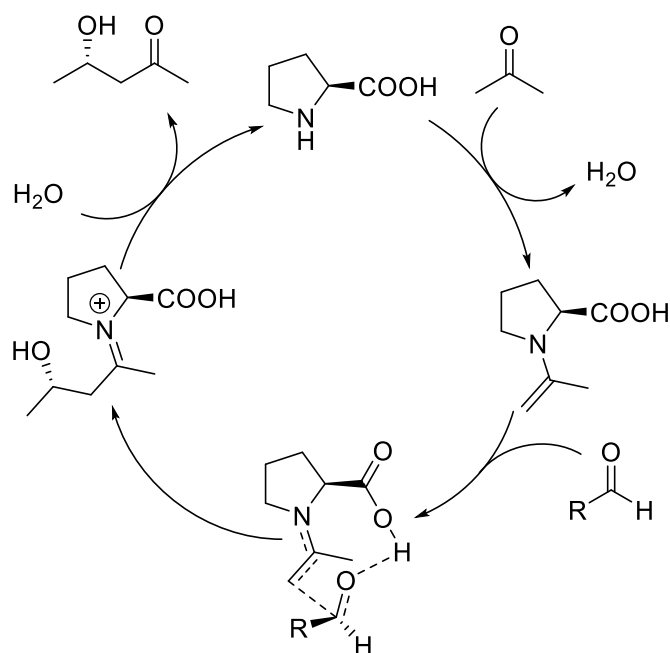


Figure 2: Mechanism of the direct Proline catalysed aldol reaction

The cycle starts with the enamine formation, generally the rate determining step, followed by the nucleophilic attack to the aldehyde, activated by proline's acid group. The hydrolysis of the iminium thus formed gives the product. By the energetic point of view, the enamine formation and the following addition have similar barrier. This means that, in some cases or changing the substrates, the rate determining step changes, like demonstrated in studies by Armstrong and Blackmond.¹⁷

Interesting is also the role of water in the reaction. It has been determined that a little amount of additional water, despite a decrease in reaction rate, can limit the formation of *off-cycle* by-product, leading to better yields. After 2001 other works on proline-catalysed aldol reaction appeared, introducing the use of different ketones.¹⁸ Since the ketone is, in most protocols, also the reaction solvent, and is also used in great molar excess, is not possible for practical reasons to use solid ketones, or very precious substrates like steroids. On the other hand, many examples have been showed with cyclohexanone and cyclopentanone. The *anti*-aldol is the favourite one in both cases: the enantioselectivity of the reaction is granted by the geometry of the transition state, where the nucleophilic attack of the enamine is governed from the carboxylic acid of the proline, that binds the aldehyde via hydrogen bond. In this way the only possible approach is through the *Si* face of enamine (**Figure 3**).

¹⁷ N. Zotova, A. Franzke, A. Armstrong and D. G. Blackmond, *J. Am. Chem. Soc.*, **2007**, *129*, 15100.

¹⁸ B. List, *Tetrahedron*, **2002**, *58*, 5573; B. List, P. Pojarliev and C. Castello, *Org. Lett.*, **2001**, *3*, 573.

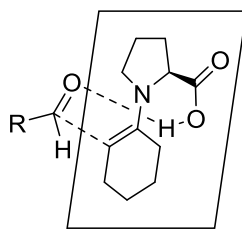


Figure 3: Transition state in the aldol reaction with cyclohexanone

It has been demonstrated that cyclohexanone gives the best diastereoselectivity, compared to cyclopentanone, probably thanks to the rigid chair conformation, that leads to more selectivity. On the other hand, cyclopentanone result to be a more reactive donor, because the enamine has a 120° hybridization sp^2 angle, and a stronger reactivity lead to a minor control in selectivity. These transformations are usually carried with 10-30 molar percent of catalyst and with very long reaction times (also days).

Without any doubt, Proline represent the most important catalyst for the asymmetric aldol reaction. Since is a natural aminoacid, is easily available in an enantiomerically pure form at a cheap price. Furthermore, like many organocatalysts, is stable to moisture and oxygen, reactions can be carried out at open air, is not toxic and easy to dispose. But despite of this, the catalyst shows also great limitations, the most important of those being the low solubility in the commonly used organic solvents, together with a poor reactivity, that requires high catalyst loadings, and offer unsatisfactory stereochemical results.¹⁹ To overcome solubility problems and concomitantly to raise the catalytic system reactivity, a huge number of proline derivatives have been designed and employed. Modification of the carboxylic acid with different groups able to donate hydrogen-bonding or the introduction of bulky substituents on the pyrrolidine ring scaffold were two of the most used strategies employed, as recently exhaustively reviewed by Trost²⁰. Moreover, the insertion of strongly hydrophobic groups can increase also the solubility in the organic phase. Some of this modified catalyst are showed in **figure 4**:

¹⁹ a) W. Notz, B. List, *J. Am. Chem. Soc.*, 2000, **122**, 7386; b) B. List, P. Pojarliev, C. Castello, *Org. Lett.*, 2001, **3**, 573; c) K. S. Sakthivel, W. Notz, T. Bui, C. F. Barbas III, *J. Am. Chem. Soc.*, 2001, **123**, 5260; d) A. Córdova, W. Notz, C. F. Barbas III, *Chem. Commun.*, 2002, 3024; e) A. I. Nyberg, A. Usano, P. M. Pihko, *Synlett*, 2004, 1891; f) Y.-Y. Peng, Q.-P. Ding, Z. Li, P. G. Wang, J.-P. Cheng, *Tetrahedron Lett.*, 2003, **44**, 3871; g) T. Darbre, M. Machuqueiro, *Chem. Commun.*, 2003, 1090; h) Y. Hayashi, W. Tsuboi, M. Shoji, N. Suzuki, *Tetrahedron Lett.*, 2004, **45**, 4353; i) Y.-S. Wu, W.-Y. Shao, C.-Q. Zheng, Z.-L. Huang, J. Cai, Q.-Y. Deng, *Helv. Chim. Acta*, 2004, **87**, 1377.

²⁰ B. M. Trost, C. S. Brindle, *Chem. Soc. Rev.*, **2010**, 39, 1600-1632.

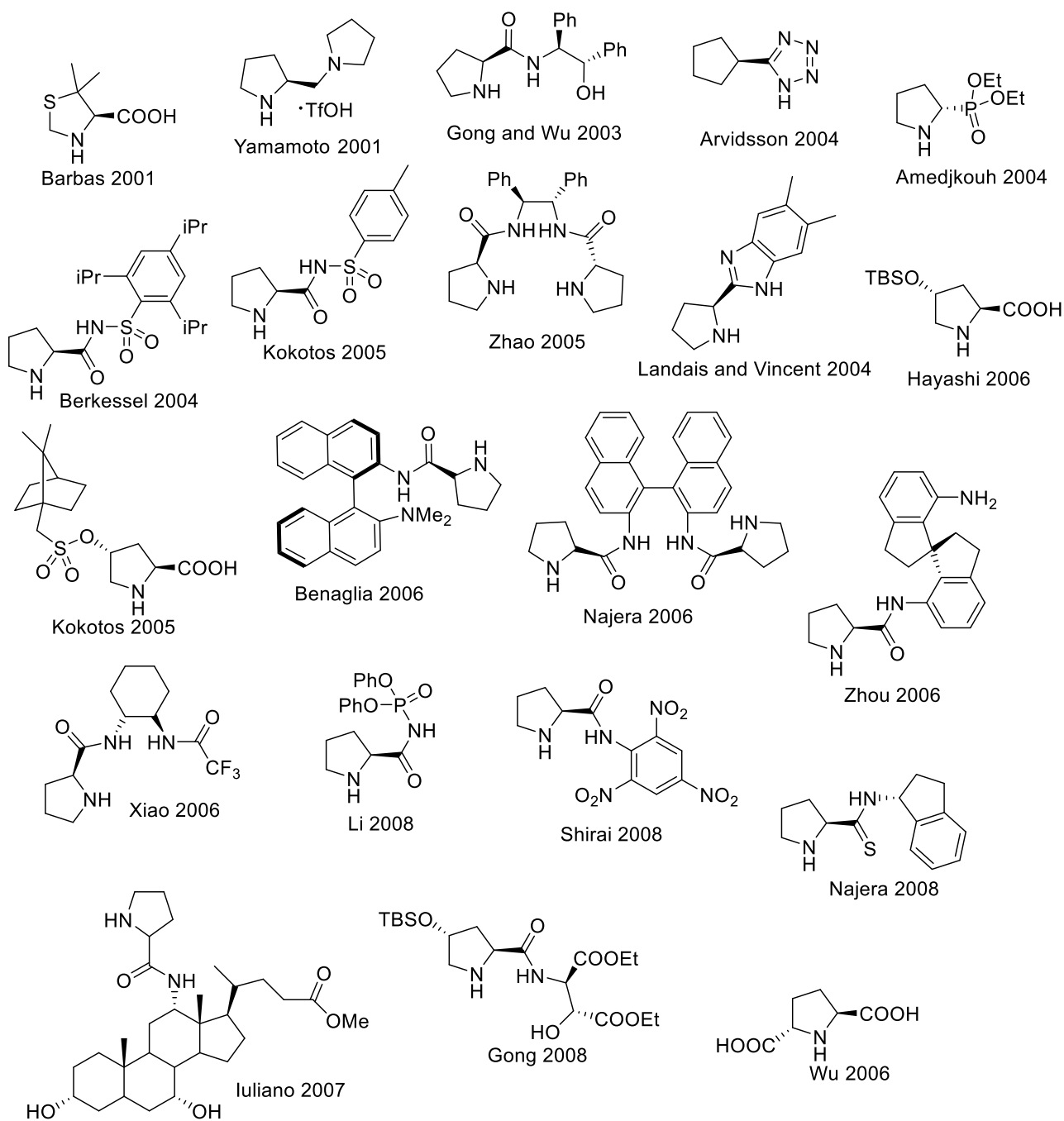
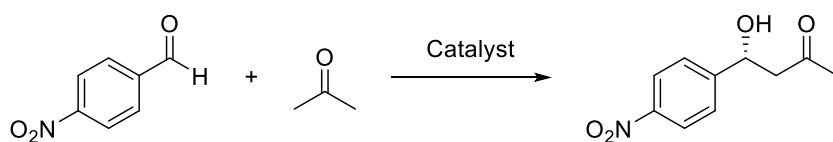
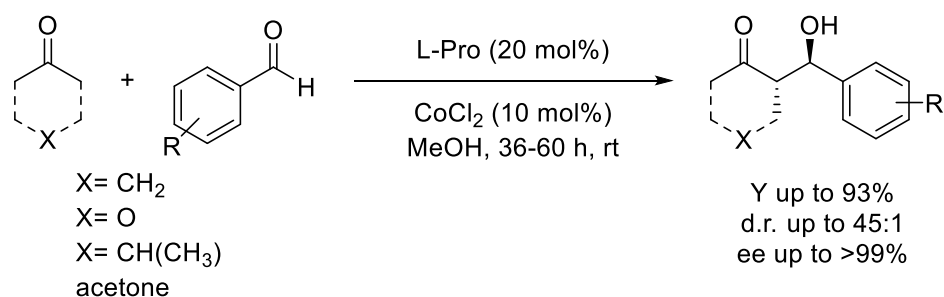


Figure 4: several examples of organocatalyst for the aldol reaction of aromatic aldehydes and ketones

Despite the outstanding levels of reactivity and selectivity achieved with these modified organocatalysts, it should be pointed out that according to the principle of green chemistry a catalyst should be a molecule possessing a low molecular weight, in order not to have a too strong impact on the reaction mass efficiency. Moreover, all proline derivatives are prepared using multi-step syntheses, increasing exponentially the mass intensity related to their preparation. From this point of view unmodified proline is the ideal candidate as a

catalyst, and in this perspective efforts should be directed in optimizing the reaction conditions to increment its activity and selectivity, rather to find different and more complex catalysts.

An interesting alternative strategy involved the use of unmodified proline together with additives, usually water, acids, diols, amines, or thioureas.²¹ In the reported examples, the co-catalyst was able to tune the solubility, the reactivity and/or the stereoselectivity of native proline, making the asymmetric aldol process more efficient and, therefore, more environmentally sustainable. Nevertheless, the achieved performances were not optimal yet (long reaction times, stereocontrol strongly depending on the substrate) and some drawbacks were still present, such as high proline loadings (10-30 mol%) and the cost of the not recovered chiral additive. Significant advances were accomplished employing metal salts as additives. In particular, Reiser and co-workers developed a strategy based on cobalt(II)-proline system²², which ensured excellent results in direct aldol reactions between aromatic aldehydes and both cyclic and acyclic ketones (**Scheme 11**).



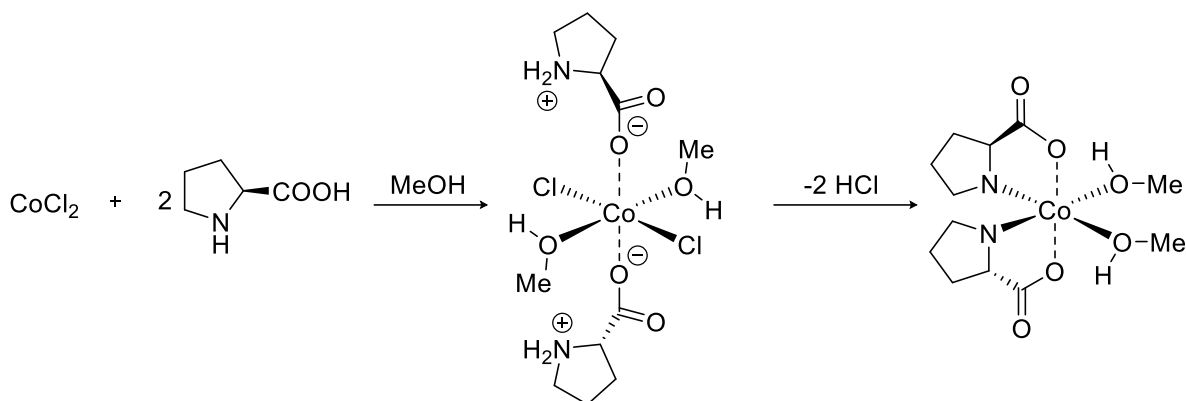
Scheme 11: Reiser's aldol reaction with Proline and CoCl_2

In previous works was demonstrated²³ that a metal salt in (II) oxidation state is able to chelate an aminoacid, allowing an amino-metallic catalysis. Reiser observed that the mechanism of the process could be a transition state in which two molecules of proline are involved, bounded through the carboxylic moiety at the Cobalt(II), while the role of methanol is the coordination of the metal to stabilise a C_2 symmetry complex (**Scheme 12**)

²¹ a) P. M. Pihko, K. M. Laurikainen, A. Usano, A. I. Nyberg, J. A. Kaavi, *Tetrahedron*, 2006, **62**, 317; b) R. L. Sutar, N. N. Joshi, *Synth. Commun.*, 2014, **44**, 352. c) D. E. Ward, V. Jheengut, *Tetrahedron Lett.*, 2004, **45**, 8347. d) Y. S. Wu, Y. Chen, D.-S. Deng, J. Cai, *Synlett*, 2005, 1627. e) Y. Zhou, Z. Shan, *Tetrahedron: Asymm.*, 2006, **17**, 1671; f) Y. Zhou, Z. Shan, *J. Org. Chem.*, 2006, **71**, 9510. g) O. Reis, S. Eymur, B. Reis, A. S. Demir, *Chem. Commun.*, 2009, 1088; h) N. El-Hamdouni, R. Rios, A. Moyano, *Chem. Eur. J.*, 2010, **16**, 1142; i) A. Sitki Demir, S. Basceken, *Tetrahedron: Asymm.*, 2013, **24**, 515

²² A. Karmakar, T. Maji, S. Wittmann, O. Reiser, *Chem. Eur. J.* **2011**, *17*, 11024 – 11029.

²³ a) Z. Damaj, A. Naveau, L. Dupont, E. H_{non}, G. Rogez, E. Guillon, *Inorg. Chem. Commun.* **2009**, *12*, 17; b) M. L. Caroline, A. Kandasamy, R. Mohan, S. Vasudevan, *J. Cryst. Growth* **2009**, *311*, 1161; c) H. J. Hsu (*J. H. Biotech Inc., Ventura*), US-A 005504055A, **1996**; d) M. Kunitamura, S. Sakamoto, K. Yamaguchi, *Org. Lett.* **2002**, *4*, 347.



Scheme 12: Hypothesis for the Cobalt-Proline Interaction

This hypothesis has been subsequently confirmed by computational investigation of Guillon et co-workers. It is interesting to see the compared results in presence of cobalt and without it. In detail, without metal the reaction with 10% Proline in methanol gives worst yields and also poor selectivity (only 4:1 diastereomeric ratio and 67% enantiomeric excess). By the way, this work by Reiser demonstrates the interest in coming back to proline as catalyst for the direct aldol reaction.

The role of the solvent in determining the aldol reaction efficiency was also addressed by several authors. Invariably, the use of unmodified proline (without additives) forced to choose polar aprotic solvents (DMSO or DMF) to obtain acceptable yields and selectivities. A peculiar case was represented by ionic liquids (ILs)²⁴, which allowed in some instances to decrease the catalyst loading (up to 1 mol%) and to confine proline in a separate phase, enabling a simple product isolation and the reuse of the catalytic system.

A number of research groups noticed that protic media were not suitable for aldol condensations promoted exclusively by native proline. However, although a plethora of studies focused on the use and the role of water (as solvent, co-solvent or additive), very few authors extended their investigations to alcohols. Alcoholic media were long-neglected because of the much worse recorded outcomes, in terms of reaction yield and/or stereoselectivity. Only when proline was used in combination with metal salts as additives, the use of methanol as solvent or co-solvent afforded acceptable results.

²⁴ a) T. P. Loh, L. C. Feng, H. Y. Yang, J. Y. Yang, *Tetrahedron Lett.*, 2002, **43**, 8741; b) P. Kotrusz, I. Kmentová, B. Gotov, S. Toma, E. Solčániová, *Chem. Commun.*, 2002, **8**, 2510; c) M. Gruttadauria, S. Riela, A. Aprile, P. L. Meo, F. D'Anna, R. Noto, *Adv. Synth. Catal.*, 2006, **348**, 82; d) T. Kitazume, Z. Jiang, K. Kasai, Y. Mihara, M. Suzuki, *J. Fluorine Chem.*, 2003, **121**, 205; e) A. Córdova, *Tetrahedron Lett.*, 2004, **45**, 3949; f) W. Miao, T.-H. Chan, *Adv. Synth. Catal.*, 2006, **348**, 1711.

2.3 Aim of the work

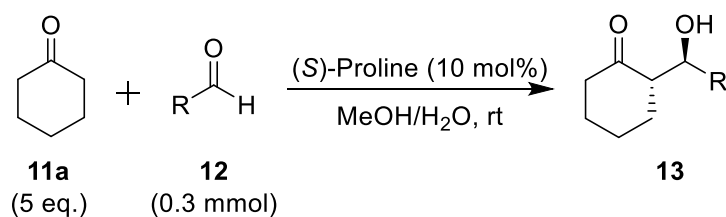
This project started with the aim to develop a really sustainable and scalable protocol for the proline catalysed direct asymmetric aldol reaction. An efficient protocol involving simple proline as catalyst would be an excellent tool for subsequent applications, due to the incredible advantages of the simple amino acid, that would allow to avoid the time- and cost-consuming catalyst preparation, and the waste of additives. On the other side, we had to face off the problem related to the low reactivity and poor solubility.

We were intrigued by the depth exploration of the methanol impact on the asymmetric intermolecular aldol condensation promoted by unmodified proline. Indeed, the development of an aldol approach based on the combination of simple unmodified proline with methanol would be highly desirable as a sustainable process. Moreover, methanol could be advantageous from an operational point of view compared with DMSO, usually required for aldol reactions catalysed by native proline. In this way, the reaction work-up and the products isolation would become easier.

All these factors could give the possibility of further exploitation of the direct asymmetric aldol reaction at production levels. Parameters taken in consideration has been the reproducibility, selectivity ad reactivity, and has been compared with data reported in literature, to investigate the effective benefits of the new approach.

2.4 Results and discussion

Reiser's work has been choosed as the starting point for the development of the new protocol for Proline catalysed aldol reaction. As fully demonstrated by literature, the employment of a minimal amount of water in the reaction mixture, despite a decrease in reactivity, plays a key role in improving the stereoselectivity of the reaction. Then we decided to use a mixture of methanol and water as co-solvent of the reaction. As model reaction we chose non enolizable aldehydes as acceptors, like differently substituted benzaldehydes, to limit the autocondensation, and cyclic ketones as cyclohexanone. The objective is to have a direct correlation between the literature results and the obtained data. We considered as model reaction the addition of cyclohexanone (**11a**, 5 equivalents) to some differently substituted aromatic aldehydes (**12a-d**, 0.3 mmol) mediated by (*S*)-proline (10 mol%) at room temperature and in the presence of a mixture MeOH/H₂O (20 μ L/10 μ L) (**Table 2**).



R (12)	Reaction conditions	Time (h)	Conv. (%) ^a	<i>ee</i> 13 (%) ^b	<i>dr</i> 13 (<i>syn:anti</i>) ^a
4-NO ₂ Ph 12a	MeOH/H ₂ O (20μL/10μL)	19	100	98	1:13
	no MeOH	19	25	99	1:19
	no H ₂ O	19	100	76	1:1.4
4-CNPh 12b	MeOH/H ₂ O (20μL/10μL)	20	81	98	1:24
	no MeOH	20	30	77	1:2.6
	no H ₂ O	20	100	98	1:1.5
4-ClPh 12c	MeOH/H ₂ O (20μL/10μL)	19	43	99	1:32
	no MeOH	19	5	100	nd
	no H ₂ O	19	64	98	1:5.6
Ph 12d^c	MeOH/H ₂ O (20μL/10μL)	30	55	97	1:7
	no MeOH	30	37	>99	>1:99
	no H ₂ O	30	55	83	1:3.7

Table 2: ^a Determined by ¹H NMR on the crude mixture. ^b Determined by chiral stationary phase (CSP)-HPLC on the crude mixture. ^c 20 mol% of (S)-proline were used. eq. = equivalents, rt = room temperature, h = hours, Conv. = conversion, nd = not determined.

The MeOH/H₂O ratio and the mixture amount were optimized to the minimum necessary to make proline soluble. To have a clear understanding about the role of each additive on the process performance, the corresponding transformations were also carried out in the absence of MeOH or H₂O (**Table 2**). For all the tested aldehydes, the best balance between conversion and stereoselectivity was achieved employing the mixture MeOH/H₂O as additive. Without MeOH the conversions dropped down. On the other hand, in the absence of H₂O a significant loss of the stereocontrol occurred. These preliminary findings confirmed the “stereoselectivity enhancer” role played by water, and, interestingly, they suggested that methanol considerably increased the reaction rate. The two protic additives seemed to act on the aldol reaction behavior in two distinct and independent ways, and, appearing these effects as additive, the use of MeOH/H₂O mixture allowed to considerably improve the process performance.

In detail in **figure 5** are showed the chiral HPLC chromatogram for the reaction of 4-NO₂-benzaldehyde **12a** with cyclohexanone **11a**, both with and without water:

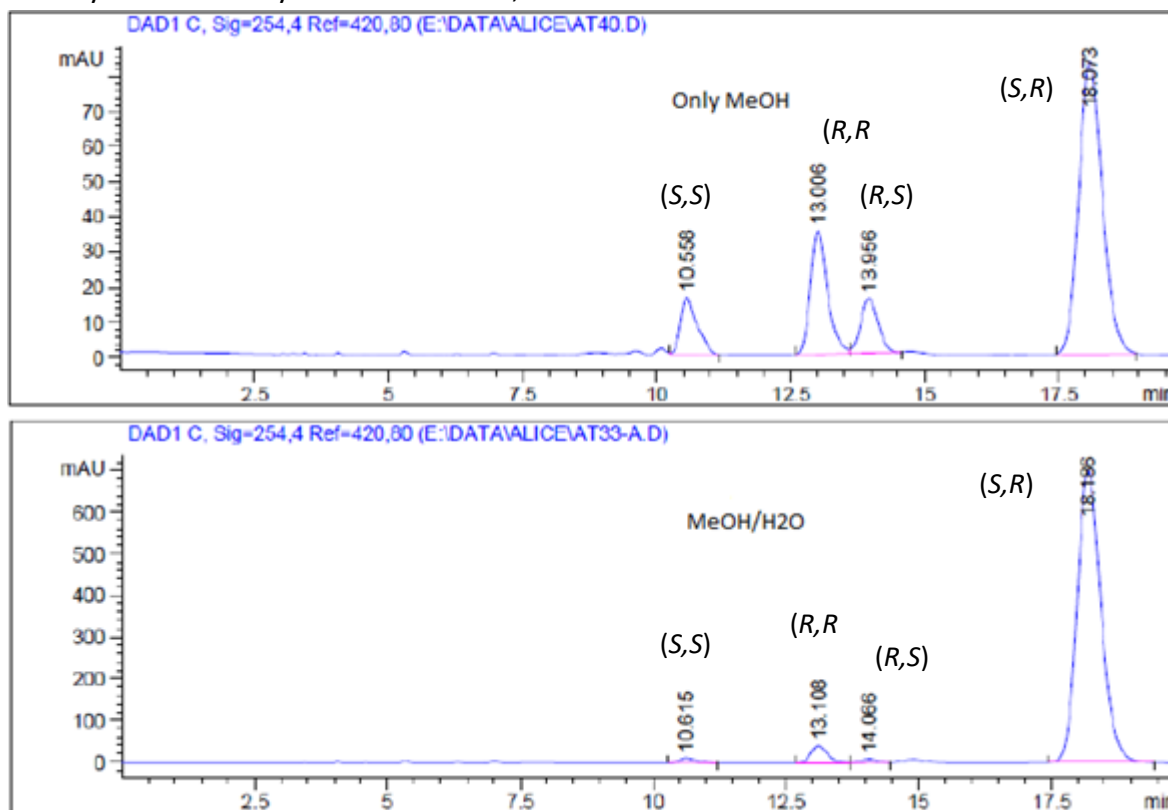


Figure 5: Chiral HPLC chromatogram for reaction between pNO₂-benzaldehyde and Cyclohexanone with and without water.

As is clearly visible, the reaction without water is extremely less selective, both in diastereo and enantioselectivity. It is noteworthy that both the accelerating effect exerted by methanol and the selectivity gave by water were observed (with slight difference) for differently substituted aldehydes, therefore it appeared as generalizable. Thus, we extended the developed protocol to a larger number of aldehydes (**Table 3**).

R (12)	Time (h)	Conv. (%) ^b	<i>ee</i> 13 (%) ^c	<i>dr</i> 13 (<i>syn:anti</i>) ^b
C ₆ F ₅ 12e	19	100	>99	>1:99
2-NO ₂ Ph 12f	19	93	95	1:5
4-BrPh 12g	19	40	99	1:49
2-naphthyl 12h	24	37	95	1:10
4-MeOPh 12i ^d	70	18	90	1:6
<i>i</i> -Pr 12j	48	30	>99	>1:99

Table 3: MeOH/H₂O-based protocol applied to different aldehydes (**12**).^a Reaction conditions: **11a** (5 equiv.), **12** (0.3 mmol), (*S*)-proline (10 mol%), MeOH/H₂O (20 μL/10 μL), rt. ^b Determined by ¹H NMR on the crude mixture. ^c Determined by CSP-HPLC on the crude mixture. ^d 20 mol% of (*S*)-proline were used.

For the most reactive electron-poor aldehydes (**12e** and **12f**) we achieved high conversion and stereocontrol in only 19 hours. These results were excellent if compared with those reported in the literature for analogous transformations promoted by unmodified (*S*)-proline and exploiting more complex protocols.²⁵ For the less reactive substrates **12g** and **12h** the conversions reached after 19 and 24 hours, respectively, were modest, but the enantio- and the diastereoselectivities were both higher than what described so far for proline-based protocols.²⁶ The electron-rich *para*-methoxy substituted aldehyde **12i** is usually not considered in the scope screening of aldol reactions mediated by proline, because of the incredibly poor reactivity. The only example we found reported low conversion (15%) and absence of diastereoselection employing (*S*)-proline (20 mol%) in DMSO.²⁷ By adding a Lewis acid and water the conversion even decreased. Exploiting our MeOH/H₂O-based protocol the product conversion remained poor (18%), but we obtained good enantio- and diastereoselectivities. Lastly, we tested the aliphatic *iso*-butyl aldehyde **12j**. Also in

²⁵ For aldehyde **12e**, see: a) W. Clegg, R. W. Harrington, M. North, F. Pizzato, P. Villuendas, *Tetrahedron: Asymmetry*, 2010, **21**, 1262. See also ref. 15l. For aldehyde **12f**, see: b) R. Tan, C. Li, J. Luo, Y. Kong, W. Zheng, D. Yin, *Journal of Catalysis*, 2013, **298**, 138; c) A. Martínez-Castañeda, H. Rodríguez-Solla, C. Concellón, V. del Amo, *J. Org. Chem.*, 2012, **77**, 10375; d) Y. Qian, X. Zheng, X. Wang, S. Xiao, Y. Wang, *Chemistry Letters*, 2009, **38**, 576; e) B. Rodríguez, A. Bruckmann, C. Bolm, *Chem. Eur. J.*, 2007, **13**, 4710; f) B. Rodríguez, T. Rantanen, C. Bolm, *Angew. Chem. Int. Ed.*, 2006, **45**, 6924.

²⁶ For aldehyde **12g**, see: a) A. Obregón-Zúñiga, M. Milán, E. Juaristi, *Org. Lett.*, 2017, **19**, 1108; b) Á. Martínez-Castañeda, B. Poladura, H. Rodríguez-Solla, C. Concellón, V. del Amo, *Org. Lett.*, 2011, **13**, 3032. See also ref.s 12, 15l and 18a,d. For aldehyde **12h**, see ref. 6d.

²⁷ R. Fernandez-Lopez, J. Kofoed, M. Machuqueiro, T. Darbre, *Eur. J. Org. Chem.*, **2005**, 5268

this case, the recorded stereoselection data were superior than those reported in the literature for unmodified proline.²⁸

The results provided by the MeOH/H₂O-based protocol were very promising in terms of both reaction rate and stereocontrol for a variety of aldehydes (Tables 2-3). These findings demonstrated the potential of the MeOH/H₂O mixture as additive in the asymmetric direct aldol condensation catalysed by native (*S*)-proline. Therefore, we focused our attention on the further improvement of the reaction performance. As observed during the preliminary studies (Table 2), the presence of a small amount of methanol in the reaction mixture exerted the main effect of increasing the reaction rate. Thus, we doubled the methanol volume (40 μ L) and the product conversions resulted significantly improved for all the tested aldehydes maintaining an excellent level of enantiocontrol (**Table 4**).

R (12)	MeOH/H ₂ O (μ L/ μ L)	Time (h)	13 , Conv. (%) ^b	<i>ee</i> 13 (%) ^c	<i>dr</i> 13 (<i>syn:anti</i>) ^b
4-NO ₂ Ph 12a	20/10	4	13aa ,47	97	1:16
	40/10	4	13aa ,82	98	1:11.6
	20+20 ^d /10	4	13aa ,84	97	1:16
4-CNPh 12b	20/10	4	13ab ,65	97	1:19
	40/10	4	13ab ,77	95	1:16
4-ClPh 12c	20/10	19	13ac ,43	99	1:32
	40/10	19	13ac ,64	98	1:19
Ph 12d	20/10 ^e	30	13ad ,55	97	1:7
	40/10	30	13ad ,75	98	1:9
C ₆ F ₅ 12e	20/10	4	13ae ,63	>99	>1:99
	40/10	4	13ae ,67	>99	>1:99
2-NO ₂ Ph 12f	20/10	4	13af ,34	>99	1:49
	40/10	4	13af ,59	>99	1:32.3
4-BrPh 12g	20/10	19	13ag ,41	99	>1:99
	40/10	19	13ag ,88	96	1:16
2-naphthyl 12h	20/10	24	13ah ,37	95	1:10
	40/10	24	13ah ,72	93	1:12
4-MeOPh 12i ^e	20/10	70	13ai ,18	90	1:6
	40/10	70	13ai ,30	90	1:4
<i>i</i> -Pr 12j ^e	20/10	72	13aj ,51	>99	>1:99
	40/10	72	13aj ,63	99	>1:99
4-CF ₃ Ph 12k	40/10	4	13ak ,78	96	1:31

²⁸ G. Szöllősi, M. Fekete, A. A. Gurka, M. Bartók, *Catal. Lett.*, 2014, **144**, 478.

2-thiophen 12l^e	40/10	48	13al,65	86	1:5
4-MePh 12m	40/10	40	13am,64	94	1:6.6

Table 4: Optimization of the MeOH/H₂O-based protocol. ^a Reaction conditions: **11a** (5 equiv.), **12** (0.3 mmol), (*S*)-proline (10 mol%), rt. ^b Determined by ¹H NMR on the crude mixture. ^c Determined by CSP-HPLC on the crude mixture. ^d 20 μL of MeOH added after 2 h. ^e 20 mol% of (*S*)-proline were used.

For the most reactive substrates (**12a**, **12b**, **12e** and **12f**) good conversions were achieved in only 4 hours, demonstrating for the MeOH/H₂O/(*S*)-proline catalytic system an unprecedented reactivity. Moreover, interesting amounts of product were obtained exploiting these reaction conditions also for less electrophilic aldehydes (**12c-d**, **12g-i**; Table 4). Concerning the diastereocontrol, the increased methanol volume produced a drop in the aldol *syn:anti* ratio, which however in most cases was slight. For benzaldehyde **12d** and 2-naphthyl aldehyde **12h** the diastereoselection resulted even improved. The most relevant diastereoselectivity deterioration was observed for the extremely reactive *para*-nitro benzaldehyde **12a**. We overcame this problem by adding the methanol in two separated portions and obtaining a complete restore of the diastereocontrol while maintaining a high reaction rate. In conclusion, the diastereoselectivity level reached with this protocol (40 μL MeOH/10 μL H₂O) remained excellent if compared with the published data obtained employing the simple proline as organocatalyst. At the same time, the reaction rates resulted significantly enhanced. Therefore, these reaction conditions demonstrated to represent the best balance between reactivity and stereoselectivity, and they were applied to some other aldehydes (**12j-m**, Table 4) with good results.

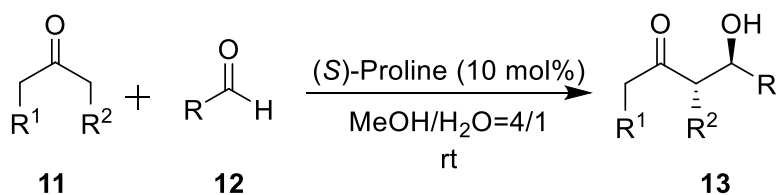
The next step of our investigation concerned the ketone partner (**11**) of the asymmetric aldol condensation.

First of all, we aimed to increase the sustainability of the process and, therefore, we planned to use unmodified proline in the presence of a lower excess of ketone, exploiting the accelerating effect of methanol additive (**Table 5**). Some aldehydes showing high or medium reactivity were selected for this study in which the ketone amount was decreased up to 2 equivalents. With almost all the tested substrates, high conversions and excellent *ee* values were obtained, although longer reaction times were required. However, the most considerable impact of the ketone decrement was observed on the diastereocontrol, which significantly decreased. One speculation could be that dilution helps to have isolated micellar-type transition states, while increased concentration disfavours it. Therefore, considering the excellent performance achieved employing the MeOH/H₂O/(*S*)-proline protocol in the presence of 5 equivalents of **1a**, we decided to maintain these as optimal reaction conditions.

R (2)	1a (eq.)	Time (h)	Conv. (%) ^b	<i>ee</i> 3 (%) ^c	<i>dr</i> 3 (<i>syn:anti</i>) ^b
4-NO ₂ Ph 2a	5	4	82	98	1:11.6
	5	19	>99	98	1:11.6
	2	19	99	95	1:11.3
	1.05	19	92	97	1:9.4
4-CNPh 2b	5	4	77	95	1:16
	2	24	98	87	1:9
C ₆ F ₅ 2e	5	4	67	>99	>1:99
	2	24	>99	92	>1:99
2-NO ₂ Ph 2f	5	4	59	>99	1:32.3
	2	24	92	93	1:15.7
4-BrPh 2g	5	19	88	96	1:16
	2	24	97	91	1:9
4-CF ₃ Ph 2k	5	4	78	96	1:31
	3	20	96	96	1:19
	2	24	93	94	1:13.3

Table 5: Effects of the cyclohexanone (**11a**) amount in the MeOH/H₂O/(*S*)-proline-based protocol. ^a Reaction conditions: **12** (0.3 mmol), (*S*)-proline (10 mol%), MeOH/H₂O (40 mL/10 mL), rt. ^b Determined by ¹H NMR on the crude mixture. ^c Determined by CSP-HPLC on the crude mixture.

Afterwards, we focused on the application of the developed catalytic system to different donor ketones (**Table 6**). For each ketone we tested three differently reactive aldehydes (**12a**, **12g** and **12d**).



R ¹ /R ² (11)	R (12)	Time (h)	Prod. (13)	Conv. (%) ^b	ee 13 (%) ^c	dr 13 (<i>syn:anti</i>) ^b
-(CH ₂) ₂ - 11b	4-NO ₂ Ph 12a	4	13ba	>95	94	1:1.6
-(CH ₂) ₂ - 11b	4-BrPh 12g	19	13bg	64	93	1:3
-(CH ₂) ₂ - 11b	Ph 12d	30	13bd	70	93	1:2.7
H/H 11c	4-NO ₂ Ph 12a	4	13ca	>99	11	/
H/H 11c^d	4-NO ₂ Ph 12a	4	13ca	>99	11	/
H/H 11c^e	4-NO ₂ Ph 12a	3	13ca	5	96	/
H/H 11c^f	4-NO ₂ Ph 12a	4	13ca	>99	23	/
H/H 11c^{d,f}	4-NO ₂ Ph 12a	4	13ca	>99	53	/
H/H 11c	4-BrPh 12g	19	13cg	43	60	/
H/H 11c	Ph 12d	30	13cd	58	51	/
-CH ₂ OCH ₂ - 11d	4-NO ₂ Ph 12a	24	13da	>99	69	1:3.8
-CH ₂ OCH ₂ - 11d	4-BrPh 12g	24	13dg	90	83	1:4
-CH ₂ OCH ₂ - 11d	Ph 12d	48	13dd	82	84	1:3.35

Table 6: Ketones (**11**) scope of the MeOH/H₂O/(*S*)-proline-based protocol. ^a Reaction conditions: **12** (0.3 mmol), **11** (5 eq.), (*S*)-proline (10 mol%), MeOH/H₂O (40 μL/10 μL), rt. ^b Determined by ¹H NMR on the crude mixture. ^c Determined by CSP-HPLC on the crude mixture. ^d %, MeOH/H₂O (20 μL/10 μL). ^e reaction at 0°C. ^f 11 eq. of **11**.

Under our conditions, cyclopentanone **11b** showed high reaction rates, similar to those observed for cyclohexanone **11a** in the presence of the same acceptors. The corresponding products **13ba**, **13bg** and **13bd** (Table 6) were obtained with excellent *ees*, whereas the diastereoselectivities were significantly lower than those recorded employing cyclohexanone **11a**. This behaviour might be due to the greater tendency

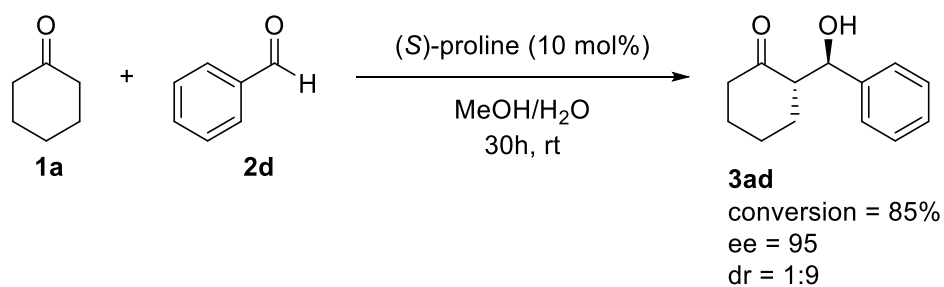
of cyclopentanone **11b**, compared to cyclohexanone **11a**, to assume a sp^2 hybridization and a 120° angle in the formation of intermediate enamine. This hypothesis is supported also by the literature data concerning the use of cyclopentanone **11b** in the presence of unmodified proline as organocatalyst coupled with an additive.²⁹ In fact, the aldol adduct **13ba** was usually isolated with low or moderate diastereomeric ratio and, in many cases, the favourite isomer was the *syn* one. In summary, the most remarkable benefits of our protocol applied to cyclopentanone **11b** were the high reaction rates and the excellent *ees* of the major *anti* isomer. These results were not trivial because obtained by using the simple unmodified proline. Switching from cyclopentanone to simpler acetone the reaction shows incredible reactivity, especially with the reactive aldehyde **12a**, with full conversion after 4 hours, but resulted in an extremely poor enantioselectivity, with only 11% ee. This could possibly be due to an excess of reactivity in the MeOH/H₂O system. Several conditions have been experimented in order to reduce the reactivity, in particular the reaction at 0°C resulted in a significant drop in reactivity with only 5% of **13ca** observed after 3 hours, but with 96% excess.

Then we diluted the reaction mixture using 11 equivalents of acetone, slightly improving the selectivity, but the maximum was reached using MeOH/H₂O in 2:1 ratio with 11 eq. of ketone, but consisted in only 53% ee. Furthermore, the use of less reactive aldehydes **12g-12d** results were not excellent with a maximum 60% ee. Considering these results, we observed that acetone is not the ideal partner for this aldol reaction protocol. Finally, to expand the scope of the ketones used, we switched to protected dihydroxyacetone **11d**, that gave good results both with reactive aldehyde **12a**, with quantitative conversion, but only 69% ee after 24 hours, while with less reactive aldehydes **12g-12d**, with a decrease in conversion, the ee was improved up to 84%. Ketone **11d** is interesting because is a useful building block for the synthesis of modified carbohydrates.³⁰ One possible explanation in this difference in enantiomeric excess can be due to the presence of supplementary oxygen atoms, that can in some way interfere in the transition state.

Finally, since this newly developed protocol is thought for possible industrial applications, we decided to perform one of the studied reactions on a medium scale, working on 10 millimol of limiting reagent, to check if any variations are visible changing the amount of material used. We decided to use as a model the reaction between cyclohexanone **11a** and simple benzaldehyde **12d**, not one of the most reactive ones.

²⁹ Z. Wang, J. Yan, X. Zhang, L. Wang, *Synthesis*, 2009, **22**, 3744

³⁰ D. Enders, C. Grondal, *Angew. Chem. Int. Ed.* **2005**, *44*, 1210–1212



Scheme 13: application of the Proline/MeOH/H₂O protocol on medium scale

The results are very good and comparable to the trials performed on 0,3 mmol scale, and in this case the product has been purified via flash chromatography leading to the aldol **13ad** in a good 78% yield.

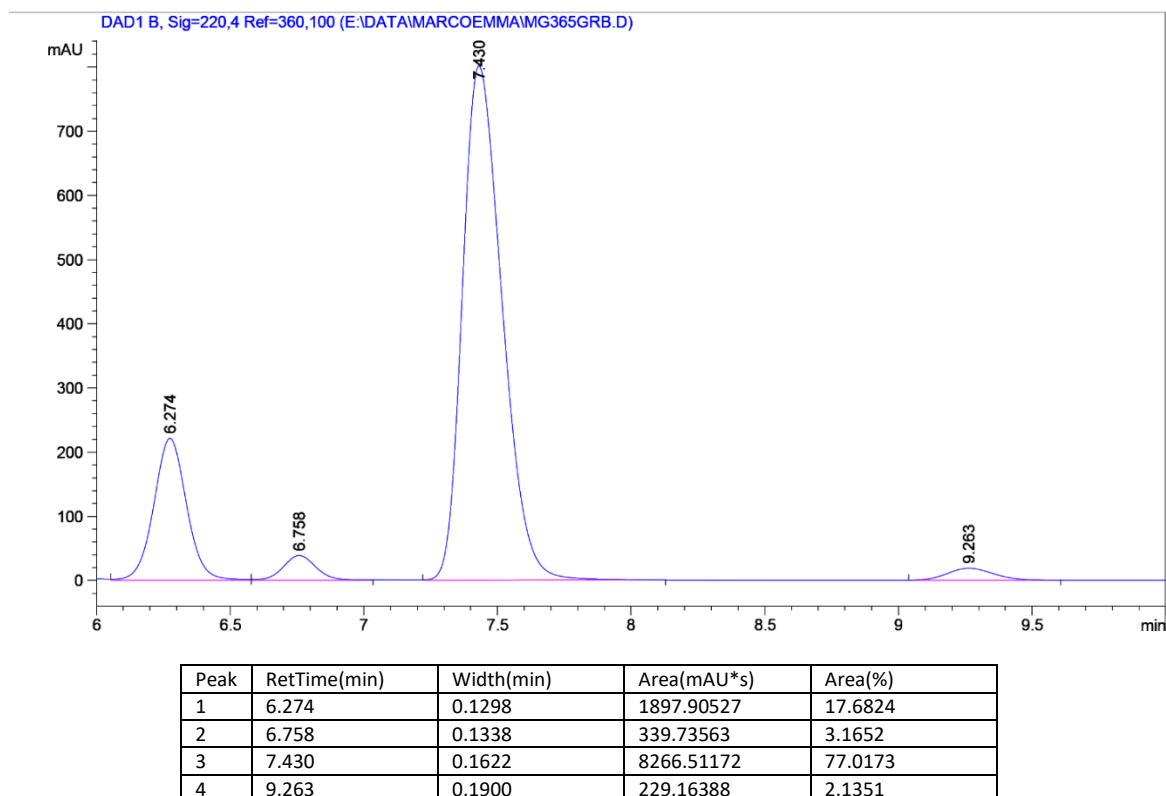


Figure 6: Chiral HPLC chromatograph and area(%) of the adduct **3ad** produced on 10 mmol scale

This trial is a starting point that gives us promising signal for the use of this reaction protocol on a medium large scale or even at production levels.

2.5 Conclusion

In this chapter a new efficient protocol for Proline catalysed aldol reaction has been studied and developed. The procedure involves the use of MeOH and water as stoichiometric additives that increase the solubility of the catalyst and the reactivity of the reaction, allowing to shorten the reaction time without losing selectivity. The implemented additives are absolutely advantageous for the use of the reaction at a production level, and are perfectly accepted as green reagents. The scope of the reaction has been expanded successfully on aromatic aldehyde and some aliphatic, and on a moderate number of ketones, with results comparable and in many cases superior to other reported protocols that involve simple proline. The reaction has been finally scaled up to 0.3 mmol to 10 mmol scale with absolutely comparable results.

2.6 General Procedures and Products Characterization

General Information. ^1H and ^{13}C NMR spectra were recorded on Varian Gemini 200 or Inova 400 NMR instruments with a 5 mm probe. Chemical shifts (δ) are reported in ppm, relative to the residual peaks of deuterated solvent signals. HPLC-MS analyses were performed on an Agilent Technologies HP1100 instrument coupled with an Agilent Technologies MSD1100 single-quadrupole mass spectrometer. A Phenomenex Gemini C18, 3 μm (100 x 3mm) column was employed for the chromatographic separation: mobile phase $\text{H}_2\text{O}/\text{CH}_3\text{CN}$, gradient from 30% to 80% of CH_3CN in 8 min, 80% of CH_3CN until 22 min, then up to 90% of CH_3CN in 2 min, flow rate 0.4 mL min^{-1} . CSP-HPLC analyses were performed on an Agilent Technologies Series 1200 instrument using Daicel[®] chiral columns and n-hexane/2-propanol (n-Hex/IPA) mixtures. Flash chromatography purifications were carried out using Merck silica gel 60 (230-400 mesh particle size). Thin layer chromatography was performed on Merck 60 F254 plates. Commercial reagents were used as received without additional purification. Ketone **2d** was prepared according to literature.³¹ All synthesized compounds were already known in literature and were not characterized.

General Procedure for the aldol condensation between aromatic aldehydes and Ketones.

The aldol reaction was conducted in a 2 mL vial. In a typical reaction, the vial was charged with S-Proline (0.03 mmol), methanol (40 μL), water (10 μL), the corresponding aldehyde (0.3 mmol) and the Ketone (1.5 mmol) successively at room temperature. The flask was capped with a stopper and sealed. Then, the reaction mixture was stirred at room temperature for the desired time. After the reaction was completed, the mixture was filtered on a pad of silica with EtOAc and concentrated under vacuum. The conversion the

³¹ M. Majewski, D. M. Gleave, P. Nowak, *Canadian Journal of Chemistry*, **1995**, 73, 1616-1626,

aldehyde and the diastereoisomeric ratio were determined by ¹H-NMR in CDCl₃. The enantiomeric excess was determined by chiral HPLC of the crude product.

Chiral-HPLC Condition: All separation conditions were optimized performing the reaction catalysed by (*RS*)-Proline, to ensure the best separation of the enantiomers.

13ab: CSP-HPLC: AD 90/10 n-Hex/IPA, flow rate 1 mL/min at 40 °C; λ 220 nm; tR = 13.9 min (syn minor), 16.9 min (syn major), 19.4 min (anti minor), 24.6 min (anti major).

13ac: CSP-HPLC: AD 90/10 n-Hex/IPA, flow rate 1 mL/min at 40 °C; λ 220 nm; tR = 7.6 min (syn minor), 8.9 min (syn major), 11.1 min (anti minor), 13.1 min (anti major).

13ad: CSP-HPLC: OD-H 90/10 n-Hex/IPA, flow rate 1 mL/min at 40 °C; λ 220 nm; tR = 6.3 min (syn major), 6.8 min (syn minor), 7.5 min (anti major), 9.5 min (anti minor).

13ae: CSP-HPLC: OJ 99/01 n-Hex/IPA, flow rate 1 mL/min at 40 °C; λ 254 nm; tR = 8.0 min (anti major).

13af: CSP-HPLC: OJ 95/05 n-Hex/IPA, flow rate 1 mL/min at 40 °C; λ 230 nm; tR = 12.4 (syn minor), 14.3 min (syn major), 17.5 min (anti minor), 21.0 min (anti major).

13ag: CSP-HPLC: AD 90/10 n-Hex/IPA, flow rate 1 mL/min at 40 °C; λ 220 nm; tR = 8.0 min (syn minor), 9.6 min (syn major), 12.2 min (anti minor), 14.7 min (anti major).

13ah: CSP-HPLC: OD 90/10 n-Hex/IPA, flow rate 0.7 mL/min at 40 °C; λ 220 nm; tR = 11.6 min (syn major), 12.5 min (syn minor), 13.8 min (anti major), 16.3 min (anti minor).

13ai: CSP-HPLC: OD-H 95/05 n-Hex/IPA, flow rate 0.8 mL/min at 40 °C; λ 230 nm; tR = 14.1 min (syn minor), 14.7 min (syn major), 17.8 min (anti minor), 22.8 min (anti major).

13aj: CSP-HPLC: OJ 99/01 n-Hex/IPA, flow rate 0.2 mL/min at 40 °C; λ 280 nm; tR = 25.3 min (anti major), 27.6 min (anti minor).

13ak: CSP-HPLC: AD 95/05 n-Hex/IPA, flow rate 1 mL/min at 40 °C; λ 230 nm; tR = 9.1 min (syn minor), 11.3 min (syn major), 14.6 min (anti minor), 20.5 min (anti major).

13al: CSP-HPLC: AD 85/15 n-Hex/IPA, flow rate 0.5 mL/min at 40 °C; λ 210 nm; tR = 15.4 min (syn minor), 16.9 min (syn major), 19.2 min (anti minor), 20.6 min (anti major).

13am: CSP-HPLC: OD-H 95/05 n-Hex/IPA, flow rate 0.7 mL/min at 40 °C; λ 210 nm; tR = 10.6 min (syn major), 11.1 min (syn minor), 13.3 min (anti major), 16.1 min (anti minor).

13ba: CSP-HPLC: AD 90/10 n-Hex/IPA, flow rate 1 mL/min at 40 °C until 17 minutes, after 0.3 mL/min; λ 254 nm; tR = 12.0 min (syn major), 15.3 min (syn minor), 20.8 min (anti minor), 23.6 min (anti major).

13bg: CSP-HPLC: AD 90/10 n-Hex/IPA, flow rate 0.4 mL/min at 40 °C; λ 230 nm; tR = 18.9 min (syn minor), 22.3 min (syn major), 27.4 min (anti major), 28.8 min (anti minor).

13bd: CSP-HPLC: OD-H 90/10 n-Hex/IPA, flow rate 1 mL/min at 40 °C; λ 220 nm; tR = 6.8 min (syn major), 8.1 min (syn minor), 8.9 min (anti major), 10.0 min (anti minor).

13ca: CSP-HPLC: OJ 90/10 n-Hex/IPA, flow rate 1 mL/min at 40 °C for 20 min, after 0.7 mL/min; λ 254 nm; tR = 27.2 min (minor), 31.3 min (major).

13cg: CSP-HPLC: AD 95/05 n-Hex/IPA, flow rate 0.4 mL/min at 40 °C; λ 220 nm; tR = 35.2 min (major), 37.7 min (minor).

13cd: CSP-HPLC: OD-H 90/10 n-Hex/IPA, flow rate 1 mL/min at 40 °C; λ 220 nm; tR = 8.5 min (minor), 8.8 min (major).

14da: CSP-HPLC: OD-H 85/15 n-Hex/IPA, flow rate 0.5 mL/min at 40 °C; λ 254 nm; tR = 14.3 min (anti major), 15.5 min (anti minor), 19.3 min (syn minor), 19.7 min (syn major).

14dg: CSP-HPLC: OD-H 85/15 n-Hex/IPA, flow rate 0.5 mL/min at 40 °C; λ 210 nm; tR = 10.6 min (anti major), 11.2 min (anti minor), 12.7 min (syn minor), 13.1 min (syn major).

14dd: CSP-HPLC: OD-H 85/15 n-Hex/IPA, flow rate 0.4 mL/min at 40 °C; λ 210 nm; tR = 12.5 min (anti major), 13.4 min (anti minor), 14.6 min (syn), 15.8 min (syn).

General Procedure for the aldol condensation between Benzaldehyde and Cyclohexanone on 10mmol scale. The aldol reaction was conducted in a 25 mL flask. In a typical reaction, the flask was charged with of S-proline (115 mg, 1 mmol), methanol (1,33 mL), water (330 μ L), the corresponding aldehyde (0.3 mmol) and cyclohexanone (5,18 mL, 50 mmol) and the mixture was stirred for 10 min at room temperature. After the mixture was cooled at 0°C and benzaldehyde (1,06 mL, 10 mmol) was slowly added. The flask was capped with a stopper and sealed. Then, the reaction mixture was stirred at room temperature for 30 h. After the reaction was completed, the mixture was filtered on a pad of silica with ethyl acetate and concentrated under vacuum. The conversion of the aldehyde and the diastereoisomeric ratio were determined by $^1\text{H-NMR}$ in CDCl_3 . Then, the residue was obtained by purification by column chromatography (ethyl acetate–cyclohexane 2-8 as the eluent) to afford the product with 78% yield. The product was further characterized by $^1\text{H-NMR}$, $^{13}\text{C-NMR}$ and HPLC-MS analysis. The enantiomeric excess was determined by chiral HPLC of the purified product. Compound already known in literature.

Chapter 3: Study of the α -Fluorination of Chiral γ -Nitroaldehydes

This chapter of the thesis is strongly based on a paper published by my research group in 2016, and treats about the study of an organocatalysed methodology for the α -fluorination of α -disubstituted chiral γ -Nitroaldehydes for the construction of fully substituted fluorinated stereocenters, a serious challenge in the field of α -functionalization of aldehyde, that can possibly open up interesting ways for the synthesis of biologically active compounds.

3.1 Organocatalysis in the synthesis of biologically active compounds

Despite their great development, the application of organocatalytic methodologies to the synthesis of active compounds in medicinal chemistry in the past years has rarely been reported. However, in most recent years organocatalytic methodologies for the synthesis of enantioenriched molecules for medicinal chemistry purposes have been gaining momentum being particularly attractive for the preparation of compounds that do not tolerate metal contamination. In academia, several groups have made a remarkable effort to show the great applicability of organocatalysts to the total synthesis of bioactive natural products³² and of drugs³³ most of them currently available in the market. These efforts mainly focused on the removal of barriers for scale-up by addressing issues such as catalyst loading, product inhibition, substrate scope, and bulk availability of designer catalysts which have drawn the attention of the companies³⁴ that have begun to incorporate organocatalysis as a synthetic tool in some industrial scale processes.¹

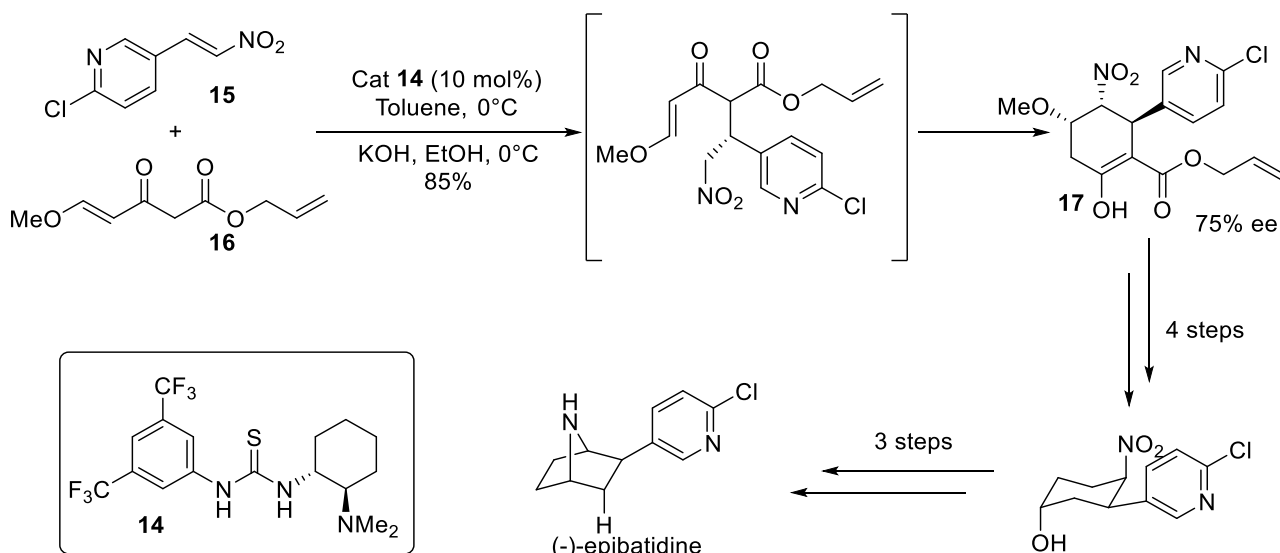
In the past 10 years, the number of chiral, non-racemic pharmaceuticals available in the market has consistently increased. It is becoming more and more important to prepare these compounds using new enantioselective technologies to minimize the losses provoked from making racemic mixtures. Due to the operational and economic advantages of asymmetric organocatalysis, this methodology has a significant impact on chemical synthesis. I will report a couple of well-known examples of organocatalysis at the service of drug synthesis. The first is the synthesis of the alkaloid (-)-epibatidine, an analgesic studied as a morphine replacer, developed by the Takemoto's group, and based on an enantioselective double Michael addition with hydrogen bond-based organocatalysis³⁵ The bifunctional thiourea-based organocatalyst **14** catalysed the first Michael addition of the γ,δ -unsaturated β -ketoester **16** to the nitroalkene **15**, and after there is a base-promoted cyclization of the intermediate to form the polysubstituted cyclohexene **17** with good yield and enantioselectivity (**Scheme 14**). The total synthesis of (-)-epibatidine was achieved in further seven steps.

³² R. M. de Figueiredo, M. Christman, *European Journal of Organic Chemistry*, **2007**, 16, 2575–2600.

³³ J. Alemán, S. Cabrera, *Chemical Society Reviews*, **2013**, 42, 2, 774–793.

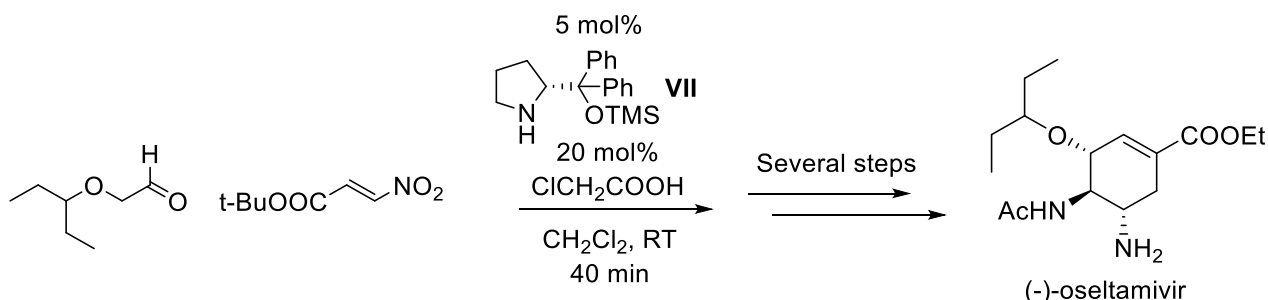
³⁴ a) H. U. Blaser, E. Schmidt, *Wiley-VCH, Weinheim, Germany*, **2004**. b) H. Groger, *Organocatalysis*, **2008**, 227–258.

³⁵ Y. Hoashi, T. Yabuta, Y. Takemoto, *Tetrahedron Letters*, **2004**, 45, 50, 9185–9188.



Scheme 14: Organocatalyzed cascade synthesis of (-)-epibatidine

Epibatidine is not a usually prescribed therapeutic because of its toxicity, but is an example of complex natural alkaloid that can be synthesized in an elegant and straightforward way using organocatalysis. As another example, Hayashi and co-workers successfully reported an efficient, enantioselective total synthesis of (-)-oseltamivir³⁶, in which the key step is a Nitro-Michael addition catalysed by the diarylprolinol **VII**, demonstrating the power of asymmetric reactions catalysed by organocatalysts.



Scheme 15: Key-step for the organocatalysed synthesis of (-)-oseltamivir

This organocatalytic step is the core of a straightforward synthesis of composed by three one-pot procedures that leads to the final compound with 57% overall yield, and is a representative example of organocatalysis at the service of drug synthesis.

However, like exposed previously, the application of organocatalysis to the synthesis of molecules of interest in various fields, including medicinal chemistry, is still facing problems such as high catalyst loading, long reaction time, difficulties in recyclability etc.

³⁶ H. Ishikawa, T. Suzuki, Y. Hayashi, *Angew. Chem. Int. Ed.* **2009**, *48*, 1304–1307

3.2 Fluorine in medicinal chemistry

The use of fluorine-containing compounds in last 30 years has grown in many different fields, from pharmaceutical to material science, as well as the study of their peculiar property.³⁷ In particular, it is well known that the introduction of one or more fluorine atoms into a biologically active molecule often incredibly enhances its activity.

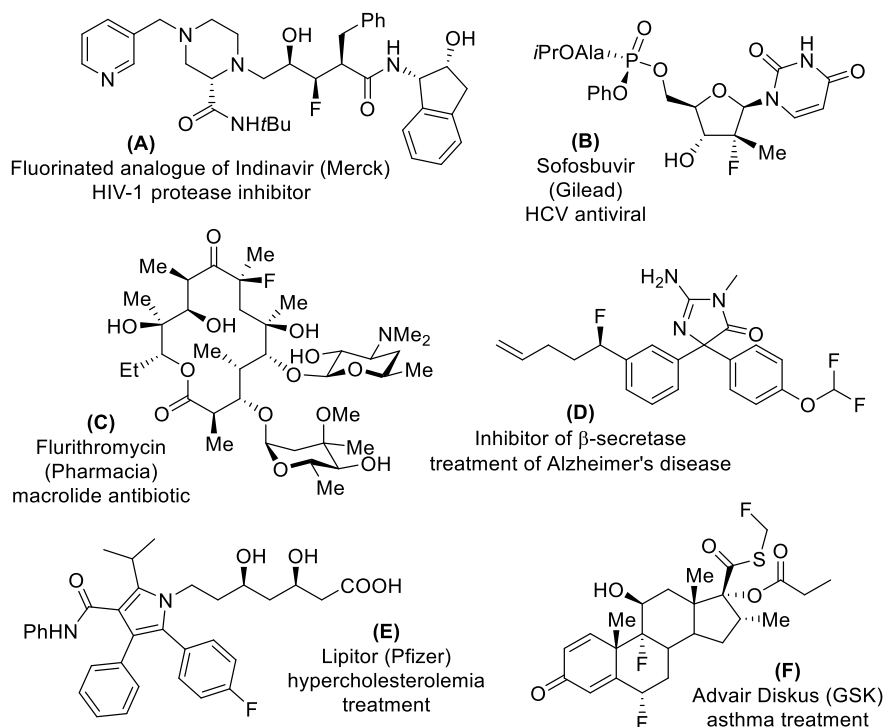


Figure 7: Examples of fluorinated drugs, characterized by very diverse structures and bioactivities.

³⁷ For reviews on various applications of fluorinated compounds, see: a) N. V. S. D. K. Bhupathiraju, W. Rizvi, J. D. Batteas, C. M. Drain, *Org. Biomol. Chem.* **2016**, *14*, 389–408; b) C. D. Murphy, *Appl. Microbiol. Biotechnol.* **2016**, *100*, 2617–2627; c) A. R. Jennings, S. T. Iacono, *Polym. Int.* **2016**, *65*, 6–10; d) T. Okazoe, *J. Fluorine Chem.* **2015**, *174*, 120–131; e) T. Sugiishi, M. Matsugi, H. Hamamoto, H. Amii, *RSC Adv.* **2015**, *5*, 17269–17282; f) P. Pengo, L. Pasquato, *J. Fluorine Chem.* **2015**, *177*, 2–10; g) C. Ni, M. Hu, J. Hu, *Chem. Rev.* **2015**, *115*, 765–825; h) D. Cosco, E. Fattal, M. Fresta, N. Tsapis, *J. Fluorine Chem.* **2015**, *171*, 18–26; i) M. Kiel, K.-H. Engesser, *Appl. Microbiol. Biotechnol.* **2015**, *99*, 7433–7464; j) M. Reindl, A. Hoffmann-Roder, *Curr. Top. Med. Chem.* **2014**, *14*, 840–854; k) C. Samojłowicz, A. Kajetanowicz, K. Grela, *Olefin Metathesis in Fluorous Phases and in Fluorinated Aromatic Solvents*, in: *Olefin Metathesis: Theory and Practice* (Ed.: K. Grela), Wiley-VCH, Weinheim, Germany, **2014**, chapter 23, p. 537–545; l) W.-B. Yi, J.-J. Ma, L.-Q. Jiang, C. Cai, W. Zhang, *J. Fluorine Chem.* **2014**, *157*, 84–105; m) D. Cahard, V. Bizet, *Chem. Soc. Rev.* **2014**, *43*, 135–147; n) F. Menaa, B. Menaa, O. N. Sharts, *J. Mol. Pharm. Org. Process Res.* **2013**, *1*, 104, DOI: 10.4172/2329-9029.1000104; o) T. Stahl, H. F. T. Klare, M. Oestreich, *ACS Catal.* **2013**, *3*, 1578–1587; p) X.-G. Hu, L. Hunter, *Beilstein J. Org. Chem.* **2013**, *9*, 2696–2708; q) F. Giornal, S. Pazenok, L. Rodefeld, N. Lui, J.-P. Vors, F. R. Leroux, *J. Fluorine Chem.* **2013**, *152*, 2–11; r) X.-J. Zhang, T.-B. Lai, R. Y.-C. Kong, *Top. Curr. Chem.* **2012**, *308*, 365–404; s) A. Belardini, *Appl. Sci.* **2012**, *2*, 682–708; t) M. Crespo, *Organometallics* **2012**, *31*, 1216–1234; u) V. Curtui, G. Brambilla, A. di Domenico, S. van Leeuwen, *EFSA J.* **2012**, *10*, 2743, p. 55; v) J. Ruiz-Cabello, B. P. Barnett, P. A. Bottomley, J. W. M. Bulte, *NMR Igaku* **2011**, *24*, 114–129; w) R. Berger, G. Resnati, P. Metrangolo, E. Weber, J. Hulliger, *Chem. Soc. Rev.* **2011**, *40*, 3496–3508; x) D. Zhi, S. Zhang, B. Wang, Y. Zhao, B. Yang, S. Yu, *Bioconjugate Chem.* **2010**, *21*, 563–577.

This is basically due to the fact that the presence of fluorine can confer several desirable characteristics to an active compound.³⁸ First of all, it can increase lipophilicity, allowing a better absorption into and across biological membranes; the electronegativity of fluorine and its low polarizability can radically change the electronic features of a biologically active molecule, changing its conformation, the pKa of neighbouring functional groups, and the hydrogen-bond network; moreover, fluorine's van der Waals radius (1.4 Å) makes it an isostere of hydrogen (van der Waals radius 1.1 Å), giving the fluorine-hydrogen substituted compound several changes in the electronic property but, at the same time, only minimal structural changes relative to a carbon–hydrogen bond. Therefore, the incorporation of fluorine atoms is used to modulate both the pharmacokinetic and pharmacodynamic properties of a drug. It has been estimated that 30 % of the leading 30 blockbuster drugs by sales contain at least one fluorine atom. In this context, fluorinated pharmaceuticals show notable and very diverse biological activities.³⁹ They include HIV-protease inhibitors⁴⁰,

³⁸ For reviews on fluorine-containing biologically active compounds, see: a) Y. Zhou, J. Wang, Z. Gu, S. Wang, W. Zhu, J. L. Acena, V. A. Soloshonok, K. Izawa, H. Liu, *Chem. Rev.* **2016**, *116*, 422–518; b) E. P. Gillis, K. J. Eastman, M. D. Hill, D. J. Donnelly, N. A. Meanwell, *J. Med. Chem.* **2015**, *58*, 8315–8359; c) B. Gomes, J. A. Loureiro, M. A. N. Coelho, M. d. Carmo Pereira, *Curr. Pharm. Des.* **2015**, *21*, 5725–5735; d) K. Kaur, V. Kumar, G. Kumar Gupta, *J. Fluorine Chem.* **2015**, *178*, 306–326; e) D. Barnes-Seeman, J. Beck, C. Springer, *Curr. Top. Med. Chem.* **2014**, *14*, 855–864; f) P. A. Gale, R. Perez-Tomas, R. Quesada, *Acc. Chem. Res.* **2013**, *46*, 2801–2813; g) M. Tredwell, V. Gouverneur, *Fluorine in Medicinal Chemistry: Importance of Chirality in Comprehensive Chirality* (Eds.: E. M. Carreira, H. Yamamoto), Elsevier, **2012**, vol. 1, chapter 5, p. 70–85; h) D. O'Hagan, *J. Fluorine Chem.* **2010**, *131*, 1071–1081; i) S. Purser, P. R. Moore, S. Swallow, V. Gouverneur, *Chem. Soc. Rev.* **2008**, *37*, 320–330; j) K. L. Kirk, *Curr. Top. Med. Chem.* **2006**, *6*, 1447–1456; k) F. M. D. Ismail, *J. Fluorine Chem.* **2002**, *118*, 27–33; l) B. E. Smart, *J. Fluorine Chem.* **2001**, *109*, 3–11.

³⁹ a) E. A. Hallinan, S. W. Kramer, S. C. Houdek, W. M. Moore, G. M. Jerome, D. P. Spangler, A. M. Stevens, H. S. Shieh, P. T. Manning, B. S. Pitzele, *Org. Biomol. Chem.* **2003**, *1*, 3527–3534; b) A. A. Sauve, Y. Cen, WO2011003018, **2011**; c) P. Wai Chia, S. C. Brennan, A. M. Z. Slawin, D. Riccardi, D. O'Hagan, *Org. Biomol. Chem.* **2012**, *10*, 7922–7927; d) U. Bothe, B. Menzenbach, P. Droescher, H.-U. Schweikert, W. Elger, A. Hillisch, G. Reddersen, B. Schneider, WO2005100376, **2005**; e) W. R. Antonios-McCrea, P. A. Barsanti, C. Hu, X. Jin, E. J. Martin, Y. Pan, K. B. Pfister, M. Sendzik, J. Sutton, L. Wan, WO2012066065, **2012**.

⁴⁰ a) A. Abouabdellah, L. Boros, F. Gyenes, J. T. Welch, *J. Fluorine Chem.* **1995**, *72*, 255–259; b) E. Kim, G. Huan Shen, J. Hee Hong, *Nucleosides Nucleotides Nucleic Acids* **2011**, *30*, 798–813; c) M. J. Boyd, C. Molinaro, A. Roy, V. L. Truong, WO2012055031, **2012**; d) R. D. Tung, F. G. Salituro, D. D. Deininger, M. A. Murcko, P. M. Novak, G. R. Bhisetti, WO95/24385, **1995**.

anticancer⁴¹ and antiviral⁴² drugs (B), antibacterials⁴³ (C), and drugs for the treatment of neurodegenerative disorders (D).⁴⁴

3.3 The Organocatalytic α -fluorination of aldehydes

In last years the scientific community started to develop new efficient fluorination protocols, using both nucleophilic and electrophilic fluorine donors, pushed by the beneficial effects related to the presence of fluorine atoms into drugs and materials. Several different synthetic approaches⁴⁵ to fluorinated products have been proposed, including, more recently, organocatalytic processes.⁴⁶

⁴¹ For reviews on fluorinated anticancer drugs, see: a) W. Tongkao-on, C. Gordon-Thomson, K. M. Dixon, E. J. Song, T. Luu, S. E. Carter, V. B. Sequeira, V. E. Reeve, R. S. Mason, *Dermato-Endocrinology* **2013**, *5*, 20-33; b) T. Goslinski, J. Piskorz, *J. Photochem. Photobiol. C* **2011**, *12*, 304-321; c) T. Fujishima, S. Fujii, T. Harayama, *Curr. Org. Chem.* **2010**, *14*, 962-976; d) C. Isanbor, D. O'Hagan, *J. Fluorine Chem.* **2006**, *127*, 303-319; e) G. Giannini, *Med. Chem. Rev. -Online* **2004**, *1*, 47-71; f) I. Ojima, *ChemBioChem* **2004**, *5*, 628-635. For selected patents on fluorinated anticancer drugs, see: g) T. J. Guzi, D. A. Parry, M. A. Labroli, M. P. Dwyer, K. Paruch, K. E. Rosner, R. Shen, J. Popovici-Muller, WO2009061781, **2009**; h) D. D. Wirth, US5559222, **1996**; i) X. Han, Y. Lou, C. Michoud, S. G. Mischke, S. Remiszewski, K. C. Rupert, WO2014009495, **2014**.

⁴² a) Q. Huang, S. Zhou, WO2013013009, **2013**; b) M. Sznajdman, US7291726B2, **2007**.

⁴³ a) N. Boechat, M. M. Bastos, *Curr. Top. Med. Chem.* **2013**, *13*, 2885-2904; b) P. Ball, *J. Antimicrob. Chemother.* **2003**, *51*, 21-27, Supplement S1.

⁴⁴ a) A. Nakazato, in: *Fluorine in Medicinal Chemistry and Chemical Biology* (Ed.: I. Ojima), Blackwell Publishing, **2009**, chapter 3, p. 67-97; b) M. S. Malamas, J. J. Erdei, W. F. Fobare, D. A. Quagliato, S. A. Antane, A. J. Robichaud, US2007/0072925A1, **2007**; c) S. J. Green, E. J. Hembre, D. J. Mergott, Y. Shi, B. M. Watson, L. L. Winneroski, Jr., US2014371212, **2014**.

⁴⁵ For different synthetic approaches to fluorinated compounds, see: a) M. Inoue, M. Shiosaki, *Curr. Org. Chem.* **2015**, *19*, 1579-1591; b) Z. U. H. Khan, D. Kong, Y. Chen, N. Muhammad, A. U. Khan, F. U. Khan, K. Tahir, A. Ahmad, L. Wang, P. Wan, *J. Ind. Eng. Chem.* **2015**, *31*, 26-38; c) C. Chatalova-Sazepina, R. Hemelaere, J.-F. Paquin, G. M. Sammis, *Synthesis* **2015**, *47*, 2554-2569; d) A. D. Dilman, V. V. Levin, *Mendeleev Commun.* **2015**, *25*, 239-244; e) B. W. Thuronyi, M. C. Y. Chang, *Acc. Chem. Res.* **2015**, *48*, 584-592; f) J.-A. Ma, S. Li, *Org. Chem. Front.* **2014**, *1*, 712-715; g) X. Mu, G. Liu, *Org. Chem. Front.* **2014**, *1*, 430-433; h) Y. Qiao, L. Zhu, B. R. Ambler, R. A. Altman, *Curr. Top. Med. Chem.* **2014**, *14*, 966-978; i) W. Kong, E. Merino, C. Nevado, *Chimia* **2014**, *68*, 430-435; j) M. C. Walker, M. C. Y. Chang, *Chem. Soc. Rev.* **2014**, *43*, 6527-6536; k) V. Gouverneur, *Nat. Chem.* **2012**, *4*, 152-154; l) V. Hugenberg, G. Haufe, *J. Fluorine Chem.* **2012**, *143*, 238-262; m) C. B. McPake, G. Sandford, *Org. Process Res. Dev.* **2012**, *16*, 844-851; n) G. Liu, *Org. Biomol. Chem.* **2012**, *10*, 6243-6248; o) X.-L. Qiu, F.-L. Qing, *Eur. J. Org. Chem.* **2011**, 3261-3278; p) Y. Zeng, C. Ni, J. Hu, *Chem. Eur. J.* **2016**, *22*, 3210-3223; q) P. A. Champagne, J. Desroches, J.-D. Hamel, M. Vandamme, J.-F. Paquin, *Chem. Rev.* **2015**, *115*, 9073-9174; r) T. A. Unzner, T. Magauer, *Tetrahedron Lett.* **2015**, *56*, 877-883; s) T. Borg, J. Danielsson, M. Mohiti, P. Restorp, P. Somfai, *Adv. Synth. Catal.* **2011**, *353*, 2022-2036; t) R. Clarkson, Z. Komsta, B. A. Mayes, A. Moussa, M. Shelbourne, A. Stewart, A. J. Tyrrell, L. L. Wallis, A. C. Weymouth-Wilson, *J. Org. Chem.* **2015**, *80*, 2198-2215; u) T. Konno, A. Ikemoto, T. Ishihara, *Org. Biomol. Chem.* **2012**, *10*, 8154-8163.

⁴⁶ For reviews on organocatalytic fluorination reactions, see: a) Y. Zhao, Y. Pan, S.-B. Derek Sim, C.-H. Tan, *Org. Biomol. Chem.* **2012**, *10*, 479-485; b) Z. Ye, G. Zhao, *Chimia* **2011**, *65*, 902-908; c) V. Guillem, X. Companyo, R. Rios, *Chem. Eur. J.* **2011**, *17*, 2018-2037; d) M. Ueda, T. Kano, K. Maruoka, *Org. Biomol. Chem.* **2009**, *7*, 2005-2012.

One of the principal fluorination organocatalytic protocols is the stereoselective α -fluorination⁴⁷ of aldehydes via enamine formation, that can open up the route to useful intermediates for the synthesis of pharmaceuticals. The fluorine is introduced using a source of electrophilic fluorine, the most common of those being molecules bearing N-F bond such as Selectfluor, *N*-fluorobenzene sulfonimide (NFSI), or various fluoropyridinium salts (**figure 8**).

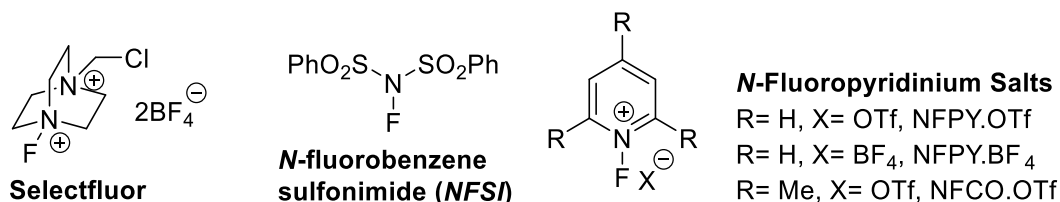
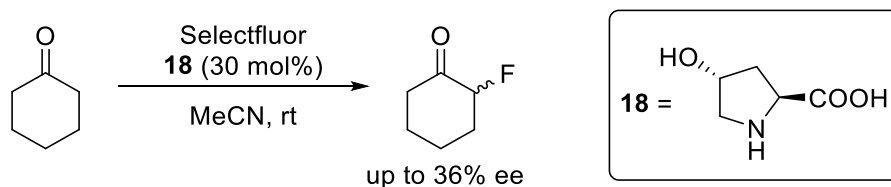


Figure 8: A selection of commonly used electrophilic fluorinating reagents.

In 2005, many enantioselective fluorination of aldehydes catalyzed by chiral secondary amines were reported. Enders and Huttli reported the organocatalytic direct α -fluorination of aldehydes and ketones employing Selectfluor and proline-related secondary amine **98** as catalyst (**Scheme 16**).⁴⁸



Scheme 16: enantioselective fluorination of ketones catalysed by **98**

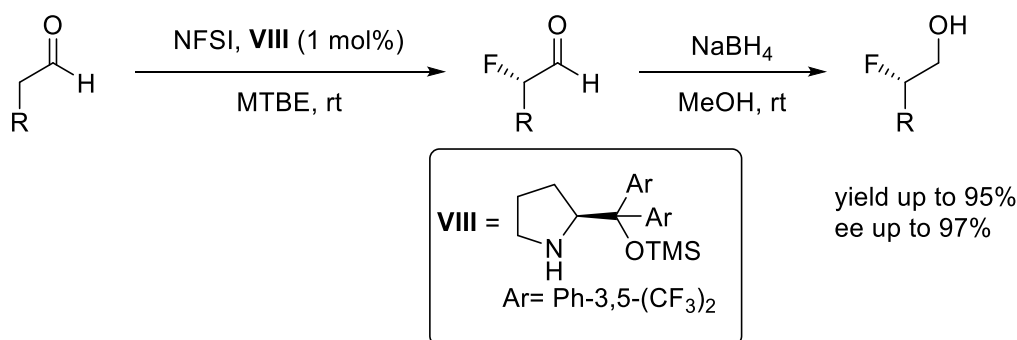
But results were still poor with only low enantioselectivity (36% ee) observed with cyclohexanone (**96**), and no selectivity for the aldehydes.

An enantioselective α -fluorination of aldehydes was proposed by Jørgensen and co-workers, catalysed by the silylated prolinol derivative **VIII**, using NFSI as fluorine source in MTBE, and reducing the α -fluorinated aldehydes to the corresponding alcohol (for stability reasons) with high enantioselectivities (up to 97%).⁴⁹

⁴⁷ X. Yang, T. Wu, R. J. Phipps, F. D. Toste, *Chem. Rev.* **2015**, *115*, 826–870

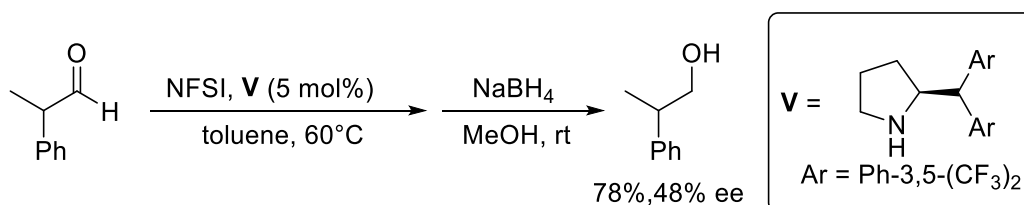
⁴⁸ D. Enders, M. R. M. Huttli, *Synlett* **2005**, *6*, 991.

⁴⁹ M. Marigo, D. Fielenbach, A. Braunton, A. Kjærsgaard, K.A. Jørgensen, *Angew. Chem., Int. Ed.* **2005**, *44*, 3703.



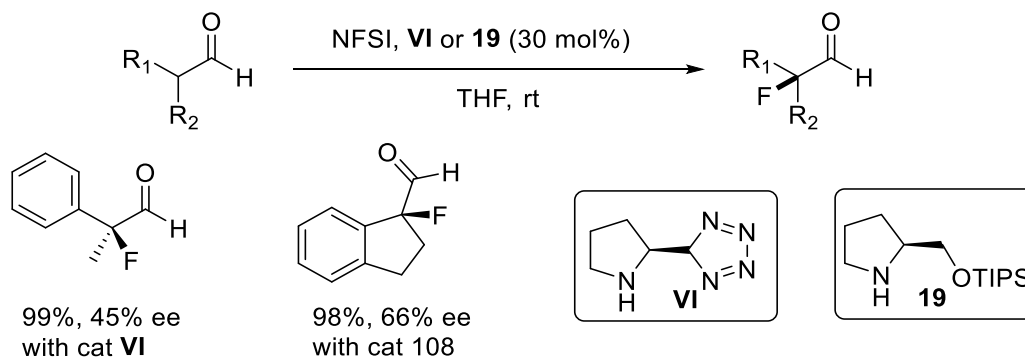
Scheme 17: Jorgensen Fluorination of aldehydes

They also tried to expand the scope on the formation of quaternary stereocenters (**Scheme 18**), using a less bulky catalyst **V** and a higher temperature, but they observed the product formation with a poor 48% ee.



Scheme 18: Jorgensen approach for the formation of fluorinated quaternary stereocenters

In a similar way, Barbas and co-workers focused on the enantioselective fluorination of α -branched aldehydes using other chiral secondary amine catalysts (**Scheme 19**).⁵⁰ The best results were obtained using catalysts **VI** and **19**, but the enantiomeric excess is only slightly improved (45% ee for **VI**; 66% ee for **19**).



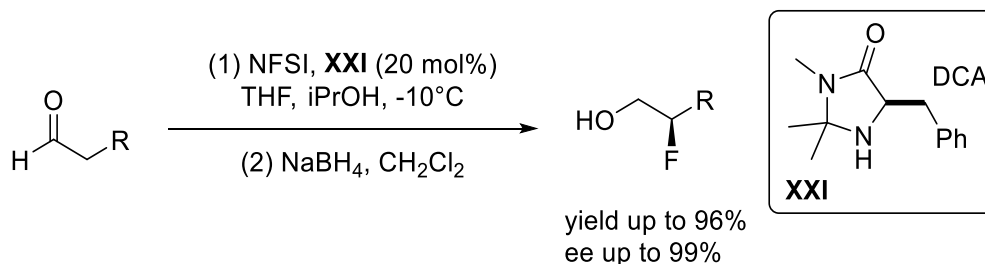
Scheme 19: Barbas fluorination of branched aldehydes

Also MacMillan and co-workers were interested in fluorination, and they reported the use of imidazolidinone dichloroacetate **XXI** for the fluorination of linear aldehydes, using NFSI in THF.⁵¹ (**Scheme 20**) In this case excellent enantioselectivity was observed (up to 99% ee), especially when isopropanol is added to the reaction mixture as a co-solvent. The reaction

⁵⁰ D. D. Steiner, N. Mase, C. F. Barbas III. *Angew. Chem, Int. Ed.* **2005**, *44*, 3706

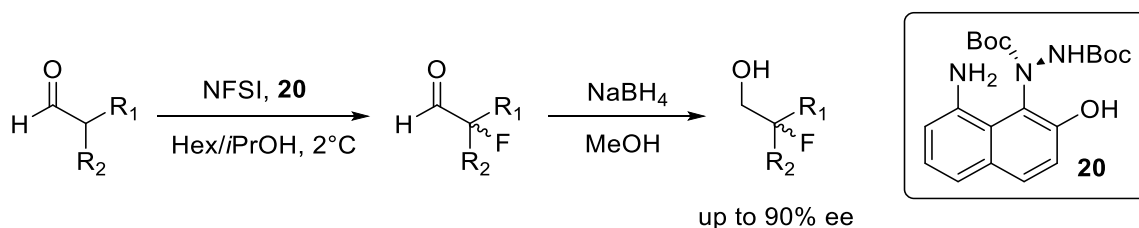
⁵¹ T. D. Beeson, D. W. C. MacMillan, *J. Am. Chem. Soc.* **2005**, *127*, 8826.

is tolerant to a wide range of functional groups and is possible to apply this protocol to several aldehydes, except for α -branched ones.



Scheme 20: Macmillan fluorination of linear aldehydes

In 2006, Jørgensen and co-workers reported the asymmetric α -fluorination of α -branched aldehydes with the use of derivative **20**, synthesized through an asymmetric Friedel–Craft amination.⁵² The results were satisfying with ee up to 90% (**Scheme 21**). In general, good enantioselectivities were achieved in presence of one aromatic group in the α position, while poorer ee were observed with alkyl groups.



Scheme 21: fluorination of α -branched aldehydes proposed by Jorgensen

Together with simple protocols, many one-pot reactions that incorporates α -fluorination of aldehydes has been reported in literature⁵³. These procedures open new routes in the design of synthetic strategies, and allows to strongly reduce the number of steps during the synthesis, to avoid also further purifications, to save time and cut costs, thus reducing the sustainability of the process.

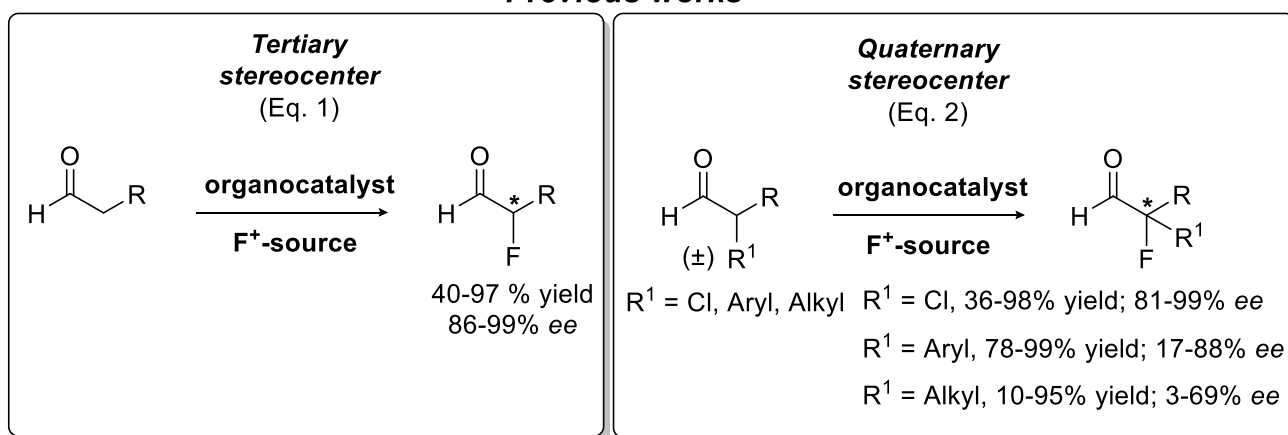
⁵² S. Brandes, B. Niess, M. Bella, A. Prieto, J. Overgaard, K. A. Jørgensen, *Chem. Eur. J.* **2006**, *12*, 6039.

⁵³ For some examples of one-pot fluorination reactions: a) Y. Huang, A. M. Walji, C. H. Larsen, D. W. C. MacMillan, *J. Am. Chem. Soc.* **2005**, *127*, 15051. b) C. Appayee, S. E. Brenner-Moyer, *Org. Lett.* **2010**, *12*, 3356. c) H. Jiang, A. Falcicchio, K. L. Jensen, M. W. Paixao, S. Bertelsen, K. A. Jørgensen, *J. Am. Chem. Soc.* **2009**, *131*, 7153. d) O. O. Fadeyi, C. W. Lindsley, *Org. Lett.* **2009**, *11*, 943.

3.4 Aim of the work

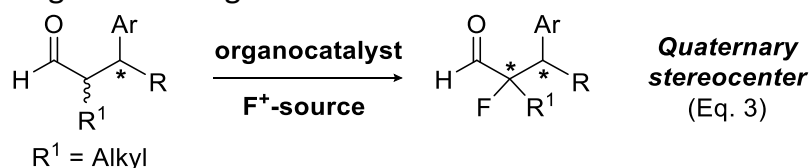
Despite the recent advantages in the organocatalytic synthesis of α -fluoro aldehydes, as exposed before, the scope of the reaction is still limited to simple achiral aldehydes, and in many cases is focused to the construction of tertiary fluorinated stereogenic centres [Scheme 22, Equation (1)]. In contrast, the stereoselective organocatalytic α -fluorination of α,α -dialkyl aldehydes appears to be way more difficult, and only a few paper have reported it, achieving only moderate levels of stereoselectivity [$ee^{\max} = 69\%$, Equation (2)].⁵⁴ Additionally, there are only few reports⁵⁵ documenting the stereoselective construction of quaternary stereocenters at the $C\alpha$ position, and the best are obtained only with α -chloro- and α -aryl-substituted aldehydes, able to stabilize the enamine formation.

Previous works



Scheme 22: Previous works

With this in mind, we wondered the study of the organocatalytic α -fluorination of chiral aldehydes containing two contiguous α and β stereocenters (Scheme 23), thus creating a quaternary stereogenic center. To the best of our knowledge, this is the first study committed to the stereoselective organocatalytic fluorination of enantioenriched α,α -dialkyl aldehydes containing two stereogenic centers.



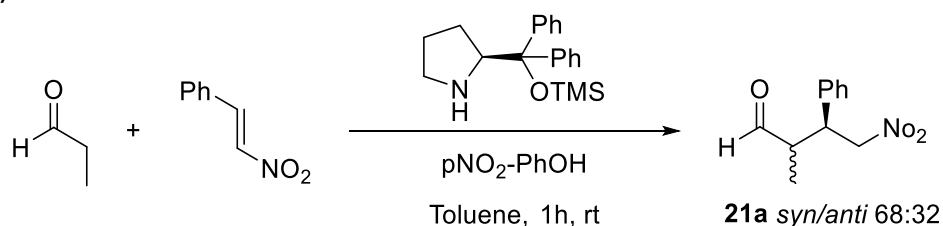
Scheme 23: aim of the work

⁵⁴ M. R. Witten, E. N. Jacobsen, *Org. Lett.* **2015**, *17*, 2772-2775, see reference 52.

⁵⁵ M. D. Hayes, M. Rodriguez-Alvarado, S. E. Brenner-Moyer, *Tetrahedron Lett.* **2015**, *56*, 4718-4720, see reference 52.

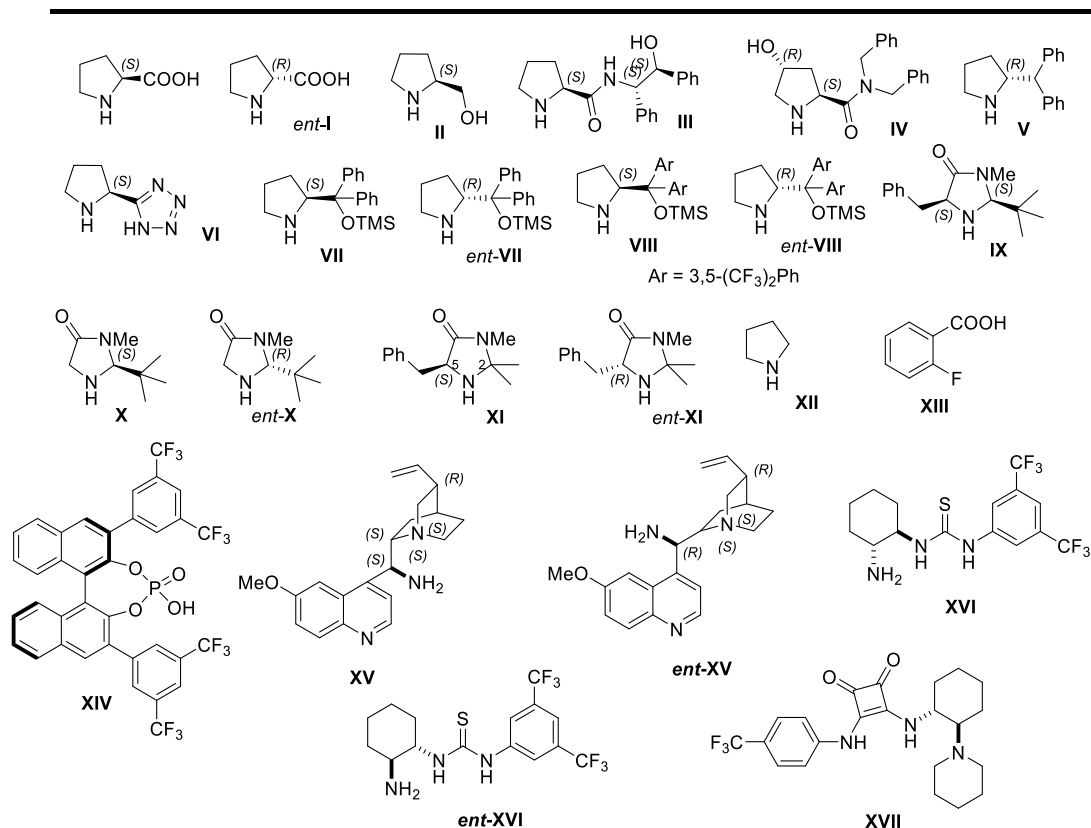
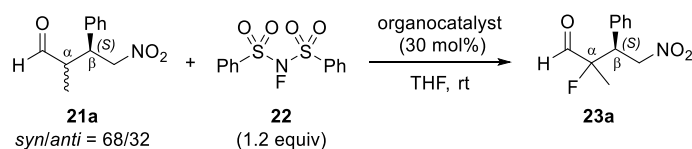
3.5 Result and discussion

We began our investigation by studying the fluorination of a mixture of (2*R*,3*S*)- and (2*S*,3*S*)-2-methyl-4-nitro-3-phenylbutanal (**21a**; *syn/anti* = 68:32). This kind of Chiral γ -nitroaldehydes are easy accessible by conjugate addition of an aldehyde to a nitroalkene catalysed by commercially available Jorgensen–Hayashi catalysts, giving products with a high stereocontrol at the β stereocenter, while lower control at the α stereocenter is present (**Scheme 24**).⁵⁶



Scheme 24: Synthesis of the starting material

This represent an ideal substrate for an ulterior α -functionalization like fluorination. Then, we started our investigation with a deepened screening of catalysts and additive the, reported in **Table 7**:



⁵⁶ a) K. Patora-Komisarska, M. Benohoud, H. Ishikawa, D. Seebach, Y. Hayashi, *Helv. Chim. Acta* **2011**, *94*, 719–745; b) X. Hu, Y.-F. Wei, N. Wu, Z. Jiang, C. Liu, R.-S. Luo, *Tetrahedron: Asymmetry* **2016**, *27*, 420–427.

Entry	Catalyst	Additive	Time	Conversion (%) ^b	dr 23a ^b	dr 21a ^b (<i>syn/anti</i>)
1	I	-	26h	77	65:35	66:34
			5d	100	64:36	-
2	<i>ent</i> -I	-	26h	65	33:67	87:13
			5d	100	32:68	-
3	II	-	24h	15	55:45	68:32
			6d	34	54:46	65:35
4	III	-	24h	36	56:44	63:37
			6d	69	48:52	67:33
5	IV	-	24h	32	53:47	71:29
			6d	51	53:47	63:37
6	V	-	24h	24	22:78	80:20
			6d	57	28:72	80:20
7	VI	-	24h	77	72:28	52:48
			3d	90	71:29	-
8	VII	-	24h	9	-	66:34
			6d	41	90:10	66:34
9	<i>ent</i> -VII	-	24h	5	-	68:32
			6d	48	50:50	70:30
10	VIII	-	24h	16	-	57:43
			5d	47	91:9	48:52
11	<i>ent</i> -VIII	-	24h	15	-	72:28
			5d	38	20:80	77:23
12	I	TFA	23h	86	71:29	-
13	VI	TFA	23h	100	77:23	-
14	VII	TFA	19h	75	92:8	56:44
			3d	94	92:8	-
15	<i>ent</i> -VII	TFA	23h	76	20:80	72:28
16	VIII	TFA	5h	53	92:8	62:38
			23h	73	90:10	55:45
			46h	76	93:7	46:54
17	<i>ent</i> -VIII	TFA	5h	37	7:93	81:19
			23h	56	8:92	78:22
			46h	69	7:93	72:28
18	IX	-	24h	9	-	67:33
			6d	43	52:48	64:36
19	IX	TFA	24h	42	69:31	64:36
			7d	95	71:29	-
20	X	TFA	24h	100	63:37	-
21	<i>ent</i> -X	TFA	24h	100	15:85	-
22	XI	DCA	24h	42	91:9	69:31
			3d	77	87:13	60:40
			6d	91	88:12	-
23	<i>ent</i> -XI	DCA	24h	39	24:76	74:26
			4d	80	20:80	83:17
			8d	94	20:80	-
24	XII	-	24h	38	51:49	69:31
			6d	61	51:49	66:34

25	XII	TFA	19h 7d	56 82	50:50 52:48	61:39 61:39
26	VII	XIII	24h 3d 7d	42 52 67	84:16 83:17 89:11	57:43 55:45 51:49
27	VII	XIV	24h 7d	18 50	77:23 74:26	64:36 59:41
28	ent- VII	XIV	24h 5d 7d	10 22 33	- 27:73 28:72	68:32 69:31 67:33
29	XI	HCl	24h 3d 6d	12 35 54	83:17 82:18 81:19	69:31 69:31 68:32
30	XV	-	24h 3d 7d	31 51 56	43:57 48:52 50:50	63:37 60:40 61:39
31	ent- XV	-	24h 3d 7d	25 46 50	37:63 29:71 31:69	66:34 61:39 61:39
32	ent- XV	HCl(3 eq.)	24h 3d	9 21	- 53:47	66:34 66:34
33	XV	-	24h 3d 7d	38 53 56	45:55 49:51 51:49	61:39 60:40 58:42
34	XVI	-	24h 3d 7d	14 32 41	45:55 49:51 51:49	61:39 60:40 58:42
35	ent- XVI	-	24h 3d 7d	14 27 52	69:31 58:42 53:47	70:30 69:31 72:28
36	XVI	TFA	24h 3d 7d	19 31 38	55:45 64:36 62:38	67:33 66:34 70:30
37	XVII	-	24h 5d 7d	29 33 43	43:57 42:58 44:56	69:31 71:29 69:31
38	XIV	-	24h	-	-	65:35

Table 7: ^a Reaction conditions: **21a** (10 mg, 0.0483 mmol), **22** (1.2 equiv), catalyst (30 mol%), tetrahydrofuran (THF, 0.4 mL), room temperature (rt). ^b Determined by ¹H NMR of the crude mixture. h = hours, d = days, TFA = trifluoroacetic acid, DCA = dichloroacetic acid.

We started testing several enantiopure secondary amines as catalysts (**I–XI**), running the reactions in THF at room temperature, and choosing *N*-fluorobenzenesulfonimide (NFSI; **22**) as the electrophilic fluorine source. First catalysts tested were the two enantiomers of proline (**I** and *ent*-**I**), and gave good conversions after 26 h (entries 1 and 2). The (*S*) enantiomer was slightly more efficient, and interestingly, the two enantiomers provided the fluorinated product (i.e., **23a**) with analogous but opposite diastereomeric ratios. (*S*-Prolinol (**II**) and two different (*S*)-prolinamides (**III** and **IV**) gave slower reactions (entries 3–5) and poor stereoselectivity. (*R*)-2-Benzhydrylpyrrolidine (**V**) showed a similar poor reactivity (entry 6), but it gave a significant diastereoselectivity (*dr* = 28:72), for the same isomer favoured by (*R*)-proline (*ent*-**I**). (*S*)-tetrazole derivative **VI** also gave interesting outcomes (entry 7). After, we screened four silylated diarylprolinols as organocatalysts (entries 8–11), observing slow reactions, but also the best diastereoselectivity of this series (*dr* = 90:10), that was achieved with (*S*)-configured catalysts **VII** and **VIII** (entries 8 and 10, respectively). This first part of the screening led us to infer that enantiomeric catalysts (**I** and *ent*-**I**, **VII** and *ent*-**VII**, **VIII** and *ent*-**VIII**) could establish matched (*S*-configured) and mismatched (*R*-configured) pairs with the chiral substrate (i.e., **21a**), favoring opposite $C\alpha$ absolute configurations of the fluorinated product (i.e., **23a**) with different efficiencies. The preferential reaction of each enantiomer of the catalyst with a particular diastereoisomer of aldehyde **21a** was also suggested by the variation of the diastereomeric ratio of **21a** during the reaction (Table 7).

Since the fastest fluorinations took place in the presence of organocatalysts bearing significantly acidic protons (**I** and **VI**), we decided to add an external acid to check if a possible enhancement in reactivity is observed. The addition of trifluoroacetic acid (TFA) increased the reaction rate for all the organocatalysts tested (entries 12–17), especially when combined with silylated diarylprolinols **VII** and **VIII**. Good conversions (73–75 %) were achieved in less than one day, together with a slightly better diastereoselectivity, in particular in the mismatched-pair using (*R*)-configured diarylprolinols (*ent*-**VII** and *ent*-**VIII**). The results with imidazolidinones **IX–XI**, which are commonly used in the presence of protic acids, confirmed the enhancement of rate and diastereoselectivity in the presence of TFA (entries 18 and 19), and also the different abilities of enantiomeric catalysts to favour opposite $C\alpha$ -configurations.

Some acids have been tested in the presence of the already studied catalysts **VII**, *ent*-**VII** and **XI**, only with moderate results. The primary bifunctional amines **XV**, *ent*-**XV**, **XVI**, *ent*-**XVI**, and the squaramide derivative **XVII** were screened with and without acid, but poorer results were invariably observed, confirming the secondary amines as the best catalysts in this fluorination reaction. Lastly, we performed the fluorination reaction using simple achiral pyrrolidine **XII** with and without acid (entries 25 and 24, respectively). No diastereoselection was observed, supporting the idea of catalyst-controlled stereodifferentiation as seen in the results of previous experiments, without notable influence of the $C\beta$ -stereocenter.

Jorgensen's diarylprolinols **VIII** and *ent*-**VIII** emerged as the best organocatalyst for the α -fluorination of α,α -dialkyl aldehyde **21a**, allowing to obtain both stereoisomers with the two opposite absolute configurations of the $C\alpha$ quaternary stereocenter (entries 16 and 17) with high levels of diastereocontrol. Furthermore, we demonstrated that the presence of TFA

improves both the rate and the stereocontrol. Using these findings as a starting point, we further examined the role of solvent and catalyst loading on the reactivity and selectivity of the fluorination reaction (**Table 8**).

Entry	Catalyst (mol%)	Solvent	Time	Conversion (%) ^b	dr 23a ^b	dr 21a ^b (<i>syn/anti</i>)
1 ^c	VIII (30)	THF	19h	72	94:6	58:42
			40h	85	93:7	58:42
2 ^c	VIII (30)	CH ₃ CN	19h	34	94:6	68:32
			40h	41	96:4	66:34
3 ^c	VIII (30)	DCM	19h	12	85:15	65:35
			40h	16	85:15	63:37
4 ^c	VIII (30)	Hexane	54h	50	90:10	55:45
5 ^c	VIII (30)	TBME	19h	95	94:6	51:49
6 ^d	<i>ent</i> - VIII (30)	TBME	19h	74	12:88	84:16
			24h	80	11:89	82:18
			44h	92	10:90	69:31
7 ^d	VIII (15)	TBME	19h	81	96:4	37:63
			44h	91	96:4	51:49
8 ^d	VIII (10)	TBME	24h	73	97:3	31:69
			4d	88	95:5	43:57
9 ^d	VIII (5)	TBME	4d	66	95:5	42:58
10 ^d	<i>ent</i> - VIII (20)	TBME	22h	65	12:88	90:10
11 ^d	<i>ent</i> - VIII (15)	TBME	24h	58	11:89	86:14
			4d	90	10:90	72:28
12 ^{c,e}	VIII (5)	TBME	23h	34	76:24	71:29
			2d	44	74:26	61:39
13 ^f	VIII (15)	TBME	18h	80	98:2	53:47
			2d	87	98:2	55:45
14 ^f	<i>ent</i> - VIII (15)	TBME	18h	35	12:88	86:14
			2d	42	14:86	73:27

Table 8: Reaction conditions optimization.^a Reaction conditions: **21a** (10 mg, 0.0483 mmol), **22** (1.2 equiv), trifluoroacetic acid (TFA, equimolar amount with the catalyst), solvent (0.2 mL), room temperature (rt). ^b Determined by ¹H NMR of the crude mixture. ^c Initial dr (**21a**): *syn/anti* = 72/28. ^d Initial dr (**21a**): *syn/anti* = 67/33. ^e Reaction set at 50 °C. ^f Initial dr (**21a**): *syn/anti* = 99/1. h = hours, d = days, THF = tetrahydrofuran, DCM = dichloromethane, TBME = *tert*-butylmethylether.

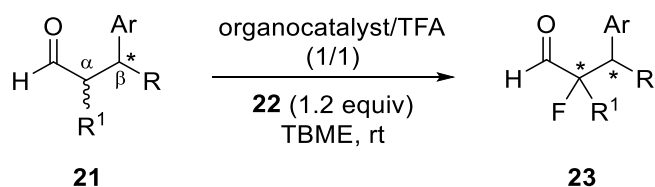
The solvent screening (entries 1–5) confirmed ethers as the best solvents in terms of both reactivity and stereoselectivity, with *tert*-butyl methyl ether (TBME; entry 5) resulting as the best. Acetonitrile slowed down the transformation (entry 2), while nonpolar or slightly polar solvents, such as dichloromethane or hexane (entries 3 and 4, respectively) gave worse diastereomeric ratios. The better performance of TBME was further confirmed by the good results obtained with enantiomeric catalyst *ent*-**VIII** (entry 6). Finally, the catalyst loading

was studied (entries 7–11), and high conversions were obtained in reasonable times using 15 mol-% of **VIII** and 20 mol-% of *ent*-**VIII** (entries 7 and 10, respectively).

However, the fluorination proceeded also using lower catalyst loadings (entries 8 and 11). With the lowest amount of catalyst (5 mol-%), we tried to speed up the reaction by increasing the temperature (50 °C), but a significant decrease in diastereomeric ratio was observed (entry 12). We carried out also trials on a *syn* enriched sample of **21a** (entries 13 and 14) to check the role of the α stereocenter in the overall catalytic cycle. A slightly improved stereocontrol was recorded for **VIII** [*dr* = 98:2 (entry 13) vs. 96:4 (entry 7)], while with *ent*-**VIII** was less selective and slower (entry 14 with entry 11). These findings further confirmed *syn*-**1a/VIII** as the matched pair, and that, even with acid additive, the *syn*-**21a** and *anti*-**21a** equilibration is a slow process. Indeed, if the *syn/anti* equilibration was fast, we should not observe a difference in terms of reaction rate between entries 11 and 14 of Table 2.

Concluding, we identified the best reaction conditions for the α -fluorination of model substrate **21a**: catalyst **VIII** (15 mol-%) or catalyst *ent*-**VIII** (20 mol-%) to obtain the two $C\alpha$ -epimers of fluorinated product **23a**; TFA as an acid additive in an equimolar amount with the organocatalyst; TBME as the reaction solvent (0.24 M) and room temperature. Based on this protocol, we investigated the wider substrate scope of the reaction (**Table 9**).

The two $C\alpha$ -epimers of fluorinated product **23a**, namely *anti*-**23a** (Table 3, entry 1) and *syn*-**23a** (entry 2), were obtained in good yields and with high stereoselectivities by fluorination of **21a** in the presence of **VIII** and *ent*-**VIII**, respectively. We applied the same protocol to (3*R*)-2-methyl-4-nitro-3-phenylbutanal (**21b**), which resulted in the stereoselective synthesis of the enantiomeric forms of compounds *anti*-**23a** and *syn*-**23a**: *anti*-**23b** from catalyst *ent*-**VIII** (Table 3, entry 4), and *syn*-**23b** from catalyst **VIII** (entry 3), respectively. As expected, **21b/VIII** acted as the mismatched pair, and **21b/ent-VIII** as the matched pair. As a result, the *anti* fluorinated products were always formed with excellent stereocontrol (*dr* **23a** = 97:3, *dr* **23b** = 96:4), while the *syn* analogs showed slightly worse diastereomeric ratios (*dr* **23a** = 89:11, *dr* **23b** = 84:16).



Entry	Substrate 21 R ¹ /Ar/R	Catalyst (mol%)	Time [h]	Product	Conversion (%) ^b (Yield %) ^c	dr 23 ^b (<i>anti:syn</i>)	er 23 ^d
1	21a Me/(<i>S</i>)- Ph/CH ₂ NO ₂	VIII (15)	22	 anti-23a	100 (75) ^e	97:3	>99:1 ^f
2	21a Me/(<i>S</i>)- Ph/CH ₂ NO ₂	<i>ent</i> - VIII (20)	20	 syn-23a	100 (85) ^e	11:89	>99:1 ^f
3	21b Me/(<i>R</i>)- Ph/CH ₂ NO ₂	VIII (20)	20	 syn-23b	95 (86) ^e	16:84	>99:1 ^f
4	21b Me/(<i>R</i>)- Ph/CH ₂ NO ₂	<i>ent</i> - VIII (15)	20	 anti-23b	100 (80) ^e	96:4	>99:1 ^f
5	21c Me/(<i>S</i>)- <i>p</i> OMePh/CH ₂ NO ₂	VIII (15)	22	 anti-23c	95 (79)	93:7	99:1 ^g
6	21d Me/(<i>S</i>)- <i>p</i> BrPh/CH ₂ NO ₂	VIII (15)	22	 anti-23d	85 (53)	95:5	>99:1 ^g
7	21e Pr/(<i>S</i>)-Ph/CH ₂ NO ₂	VIII (20)	72	 anti-23e	32	97:3	>99:1 ^g

8 ^h	21e Pr/(S)-Ph/CH ₂ NO ₂	VIII (20)	48		69 (35)	85:15	>99:1 ^g
9 ^h	21f iPr/(S)-Ph/CH ₂ NO ₂	VIII (20)	48		19	80:20	>99:1 ^g
10	21g Me/(S)-Ph/CH(Me)NO ₂	VIII (20)	72		74 (35) ⁱ	96:4	>99:1 ^g
11	<i>rac</i> - 21h Me/C ₆ H ₃ OCH ₂ O/ H	<i>ent</i> -VIII (20)	48		81 (75)	-	82:18 ^f
12	21i Me/(S)-Cy/CH ₂ NO ₂	VIII (15)	24		100 (85)	91:9	>99:1 ^g
13	21j Me/(S)-iBu/CH ₂ NO ₂	VIII (15)	17		100 (81)	90:10	nd
14	21k Me/(S)-iPr/CH ₂ NO ₂	VIII (15)	24		100 (25) ¹	86:14	>99:1 ^g

Table 9: Substrates scope.^a Reaction conditions: **1** (0.1448 mmol), **2** (NFSI, 1.2 equiv), TFA (equimolar amount with the catalyst), TBME (0.6 mL), rt. ^b Determined by ¹H NMR of the crude mixture. ^c Determined after chromatographic purification. ^d Determined by chiral stationary phase (CSP)-HPLC on isolated product. ^e Reaction set at 50 °C. ^f Determined on product reduced with NaBH₄. ^g Derived from *ee* of starting aldehyde **1**. ^h Reaction carried out at 50 °C. ⁱ Data obtained from a not optimized process. nd = not determined. Cy = cyclohexyl, iBu = isobutyl, iPr = isopropyl.

The developed asymmetric fluorination was applied to differently substituted α,α -dialkyl aldehydes **21c–21k** (Table 3). The introduction of electron-donating (entry 5, **21c**) and electron-withdrawing (entry 6, **21d**) groups on the C β -aromatic ring did not interfere with the successful fluorination reaction. Conversely, increasing the steric hindrance at the C α position significantly affected the efficiency of the construction of the quaternary carbon (entries 7–9). With an *n*-propyl substituent (**21e**), the conversion was low at room

temperature (entry 7), and it increased at 50 °C (entry 8), although the diastereomeric ratio decreased slightly. For the isopropyl derivative (i.e., **21f**) the fluorination proceeded very slowly, despite a higher temperature (entry 9). Afterwards, we applied our protocol to (3*S*,4*R*)-2-methyl-4-nitro-3-phenylpentanal (**21g**), which contains three stereocenters, and was used as mixture of two C α epimers (*dr* = 84:16). The α -fluorination took place, and although the process was not optimized, product **23g** was obtained with excellent stereoselectivity (Table 3, entry 10).

Next, racemic 2-methyl-3-(3,4-methylenedioxyphenyl) propanal (**21h**) was subjected to the organocatalytic asymmetric fluorination (entry 11). The reaction proceeded smoothly in the presence of catalyst *ent*-**VIII**, and the two enantiomers of product **23h** were formed in a noteworthy 82:18 ratio.⁵⁷ This result represents the second most enantioselective fluorination of a racemic α,α -dialkyl aldehyde, and the best ever result obtained using a commercially available secondary amine as an organocatalyst. The enantiocontrol recorded for C β -unsubstituted product **23h** did not reflect the diastereocontrol observed for the C β -substituted compounds **23a–23g**. Although in many examples we obtained evidence of a catalyst-controlled process, in the case of **21h** the steric and geometric constraints imposed by a longer branched chain significantly affect the distribution of the enamines and/or their reactivity with the fluorinating agent.

We also successfully applied our protocol to α,α -dialkyl aldehydes derived from aliphatic nitroalkenes (**21i–21k**, entries 12–14), demonstrating the efficiency of the developed asymmetric fluorination process.

The α -fluorination of substrates similar as aldehyde **21h** has been studied also by Shibatomi and coworkers.⁵⁸ They revealed that a kinetic resolution of the starting aldehydes was involved. We decided to further investigate the α -fluorination of **21h** under different reaction conditions (Table 10).

Entry ^a	Catalyst	TFA (%)	t (h)	Conversion (%) ^b	er ^c
1	<i>Ent</i> - VIII	20	20 h	70	-
			48 h	81	18:82
2	VIII	20	3.5 h	85	73:27
3	<i>Ent</i> - VIII	-	3.5 h	31	-
			24h	59	46:54

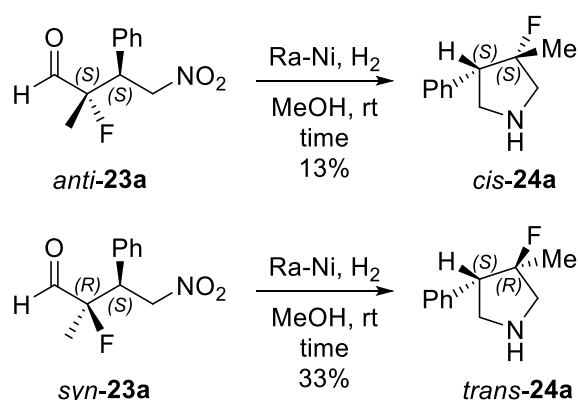
Table 10: a Reaction conditions: **1a** (30 mg, 0.048 mmol), NFSI (1.2 equiv), catalyst (20 mol%), TBME (0.6 mL), room temperature (rt). b Determined by ¹H NMR of the crude mixture. c Determined by chiral stationary phase (CSP)-HPLC after reduction to the corresponding alcohol. h = hours, TFA = trifluoroacetic acid, TBME = tert-butylmethylether.

⁵⁷ For the synthesis and stereochemical determination of substrate **1g**, see: G. Sahoo, H. Rahaman, A. Madarasz, I. Papai, M. Melarto, A. Valkonen, P. M. Pihko, *Angew. Chem. Int. Ed.* **2012**, *51*, 13144–13148; *Angew. Chem.* **2012**, *124*, 13321–13325.

⁵⁸ K. Shibatomi, T. Okimi, Y. Abe, A. Narayama, N. Nakamura, S. Iwasa, *Beilstein J. Org. Chem.* **2014**, *10*, 323.

As showed by the data summarized in Table 10, catalyst *ent*-**VIII** provided the fluorinated product **23h** with higher stereocontrol (*er* = 18/82, entry 1), but catalyst **VIII** promoted a faster reaction (entry 2). Moreover, we further demonstrated that the acid additive was able to increase both reaction rate and stereocontrol (cf. entry 1 with entry 3).

In order to determinate the absolute configuration of compounds *anti*-**23a** and *syn*-**23a**, we reduced and cyclized giving the corresponding cyclized substitute pyrrolidine (i.e., *cis*-**24** and *trans*-**24**; **Scheme 25**) and recorded several nOe experiments. The stereochemistry determined in this way was extended to all the molecules of the series (Table 9) provided by the same organocatalytic protocol (see Chapter 3.8 for the spectra).



Scheme 25: Synthesis of fluorinated pyrrolidines *cis*-**24** and *trans*-**24**, derived from the stereochemically defined α -fluoro- γ -nitro aldehydes *anti*-**23a** and *syn*-**23a**, respectively.

In order to investigate the enamine formation in the developed fluorination reaction we studied the enamine formation by mixing **21a** (*syn/anti* = 68:32) and catalyst **VII** or *ent*-**VII** (30 mol-%) in *d*₈-THF in a standard 5 mm NMR tube at the same concentrations used for the synthetic experiments.

Entry ^a	Catalyst	Time (h)	Conversion (%) ^b	dr enamine <i>E/Z</i> ^b	dr 21a ^b (<i>syn/anti</i>)
1	<i>ent</i> - VII (30%)	1	20	92/8	74/26
		2.5	24	92/8	76/24
		5.5	26	88/12	76/24
2	VII (30%)	1	22	94/6	54/46
		2.5	23	94/6	52/48
		5.5	30	94/6	52/48

Table 11: Scanning of enamine formation with catalyst **VII** and *ent*-**VII**. ^a Reaction conditions: **1a** (30 mg, 0.145 mmol), catalyst (14 mg, 30 mol%), THF-*d*₈ (0.6 mL), room temperature (rt), reaction carried out into NMR sample tube. ^b Determined by ¹H NMR of the crude mixture. h = hours.

The enamine formation was almost complete after 1 h at room temperature (24 % conversion, with respect to 30 mol-% of catalyst present) for catalyst **VII**, while a slower

reaction was observed for *ent*-**VII** (17 % conversion). After 5.5 h, the conversion reached 30 % for **VII** and 21 % for *ent*-**VII**. In both cases, only two enamine intermediates were detected, in ratios of 95:5 and 90:10, respectively. These observations agree with the results of the fluorination reported, which identify **VII/1a** and *ent*-**VII/1a** as the matched and the mismatched pair, respectively. nOe experiments showed how the major enamine formed is an *E*-configured *s-trans* enamine (**25a** or **26a**); the minor enamine was presumably the less stable *Z*-configured *s-trans* enamine (**25c** or **26c**).

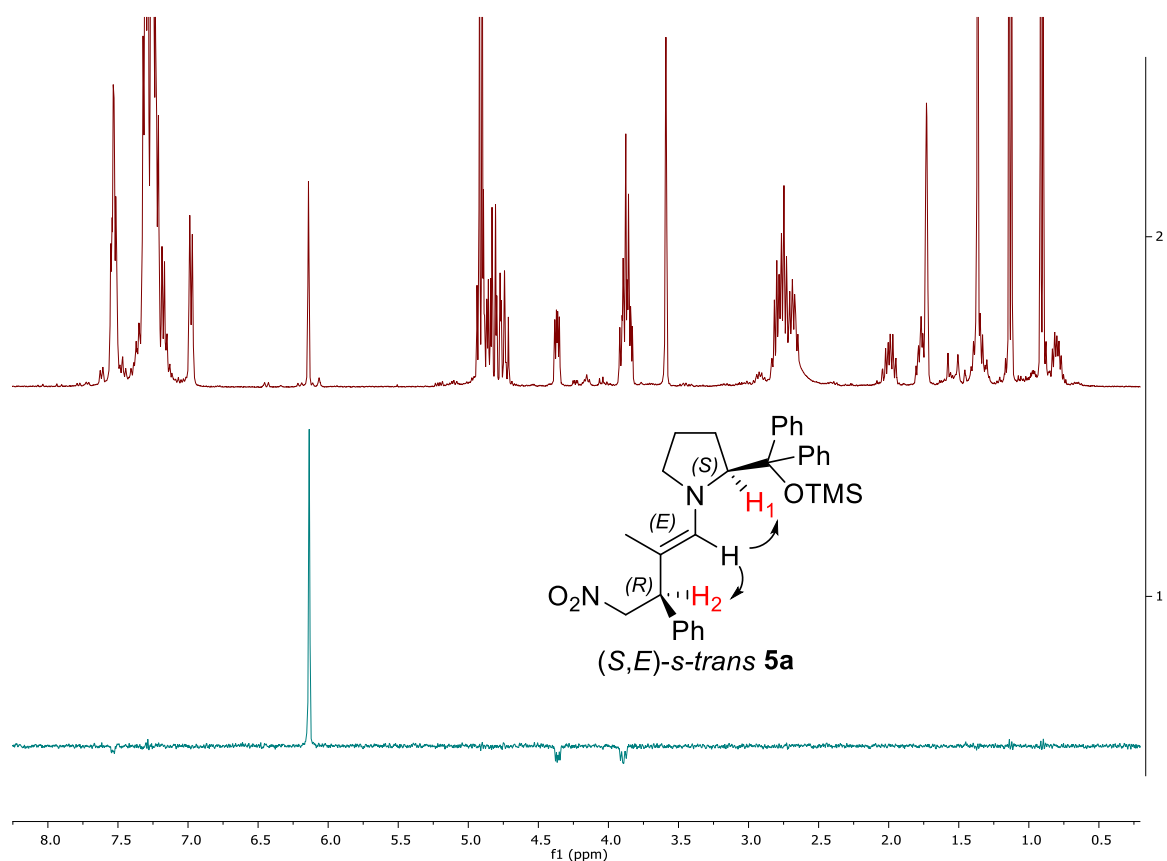


Figure 9: $^1\text{H-NMR}$ at 5.5 h with catalyst **VII** (entry 2) / 1D NOESY, irradiation at 6.1 ppm

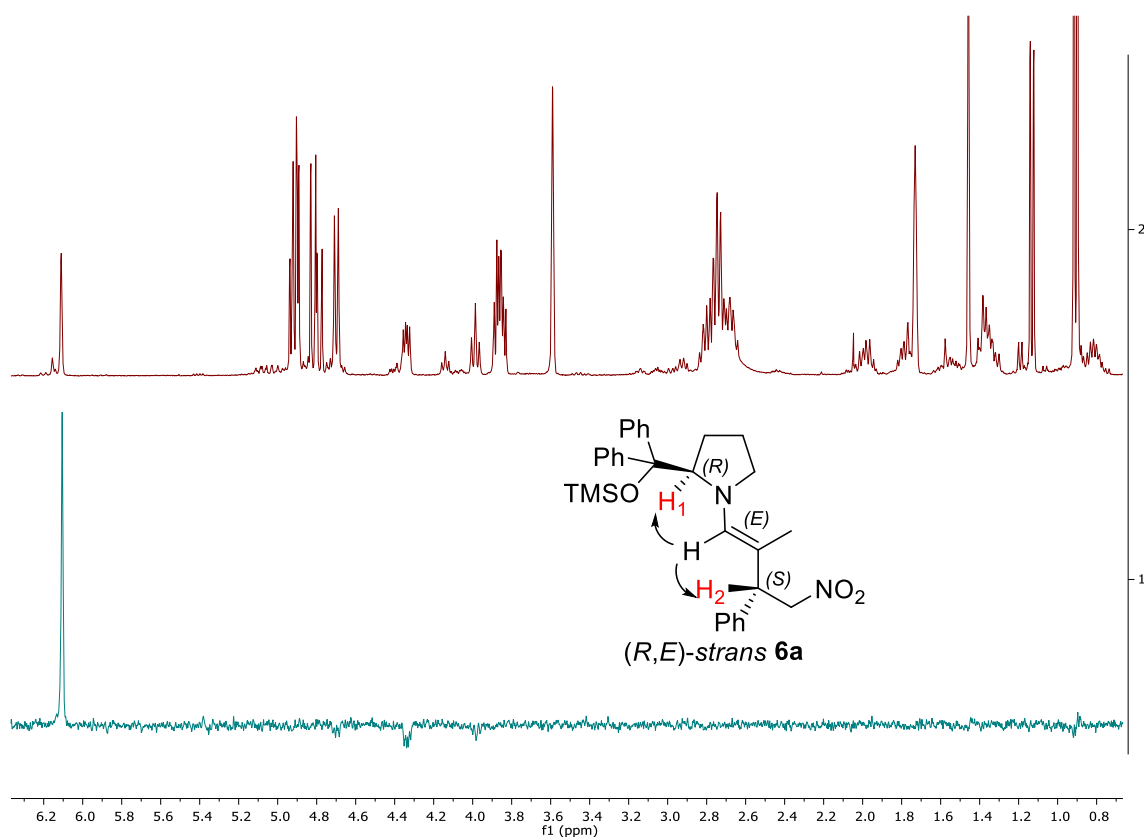
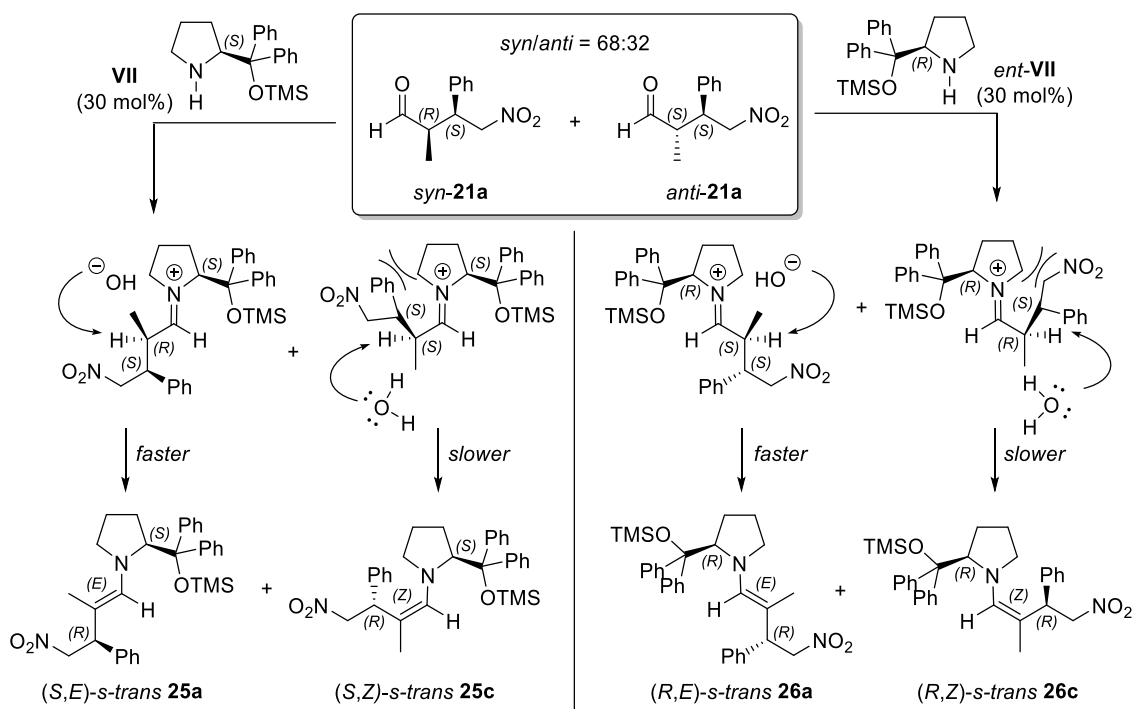


Figure 10: $^1\text{H-NMR}$ at 5.5 h with catalyst *ent-VII* (entry 1) / 1D NOESY, irradiation at 6.1 ppm

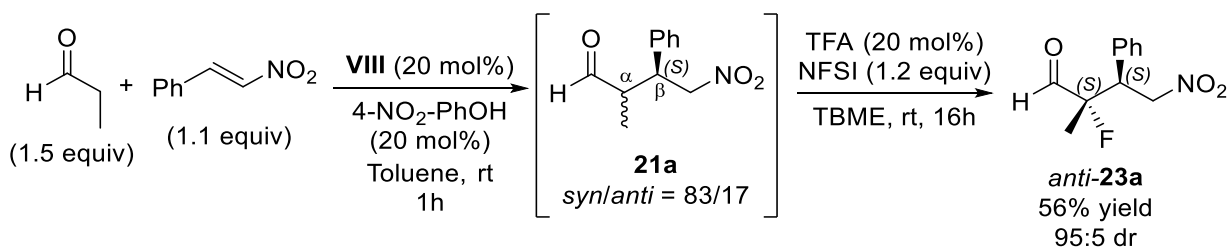
The 1D NOESY spectra of enamines showed no answer for the CH_3 signals for both the catalysts **VII** and *ent-VII*, confirming the *E*-configuration of the double bond. The nOe signal for proton H1 confirmed also the preferential *s-trans* conformation.

Moreover, during the NMR experiments, we confirmed that when (*S*)-configured catalyst **VII** was used, the *syn-21a* isomer was consumed preferentially (**21a** *syn/anti* = 52:48 after 5.5 h). The *anti-21a* isomer was the favoured substrate when (*R*)-configured catalyst *ent-VII* (**21a** *syn/anti* = 76:24 after 5.5 h) was used. The preferential formation of *E*-configured *s-trans* enamines was not unexpected, since according to the most credited reaction mechanism for the formation of enamines from the corresponding iminium intermediates, deprotonation must occur opposite to the side of the bulky substituent of the pyrrolidine ring, arranging the hydrogen parallel to the iminium π -orbital system. Based on this result, we propose a mechanism for the formation of the enamines as reported in **Scheme 26**.



Scheme 26: Proposed reaction mechanism for the formation of enamine intermediates **25a**, **25c** and **26a**, **26c** using catalysts **VII** and *ent*-**VII**, respectively.

Finally, we integrated into a one-pot process the synthesis of *anti*-**23a** starting from propanal and *trans*-nitro-styrene, thus carrying out the Michael–fluorination sequence with the same organocatalyst, and avoiding the intermediate purification step (**Scheme 27**). The good results obtained reflects the performances of the separate synthetic steps, and allow us to save catalyst, solvent, and time.



Scheme 27: One-pot Michael/fluorination sequence, stereoselectively giving compound *anti*-**23a** starting from propanal and *trans*- β -nitrostyrene.

3.6 Conclusion

In conclusion a new organocatalysed protocol for the α -fluorination of α,α -dialkyl aldehydes has been accomplished. The results are comparable and superior to the one reported in literature. The presence of β stereocenters does not interfere with the diastereoselection of the reaction, that appears to be catalyst-governed. The transformation allows easily to build fully substituted quaternary stereocenters, often presents in pharmaceuticals and drugs. The one-pot nitromichael-fluorination reaction gives results similar to the single steps. The absolute configuration of the intermediates has been determined and the mechanism of the reaction has been clarified.

3.7 General Procedures and Products Characterization

General Information. ^1H and ^{13}C NMR spectra were recorded on Varian Gemini 200 or Inova 400 NMR instruments with a 5 mm probe. Chemical shifts (δ) are reported in ppm, relative to the residual peaks of deuterated solvent signals.

HPLC-MS analyses were performed on an Agilent Technologies HP1100 instrument coupled with an Agilent Technologies MSD1100 single-quadrupole mass spectrometer. A Phenomenex Gemini C18, 3 μm (100 x 3mm) column was employed for the chromatographic separation: mobile phase $\text{H}_2\text{O}/\text{CH}_3\text{CN}$, gradient from 30% to 80% of CH_3CN in 8 min, 80% of CH_3CN until 22 min, then up to 90% of CH_3CN in 2 min, flow rate 0.4 mL min^{-1} . Mass spectrometric detection was performed in full-scan mode from m/z 50 to 2500, scan time 0.1 s in positive ion mode, ESI spray voltage 4500 V, nitrogen gas 35 psi, drying gas flow rate 11.5 mL min^{-1} , fragmentor voltage 30 V.

GC-MS spectra were taken by EI ionization at 70 eV on a Hewlett-Packard 5971. They are reported as: m/z (rel. intense).

CSP-HPLC analyses were performed on an Agilent Technologies Series 1200 instrument using Daicel[®] chiral columns and *n*-hexane/2-propanol (*n*-Hex/IPA) mixtures.

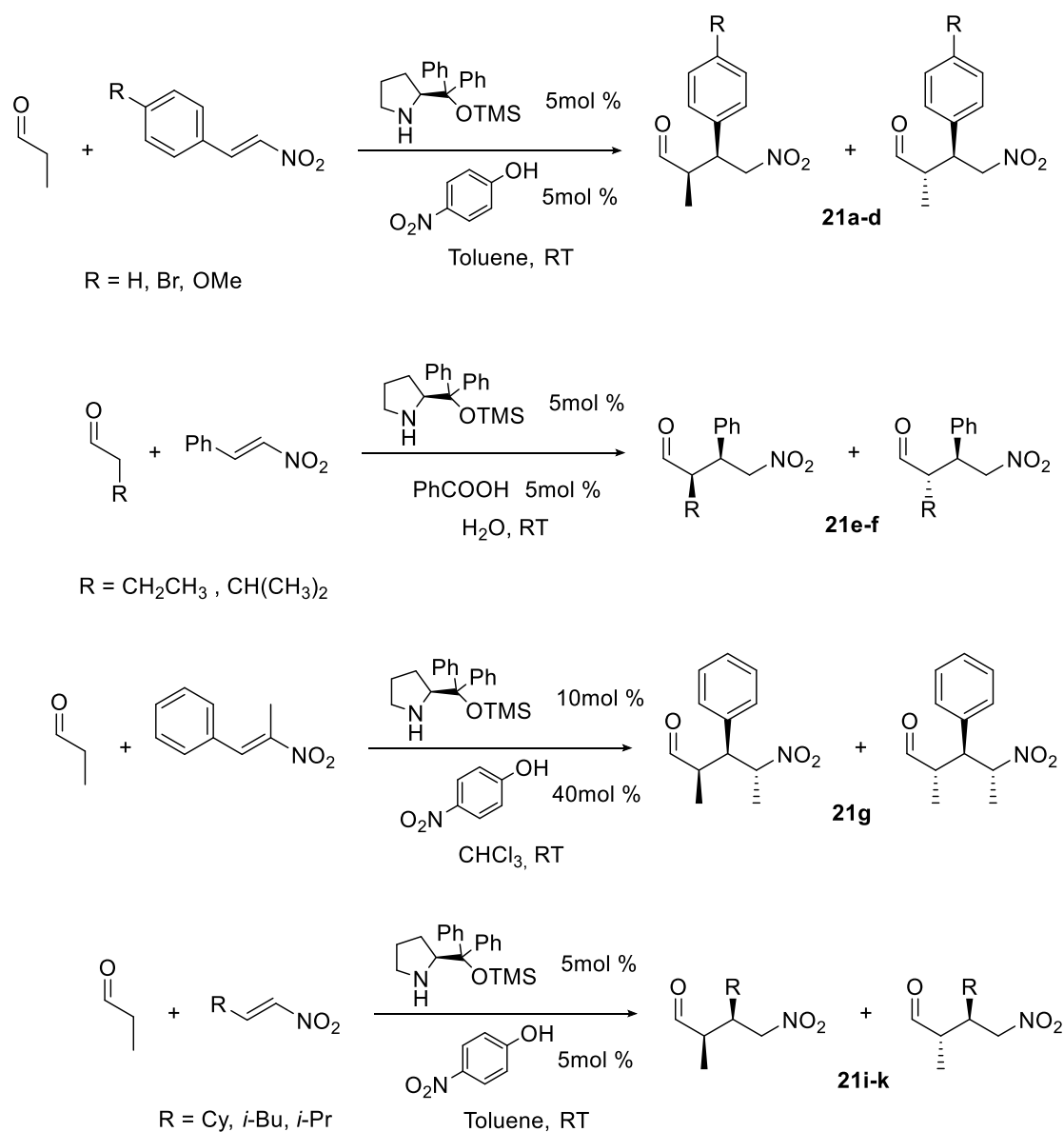
Optical rotation measurements were performed on a polarimeter Schmidt+Haensch UniPol L1000.

Flash chromatography purifications were carried out using Merck silica gel 60 (230-400 mesh particle size). Thin layer chromatography was performed on Merck 60 F254 plates.

Commercial reagents were used as received without additional purification.

Synthesis of aldehydes 1a-g.

Compounds **21a-g** are known and were prepared according to the literature procedures.⁵⁹ Aliphatic nitroalkenes are also known and were prepared according to the literature procedures.⁶⁰ Compound **21h** is commercially available and was used without further purification.



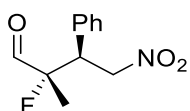
Scheme 28: synthesis of the starting materials

⁵⁹ a) K. Patora-Komisarskaa, M. Benohouda, H. Ishikawaa, D. Seebach, Y. Hayashi, *Helvetica Chimica Acta*, **2011**, *94*, 719. b) S. Zhu, S. Yu, D. Ma, *Angew. Chem. Int. Ed.* **2008**, *47*, 545 c) G. Sahoo, H. Rahaman, A. Madarász, I. Pápai, M. Melarto, A. Valkonen, P. M. Pihko, *Angew. Chem.*, **2012**, *124*, 13321.

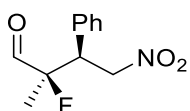
⁶⁰ a) Q. Yan, M. Liu, D. Kong, G. Zi, G. Hou, *Chem. Commun.* **2014**, *50*, 12870. b) Sivakumar, B. Venkata et al, *PCT Appl*, 2008117305, 02 oct **2008**.

General Procedure for the Organocatalyzed Fluorination of aldehydes **21**.

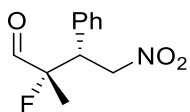
NFSI (0.058 mmol, 1.2 equiv) was added to a solution of aldehyde **21** (0.048 mmol, 1 equiv), **VIII** (20 mol%) and TFA (20% mol) in MTBE (0.2 mL). The mixture was stirred at room temperature and the conversion was monitored by TLC and ^1H NMR. The crude mixture was quenched with 0.1 mL of NH_4Cl (saturated solution) and extracted with AcOEt (3 \times 2 mL). The organic phases were collected and dried over Na_2SO_4 , the solvent was evaporated under reduced pressure without heating, and the product was purified by flash chromatography on silica gel (cyclohexane/ethyl acetate = 90/10).



anti-**23a** (*anti/syn* = 97:3): 75% yield, brown oil. ^1H NMR (400 MHz, CDCl_3) δ = 9.8 (d, J = 5 Hz, 1H, maj), 9.40(d, J = 5.3 Hz, 1H, min), 7.32(m, 5H,) 4.83 (dd, J = 10.3, 13.2 Hz, 1H, maj), 4.67(dd, J = 4.7, 13.2 Hz, 1H, maj), 3.98(ddd, J = 4.7, 10.2, 28.5 Hz, 1H, maj), 1.20(d, J = 22.3 Hz, 3H, maj). ^{13}C NMR (100 MHz, CDCl_3) δ = 199.9 (d, J = 39.2 Hz, 1C), 133.7, 129.33, 129.31, 129.3 (2C), 128.9, 99.6 (d, J = 185 Hz, 1C), 75.7 (d, J = 6.3 Hz, 1C), 48.6 (d, J = 19.2 Hz, 1C), 20.0 (d, J = 23.6 Hz, 1C). ^{19}F NMR (400 MHz, CDCl_3) δ = -169.7 (m, 1F). GC-MS: t_R = 13.58 min, m/z = 225 (2.8, M), 178 (18.5, M - HNO_2), 104 (100, PhCH_2CH_2). $[\alpha]_D^{25}$ = 38 (c = 0.50, CH_2Cl_2). $[\alpha]_D^{25}$ = -16 (c = 0.84, CH_2Cl_2). The enantiomeric excess was determined after reduction to the corresponding alcohol.

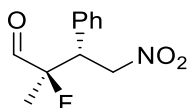


syn-**23a** (*anti/syn* = 11:89): 85% yield, brown oil. ^1H NMR (400 MHz, CDCl_3) δ = 9.8 (d, J = 5 Hz, 1H, min), 9.40 (d, J = 5.3 Hz, 1H, maj), 7.30 (m, 5H), 4.97 (dd, J = 5, 13.3 Hz, 1H, maj), 4.84 (dd, J = 9.8, 13.4 Hz, 1H, maj), 4.67 (dd, J = 4.7, 13.2 Hz, 1H, min), 3.95 (ddd, J = 5.1, 9.7, 26.9 Hz, 1H, maj), 1.54 (d, J = 21.7 Hz, 3H, maj). ^{13}C NMR (100 MHz, CDCl_3) δ = 199.7 (d, J = 39.2 Hz, 1C), 133.5, 129.14, 129.12, 129.07 (2C), 128.8, 99.4 (d, J = 185 Hz, 1C), 75.5 (d, J = 6.3 Hz, 1C), 48.4 (d, J = 19.2 Hz, 1C), 19.8 (d, J = 23.6 Hz, 1C). ^{19}F NMR (400 MHz, CDCl_3) δ = -168.3 (m, 1F, maj), -170.5 (m, 1F, min). GC-MS: t_R = 13.65 min, m/z = 225 (1, M), 178 (17.6, M - HNO_2), 104 (100, PhCH_2CH_2). The enantiomeric excess was determined after reduction to the corresponding alcohol.

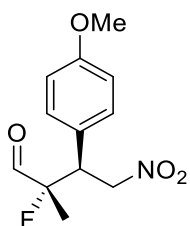


syn-**23b** (*anti/syn* = 16:84): 86% yield, brown oil. ^1H NMR (400 MHz, CDCl_3) δ = 9.8 (d, J = 5 Hz, 1H, min), 9.40 (d, J = 5.3 Hz, 1H, maj), 7.30 (m, 5H), 4.95 (dd, J = 5.0, 13.4 Hz, 1H, maj), 4.83 (dd, J = 9.7, 13.4 Hz, 1H, maj), 4.67(dd, J = 4.7, 13.2 Hz, 1H, min), 3.94 (ddd, J = 5.1, 9.7,

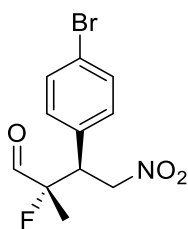
26.8 Hz, 1H, maj), 1.53 (d, $J = 21.8$ Hz, 3H, maj), 1.20(d, $J = 22.3$ Hz, 3H, min). ^{13}C -NMR (100 MHz, CDCl_3) $\delta = 199.7$ (d, $J = 39.2$ Hz, 1C), 133.5, 129.14, 129.12, 129.07(2C), 128.8, 99.4 (d, $J = 185$ Hz, 1C), 75.5 (d, $J = 6.3$ Hz, 1C), 48.4 (d, $J = 19.2$ Hz, 1C), 19.8 (d, $J = 23.6$ Hz, 1C). ^{19}F NMR (400 MHz, CDCl_3) $\delta = -168.3$ (m, 1F, maj), -170.5 (m, 1F, min). GC-MS: $t_{\text{R}} = 13.65$ min, $m/z = 225$ (1, M), 178 (17.6, M - HNO_2), 104 (100, PhCH_2CH_2). The enantiomeric excess was determined after reduction to the corresponding alcohol.



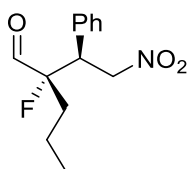
anti-23b (*anti/syn* = 96:4): 80% yield, brown oil. ^1H NMR (400 MHz, CDCl_3) $\delta = 9.8$ (d, $J = 5$ Hz, 1H, min), 9.40 (d, $J = 5.3$ Hz, 1H, maj), 7.30 (m, 5H), 4.97 (dd, $J = 5, 13.3$ Hz, 1H, maj), 4.84 (dd, $J = 9.8, 13.4$ Hz, 1H, maj), 4.67 (dd, $J = 4.7, 13.2$ Hz, 1H, min), 3.95 (ddd, $J = 5.1, 9.7, 26.9$ Hz, 1H, maj), 1.54 (d, $J = 21.7$ Hz, 3H, maj). ^{13}C NMR (100 MHz, CDCl_3) $\delta = 199.9$ (d, $J = 39.2$ Hz, 1C), 133.7, 129.33, 129.31, 129.3 (2C), 128.9, 99.6 (d, $J = 185$ Hz, 1C), 75.7 (d, $J = 6.3$ Hz, 1C), 48.6 (d, $J = 19.2$ Hz, 1C), 20.0 (d, $J = 23.6$ Hz, 1C). ^{19}F NMR (400 MHz, CDCl_3) $\delta = -169.7$ (m, 1F). GC-MS: $t_{\text{R}} = 13.58$ min, $m/z = 225$ (2.8, M), 178 (18.5, M - HNO_2), 104 (100, PhCH_2CH_2). The enantiomeric excess was determined after reduction to the corresponding alcohol.



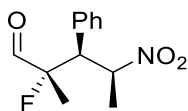
anti-23c (*anti/syn* = 93:7): 79% yield, brown oil. ^1H NMR (400 MHz, CDCl_3) $\delta = 9.77$ (d, $J = 5.1$ Hz, 1H, maj), 9.38(d, $J = 5.4$ Hz, 1H, min), 7.18(d, $J = 8.6$ Hz, 2H, maj), 6.87 (m, 2H, maj), 6.83(m, 2H, min), 4.91(dd, $J = 5, 13.1$ Hz, 1H, min), 4.76 (dd, $J = 10.4, 13$ Hz, 1H, maj), 4.61 (dd, $J = 4.7, 13$ Hz, 1H, maj), 3.90 (ddd, $J = 4.7, 10.4, 28.5$ Hz, 1H, maj), 3.78 (s, 3H, maj), 3.76 (s, 3H, min), 1.18 (d, $J = 22.4$ Hz, 3H, maj). ^{13}C NMR (100 MHz, CDCl_3) $\delta = 199.9$ (d, $J = 5, 39$ Hz, 1C), 159.8, 130.2 (2C), 125.3, 114.4 (2C), 99.6 (d, $J = 184.4$ Hz, 1C), 75.7 (d, $J = 6.2$ Hz, 1C), 55.2, 47.8 (d, $J = 19.3$ Hz, 1C), 19.8 (d, $J = 23.4$ Hz, 1C). ^{19}F NMR (400 MHz, CDCl_3) $\delta = -167.8$ (m, 1F, min), -169.8 (dq, $J = 27.3, 22.4, 5.3$ Hz 1F, maj). GC-MS: $t_{\text{R}} = 16.49$ min, $m/z = 255$ (9.2, M), 208 (8.6, M - HNO_2), 134 (100, $\text{CH}_3\text{OPhCH}_2\text{CH}_2$). $[\alpha]_{\text{D}}^{25} = -26.4$ ($c = 1.2, \text{CH}_2\text{Cl}_2$). The enantiomeric excess was not determined.



anti-23d (*anti/syn* = 95:5): 53% yield, brown oil. ^1H NMR (400 MHz, CDCl_3) δ = 9.79 (d, J = 4.8 Hz, 1H, maj), 9.41 (d, J = 5.1 Hz, 1H, min), 7.52 (d, J = 8.5 Hz, 2H, maj), 7.18 (d, J = 8.5, 2H, maj), 4.78 (dd, J = 10.6, 13.1 Hz, 1H, maj), 4.63 (dd, J = 4.5, 13.3 Hz, 1H, maj), 3.95 (ddd, J = 4.6, 10.6, 28.8 Hz, 1H, maj), 1.20 (d, J = 22.3 Hz, 3H, maj). ^{13}C NMR (100 MHz, CDCl_3) δ = 199.4 (d, J = 39.6 Hz, 1C), 132.6, 130.3 (2C), 130.8 (2C), 123.1, 99.1 (d, J = 185 Hz, 1C), 75.3 (d, J = 6.1 Hz, 1C), 47.9 (d, J = 19.1 Hz, 1C), 19.9 (d, J = 23.4 Hz, 1C). ^{19}F NMR (400 MHz, CDCl_3) δ = -170 (m, 1F, min), -168 (dq, J = 27.4, 22.2, 8.4 Hz 1F, maj). GC-MS: t_R = 16.90 min, m/z = 305 (8.3, M), 258 (22, M - HNO_2), 182 (100, $\text{BrPhCH}_2\text{CH}_2$). $[\alpha]_D^{25}$ = -20 (c = 1.12, CH_2Cl_2). The enantiomeric excess was determined for the corresponding starting aldehyde **21d**.

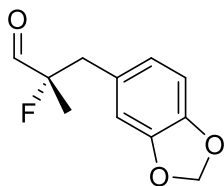


anti-23e (*anti/syn* = 82:15): 35% yield, brown oil. ^1H NMR (400 MHz, CDCl_3) δ = 9.81 (d, J = 5.6 Hz, 1H, maj), 9.40 (d, J = 5.9 Hz, 1H, min), 7.33 (m, 5H), 4.94 (dd, J = 4.9, 13.4 Hz, 1H, min), 4.81 (dd, J = 10.3, 13.2 Hz, 1H, maj), 4.61 (dd, J = 4.5, 13.2 Hz, 1H, maj), 3.97 (ddd, J = 4.4, 10.4, 28.9 Hz, 1H, maj), 1.53 (m, 2H), 1.28 (m, 2H), 0.93 (t, J = 7.4 Hz, 3H, min), 0.78 (t, J = 7.3 Hz, 3H, min). ^{13}C NMR (100 MHz, CDCl_3) δ = 199.7 (d, J = 39.2 Hz, 1C, maj), 133.5, 129.14, 129.12, 129.07 (2C), 128.8, 99.4 (d, J = 185 Hz, 1C), 75.5 (d, J = 6.3 Hz, 1C), 48.4 (d, J = 19.2 Hz, 1C), 19.8 (d, J = 23.6 Hz, 1C). ^{19}F NMR (400 MHz, CDCl_3) δ = -176.5 (m, 1F, min), -177 (ddt, J = 5.6, 10.4, 29.7 Hz, 1F, maj). GC-MS: t_R = 15.56 min (maj), m/z = 206 (8.3, M - HNO_2), 150 (22, M - $\text{PhC}_2\text{H}_3\text{NO}_2$), 104 (100, $\text{PhC}_2\text{H}_2\text{NO}_2$), t_R = 15.66 min (min), m/z = 206 (8.3, M - HNO_2), 104 (100, $\text{PhC}_2\text{H}_2\text{NO}_2$). The enantiomeric excess was determined for the corresponding starting aldehyde **21e**.

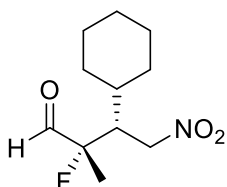


anti-23g (*anti/syn* = 96:4): 35% yield, brown oil. ^1H NMR (400 MHz, CDCl_3) δ = 9.91 (d, J = 5.1 Hz, 1H), 7.34 (m, 5H), 5.11 (dq, J = 10.3, 6.8 Hz, 1H), 3.78 (dd, J = 30.4, 10.2 Hz, 1H), 1.54 (d, J = 6.7 Hz, 3H), 1.97 (d, J = 22.5 Hz, 3H). ^{13}C NMR (100 MHz, CDCl_3) δ = 200.5 (d, J = 40.1 Hz, 1C), 134.7, 129.5 (2C), 129.1 (2C), 128.8, 100.2 (d, J = 186.5 Hz, 1C), 85.7 (d, J = 6.0 Hz, 1C), 54.2 (d, J = 18.8 Hz, 1C), 21.5 (d, J = 23.6 Hz, 1C), 20.5. ^{19}F NMR (400 MHz, CDCl_3) δ = -172.4

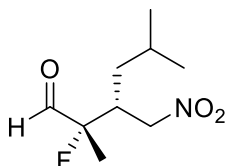
(m, 1F). GC-MS: t_R = 14.11 min, m/z = 221 (8, M-F), 118 (100, PhCHCHCH₃), 91 (60, PhCH₂)
[α]_D²⁵ = 5 (c = 0.11, CH₂Cl₂). The enantiomeric excess was not determined.



23h: 75% yield, brown oil. ¹H NMR (400 MHz, CDCl₃) δ = 9.7 (d, J = 5 Hz, 1H), 6.70 (m, 4H), 5.95 (s, 2H), 3.05 (dd, J = 14.6, 24.6 Hz, 1H), 2.89 (dd, J = 14.6, 23.3 Hz, 1H), 1.38 (d, J = 21.5 Hz, 3H). ¹³C NMR (100 MHz, CDCl₃) δ = 202 (d, J = 40.6 Hz, 1C), 147.1 (d, J = 84.1, 1C), 127.3, 123.6, 110.7, 108.1, 101.0, 98.7 (d, J = 179.2, 1C), 41.6 (d, J = 21.5 Hz, 1C), 20.3 (d, J = 23.6 Hz, 1C). ¹⁹F NMR (400 MHz, CDCl₃) δ = -155.4 (m, 1F). GC-MS: t_R = 12.88 min, m/z = 218 (20, M), 135 (100, PhC₂H₄O₂). The enantiomeric excess was determined after reduction to the corresponding alcohol.

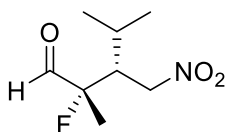


23i: (*anti/syn* = 91:9): 85% yield, yellow oil. ¹H NMR (400 MHz, CDCl₃) δ = 9.79 (d, J = 5.9 Hz, 1H, maj), 9.74 (d, J = 5.4 Hz, 1H, min), 4.60 (dd, J = 14.6, 6.5 Hz, 1H, min), 4.51 (dd, J = 14.1, 5.9 Hz, 1H, maj), 4.44 (dd, J = 14.5, 5.1 Hz, 1H, maj), 2.84 (dtd, J = 20.0, 5.8, 2.9 Hz, 1H, maj), 1.72 (m, 4H, maj), 1.47 (d, J = 22.4 Hz, 3H, maj), 1.16 (s, 7H, maj). ¹³C NMR (100 MHz, CDCl₃) δ = 200.1 (d, J = 39.2 Hz, 1C), 99.5 (d, J = 182.2 Hz, 1C), 72.4 (d, J = 7.7 Hz, 1C), 47.6 (d, J = 20.5 Hz, 1C), 36.9 (d, J = 1.5 Hz, 1C), 31.8 (d, J = 1.1 Hz, 1C), 28.9 (d, J = 2.3 Hz, 1C), 26.7, 26.4, 26.0, 19.4 (d, J = 23.7 Hz, 1C). ¹⁹F NMR (400 MHz, CDCl₃) δ = -162.3 (dp, J = 22.1, 5.4 Hz, 1F, maj), -167.6 (m, 1F, min). GC-MS: t_R = 14.15 min, m/z = 202 (5, M-CHO), 83 (60, Cycloesyl) 55 (100, CH₃CHCHCH₂).



23j: (*anti/syn* = 84:16): 81% yield, yellow oil. ¹H NMR (400 MHz, CDCl₃) δ = 9.73 (d, J = 5.4 Hz, 1H, maj), 9.69 (d, J = 5.5 Hz, 1H, min), 4.55 (dd, J = 13.4, 6.4 Hz, 1H, maj), 4.40 (dd, J = 12.5, 7.2 Hz, 1H, min), 4.29 (ddd, J = 13.4, 5.3, 1 Hz, 1H, maj), 2.89 (m, 1H, maj), 1.57 (m, 2H, maj), 1.40 (d, J = 22.4 Hz, 3H, maj), 1.18 (m, 1H, maj), 0.91 (dd, J = 7.0 Hz, 3H, maj), 0.92 (d, J = 6.6 Hz, 3H, maj), 0.90 (d, J = 6.4 Hz, 3H, maj). ¹³C NMR (100 MHz, CDCl₃) δ = 199.9 (d, J = 39.9 Hz, 1C), 99.9 (d, J = 179.6 Hz, 1C), 75.1 (d, J = 6.1 Hz, 1C), 40.2 (d, J = 21.4 Hz, 1C), 36.2 (d, J =

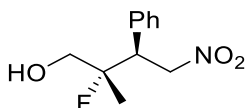
3.5 Hz, 1C), 25.8, 23.4, 21.4, 17.7 (d, $J = 23.6$ Hz, 1C). ^{19}F NMR (400 MHz, CDCl_3) $\delta = -161.9$ (dq, $J = 22.5, 14.1, 4.6$ Hz 1F, maj), -167.6 (m, 1F, min). GC-MS: $t_R = 9.97$ min, $m/z = 192$ (100, isobutylene).



23k: (*anti/syn* = 83:17): 25% yield, brown oil. ^1H NMR (400 MHz, CDCl_3) $\delta = 9.78$ (d, $J = 6.0$ Hz, 1H, maj), 9.69 (d, $J = 5.5$ Hz, 1H, min), 4.59 (dd, $J = 14.6, 6.6$ Hz, 1H, min), 4.50 (dd, $J = 14.1, 6.1$ Hz, 1H, maj), 4.38 (ddd, $J = 14.2, 5.2, 1$ Hz, 1H, maj), 2.86 (dtd, $J = 21.0, 5.9, 2.9$ Hz, 1H, maj), 2.20 (pd, $J = 7.0, 3.0$ Hz, 4H, maj), 1.46 (d, $J = 22.4$ Hz, 3H, maj), 1.38 (d, $J = 22.0$ Hz, 3H, min), 1.01 (d, $J = 7.0$ Hz, 3H, maj), 0.9 (dd, $J = 6.9, 1.3$ Hz, 3H, maj). ^{13}C NMR (100 MHz, CDCl_3) $\delta = 200.2$ (d, $J = 39.7$ Hz, 1C), 99.7 (d, $J = 182.5$ Hz, 1C), 71.8 (d, $J = 7.1$ Hz, 1C), 47.5 (d, $J = 20.3$ Hz, 1C), 29.8, 21.6, 19.4 (d, $J = 23.8$ Hz, 1C), 18.2. ^{19}F NMR (400 MHz, CDCl_3) $\delta = -164.3$ (dq, $J = 22.1, 21.6, 4.6$ Hz 1F, maj), -169.4 (m, 1F, min). GC-MS: $t_R = 9.45$ min, $m/z = 115$ (50, $\text{NO}_2\text{CHCHCH}(\text{CH}_3)_2$).

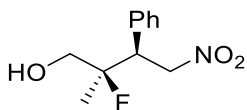
General Procedure for the reduction of fluorinated aldehydes **23**.

NaBH_4 (0.45 mmol, 3 equiv) was added to a solution of the aldehyde **23** (0.15 mmol, 1 equiv) in MeOH (1.5 mL) at 0°C . The mixture was stirred at room temperature and the conversion was monitored by TLC. The crude mixture was quenched with 1 mL of NH_4Cl (saturated solution) and extracted with AcOEt (3×3 mL). The organic phases were collected and dried over Na_2SO_4 , the solvent was evaporated under reduced pressure and the product was purified by flash chromatography on silica gel (cyclohexane/ethyl acetate = 85/15).

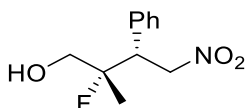


anti-27a (*anti/syn* = 97:3): ^1H NMR (400 MHz, CDCl_3) $\delta = 7.32$ (m, 5H), 5.04 (m, 1H), 4.89 (dd, $J = 10.1, 13.2$ Hz, 1H), 4.21 (ddd, $J = 13.5, 10.1, 5.8$ Hz, 1H, maj), 3.88 (ddd, $J = 14.9, 8.4, 6.6$ Hz, 1H, min), 1.36 (d, $J = 22.2$ Hz, 3H, min), 1.23 (d, $J = 22.4$ Hz, 3H, maj). ^{13}C NMR (100 MHz, CDCl_3) $\delta = 135.5$ (d, $J = 5.0$ Hz, 1C, min), 135.3 (d, $J = 6.6$ Hz, 1C, maj), 129.2, 129.0 (3C), 128.4, 98.2 (d, $J = 175.5$ Hz, 1C, maj), 97.6 (d, $J = 177.1$ Hz, 1C, min), 76.5 (d, $J = 5.7$ Hz, 1C, min), 75.7 (d, $J = 5.2$ Hz, 1C, maj), 66.8 (d, $J = 23.5$ Hz, 1C, maj), 66.2 (d, $J = 24.6$ Hz, 1C, min), 51.1 (d, $J = 21.0$ Hz, 1C, min), 47.9 (d, $J = 21.3$ Hz, 1C, maj), 21.7 (d, $J = 23.3$ Hz, 1C, min), 18.7 (d, $J = 23.4$ Hz, 1C, maj). ^{19}F NMR (400 MHz, CDCl_3) $\delta = -159.1.7$ (m, 1F, maj), -160.0 (m, 1F, min). GC-MS: $t_R = 15.75$ min, $m/z = 227$ (2.4, M), 180 (10, M - HNO_2), 150 (15, M - CHOH), 104 (100, PhCH_2CH_2). $[\alpha]_D^{25} = -9.6$ ($c = 0.16$, CH_2Cl_2). CSP-HPLC: IC 95/5 *n*-Hex/IPA, flow rate 0.5

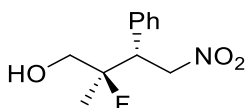
mL/min at 40 °C; λ 214 nm; t_R = 26.3 min (*syn* major), 30.1 min (*syn* minor), 37.2 min (*anti* major), 43.1 min (*anti* minor).



syn-27a (*anti/syn* = 11:89): ^1H NMR (400 MHz, CDCl_3) δ = 7.32 (m, 5H), 5.04 (m, 1H), 4.89 (dd, J = 10.1, 13.2 Hz, 1H), 4.21 (ddd, J = 13.5, 10.1, 5.8 Hz, 1H, min), 3.88 (ddd, J = 14.9, 8.4, 6.6 Hz, 1H, maj), 1.36 (d, J = 22.2 Hz, 3H, maj), 1.23 (d, J = 22.4 Hz, 3H, min). ^{13}C NMR (100 MHz, CDCl_3) δ = 135.5 (d, J = 5.0 Hz, 1C, maj), 135.3 (d, J = 6.6 Hz, 1C, min), 129.2, 129.0 (3C), 128.4, 98.2 (d, J = 175.5 Hz, 1C, min), 97.6 (d, J = 177.1 Hz, 1C, maj), 76.5 (d, J = 5.7 Hz, 1C, maj), 75.7 (d, J = 5.2 Hz, 1C, min), 66.8 (d, J = 23.5 Hz, 1C, min), 66.2 (d, J = 24.6 Hz, 1C, maj), 51.1 (d, J = 21.0 Hz, 1C, maj), 47.9 (d, J = 21.3 Hz, 1C, min), 21.7 (d, J = 23.3 Hz, 1C, maj), 18.7 (d, J = 23.4 Hz, 1C, min). ^{19}F NMR (400 MHz, CDCl_3) δ = -159.1.7 (m, 1F, min), -160.0 (m, 1F, maj). GC-MS: t_R = 15.76 min, m/z = 227 (0.5, M), 180 (17, M - HNO_2) 150 (17.5, M - CHOH), 104 (100, PhCH_2CH_2). CSP-HPLC: IC 95/5 *n*-Hex/IPA, flow rate 0.5 mL/min at 40 °C; λ 214 nm; t_R = 26.3 min (*syn* major), 32.5 min (*syn* minor), 37.3 min (*anti* major), 43.1 min (*anti* minor).

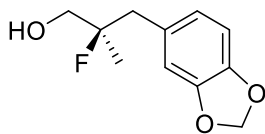


syn-27b (*anti/syn* = 16:84): ^1H NMR (400 MHz, CDCl_3) δ = 9.8 (d, J = 5 Hz, 1H, min), 9.40 (d, J = 5.3 Hz, 1H, maj), 7.30 (m, 5H), 4.95 (dd, J = 5.0, 13.4 Hz, 1H, maj), 4.83 (dd, J = 9.7, 13.4 Hz, 1H, maj), 4.67 (dd, J = 4.7, 13.2 Hz, 1H, min), 3.94 (ddd, J = 5.1, 9.7, 26.8 Hz, 1H, maj), 1.53 (d, J = 21.8 Hz, 3H, maj), 1.20 (d, J = 22.3 Hz, 3H). ^{13}C NMR (100 MHz, CDCl_3) δ = 135.5 (d, J = 5.0 Hz, 1C, maj), 135.3 (d, J = 6.6 Hz, 1C, min), 129.2, 129.0 (3C), 128.4, 98.2 (d, J = 175.5 Hz, 1C, min), 97.6 (d, J = 177.1 Hz, 1C, maj), 76.5 (d, J = 5.7 Hz, 1C, maj), 75.7 (d, J = 5.2 Hz, 1C, min), 66.8 (d, J = 23.5 Hz, 1C, min), 66.2 (d, J = 24.6 Hz, 1C, maj), 51.1 (d, J = 21.0 Hz, 1C, maj), 47.9 (d, J = 21.3 Hz, 1C, min), 21.7 (d, J = 23.3 Hz, 1C, maj), 18.7 (d, J = 23.4 Hz, 1C, min). ^{19}F NMR (400 MHz, CDCl_3) δ = -159.1.7 (m, 1F, min), -160.0 (m, 1F, maj). GC-MS: t_R = 15.76 min, m/z = 227 (0.5, M), 180 (17, M - HNO_2) 150 (17.5, M - CHOH), 104 (100, PhCH_2CH_2). CSP-HPLC: IC 95/5 *n*-Hex/IPA, flow rate 0.5 mL/min at 40 °C; λ 214 nm; t_R = 26.3 min (*syn* minor), 30.1 min (*syn* major), 37.4 min (*anti* minor), 42.3 min (*anti* major).



anti-27b (*anti/syn* = 96:4): ^1H NMR (400 MHz, CDCl_3) δ = 7.32 (m, 5H), 5.04 (m, 1H), 4.89 (dd, J = 10.1, 13.2 Hz, 1H), 4.21 (ddd, J = 13.5, 10.1, 5.8 Hz, 1H, maj), 3.88 (ddd, J = 14.9, 8.4, 6.6 Hz, 1H, min), 1.36 (d, J = 22.2 Hz, 3H, min), 1.23 (d, J = 22.4 Hz, 3H, maj). ^{13}C NMR (100 MHz, CDCl_3) δ = 135.5 (d, J = 5.0 Hz, 1C, min), 135.3 (d, J = 6.6 Hz, 1C, maj), 129.2, 129.0 (3C), 128.4, 98.2 (d, J = 175.5 Hz, 1C, maj), 97.6 (d, J = 177.1 Hz, 1C, min), 76.5 (d, J = 5.7 Hz, 1C, min), 75.7 (d, J = 5.2 Hz, 1C, maj), 66.8 (d, J = 23.5 Hz, 1C, maj), 66.2 (d, J = 24.6 Hz, 1C, min), 51.1

(d, $J = 21.0$ Hz, 1C, min), 47.9 (d, $J = 21.3$ Hz, 1C, maj), 21.7 (d, $J = 23.3$ Hz, 1C, min), 18.7 (d, $J = 23.4$ Hz, 1C, maj)¹⁹F NMR (400 MHz, CDCl₃) $\delta = -159.1.7$ (m, 1F, maj), -160.0 (m, 1F, min). GC-MS: $t_R = 15.75$ min, $m/z = 227$ (2.4, M), 180 (10, M - HNO₂), 150 (15, M - CHO), 104 (100, PhCH₂CH₂). CSP-HPLC: IC 95/5 *n*-Hex/IPA, flow rate 0.5 mL/min at 40 °C; λ 214 nm; $t_R = 26.4$ min (*syn* minor), 29.9 min (*syn* major), 37.4 min (*anti* minor), 43.1 min (*anti* major).



27h: ¹H NMR (400 MHz, CDCl₃) $\delta = 6.73$ (m, 2H), 6.66 (m, 1H), 5.92 (s, 2H), 3.56 (d, $J = 19.4$ Hz, 2H), 2.89 (m, 2H), 1.24 (d, $J = 21.9$ Hz, 3H). ¹³C NMR (100 MHz, CDCl₃) $\delta = 146.1$ (d, $J = 112.1$, 1C), 129.5, 123.3, 110.7, 108.0, 100.8, 97.2 (d, $J = 169.8$, 1C), 67.5 (d, $J = 24$ Hz, 1C), 41.9 (d, $J = 23$ Hz, 1C), 20.8 (d, $J = 23.7$ Hz, 1C). ¹⁹F NMR (400 MHz, CDCl₃) $\delta = -155.4$ (m, 1F). GC-MS: $t_R = 14.37$ min, $m/z = 192$ (83, M - HF), 135 (100, CH₃PhO₂CH₂). CSP-HPLC: OD-H, 95/5 *n*-Hex/IPA, for 10 min, flow rate 0.5 mL/min at 40 °C; λ 214 nm; $t_R = 22.7$ min (minor), 23.9 min (major).

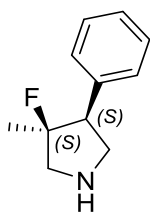
General Procedure for the Michael/Fluorination one-pot reaction.

Propanal (0.15 mmol, 1.5 equiv) was added dropwise to a solution of *trans*- β -nitrostyrene (0.1 mmol, 1 equiv), *p*-nitrophenol (20 mol%) and catalyst **VIII** (20 mol%) in toluene (600 μ L). The reaction was stirred at room temperature for 1 h. Then the solvent was evaporated under reduced pressure and the crude mixture was dissolved in MTBE (600 μ L). TFA (20 mol%) and NFSI (0.12 mmol, 1.2 equiv) were added and the mixture was stirred at room temperature for 16 h. The crude mixture was quenched with 1 mL of NH₄Cl (saturated solution) and extracted with AcOEt (3 \times 2 mL). The organic phases were collected and dried over Na₂SO₄, the solvent was evaporated under reduced pressure without heating, and the product was purified by flash chromatography on silica gel (cyclohexane/ethyl acetate = 90/10).

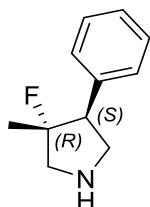
General Procedure for the synthesis of pyrrolidines **4**.⁶¹

Ni-Raney (2.1 mmol, 5 equiv) was added at room temperature to the fluorinated aldehyde *anti*-**23a** or *syn*-**23a** (0.42 mmol, 1 equiv) dissolved in MeOH (3.5 mL). After stirring the reaction mixture for 24 h under hydrogen atmosphere (balloon, 1 bar), the reaction was filtered through a pad of celite and the solvent was evaporated under reduced pressure. The crude product was purified by flash chromatography (DCM/MeOH/NH₄OH = 80:19:1) to provide the pure product **24**.

⁶¹ D. Petruzzello, A. Gualandi, S. Grilli, P. G. Cozzi, *Eur. J. Org. Chem.* **2012**, 6697.



cis-**24**: 13% yield, yellow oil. ^1H NMR (400 MHz, CDCl_3) δ = 7.34 (m, 2H), 7.25 (m, 3H), 3.74 (dd, J = 11.8, 8.1, 1H), 3.43 (dt, J = 26.1, 7.1, 3H), 3.35 (dd, J = 17.3, 13.1, 1H), 3.25 (dd, J = 11.8, 5.7 Hz, 1H), 2.96 (dd, J = 34.3, 13.2 Hz, 1H), 1.11 (d, J = 22.1 Hz, 3H). ^{13}C NMR (100 MHz, CDCl_3) δ = 135.2, 129.6, 129.5, 128.5 (2C), 127.6, 101.6 (d, J = 179.8 Hz, 1C), 58.0 (d, J = 24.4 Hz, 1C), 54.8 (d, J = 19.2 Hz, 1C), 51.3, 20.1 (d, J = 27.1 Hz, 1C). ^{19}F NMR (400 MHz, CDCl_3) δ = -155.5(m, 1F). HPLC-MS (ESI) t_r = 2.43 min; $[\text{M}+\text{H}]^+$ 180.0 m/z. $[\alpha]_{\text{D}}^{25}$ = -55 (c = 0.31, CH_2Cl_2).



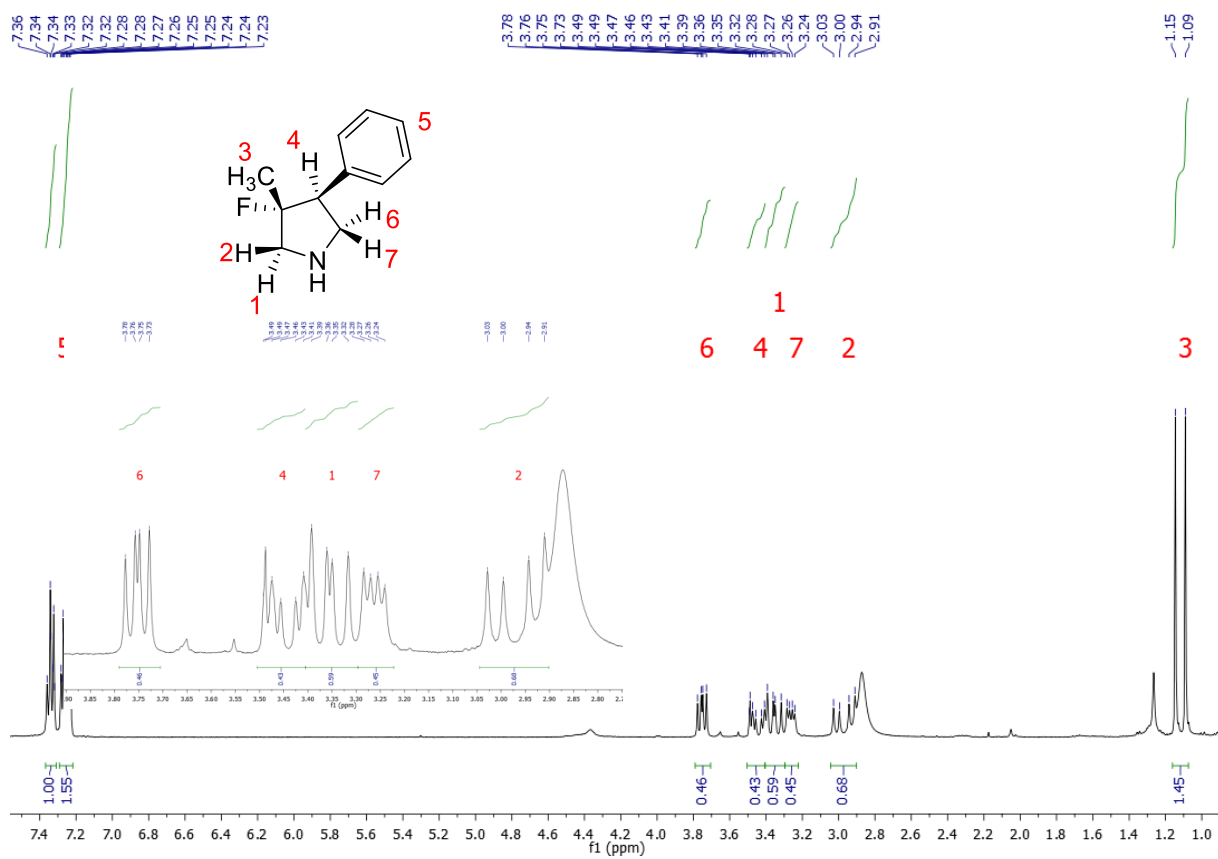
trans-**24**: 33% yield, yellow oil. ^1H NMR (400 MHz, CDCl_3) δ = 7.30 (m, 5H), 3.56 (m, 3H), 3.34 (dd, J = 34.8, 13.1, 1H), 3.19 (dt, J = 30.5, 9.8 Hz, 1H), 1.37 (d, J = 20.8 Hz, 3H). ^{13}C NMR (100 MHz, CDCl_3) δ = 139.9 (d, J = 8.7 Hz, 1C), 128.8 (1C), 128.4 (1C), 127.3, 105.7 (d, J = 175.2 Hz, 1C), 57.8 (d, J = 25.1 Hz, 1C), 55.7 (d, J = 24.3 Hz, 1C), 53.1, 19.9 (d, J = 26.0 Hz, 1C). ^{19}F NMR (400 MHz, CDCl_3) δ = -130.9(m, 1F). HPLC-MS (ESI) t_r = 2.48 min; $[\text{M}+\text{H}]^+$ 180.0 m/z. $[\alpha]_{\text{D}}^{25}$ = 21 (c = 1.13, CH_2Cl_2).

Determination of Stereochemistry of Pyrrolidines *cis*-**24** and *trans*-**24**

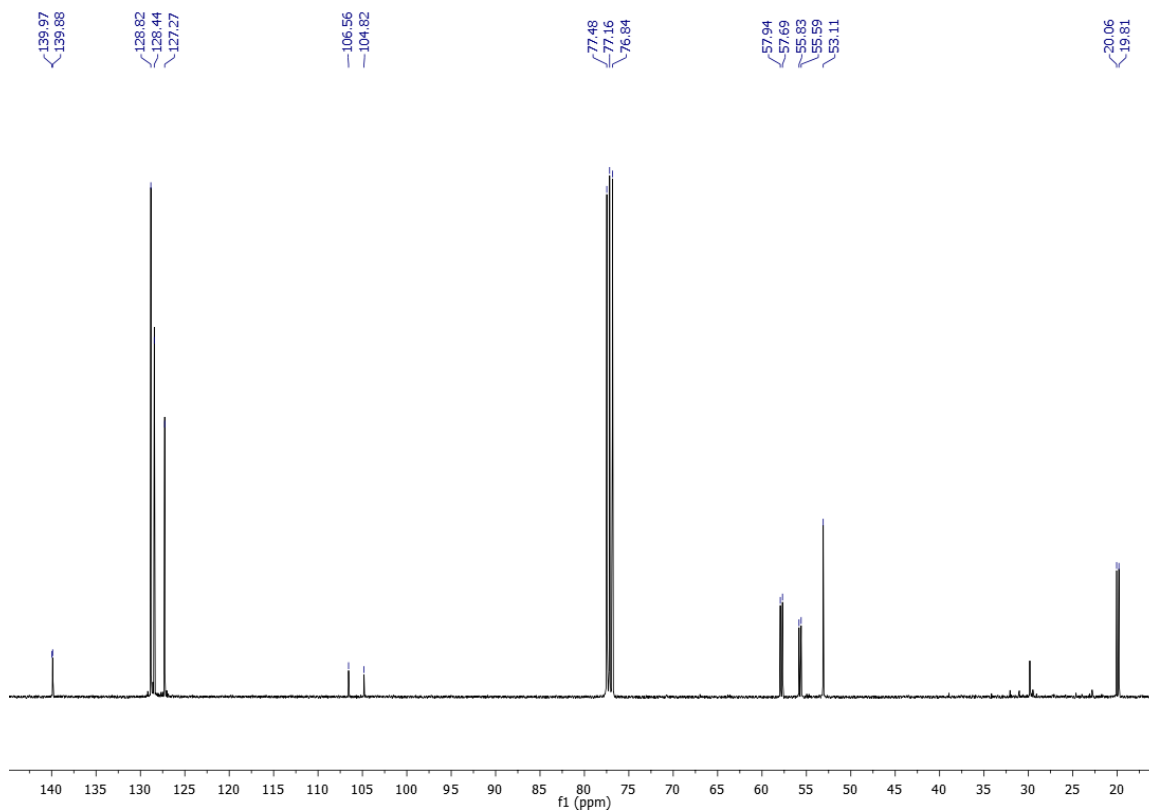
1D NOESY experiments on both the stereoisomers of compound **24** allowed us to establish the relative configuration of the two stereocenters present in the molecules.

Based on the known absolute stereochemistry of the $\text{C}\beta$ stereocenter of starting aldehyde **21a**, we were able to establish also the absolute stereochemistry of products **24**.

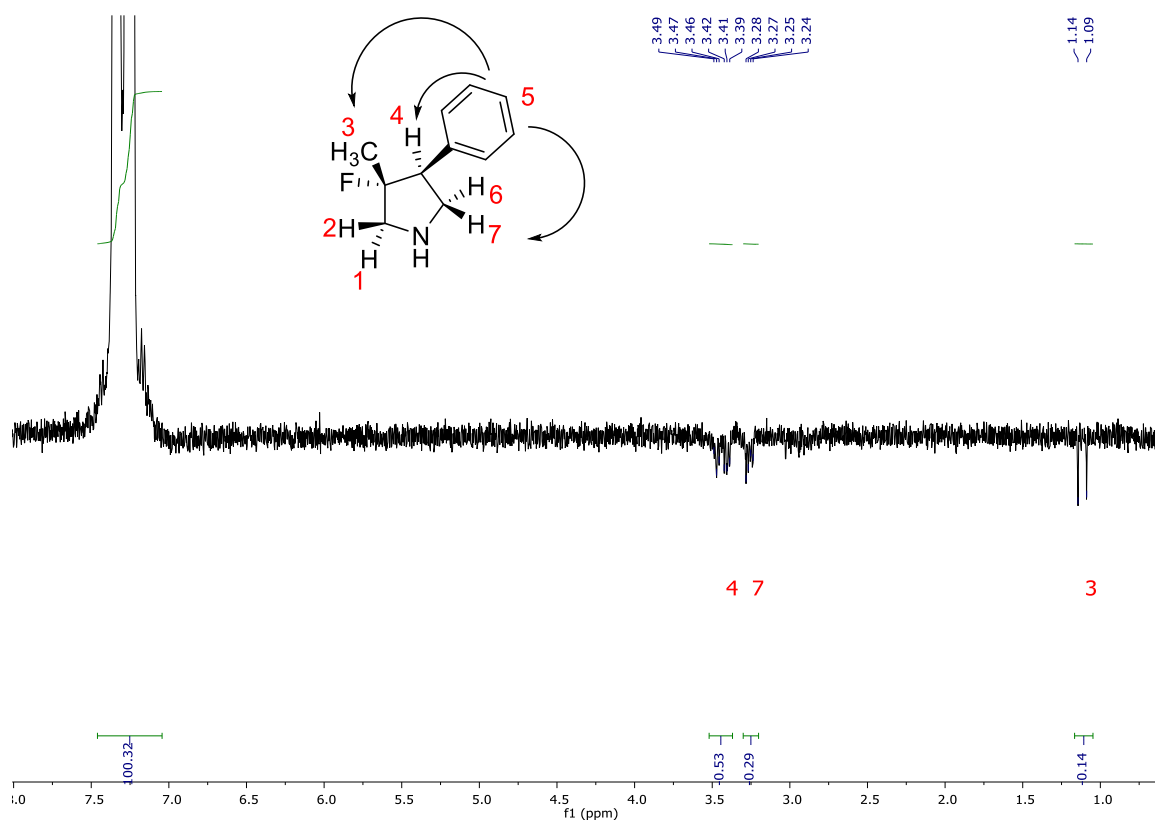
The stereochemistry established for the two isomers of pyrrolidine **24** was extended to all the products of this series, obtained with the same catalytic system.



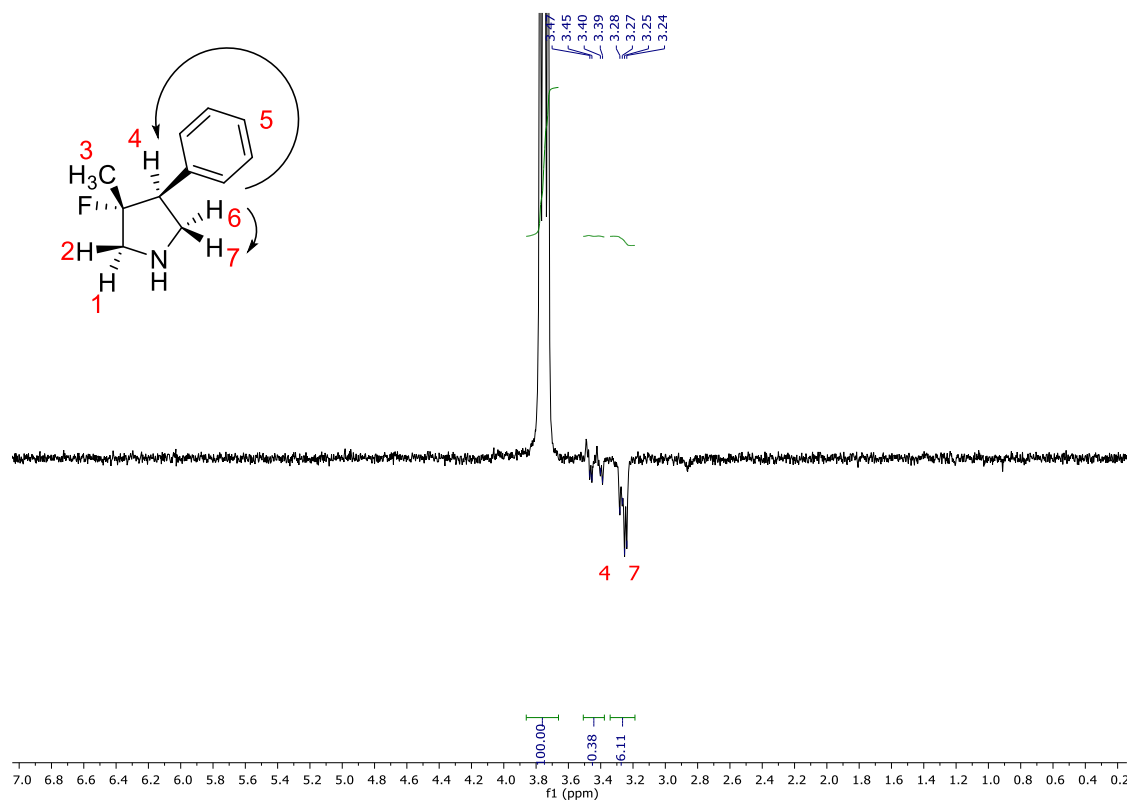
¹H NMR spectrum of isomer *trans*-24.



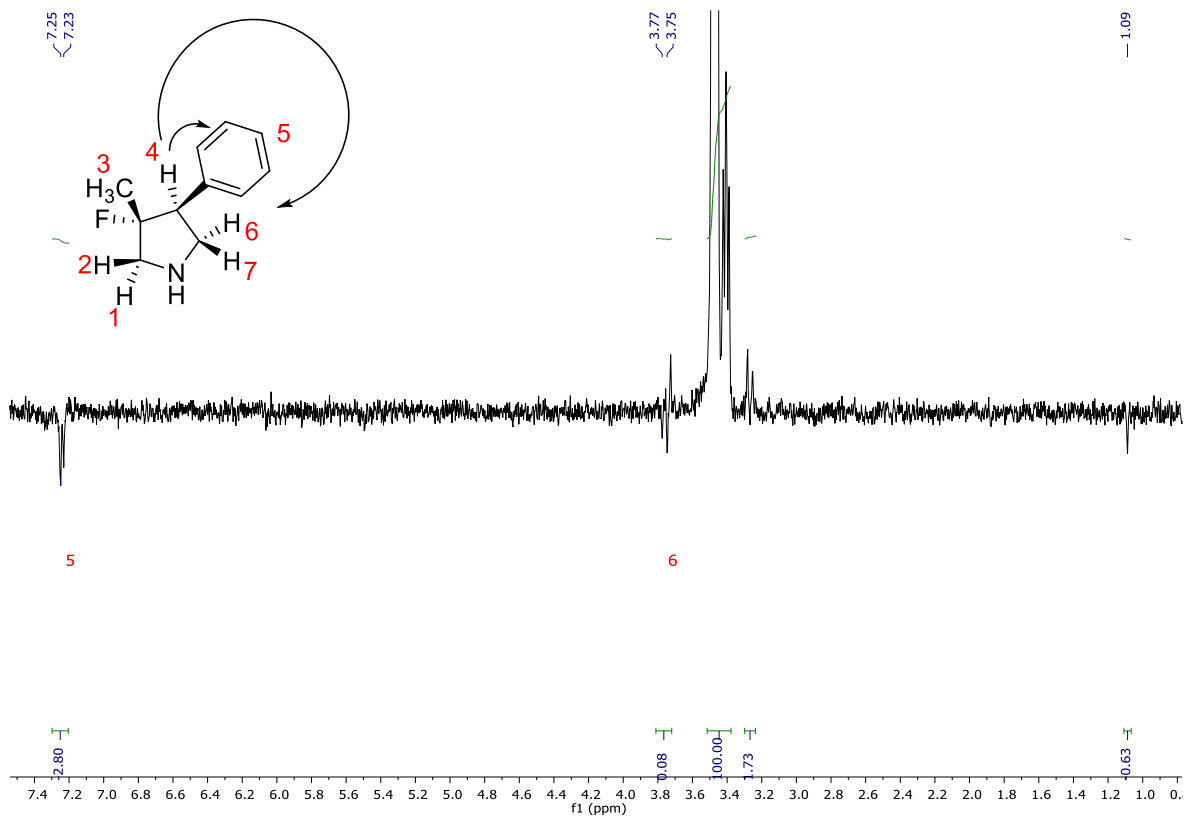
¹³C-NMR spectrum of *trans*-24.



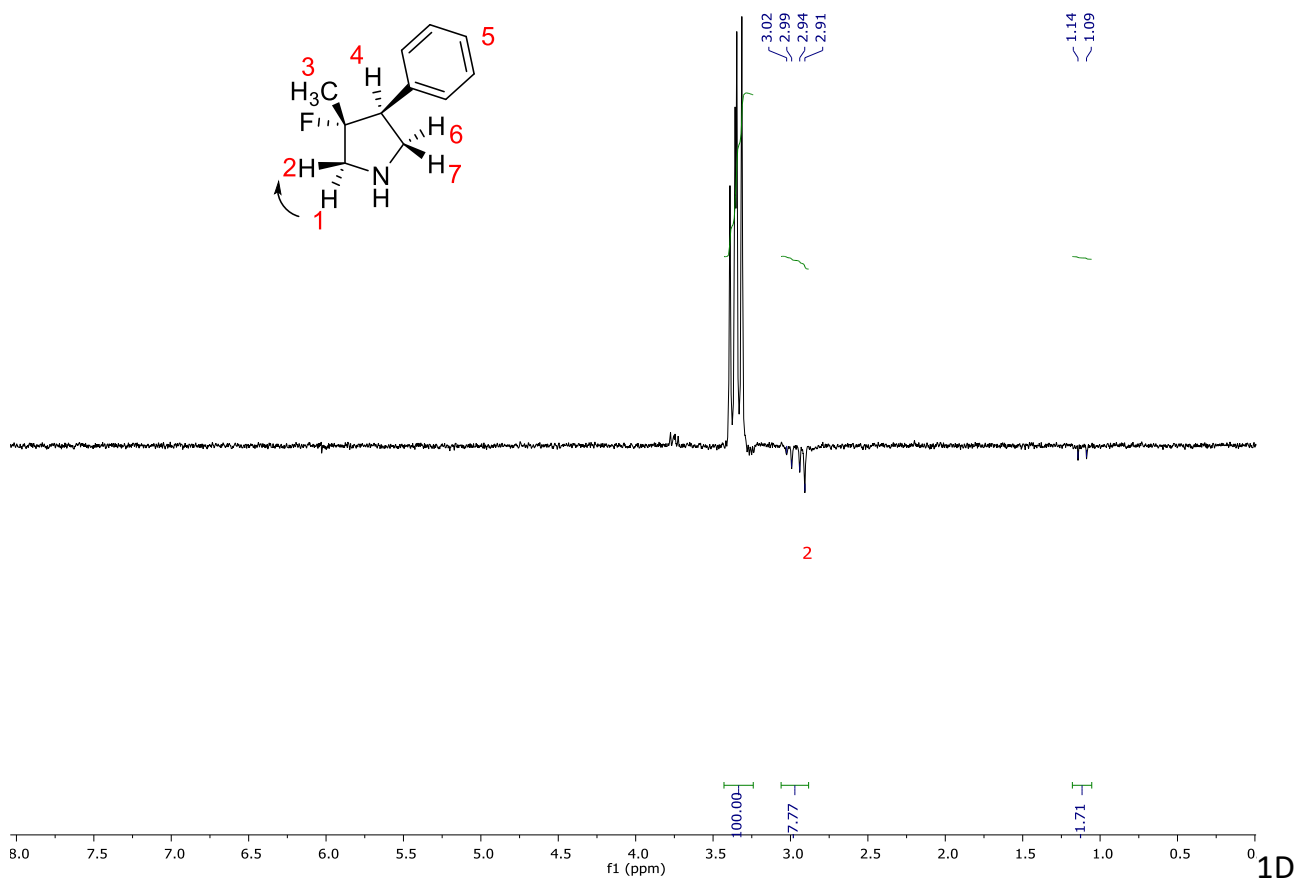
1D NOESY spectrum of isomer *trans*-24, irradiation at 7.3 ppm



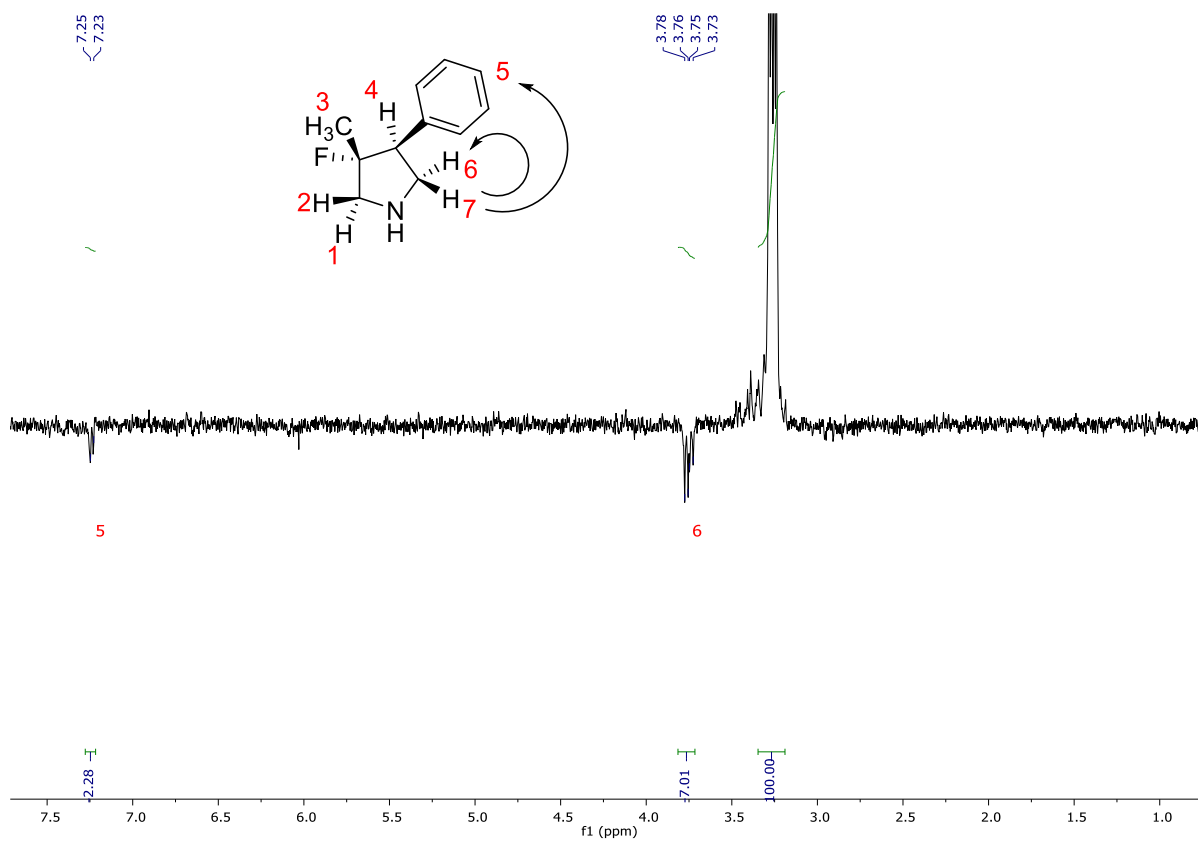
1D NOESY spectrum of isomer *trans*-24, irradiation at 3.75 ppm



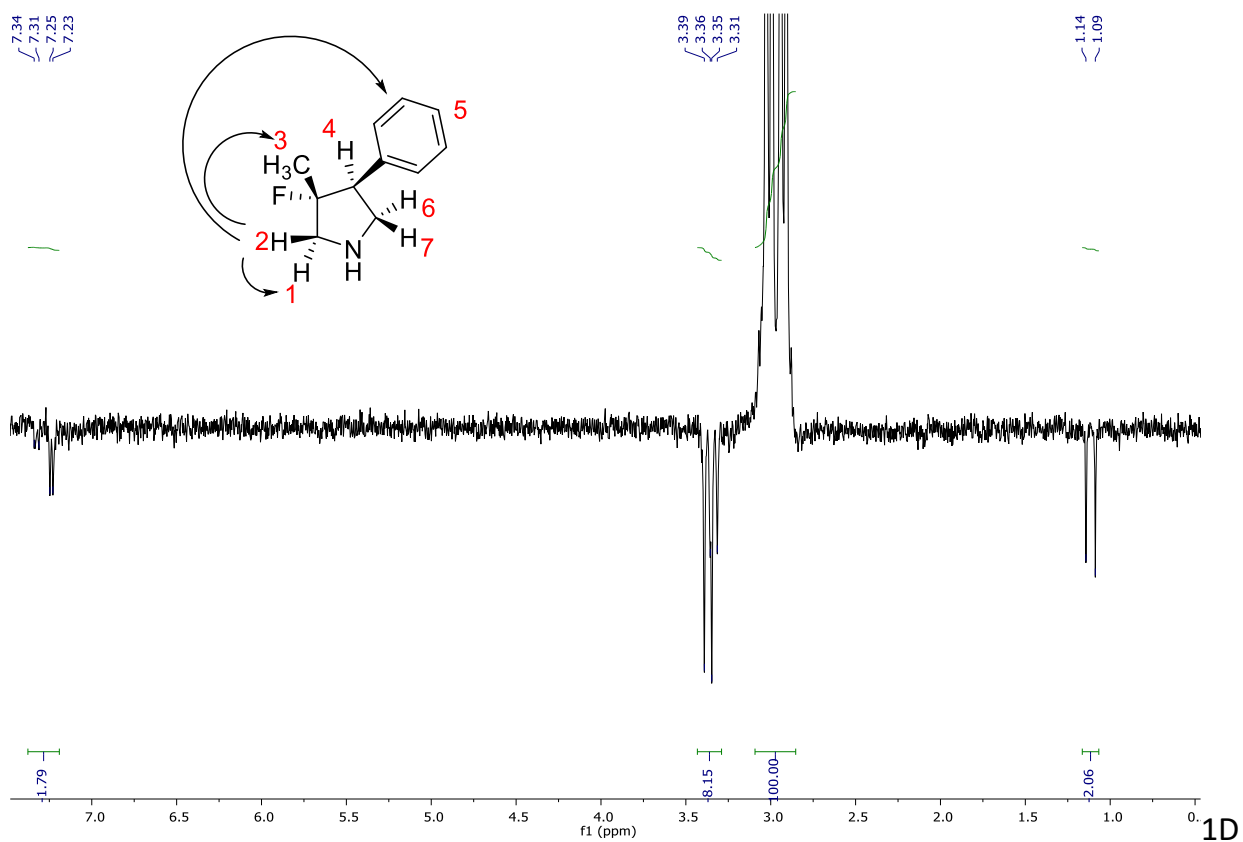
1D NOESY spectrum of isomer *trans*-24, irradiation at 3.5 ppm



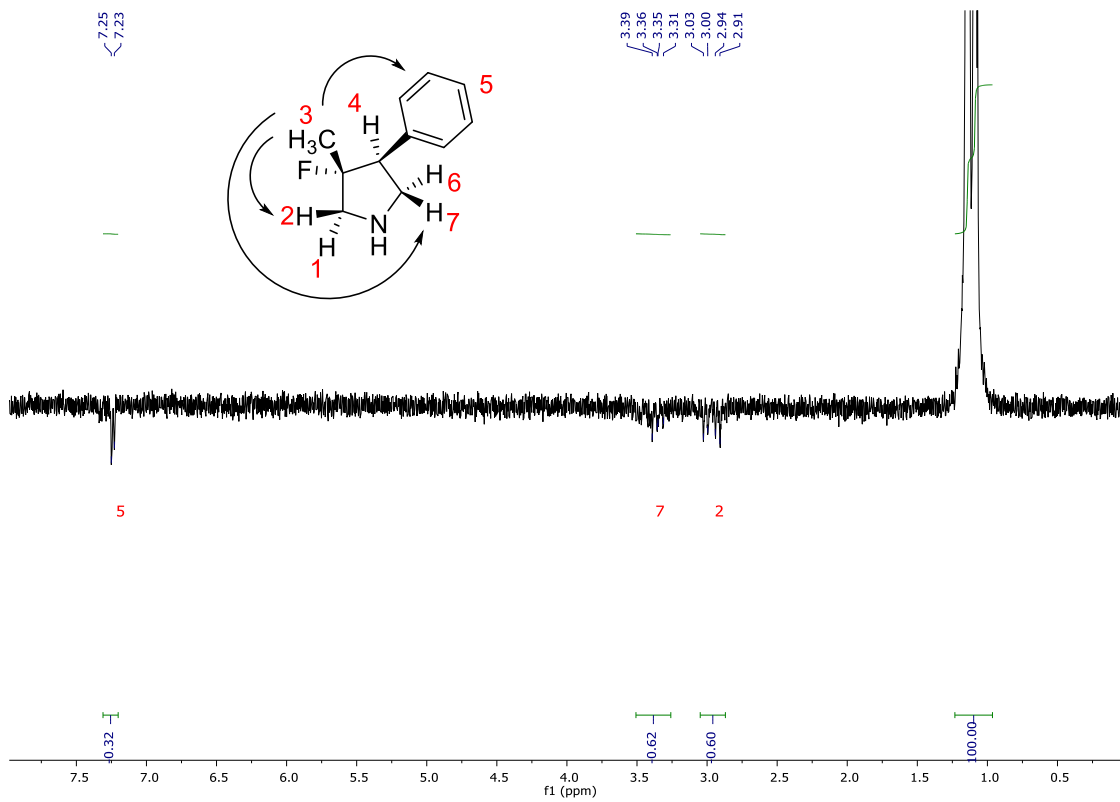
NOESY spectrum of isomer *trans*-24, irradiation at 3.4 ppm



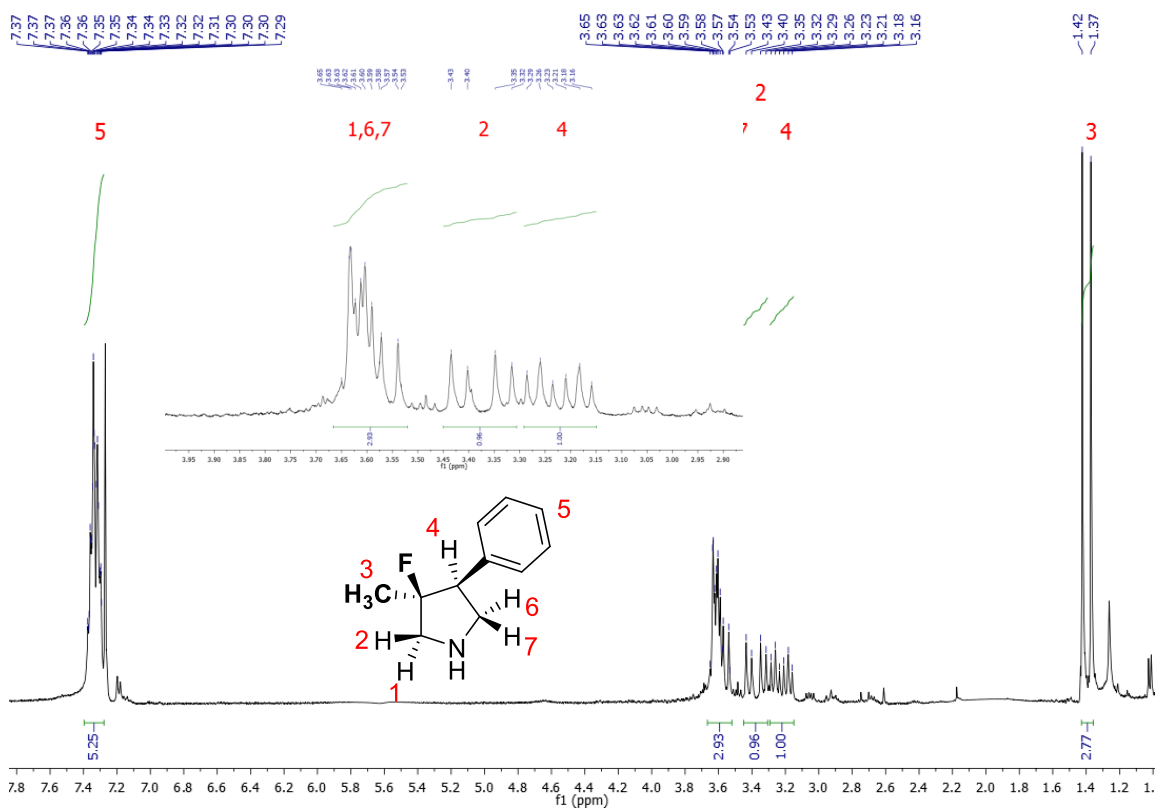
1D NOESY spectrum of isomer *trans*-**24**, irradiation at 3.25 ppm



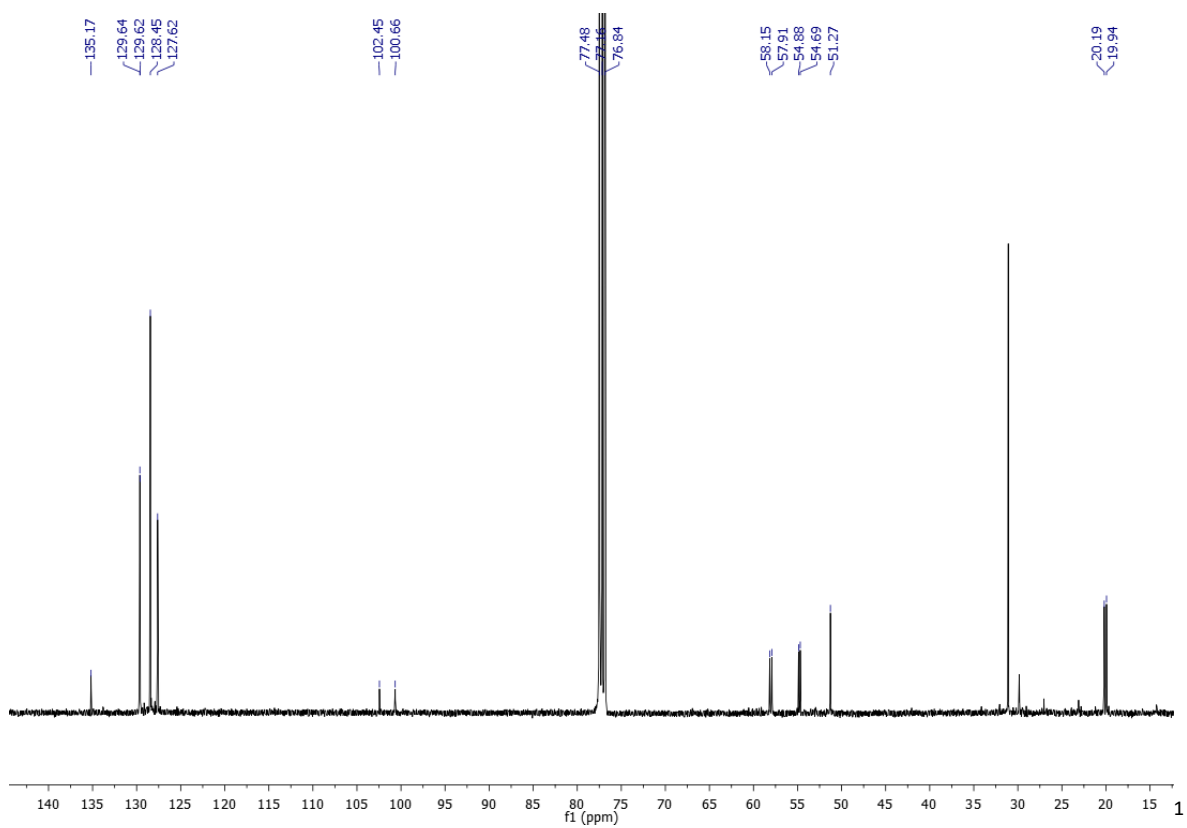
NOESY spectrum of isomer *trans*-**24**, irradiation at 3.0 ppm



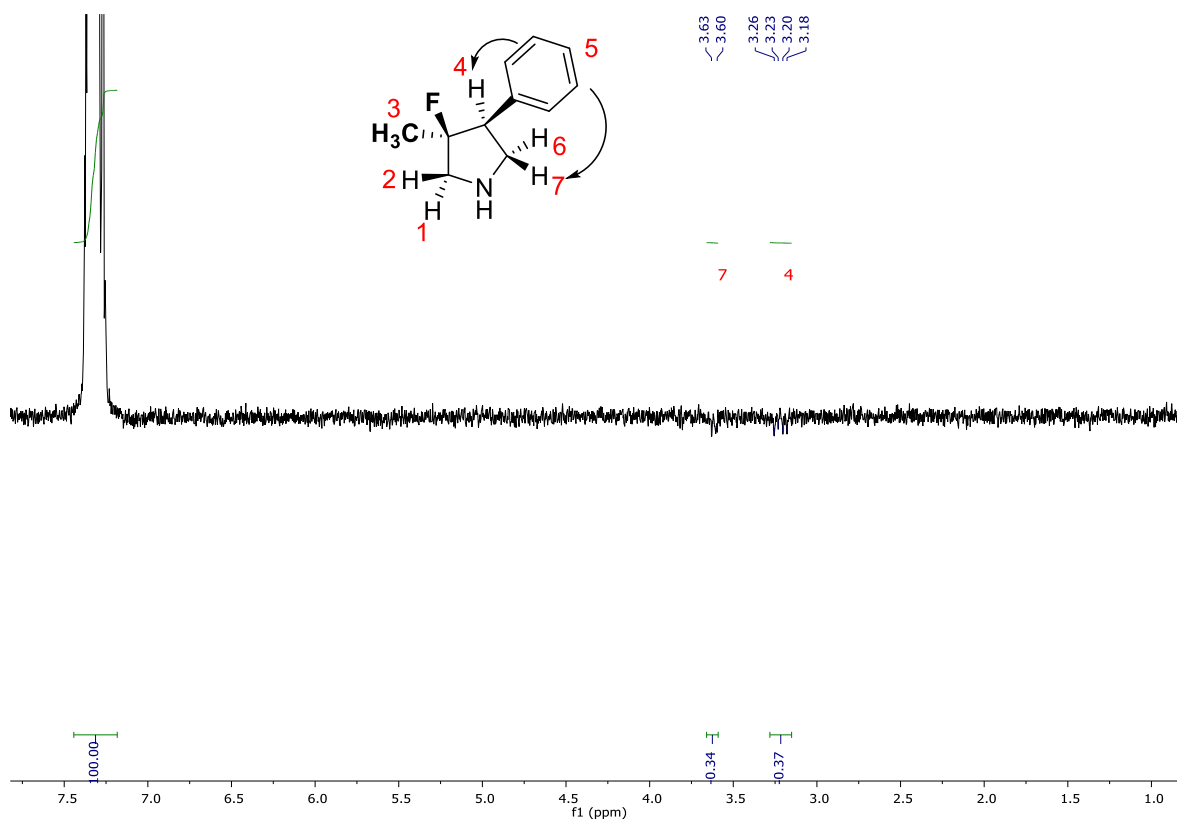
1D NOESY spectrum of isomer *trans*-24, irradiation at 1.1 ppm



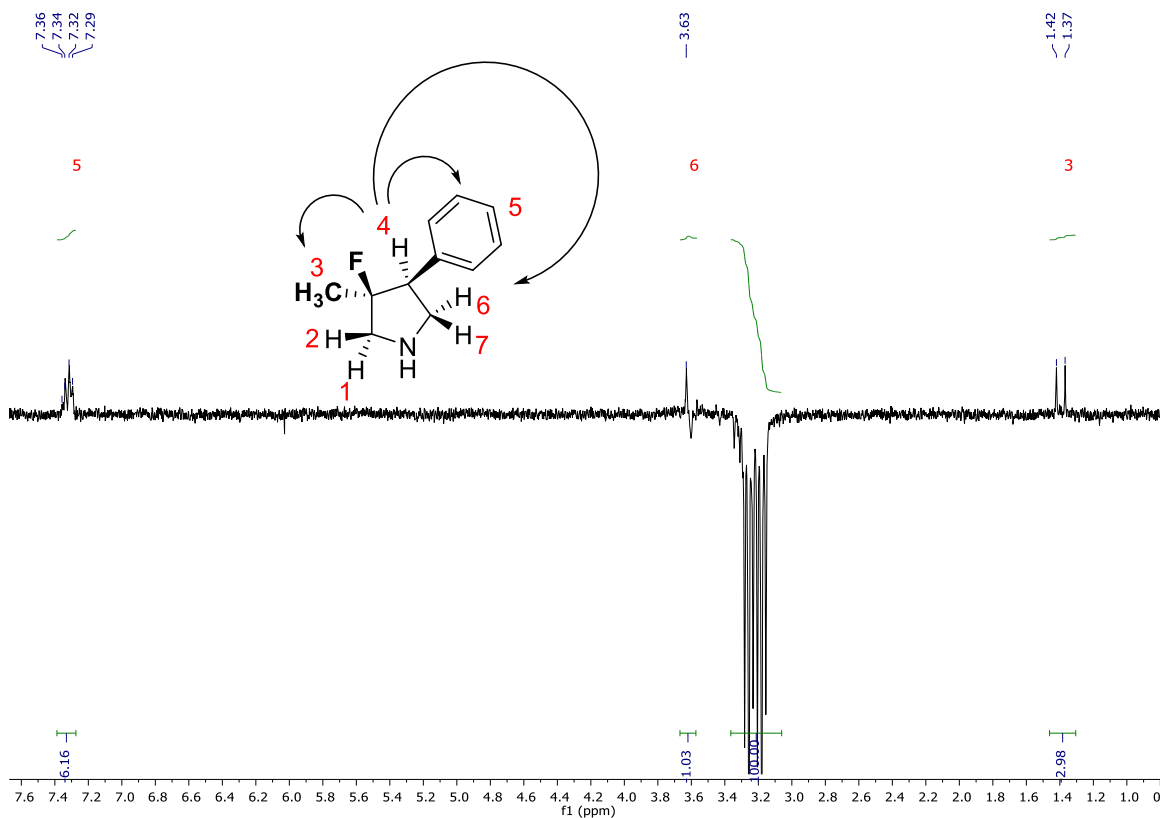
^1H -NMR spectrum of isomer *cis*-24



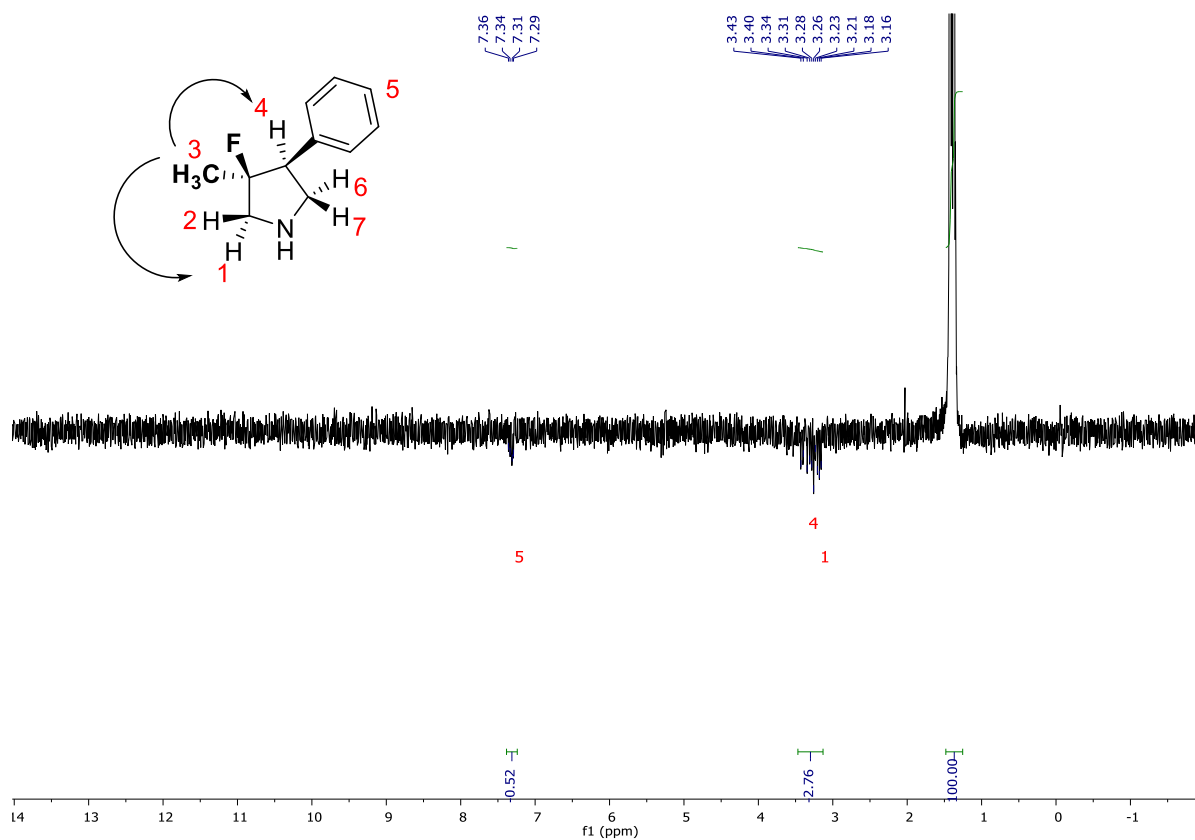
^{13}C -NMR spectrum of isomer *cis*-**24**



1D NOESY spectrum of isomer *cis*-**24**, irradiation at 7.4 ppm



1D NOESY spectrum of isomer *cis*-**24**, irradiation at 3.2 ppm



1D NOESY spectrum of isomer *cis*-**24**, irradiation at 1.4 ppm

Chapter 4: Organocatalysis with carbon-based nanomaterials

This part of the thesis focuses on a work done in collaboration with Prof. Maurizio Prato and co-workers from the University of Trieste, and treats the functionalization of Carbon Nanotubes and Fullerene with stable organocatalysts synthesized during my PhD, with the aim to study the use of these nanomaterials in organocatalytic transformations with the possibility to recycle the catalyst. These results will be soon submitted for publication.

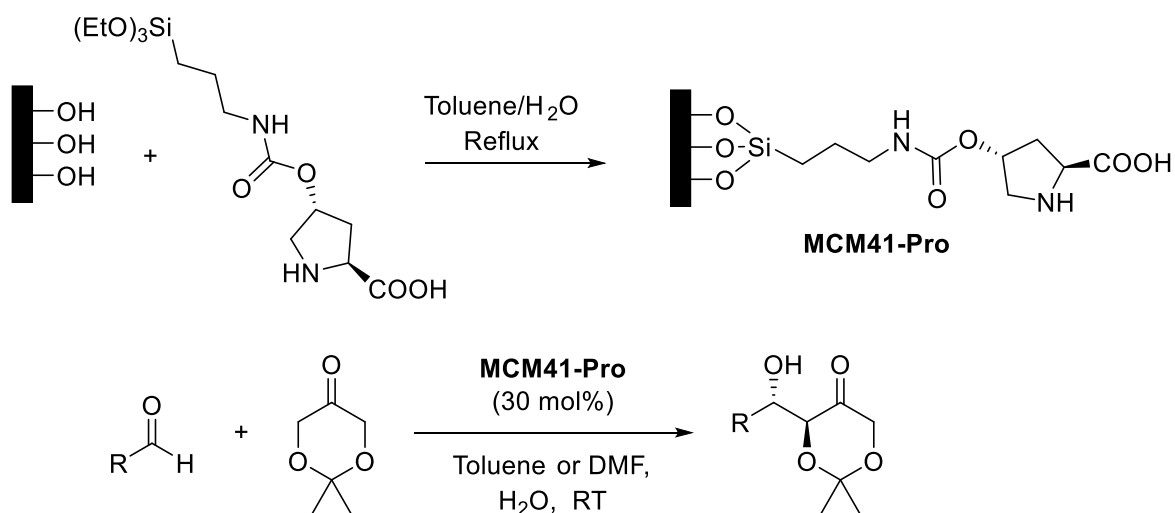
4.1 Organocatalysis on different supported materials

Although organocatalyzed transformations can be considered as a green process, one of the principal drawback is the need for high catalyst loading. Usually a quantity between 5 and 20 percent of catalyst is used in principal organocatalyzed reactions, while organometallic catalyst are often used less than 1 molar percent. Apart from economic advantages it is also very essential to elude the accumulation of unwanted waste products to make the processes environmentally benign. One way to overcome this lack is to make the organocatalyst highly recoverable. It is therefore of interest to develop efficient approaches for the recovery and reuse of asymmetric organocatalysts, which will make the reactions economical and environmentally friendly. Undoubtedly, the immobilization of catalysts onto different platforms is one of the promising processes and displays some advantage since it can allow simple product separation while offering the possibility of catalyst recycling as an additional bonus. Up to now, several papers have been reported describing how to immobilize the asymmetric organocatalysts on different supports.

There are different example and approaches. One could be the immobilization of an organocatalyst on a silica support⁶², like the one reported by Fernandez-Mayoralas⁶³ in **Scheme 29**, where the link is between the catalyst functionalized with a silyl group and MCM-41 (a mesoporous silica).

⁶² S. Rostamnia, E. Doustkhah; *RSC Adv.*, **2014**, *4*, 28238–28248

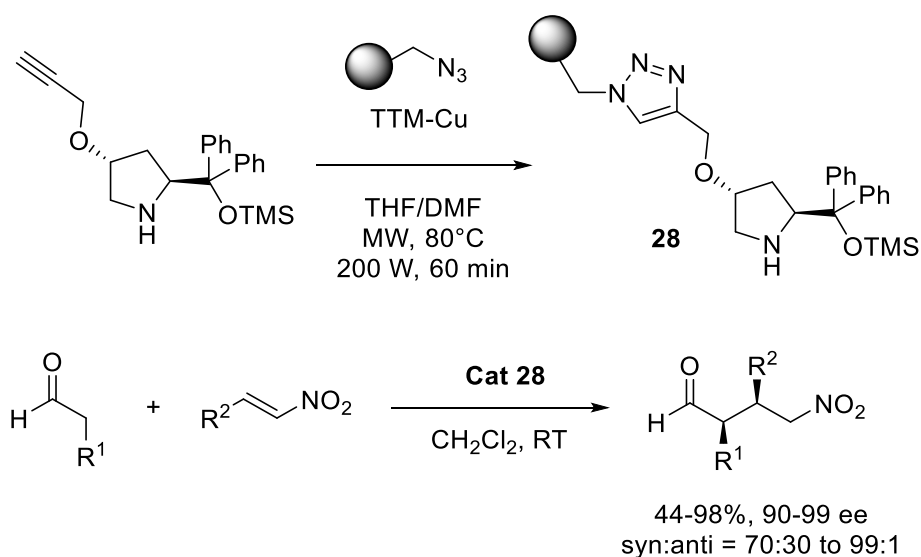
⁶³ E. G. Doyaguez, F. Calderon, F. Sanchez, and A. Fernandez-Mayoralas; *J. Org. Chem.* **2007**, *72*, 9353-9356



Scheme 29: Functionalization of MCM41 and aldol reaction catalysed by MCM41-Pro

The supported catalyst is used for the reaction of aldehyde with a derivative of dihydroxyacetone and the paper investigates the role of different solvents in the reaction system.

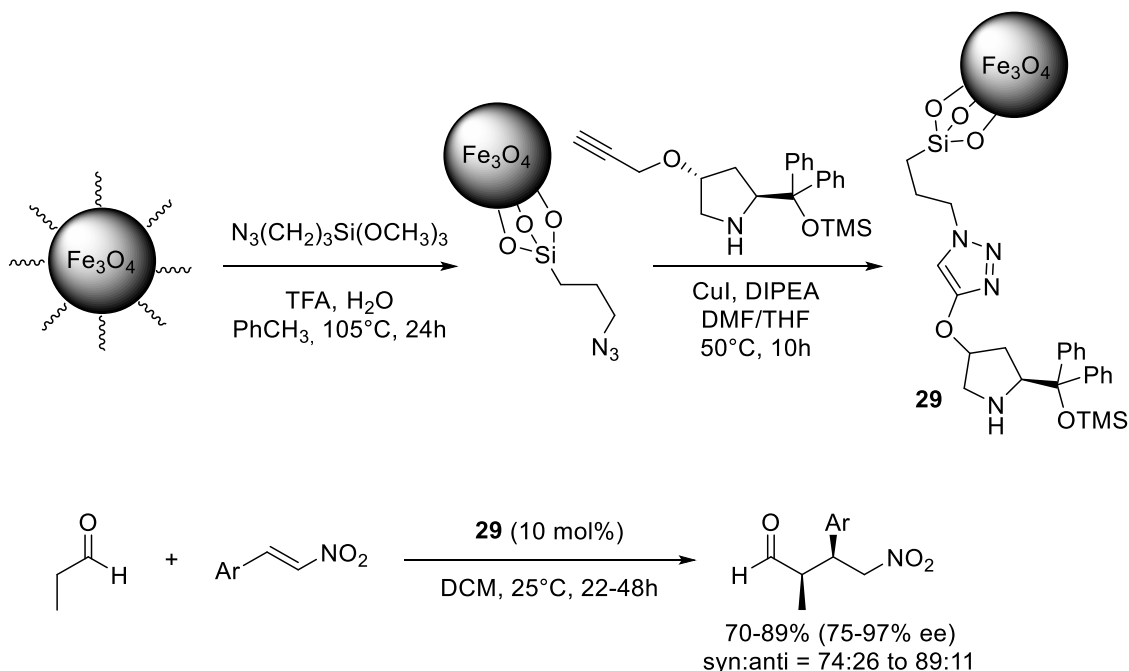
Another approach could be the use of a polymer, such as PEG or polystyrene, as a solid support for an organocatalyst. This support can also be used for flow processes. In this case, a great work has been done by Prof. Pericas and co-workers, who successfully investigated the immobilization of catalyst and the improvement of organocatalyzed reactions using a flow process. In the example reported in **Scheme 30**⁶⁴, an analog of Hayashi catalyst is covalently binded via click reaction to a functionalized polystyrene polymer. The catalyst is used, both in batch and flow processes, in nitro Michael reaction with very good results.



Scheme 30: Immobilization of catalyst on Polystyrene bound and application in nitro Michael reaction

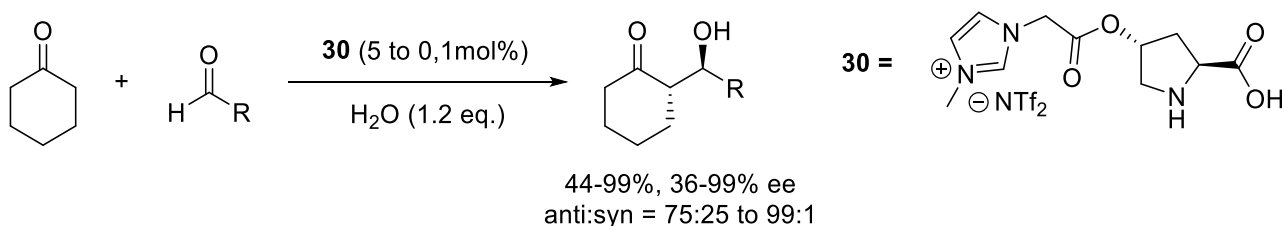
⁶⁴ E. Alza, S. Sayalero, P. Kasaplar, D. Almas, M. A. Pericas; *Chem. Eur. J.*, **2011**, *17*, 11585 – 11595

Another strategy could be the immobilization of catalyst on magnetic materials, to use the magnetic property of it for recycle, like magnetic nanoparticles⁶⁵. In this case, an example always by Prof. Pericas is the immobilization of the Hayashi catalyst on Ferromagnetic nanoparticles and their use in nitro Michael reaction,⁶⁶ showed in **Scheme 31**.



Scheme 31: Immobilization of catalyst on ferromagnetic nanoparticles and application in nitro Michael reaction

And another way can be the functionalization of catalyst in order to modify its property, in particular the solubility in organic solvent, and use it for recycling. An example is the use of ionic liquids, which solubility can be very different. In particular, an example reported by my research group in 2009⁶⁷ and showed in **Scheme 32**, is the development of an ion-tagged proline, and its application in aldol reaction of cyclohexanone with different aldehydes, that showed an incredible reactivity and a very good recyclability.



Scheme 32: Application of ion-tagged Proline in the enantioselective aldol reaction.

In this last years a new trend in material chemistry is the use of carbon-based nanomaterials. One of carbon atom's most important feature is the possibility to form compound built only

⁶⁵ Y. Huang, W. Zhang; *Green Process Synth*, **2013**; *2*, 603-609

⁶⁶ Riente P, Mendoza C, Pericas MA. *J. Mater. Chem.* 2011, *21*, 7350-7355.

⁶⁷ M. Lombardo, S. Easwar, F. Pasi, C. Trombini; *Adv. Synth. Catal.*, **2009**, *351*, 276 – 282

by his atoms, named usually allotropes. The first known are carbon, diamonds or graphite, but several other have been discovered among the years, starting from fullerenes in 1985⁶⁸, and after carbon nanotubes, endohedral fullerenes, nanohorns, nano-onions, nanodots and graphenes. Every allotrope has particular chemical and physical properties, that allows particular functionalization for different applications. During my thesis work I have focused my attention on fullerenes and nanotubes, so I will elucidate the main features of this nanomaterials.

4.2 Fullerene

Fullerenes are a family of compounds in which the most studied and most interesting is C₆₀, also called “buckminsterfullerene”, which is made of 20 hexagons and 12 pentagons fused together giving his classical hollow spherical shape. From the chemical point of view is a polyenic structure⁶⁹, with two different types of covalente bond: the one that binds two hexagons is 1,38 Å long, while the other that binds a pentagon to an hexagon is 1,45 Å long.

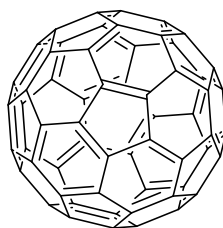


Figure 11: Fullerene C₆₀

Although Fullerene is a stable molecule, it is not totally unreactive. Fullerenes reactivity is based on the deviation of planarity of double bonds, with the angle strain that is significantly released during a reaction that leads to a change in the ibridation of carbon to sp² to sp³.⁷⁰ Professor Wuld was the first to study C₆₀ reactivity, and its electrophilic nature.⁷¹ Fullerene functionalization is interesting because it allows to increase solubility in common organic solvents, or to modify their property, and usually the site involved in functionalization is the junction between two six-membered rings. The typical functionalization reactions are cicloadizione [1+2], [2+2], [3+2], [4+2] cycloaddition reaction, Bingel-Hirsch nucleofilic addition with bromomalonates, organometallic addition, radicalic reaction etc.

⁶⁸ H. W. Kroto, J. R. Heath, S. C. O'Brien, R. F. Curl, R. E. Smalley, *Nature* **1985**, 318, 162.

⁶⁹ J. M. Hawkins, A. Meyer, T. A. Lewis, S. Loren, F. J. Hollander, *Science* **1991**, 252, 312–313.

⁷⁰ R. C. Haddon, *Science* **1993**, 261, 1545–1550., R. C. Haddon, *Acc. Chem. Res.* **1992**, 25, 127–133.

⁷¹ F. Wudl, A. Hirsch, K. C. Khemani, T. Suzuki, P. M. Allemand, A. Kosh, H. Eckert, G. Srdanov, H. M. Webb, *ACS Symp. Ser.* **481**, ACS Washingt. DC **1992**, 161.

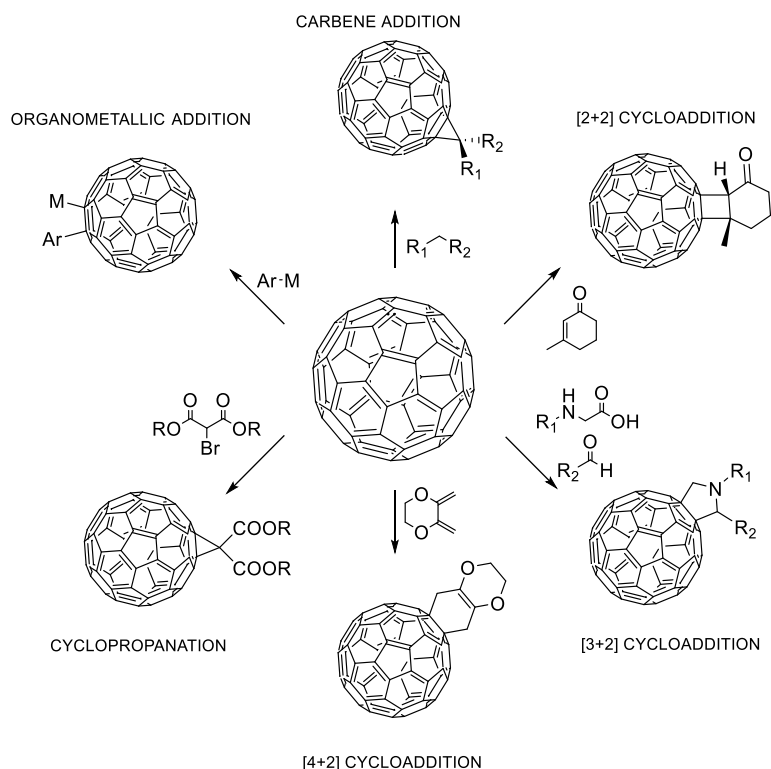
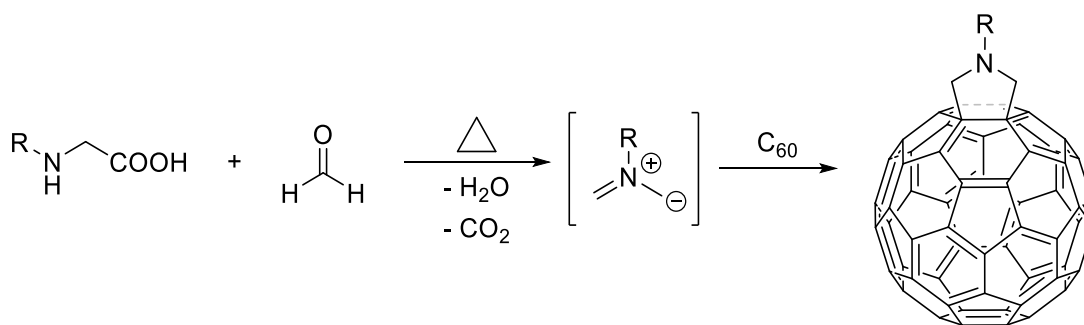


Figure 12: Some commonly known C₆₀ functionalization ⁷²

Since has been used in this work, in this thesis the attention will be focused in particular only in one particular functionalization, the [3+2] 1,3-dipolar cycloaddition usually named “Prato reaction”. In this reaction the dipolar compound is an azomethyne ylide, formed *in situ* from an aminoacid and formaldehyde, while the dipolarophile compound is fullerene. The product of this reaction is a substituted pyrrolidine located on a 6,6-fullerene junction:



Scheme 33: generic “Prato Reaction”

In this case azomethine ylide generation is based on a decarboxylation and a dehydration step, which is the common way, but there are also other tipe like termic degradation of aziridine or desilylation of silyl-derivatives, but are usually less common.

These products are usually characterized by ¹H e ¹³C-NMR. In particular, in the proton spectra are very well visible the pyrrolidinic ring CH₂ signals, more or less around 4 ppm

⁷² A. M. López, A. Mateo-Alonso, M. Prato, *J. Mater. Chem.* **2011**, *21*, 1305–1318.

depending on substitution, while in carbon spectra 16 signals are usually observed between 136 and 155 ppm, related to fullerene's sp^2 atoms, 2 signals around 70 ppm related to fullerene's sp^3 atoms and other 2 signals around 70 ppm, related to pyrrolidine's CH_2 groups. Another important tool for characterization is HRMS, in particular MALDI-TOF analysis.

The first Prato reaction involves the *N*-methyl glycine, also known as sarcosine, and paraformaldehyde, a stable polymer of formaldehyde, to form an *N*-methyl pyrrolidine on a 6,6-fullerene junction. This compound has a C_{2v} symmetry.⁷³

By variation of the substituent of the N atom of the amino acid it is possible to obtain several *N*-substituted pyrrolidines, while using different aldehydes leads to the synthesis of pyrrolidine with a substituent in the 2-position:

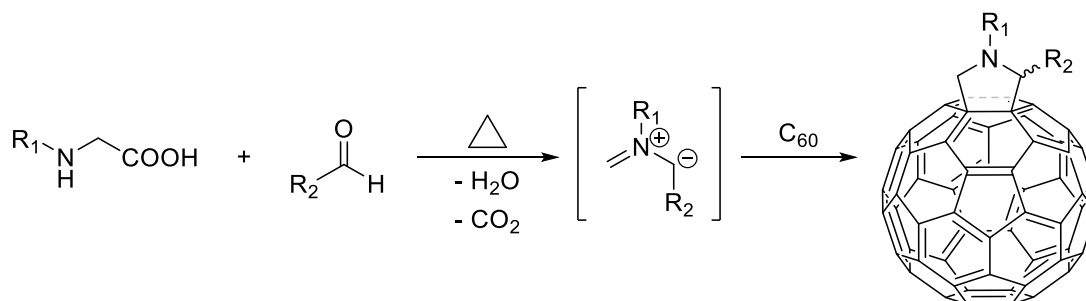


Figure 13: Formation of substituted fullerene-pyrrolidine

In this way it is possible to obtain several libraries of compounds for many applications, both chemical and related to material science. Other important advantages of the “*Prato Reaction*” are the use of simple and cheap reagents, the possibility to obtain both monoadducts and multiadducts depending on reaction conditions, and finally the possibility to insert two different substituents on the pyrrolidinic ring, in order to modulate solubility and chemical property of the desired product. A disadvantage is that the substituent in the 2-position gives racemic products, and if other stereocenters are present this leads to a complex mixture of diastereoisomers⁷⁴. Pristine Fullerene is soluble in Toluene forming a deeply purple solution. They are slightly soluble in Chloroform and very soluble in 1,2-dichlorobenzene. Functionalized fullerenes are soluble in several solvents depending on the nature of the substituents.

This is a simplified mechanism for a common “*Prato Reaction*”:

⁷³ M. Maggini, G. Scorrano, M. Prato, *J. Am. Chem. Soc.* **1993**, *115*, 9798–9799.

⁷⁴ M. Prato, M. Maggini, *Acc. Chem. Res.* **1998**, *31*, 519–526.

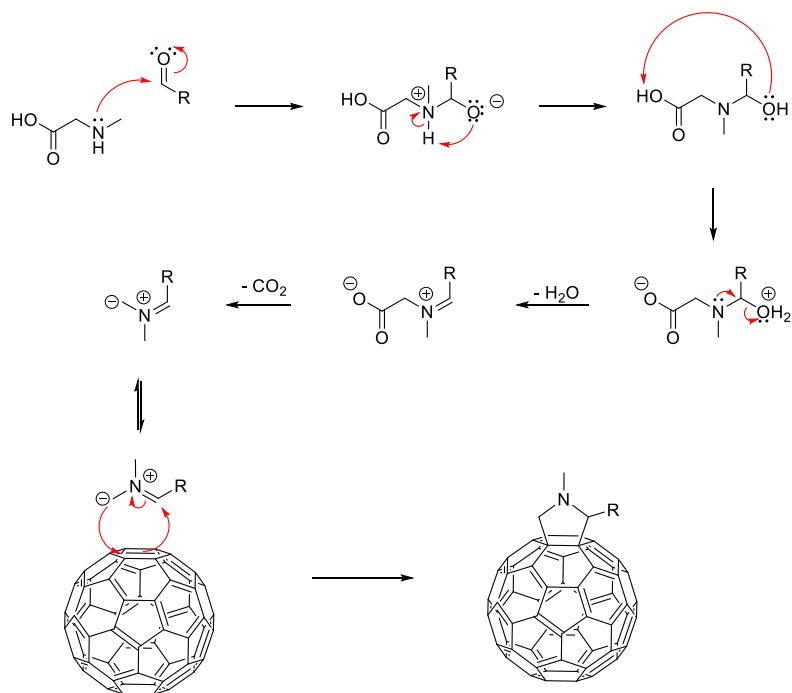


Figure 14: simplified mechanism for a common “Prato Reaction”

The amino acid reacts with the aldehyde forming an immonium ion, after there is the decarboxylation that gives the corresponding azomethine ylide, that reacts with fullerene’s 6,6 double bond in a 1,3-dipolar cycloaddition. Theoretical studies have demonstrated that the yield of the reaction depends directly the HOMO – LUMO difference between the two partners and also from the substituent of the aldehyde.⁷⁵

These functionalized fullerenes are comparable to mostly apolar organic molecules, and they can be derivatized giving other interesting compounds with classic organic chemistry. All this important property allowed to their discoverer Prof. Kroto⁷⁶ to win the Noble Prize for Chemistry in 1996, and fullerene is still used in many fields of scientific research.

4.3 Carbon Nanotubes

Carbon nanotubes (CNTs) are allotropes of carbon with a cylindrical nanostructure. They can be considered like graphene sheets, with hexagon made up only of sp^2 carbon atoms, rolled together to form a cylindrical structure, closed on both edges by half fullerenic structures. These objects have incredible electronic and mechanic property and are broadly studied in many scientific areas. The exact structure of CNTs is dependent from their rolling angle, and different nanotubes has different electronic property. Usually CNTs are 1 μm long and their diameter is variable from 0,5 to more than 100 nm. They often tend to form aggregate, and

⁷⁵ P. Piotrowski, J. Pawłowska, J. Pawłowski, A. Więckowska, R. Bilewicz, A. Kaim, *J. Mater. Chem. A* **2014**, 2, 2353–2362.

⁷⁶ H. W. Kroto, J. R. Heath, S. C. O’Brien, R. F. Curl, R. E. Smalley, *Nature* **1985**, 318, 162.

usually are divided in Single Walled Carbon Nanotubes “SWCNTs” and Multi Walled Carbon Nanotubes “MWCNTs”, with different dimension and property.

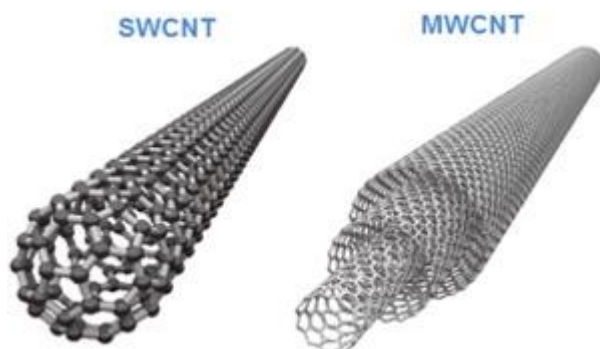


Figure 15: SWCNT e MWCNT^[55]

In fact, SWCNT are really tiny with a diameter of only 0,8-1,5 nm, while MWCNT usually 20-30 nm, depending on the production method. SWCNT then have a bigger superficial area, that leads to a different reactivity. First MWCNT were discovered by Iijima group in 1991 during arc discharge evaporation of fullerene. He discovered tube of carbon atom with 2 to 50 layers.⁷⁷ After two years also SWCNT were discovered by Iijima, Ichihashi e Bethune⁷⁸.

Actually, carbon nanotubes are produced using the “*chemical vapour deposition*” method (CVD), that allows to have a better control on length, orientation, diameter, purity and density of the CNTs synthesized. Other methods, like pyrolysis or “bottom-up” syntheses are less common. Different synthesis leads to different kind of impurities. Usually the principal impurities are traces of other carbon-based materials, such as graphite, amorphous carbon, IPA, fullerenes or, when are used for synthesis, transition metals. Usually, CNT undergoes to acid treatment in order to eliminate some impurities.⁷⁹

Moreover, in the regular structure often some defects are present. Most of the times are dislocations, holes or other topological variation, like the presence of pentagons and heptagons next to each other, named “Stone-Wales defects”. This are the most common and leads to a distortion in the graphitic nanotube’s structure. They usually start to a local rotation of 90° of a C-C bond of a hexagon that form two pentagons and two heptagons.⁸⁰

⁷⁷ S. Iijima, *Nature* **1991**, *354*, 56–58.

⁷⁸ N. Karousis, N. Tagmatarchis, D. Tasis, *Chem. Rev.* **2010**, *110*, 5366–5397.
D. Tasis, N. Tagmatarchis, A. Bianco, M. Prato, D. Tasis, N. Tagmatarchis, A. Bianco, M. Prato, *Chem. Rev.* **2006**, *106*, 1105–1136.

⁷⁹ J. Prasek, J. Drbohlavova, J. Chomoucka, J. Hubalek, O. Jasek, V. Adam, R. Kizek, *J. Mater. Chem.* **2011**, *21*, 15872–15884.

⁸⁰ Y. Miyamoto, A. Rubio, S. Berber, M. Yoon, D. Tománek, *Phys. Rev. B* **2004**, *69*, 1–4.

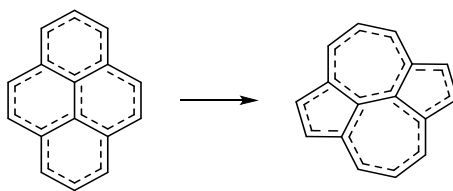


Figure 16: Stone-Wales defect formation

The propagation of these defect along the structure of nanotubes can represent a problem in CNTs growth during their synthesis. Despite of this, defects are also the most reactive sites in all their structure, and they can be exploited to carry out functionalization reactions. In order to use CNTs for organic synthesis chemists have to face off a big problem in solubility. Nanotubes are almost insoluble in both common organic and inorganic solvents, due to the strong Van der Waals interactions occurring, and they tend to form complex aggregates. To face off this problem and expand the reactivity of nanotubes is possible to functionalize them, in a covalent or non covalent way, or to use endohedral inclusion inside their cavity. The first is the most used one, while the second exploits the possibility to use π - π stacking on NTs structure. In this way is possible to obtain modified CNTs that can be partially dispersed in organic solvents, and after they can be used for other functionalization reactions. It is possible in fact to bind also complex organic molecules and even biological ones to give very interesting nanomaterials.

Now we will focus our attention on covalent functionalization of carbon nanotubes. The most common way is oxidation. With oxidative treatment is possible to introduce, in particular on the lateral wall where defects are present, oxygen-containing functional groups, carboxylic acids in most of the cases. In this process the nanotubes are broken, consequentially a significant shortening of the material is observed.

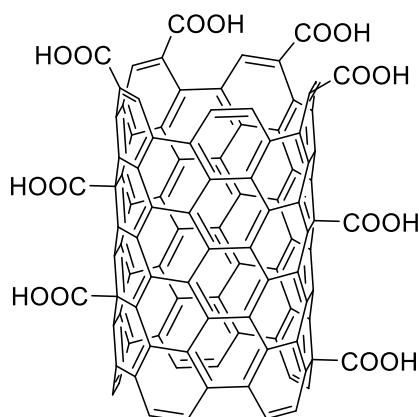


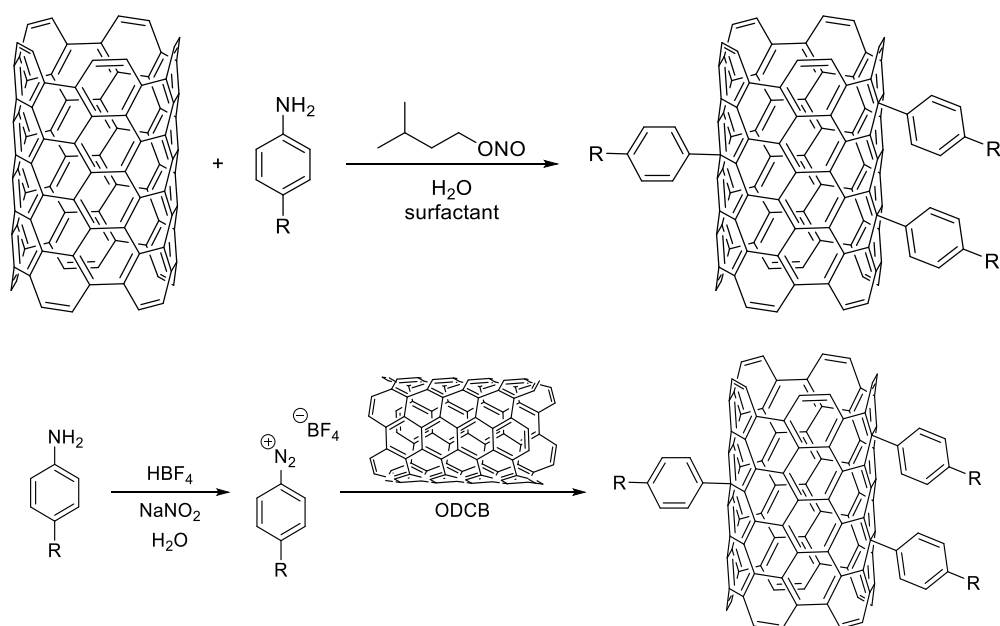
Figure 17: Carbon nanotube functionalized on their edges using oxidation (simplified representation)

Also in this case, the change in hybridization of functionalized carbon from sp^2 to sp^3 leads to a deplanarization of the local structure, that is the proper “driving force” for functionalization

reaction. Moreover, they are more reactive respect to graphene because of the curvature of CNTs scheleton, that helps the carbon pyramidalization.⁸¹ Moreover, is demonstrated by theoretical studies⁸² that another functionalization site is in presence of Stone-Wales defects. The percentage of functionalization reported in literature, referred to COOH groups, is almost 1,7 $\mu\text{mol}/\text{mg}$ (2% molar) for MWCNT⁸³, and 3,5-7 $\mu\text{mol}/\text{mg}$ (5-10% molar) for SWCNT⁸⁴, depending on reaction conditions. The oxidation reaction is carried with aqueous nitric acid, sometimes mixed with sulphuric acid at 100°C.⁸⁵ Other oxidant can be used to modify the oxidation grade and the length of the resulting material.

Introduction of carboxylic groups on nanotube surface open the way for many other re-functionalization process, first of all the formation of an amidic bond with an amine, that will be treated more deeply in this chapter.

Another important methodology for CNT functionalization is arylation. First proposed by Tour, involves the addition of diazonium salt, both in situ or ex situ, to the lateral wall of nanotube to give aryl-derivatives more soluble and easy to functionalize.⁸⁶



Scheme 34: Generic arylation reaction of nanotube, with in situ and ex situ formation of diazonium salt.

⁸¹ N. Karousis, N. Tagmatarchis, D. Tasis, *Chem. Rev.* **2010**, *110*, 5366–5397.

⁸² C. Wang, G. Zhou, H. Liu, J. Wu, Y. Qiu, B.-L. Gu, W. Duan, *J. Phys. Chem. B* **2006**, *110*, 10266–10271.

⁸³ D. D. Chronopoulos, C. G. Kokotos, N. Karousis, G. Kokotos, N. Tagmatarchis, *Nanoscale* **2015**, *7*, 2750–7.

⁸⁴ K. J. Ziegler, Z. Gu, H. Peng, E. L. Flor, R. H. Hauge, R. E. Smalley, *J. Am. Chem. Soc.* **2005**, *127*, 1541–1547.

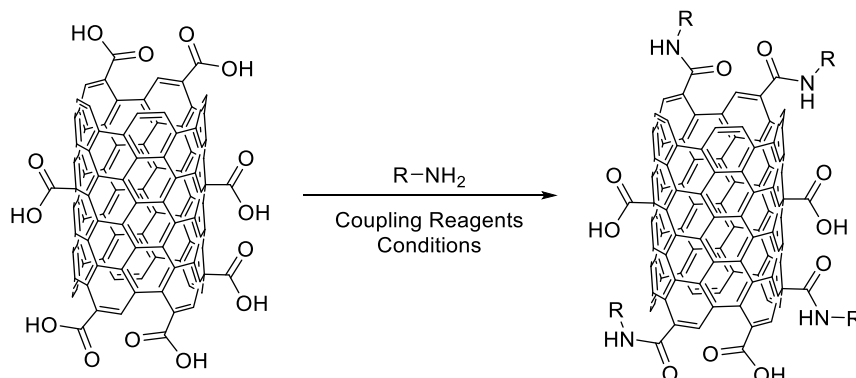
⁸⁵ J. Liu, A. G. Rinzler, H. Dai, J. H. Hafner, R. K. Bradley, P. J. Boul, A. Lu, T. Iverson, K. Shelimov, C. B. Huffman, et al., *Science* **1998**, *280*, 1253–1256.

⁸⁶ B. K. Price, J. M. Tour, *J. Am. Chem. Soc.* **2006**, *128*, 12899–12904.

C. D. Doyle, J. R. Rocha, R. B. Weisman, J. M. Tour, *J. Am. Chem. Soc.* **2008**, *130*, 6795–6800.

The functionalization percentage for arylation is almost 2 $\mu\text{mol}/\text{mg}$ (3% molar) for SWCNT⁸⁷ and 0,8 $\mu\text{mol}/\text{mg}$ (1% molar) for MWCNT⁸⁸. The presence of substituent on the aromatic ring can affect these results.

The functionalization of CNT with carboxylic moiety is very important because it allows a rapid re-functionalization of the material, in particular through amide-formation using amide coupling reactions.



Scheme 35: Generic Amide coupling on CNT

In literature are present many publications about amide coupling reactions, often using classic coupling reagents as EDC/HOBt⁸⁹, EDC/NHS⁹⁰, or $\text{SOCl}_2/\text{pyridine}$ ⁹¹. Other common coupling reagents are TBTU or HATU.

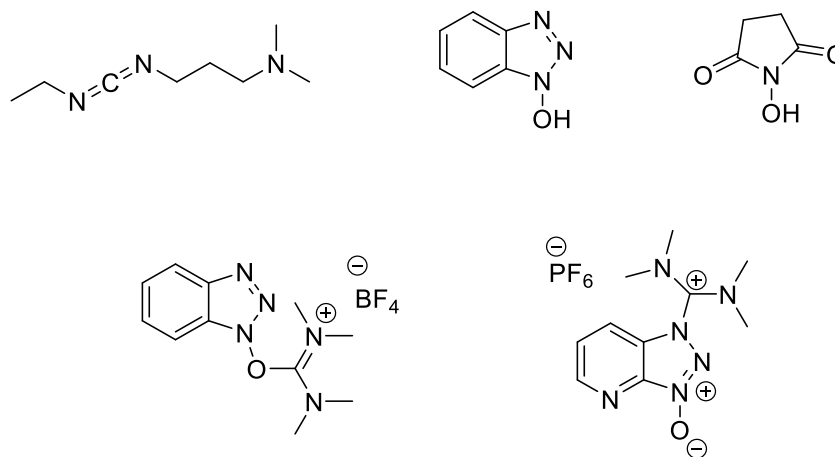


Figure 18: Common coupling reagents (EDC, HOBt, NHS, TBTU, HATU)

These reactants are able to activate the carboxylic moiety present on CNTs surface, allowing the nucleophilic substitution with an amine, allowing the formation of the amide bond. This

⁸⁷ C. A. Dyke, J. M. Tour, *Nano Lett.* **2003**, *3*, 1215–1218.

⁸⁸ J. J. Stephenson, A. K. Sadana, A. L. Higginbotham, J. M. Tour, *Chem. Mater.* **2006**, *18*, 4658–4661.

⁸⁹ W. Wu, H. Zhu, L. Fan, S. Yang, *Chem. Eur. J.* **2008**, *14*, 5981–5987.

⁹⁰ Z. Wang, A. Korobeinyk, R. L. D. Whitby, S. T. Meikle, S. V. Mikhalovsky, S. F. A. Acquah, H. W. Kroto, *Carbon* **2010**, *48*, 916–918.

⁹¹ Y. Lin, A. M. Rao, B. Sadanadan, E. A. Kenik, Y. P. Sun, *J. Phys. Chem. B* **2002**, *106*, 1294–1298.

connection is usually very stable, and usually only strong acidic conditions are able to cleave it, and this is ideal for application of this nanomaterial in organic synthesis.

These reactions on CNT need very diluted conditions because of the low dispersion in common solvents for coupling reactions. Usually, the concentration is around 1 mL of solvent for mg of material for MWCNT, while for SWCNT sometimes also 10 mL for 1 mg of SWCNT. The solvents used are DMF, CH₃CN, DCM etc. In some cases it is also possible to form an ester using an alcohol instead of an amine, always using coupling reagents with catalytic DMAP (*N,N*-dimethyl-4-aminopyridine), but they are usually less common because alcohols are less reactive.

A critical point in carbon nanomaterials and in particular in nanotubes is the qualitative and quantitative characterization of the functionalized products. In fact, differently from common organic molecules, nanomaterials need a totally different analytical approach for the determination of their structure, and that cannot lead to the complete elucidation of it. In fact, these materials are not made up of precise single entities such as organic molecules, but aggregates of nanometric structures insoluble in organic solvents, that is not enhanced with functionalization. It is easy to understand that, differently from fullerene derivatives, nuclear magnetic resonance spectroscopy and chromatographic techniques are not useful for the characterization of CNT, but other methodologies are needed. In particular, are used measurement of other properties that doesn't need to solubilize the adduct. The most important are analytical thermogravimetry (TGA), UV-VIS spectroscopy, IR and Raman analysis, elemental analysis, Electronic microscopy (SEM, TEM, AFM, STM) X-ray diffraction (XRD), etc. Thanks to these analyses it is possible to measure in a general way the dimension, the chemical composition, the electronic and optical properties, and the percentage of functionalization of examined nanomaterials. In particular, TGA and Raman analysis have been used in this thesis work.

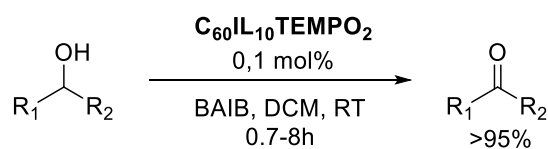
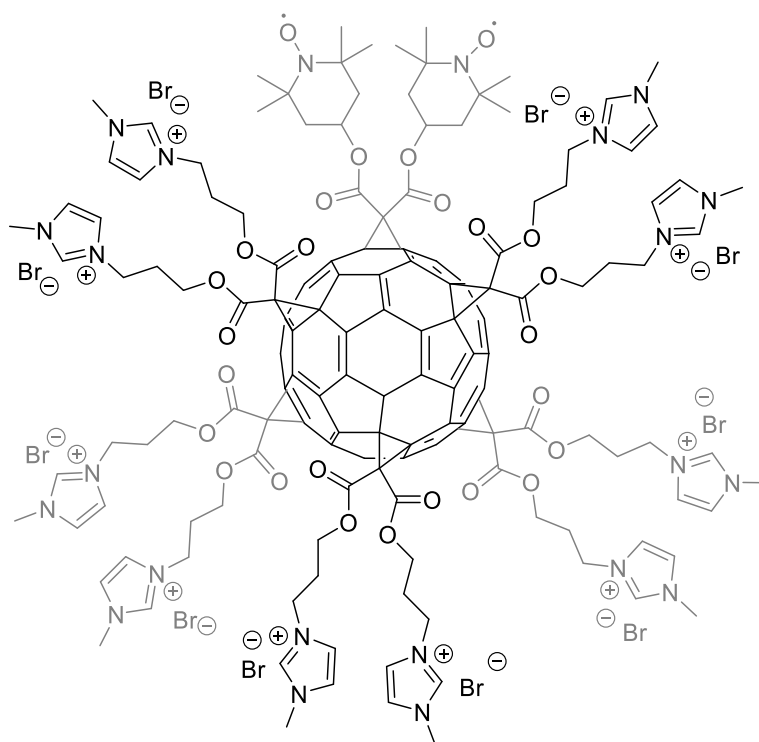
Analytical thermogravimetry (TGA) is the most common characterization of carbon-based nanomaterials and in particular of nanotubes. It measures the loss of mass on a sample exposed to heating under inert and oxidant conditions. In this thesis work it has been applied for measuring the percentage of functionalizations of the synthesized materials, because the loss of mass is attributed to the molecules covalently bound to the nanotube's surface. With this it is possible to calculate the number of moles of molecules on the material and the functionalization percentage. Of course, the data should be corrected with the loss of mass of pristine CNT. It's appropriate to remember that these data are not precise due to approximations, but TGA can give a useful indication on functionalization, and the quality of data is enhanced if compared with other analyses like Raman spectroscopy.

Raman spectroscopy is broadly used for qualitative and semi-quantitative analysis, in particular with SWCNT. It is based on anelastic scattering of incident light on a sample. During this, an electron is excited from the valency band to the conduction band of the nanomaterial by photon absorption. After there is relaxation to the ground state with emission of a photon with less energy than the incidental photon. Then, the Raman spectra is made on this difference in the wavenumber of emitted radiation, called Raman shift. In these spectra are always present characteristic band of CNT and of CNT's defects, and from them is possible to take information on their functionalization. Also in this case, the bands are normalized on pristine CNTs. As said before, the results of TGA analysis can be implemented by Raman analysis, and a high level of functionalization in TGA has to be confirmed by high presence of defects-band. If this is not, the data can't be associated to CNT functionalization but to other impurities or byproducts not directly binded to CNT.

4.4 Fullerene and Carbon Nanotubes in catalysis

If on one side the poor solubility in organic solvents of functionalized CNT and in some cases of fullerene can be seen as a limitation, on the other side the use of non-solvent during the work up procedures can allow an easily recycle of this material, if used as catalyst. For these characteristics these materials are now used as solid support for the synthesis of catalytic systems. Since the field is quite new, there are not a lot of examples of application in catalysis. For example, Prof. Gruttadauria and co-workers reported the synthesis of many supported systems for oxidation, both with C₆₀ and CNTs. For example, in **Scheme 36** is showed a multifunctionalized fullerene derivative bearing both imidazolium salts and TEMPO, used for catalysed oxidation of alcohols with good results. The catalyst can be fully recovered and also used in combination with silica gel in a “*release and catch*” protocol⁹².

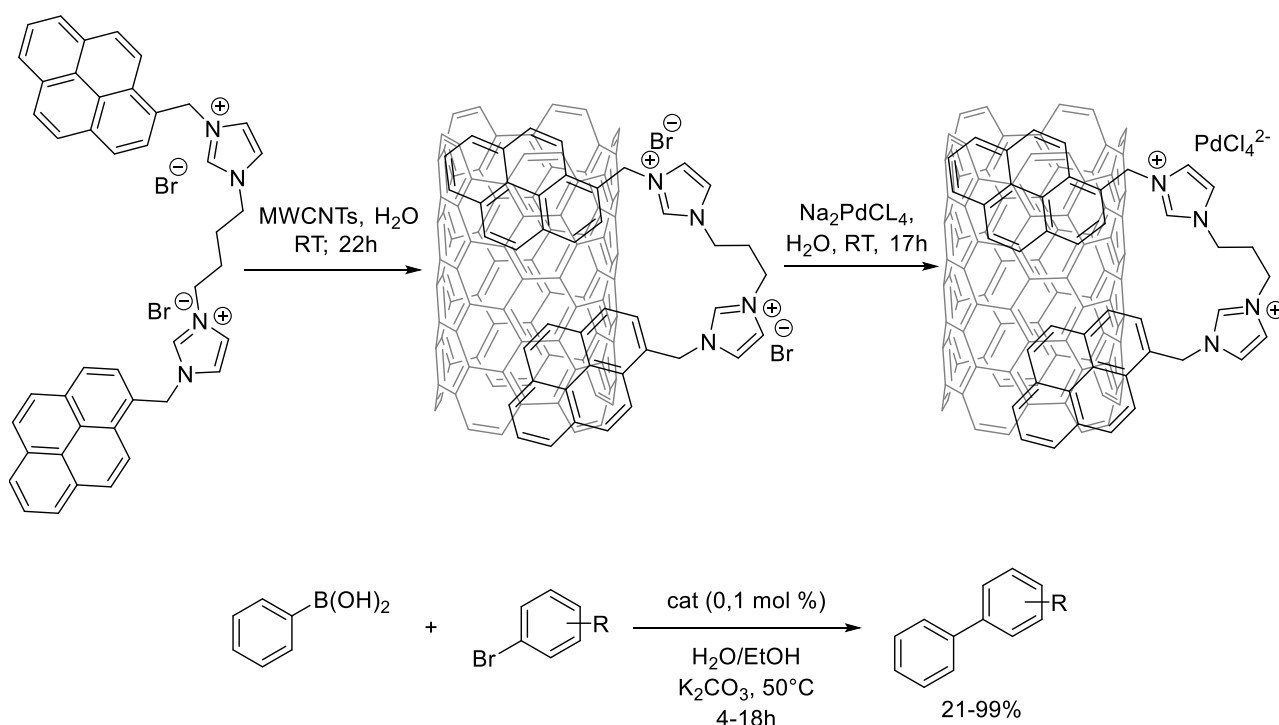
⁹² V. Campisciano, V. La Parola, L. F. Liotta, F. Giacalone, M. Gruttadauria; *Chem. Eur. J.*; **2015**, *21*, 3327 – 3334



Scheme 36: Oxidation of alcohol promoted by TEMPO-IL-functionalized fullerene

Similar examples of these systems are reported also with CNTs. Another peculiar approach is the use of non-covalent functionalization of CNT. Using catalyst tagged with proper aromatic moieties, is possible to exploit the π -stack interactions to adsorb the molecule on the nanotube surface. An example is reported always from Prof. Gruttadauria⁹³, and showed in **Scheme 37**:

⁹³A. M. P. Salvo, V. La Parola, L. F. Liotta, F. Giacalone, M. Gruttadauria; *ChemPlusChem*, **2016**, *81*, 471 – 476



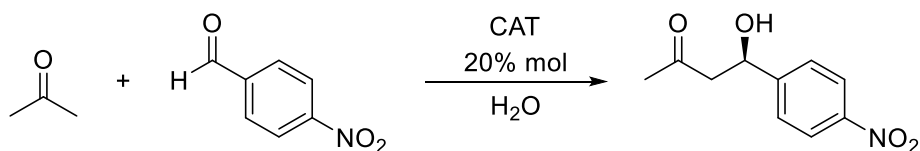
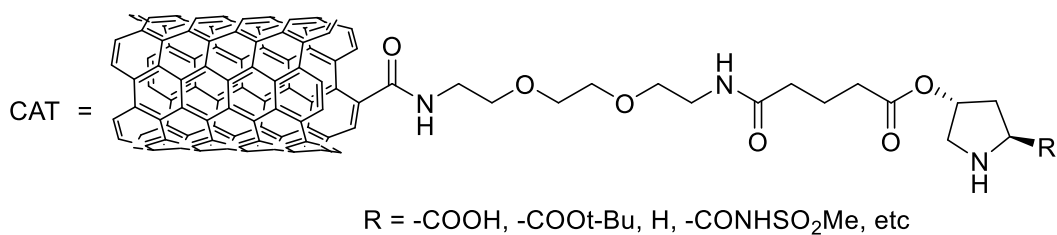
Scheme 37: Synthesis of non-covalently nanotube-supported catalyst and application to Suzuki cross-coupling using a “release and catch” approach.

In this case a bis imidazolium salt is adsorbed on CNTs using pyrene groups. After, the cations are used to bind Palladium on the surface and catalyse a classic Suzuki Cross Coupling reaction with good results.

Regarding organocatalysis, there are only a few examples. The group of Prof. Kokotos and co-workers reported the functionalization of CNT with proline derivatives to promote the enantioselective aldol reaction between acetone and 4-nitrobenzaldehyde.⁹⁴⁹⁵ The example is showed in **Scheme 38**.

⁹⁴ D. D. Chronopoulos, C. G. Kokotos, N. Karousis, G. Kokotos, N. Tagmatarchis, *Nanoscale* **2015**, *7*, 2750–7.

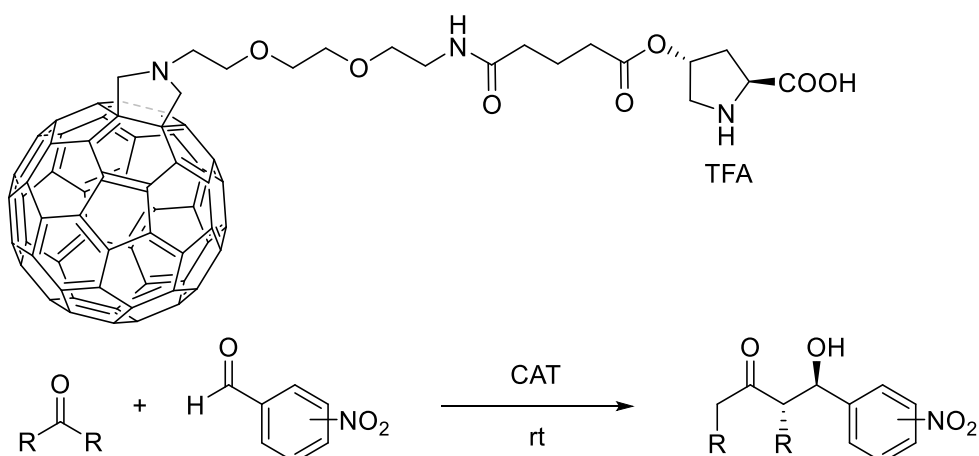
⁹⁵ D. D. Chronopoulos, C. G. Kokotos, M. Tsakos, N. Karousis, G. Kokotos, N. Tagmatarchis, *Mater. Lett.* **2015**, *157*, 212–214.



Scheme 38: Kokotos aldol reaction catalysed by nanotube-supported proline derivatives.

In this example the yield is generally good (70-99%) while the enantiomeric excess is not very satisfying (up to 76%).

Another example always by Kokotos is the functionalization of fullerene with proline, using the classic "*Prato Reaction*" and a proper spacer, and the application in aldol reaction., showed in **Scheme 39**.



Scheme 39: Kokotos aldol reaction catalysed by fullerene-supported Proline

In this case the best results in ee are with the longer spacer, due to the fact that there is less hindrance during the formation of the active conformations.

4.5 Aim of the work

The aim of this work is the use of Carbon-based Nanomaterials as solid support for organocatalyst.

The first part of the work is really innovative, and concern the use of nanomaterials, and in particular carbon nanotubes, in order to hinder one of the diastereotopic face of the iminium ion formed by reaction of the chiral catalyst and $\alpha,\beta\text{-}\gamma,\delta$ -saturated aldehyde, favouring the 1,6 reaction the only possible and most of all stereocotrolled. For doing this, the secondary amine has to be binded covalently to the CNT and very near to the surface.

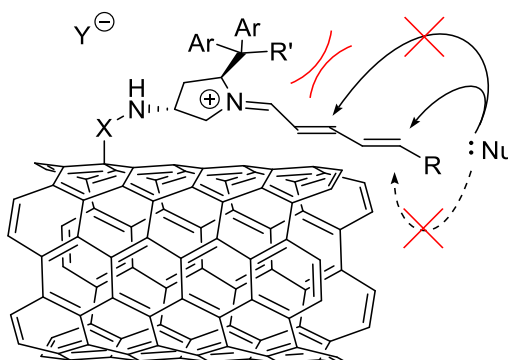
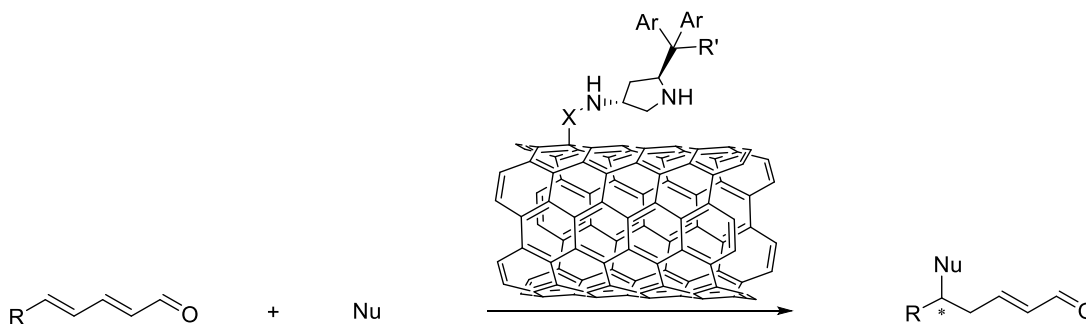


Figure 19: Mechanism of asymmetric induction of CNTs

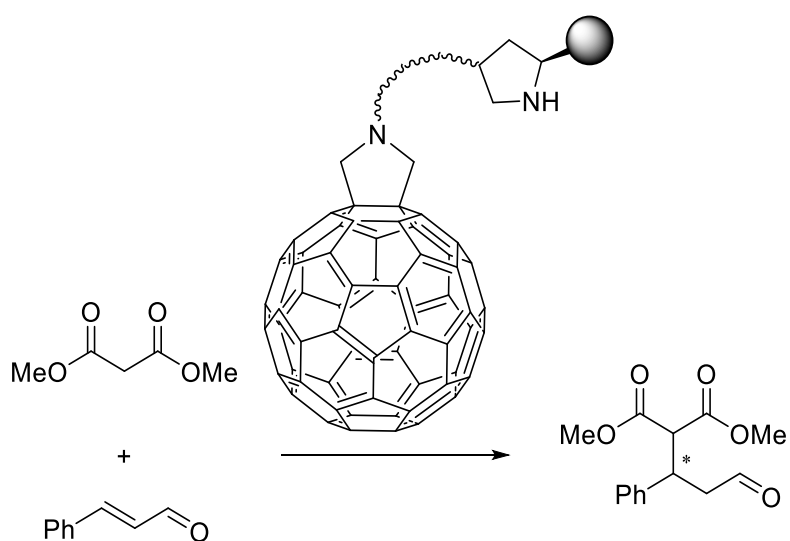
In **Figure 19**: the mechanism of stereocontrolled addition is showed, and is mediated by the CNT. The catalyst should be a modified diarylprolinol. The key-concept is the $\pi\text{-}\pi$ stacking interaction between the conjugated double bonds of the iminium and the aromatic system of the material, that allows to the substrate to be totally stretched on the surface on the CNT, by fact blocking completely one face. On the other side, the presence of a highly hindered group on the other face prevent the 1,4 addition, usually very favoured. In conclusion, theoretically the only reaction possible should be the 1,6 of the face opposite to the material, obtaining only one defined product. The nucleophile should be a “soft” one like a thiol.



Scheme 40: 1,6 stereocontrolled addition to $\alpha,\beta\text{-}\gamma,\delta$ -unsaturated aldehyde

Moreover, the catalyst should be easily recycled via filtration or centrifugation, and recovered.

The catalytic unity, should be a very stable one, and we need to synthesize a proper catalyst. In fact, the classic Hayashi-Jorgensen catalyst suffer from stability problems due to the presence of the silylether group that is unstable in particular in acidic conditions. Finally, the last part of the work is the functionalization of Fullerene with the synthesized catalysts, in order to promote enantioselective Michael reactions. Also in this case is interesting to recover the catalyst for several reactions.

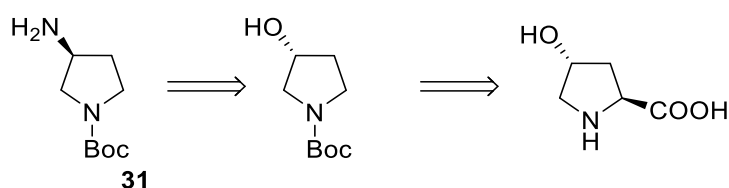


Scheme 41: Fullerene supported Modified pyrrolidine to promote racemic of diastereoselective michael addition reaction.

4.6 DISCUSSION AND RESULTS

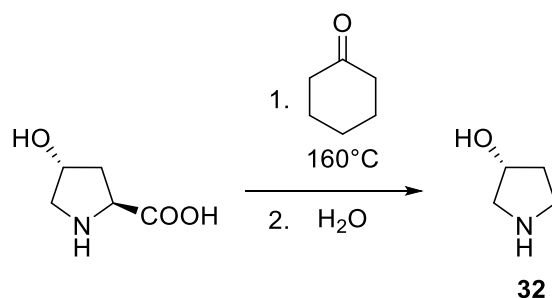
Since the synthesis of very complex molecules without any information about the possible results can be seriously risky, in the beginning we decided to start this study with the synthesis of a simple pyrrolidinic catalyst **1**, able to promote a simple Michael reaction, even if not stereoselective. This allows us not to waste time and resources.

The catalyst **31** can be obtained in some synthetic steps starting from relatively simple L-4-trans-hydroxyproline, as shown in **Scheme 42**:



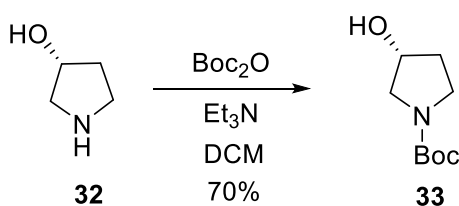
Scheme 42: retro-synthesis of catalyst 1

The synthesis starts with decarboxylation of commercial hydroxyproline using cyclohexanone, heating at reflux and removing the water formed during the process with the use of a Dean-Stark apparatus. The reaction is based on the formation of the corresponding iminium ion that leads to the enamine via decarboxylation. After, the enamine is hydrolysed giving the corresponding hydroxypyrrolidine **32**.



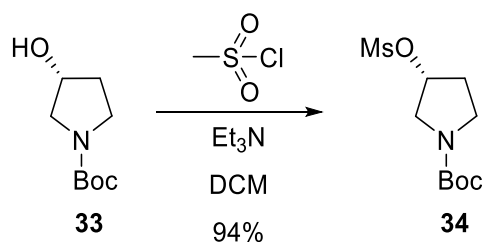
Scheme 43: L-4-trans-hydroxyproline decarboxylation

3-hydroxypyrrolidine **32** is then protected using Boc Anhydride and triethylamine in DCM to give the protected pyrrolidine **33**, with 70% yield on this first two steps.



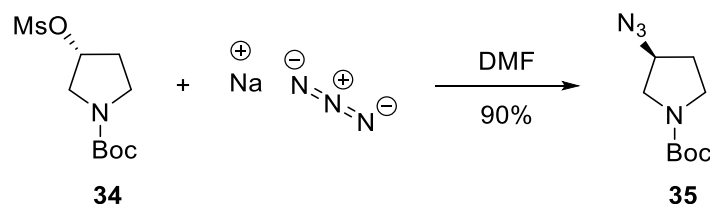
Scheme 44: Boc Protection of **32**

This protection is necessary because the free amine can interfere in the next steps. After, the alcohol is turned into a good leaving group through a mesylation reaction with mesyl chloride and triethylamine to give compound **34** in 94% yield.



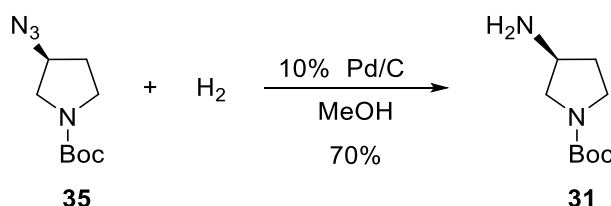
Scheme 45: Mesylation of **34**

Mesyated compound **7** is turned into the azide **35** via nucleophilic substitution with sodium azide in DMF, with 90% yield. This last two passages have been performed according to literature procedures.⁹⁶



Scheme 46: Nucleophilic substitution on mesylated **35**

Finally, the azido-derivative **8** is reduced to the corresponding amine through catalytic hydrogenation with Palladium/Carbon as catalyst in methanol, to give the product **1** with 70% yield.

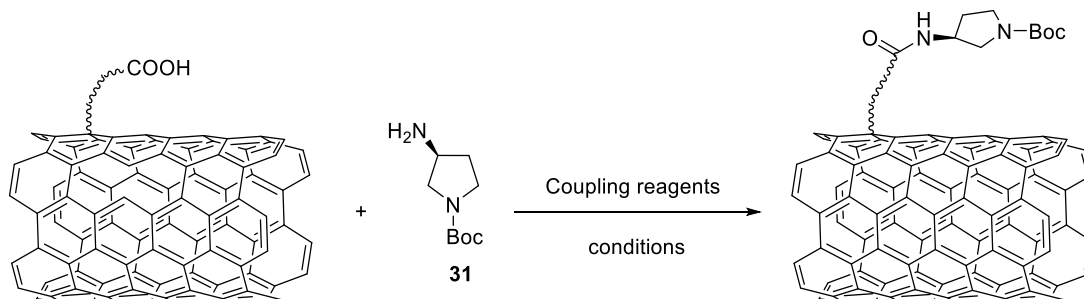


Scheme 47: Hydrogenation of derivative **35**

The critical point in this synthetic procedure are the difficult decarboxylation reaction, with a difficult work up, that can be avoided using directly the commercially available chlorohydrate pyrrolidinol, and the final reduction, due to the poisoning of the catalyst in presence of the free amine, and to the difficult in column chromatography. The reaction can be better performed in presence of acid, or even in acid solvent instead of MeOH, and by using Al₂O₃ instead of silica for chromatography.

⁹⁶ H. Zhang, Y. Chuan, Z. Li, Y. Peng, *Adv. Synth. Catal.* **2009**, *351*, 2288–2294.

From the point of view of nanomaterial, we started with the use of CNTs. The idea was to functionalize the nanotubes introducing carboxylic moieties, that can be coupled with the free anime of catalyst **1** in presence of coupling reagents to form an amide bond, as shown in **Scheme 48**.

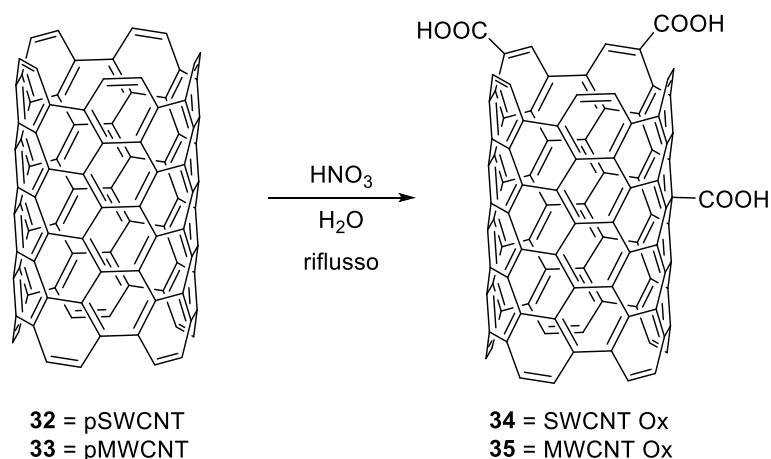


Scheme 48: functionalization of oxidized nanotube

The work of functionalization of CNTs has been done collaborating with the research group of Prof. Maurizio Prato from the University of Trieste, for their long expertise in functionalization of carbon-based nanomaterials. As functionalization reaction we chosed the simple oxidation of CNT and the Arylation with the use of diazonium salts, and the functionalization was tried on both single and multiwalled carbon nanotubes, in order to understand which material is the best for our purposes. The two functionalizations reaction has been chosen because simple oxidation often gives nanotubes functionalized on the borders and edges, while the arylation could give product with different functionalization points.

The reaction has been carried out using a great dilution, generally 1 mL for mg of material, in order to have a better dispersion. Moreover, sonication of the solution is very important. TGA is the principal technique used for the determination of the functionalization percentage.

We started with the oxidation of both pSWCNT **32** and pMWCNT **33**, using 4M nitric acid in water at reflux, obtaining the oxidized product **34** and **35**.



Scheme 49: Oxidation of carbon nanotubes

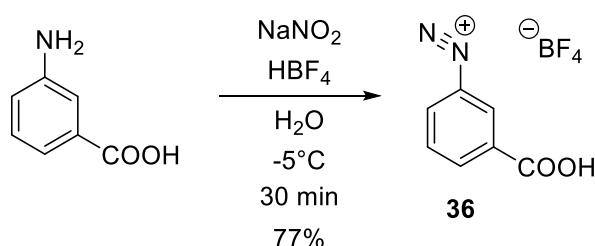
The results are showed in the following table.

Entry	Nanotubes	Functionalization %	$\mu\text{mol}/\text{mg}$
1	SWCNT Ox 34	5,4 %	3,8
2	MWCNT Ox 35	0,5 %	0,4

Table 12: results ofr the oxidation of CNTs

The value of functionalization for the SWCNT Ox is similar to other reported in literature, while for MWCNT OX is too low. Then, another oxidation on the same nanotubes is performed, using 8M nitric acid, that increase the functionalization up to 1%, almost 0,8 $\mu\text{mol}/\text{mg}$ of material.

For the arylation reaction we decided to use 3-carboxybenzediazonium tetrafluoroborate **36**, synthesized starting from 3-aminobenzoic acid with HBF_4 and sodium nitrite with 77% yield, as reported in literature.⁹⁷ (**Scheme 50**)

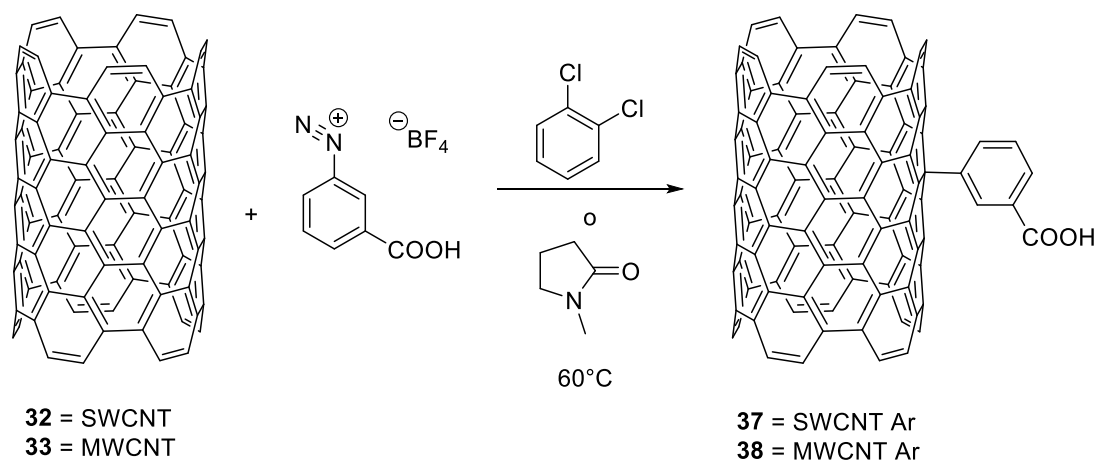


Scheme 50: Synthesis of diazonium salt

The choice of this particular diazonium salt is due to the presence of the carboxylic acid, that is needed for the coupling reaction with the catalyst. Moreover, the *meta* position gives the best compromise between proximity to the wall and steric hindrance.

⁹⁷ G. F. Kolar, *Zeitschrift fur Naturforsch. - Sect. B J. Chem. Sci.* **1972**, 27, 1183–1185.

Once the diazonium salt has been synthesized, we proceeded with the arylation of both pSWCNT and pMWCNT in orthodichlorobenzene or *N*-methyl-pyrrolidone as solvent at 60°C to obtain the arylated materials **37** and **38**.



Scheme 51: Arylation of CNTs

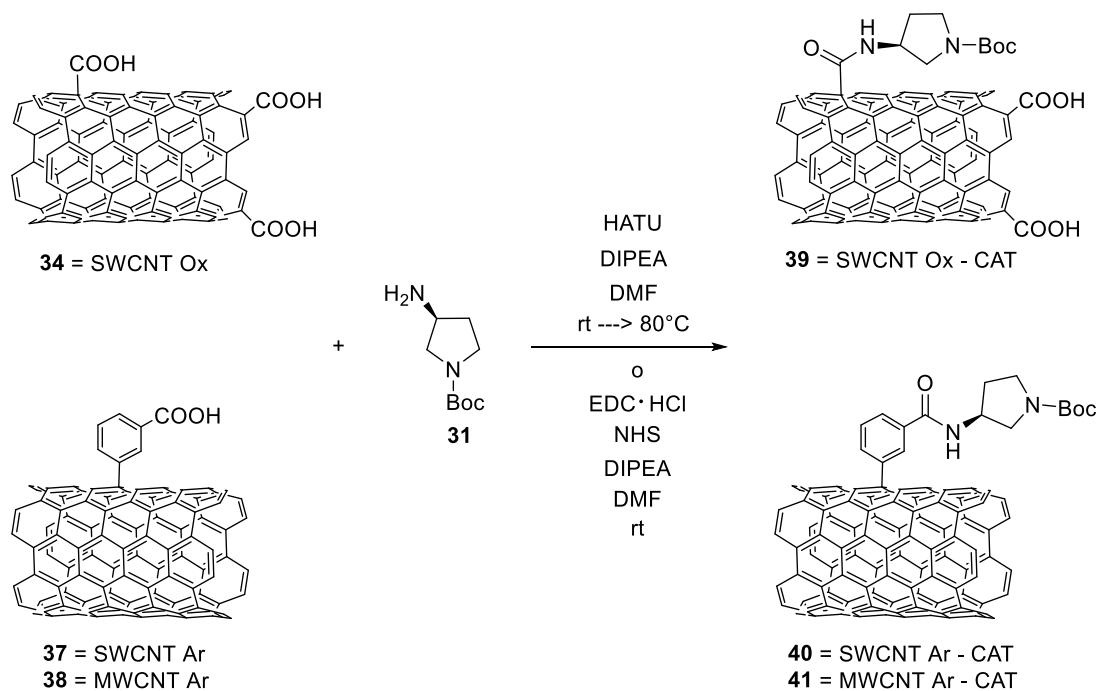
The results are showed in the following table.

Entry	Nanotubes	Solvent	Functionalization %	μmol/mg
1	SWCNT Ar 37	ODCB	1,6 – 2,7 %	1,1 – 1,8
2	SWCNT Ar 37	NMP	2,8 %	1,8
3	MWCNT Ar 38	OCDB	0,5 %	0,4

Table 13: Results for Arylation of CNTs

As shown in the table, the reaction proceeded almost in the same way using ODCB or NMP as solvents, So ODCB was chosen as solvent for next arylation. Concerning the results, they are similar to the one reported in literature. Both arylation has been repeated on the arylated material but only with a slight increase in functionalization in case of SWCNT (from 1,6 to 1,8%).

After these functionalization of pristine CNT, we proceeded with the amide coupling with catalyst **31**, both with oxidized SWCNT Ox **34** and with the arylated SWCNT Ar **37** and MWCNT Ar **38**. MWCNT Ox have not been functionalized for time reason. HATU and EDC/NHS has been chosen as coupling reagents in DMF. The reaction time is several days, as usual for nanomaterials. In particular, the amine is added one day after, respect to the coupling reagents.



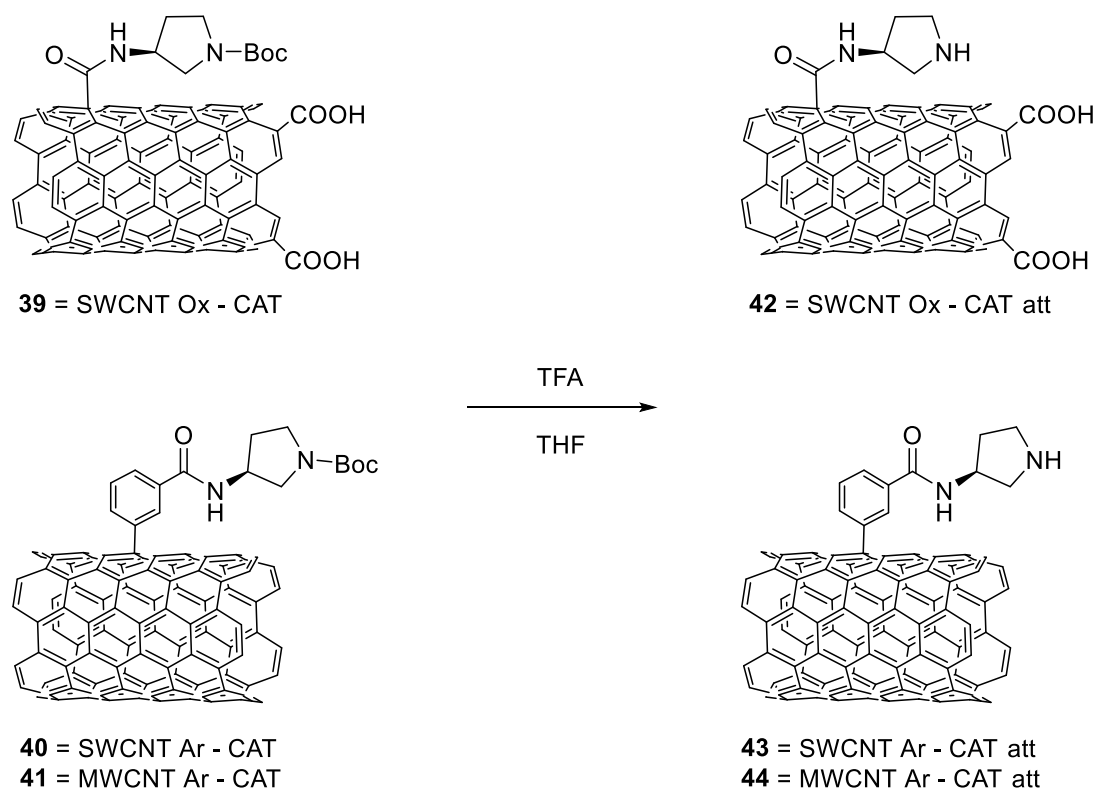
Scheme 52: Peptide coupling between oxidated and arylated CNTs and catalyst **31**

In this way the derivatized materials **39**, **40** e **41** has been obtained. The functionalization has been calculated considering that the molecular weight of the residue is increased respect to the starting material. In **Table 14** the changes in functionalization are showed.

Entry	Nanotubes	Coupling reagent	Dilution (mg/mL)	% funz	$\mu\text{mol/mg}$	$\Delta\%$ funz	Δ $\mu\text{mol/mg}$
1	SW Ox – CAT 39	HATU	0,1	1,8 %	1,1	- 3,6 %	- 2,7
2	SW Ox – CAT 39	EDC/NHS	0,1	1,1 %	0,8	- 4,3 %	- 3,0
3	SW Ar – CAT 40	HATU	0,25	1,2 %	0,8	- 0,4 %	- 0,3
4	MW Ar – CAT 41	HATU	0,25	0,2 %	0,2	- 0,3 %	- 0,2

Table 14: results for amide coupling on functionalized CNTs

What is soon evident is that the percentage are decreased, also dramatically in some cases. We can also observe that arylated nanotubes are less affected by this loss. Despite of the unpromising result, we proceeded with the last step, the removal of the Boc protective group, that release the active catalyst. The deprotection is carried out in presence of trifluoroacetic acid in THF.



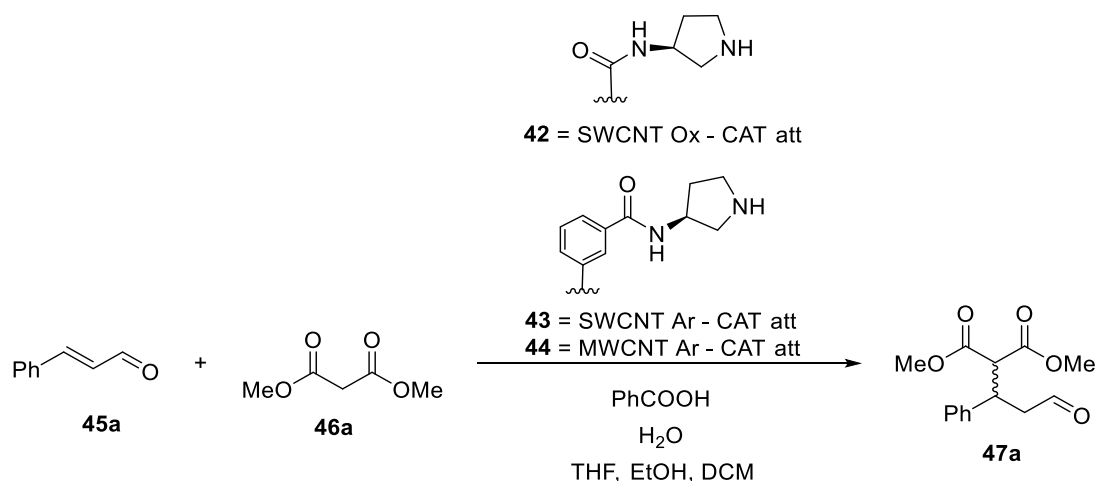
Scheme 53: Deprotection of the catalysts

The last step allowed to obtain the active materials **42**, **43** and **44**. Also in this case the variations in functionalization are showed in **Table 15**:

Entry	Nanotubes	[TFA] (mL/mL THF)	% funct	$\mu\text{mol/mg}$	$\Delta\%$ funz	$\Delta \mu\text{mol/mg}$
1	SW Ox – CAT att 42	0,2	2,7 %	1,8	+ 1,6 %	+ 1,0
2	SW Ar – CAT att 43	0,2	1,6 %	1,1	+ 0,4 %	+ 0,3
3	MW Ar – CAT att 44	0,2	0,4 %	0,3	+ 0,2 %	+ 0,1

Table 15: Results for boc deprotection

The work up of the reaction is the similar to the other, but a basic wash with saturated NaHCO_3 is added in order to neutralize the ammonium salt formed during the reaction. We can observe an increase in functionalization, even if there is not a direct explanation for this. Entry 1 is relative to amide coupling with EDC/NHS. Once the catalytic system is ready, the materials were tested in the classic Michael addition reaction between cinnamaldehyde and dimethyl malonate in different condition.



Scheme 54: Organocatalyzed Michael Reaction

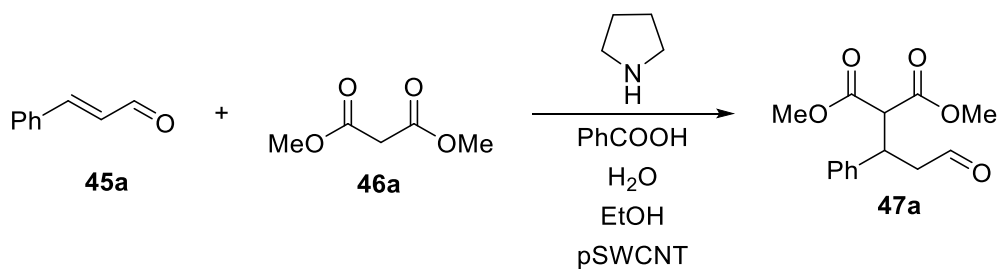
The reactions were carried out with 7,5 mol % of active catalyst, considering the different load between the materials. The results were verified by ¹H-NMR of the reaction mixture. The reaction condition and the results are reported in **Table 16**.

Entry	Nanotubes	Solvent	funct μmol/mg	[C] (mg/mL)	47a
1 ^x	SW Ox – CAT att 42	THF	1,8	1,8	-
2	SW Ar – CAT att 43	THF	1,1	2	-
3	SW Ar – CAT att 43	EtOH	1,1	2	traces
4	SW Ar – CAT att 43	DCM	1,1	2	-
5 [≠]	SW Ar – CAT att 43	EtOH	1,1	2	-
6 [≠]	SW Ar – CAT att 43	EtOH/THF 4:1	1,1	2	-
7	SW Ar – CAT att 43	EtOH	1,1	2	-
8 ^{x≠}	SW Ox – CAT att 42	EtOH	1,8	1,8	-
9	MW Ar – CAT att 44	EtOH	0,3	4,5	traces

Table 16: results for the organocatalysed Michael addition. Conversion determined by ¹H-NMR of the reaction mixture.

Entry signed with (x) are relative to CNT functionalized with EDC/NHS coupling, while entry signed with (≠) to CNTs recovered from previous catalysis. Reactions were checked until 4 days. Entry 7 and 9, after this period, were heated at 40°C for another day without any difference. The important data is that none of the entries gives any Michael adduct, and only traces in some cases were observed without any reproducibility. The percentage of functionalization is only from 0,3 to 1 μmol/mg.

Before going on some control reaction were performed, using simple pyrrolidine as a catalyst, and also adding pristine SWCNT, in order to verify if the simple reaction works or, for some reason, the presence of the nanomaterial itself disfavour the reaction.



Entry	Nanotube	Loading	47a
1	-	7,5% mol	> 50% in 2h
2	pSWCNT	7,5% mol	> 50% in 2h

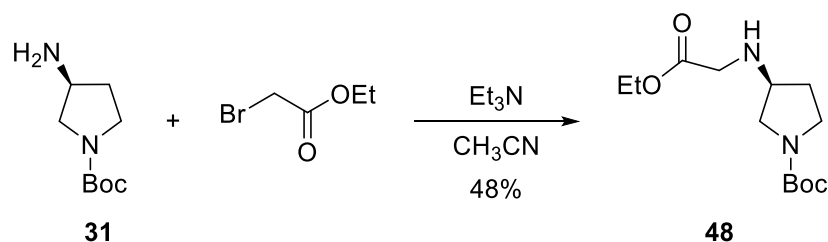
Table 17: results for Michael addition with pyrrolidine. Conversion determined by $^1\text{H-NMR}$ of the reaction mixture.

As showed in **Table 17** the control reactions lead easily to the formation of product. Moreover, the introduction of pSWCNT does not interfere with the reaction. Then, the absence of product in presence of the new materials is due to other factors.

The low percentage in functionalization of CNT is probably the most important factor: despite it is comparable to results reported in literature, is clearly not enough to have a good load of active catalyst during the reaction. Moreover, even the use of large quantities of nanomaterial, a great dilution is necessary for its dispersion. This limitation in functionalization of the CNTs convinced the research group in abandon this first part of the work, and also the idea to use the surface of carbon-based nanomaterials for perform stereoselective 1,6 addition.

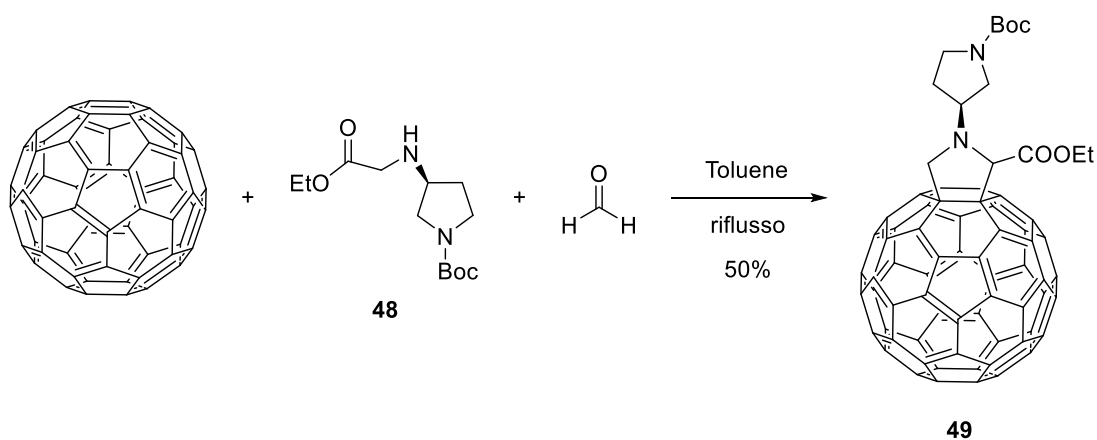
Despite of this, the work with nanotubes highlighted the right features that are essentials for a good supported catalyst. The need for high loading and solid analytical procedures are extremely important. In this sense, Fullerene is comparable to common organic molecules: is soluble, relatively easy to functionalize with solid protocols, can be purified via simple flash chromatography, and can be characterized with NMR and HRMS. Is clear that fullerenes are not useful for 1,6-reaction, because of their shape and dimension, but however is possible to carry out simple 1,4 Michael reaction, and in the end to recycle the catalyst using specific non-solvents.

The first step is to bind the catalyst **31**, already synthesized, to fullerene C_{60} and to test this system in the simple Michael reaction, even with racemate product. First of all, the catalyst has to be modified for being suitable for Michael reaction, and then the first step is the reaction of catalyst **1** with ethyl bromoacetate in presence of triethylamine, to give the amino acid **25** with 48% yield after purification.



Scheme 55: Alkylation of N-Boc-4-aminopyrrolidine **31**

Now with compound **48** is possible to perform a Prato reaction with paraformaldehyde and fullerene. The experimental conditions are toluene as solvent, 1 mL for 1 mg of fullerene, and heating to reflux.



Scheme 56: Prato reaction between formaldehyde, fullerene and compound **48**

The aim is to obtain only the monoadduct **49**, then the reaction needs to be stopped when the TLC of reaction mixture shows the formation of poly adducts. At that point the conversion is almost 50%. Poly adducts, like for example the double adduct **50** are not desirable gives a mixture of diastereoisomers. Thanks to this functionalization the adduct is soluble in slightly polar solvents like chloroform, despite of pristine fullerene.

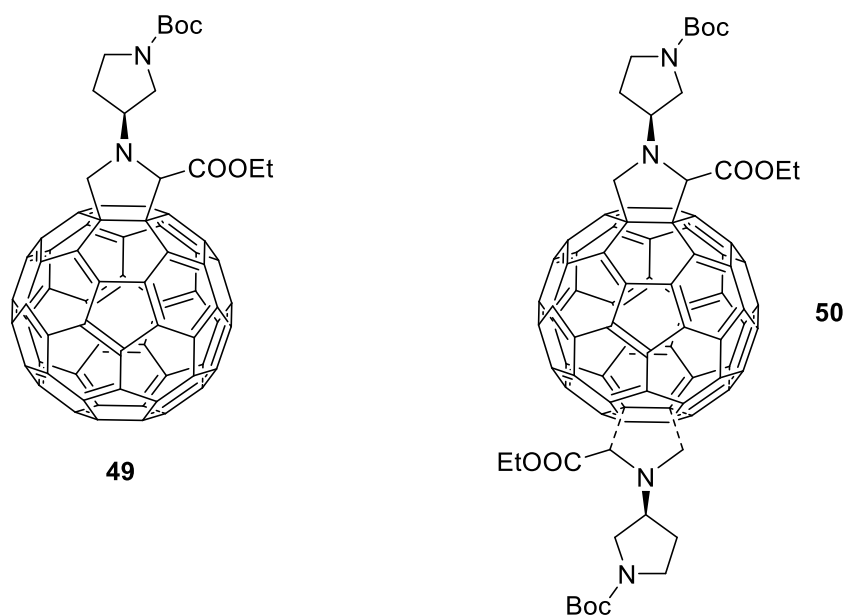
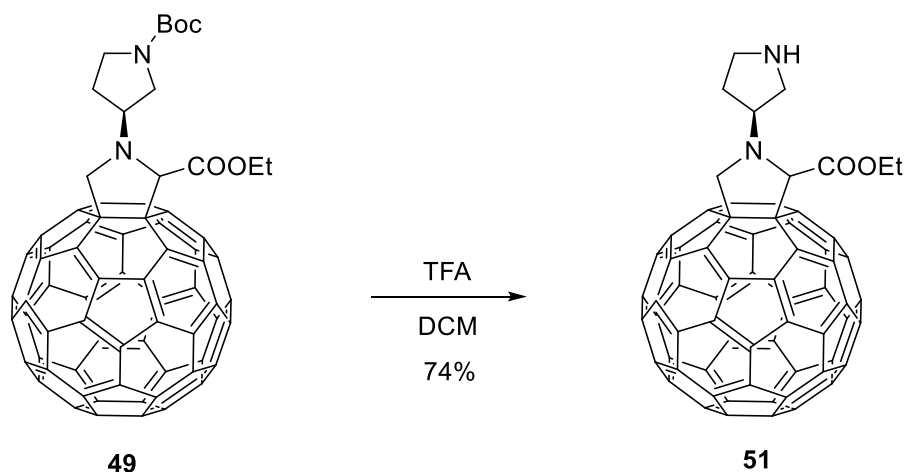


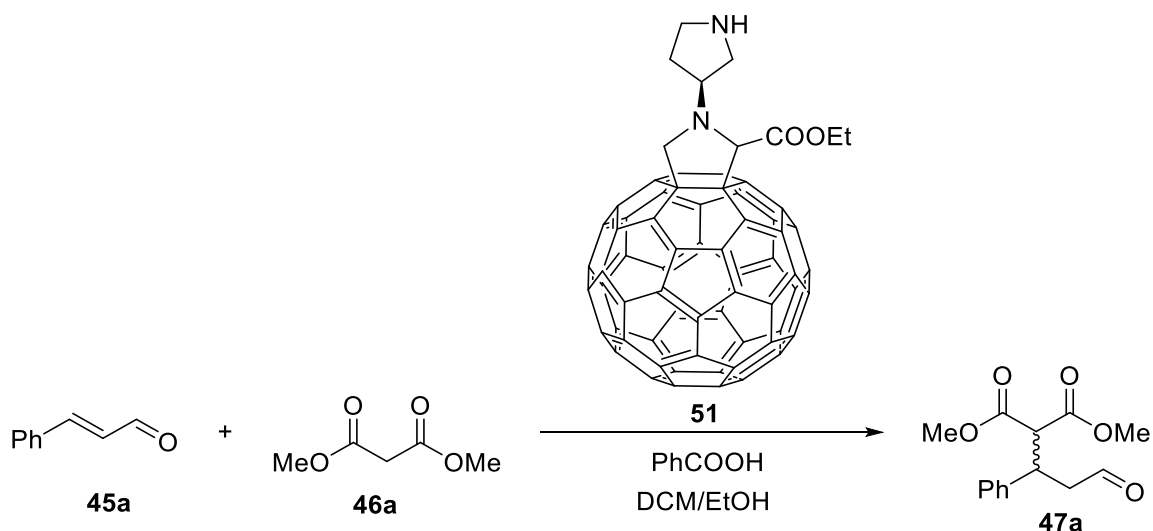
Figure 20: Mono adduct **49** and double adduct **50**

The work up of the Prato reaction is a direct flash chromatography, that is possible thanks to a great difference in polarity between pristine Fullerene, mono adduct **49** and double adduct **50**. After, the product is centrifuged with chloroform /methanol to remove traces of reagents. After, compound **49** is treated with a mixture of trifluoroacetic acid and dichloromethane for the removal of boc group, leading to the active catalyst **51**. The yield of the reaction is 74%, after a neutralization with saturated NaHCO_3 .



Scheme 57: Deprotection of the amine of compound **49**

Once catalyst **51** has been obtained is possible to test its reactivity in the organocatalyzed Michael reaction between Cynamaldehyde and dimethyl malonate.



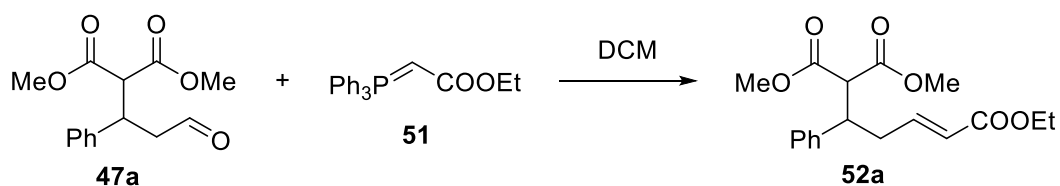
Scheme 58: Michael addition catalyzed by **51**

The result is reported in **Table 18**:

Entry	Solvent	Concentration 3	Loading 3	Additive	time	Conversion
1	DCM/EtOH 1:1	20 mg/mL	30% mol	PhCOOH	3 d	90 %

Table 18: results for Michael addition. Conversion determined by $^1\text{H-NMR}$ of the reaction mixture. d = days

This time, the catalyst supported on fullerene gave the first promising results, with 90% conversion after 3 days determined by $^1\text{H-NMR}$. The mixture of solvents is necessary for the solubility of the material, even if not complete. It's clear that the conversion is not due to background reaction, never observed in the other cases, even after several days. After, the supernatant, containing the reagents and the product, is removed, while the catalyst is washed with diethyl ether and centrifuged for recycle. For the determination of the enantiomeric excess the product is derivatized via Wittig reaction, that gives the corresponding α,β -unsaturated ester.



Scheme 59: Derivatization of the Michael adduct via Wittig reaction

The Chiral HPLC analysis showed, as expected, that the product obtained with catalyst **3** is a racemic mixture. the two enantiomers were present at almost 50%. Since this part of the project gave promising results, we decided to go on with the synthesis of a new catalyst, able to perform enantioselective reaction, to support on Fullerene.

Encouraged by these first promising trials, we started wondering about the synthesis of a secondary amine capable both to induce asymmetric Michael reactions, and at the same

time to be covalently supported on fullerene. A molecular linker should be incorporated in the catalyst, both for binding the two parts of the catalyst, and to act as a spacer between them.

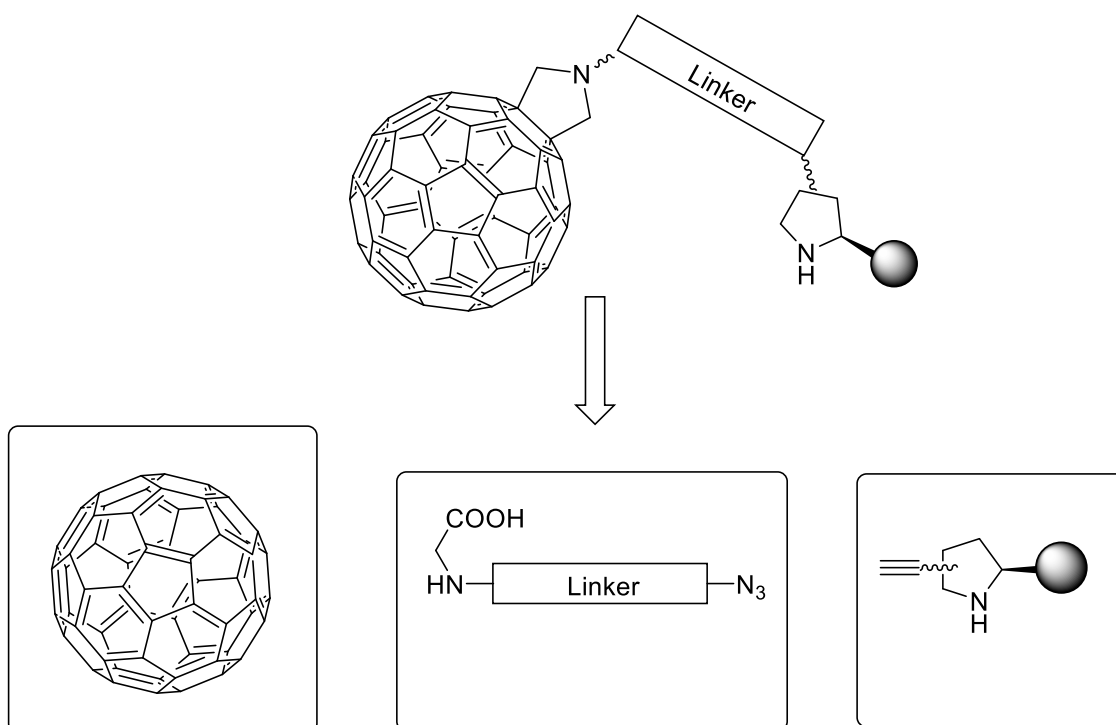


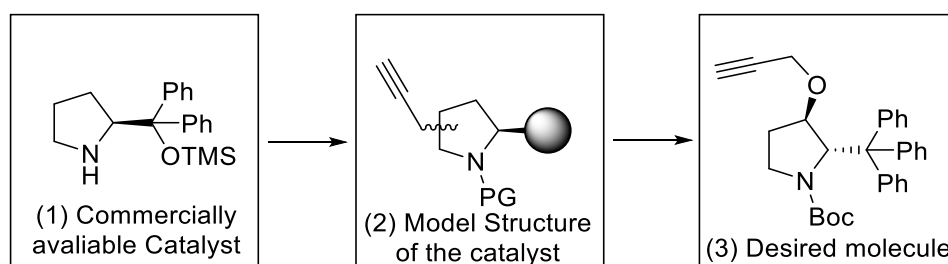
Figure 21: Project of the active catalyst

For covalently bind the catalyst to the spacer, we decided to perform a classic Huisgen cycloaddition reaction, placing an azide functional group on the linker (easy obtainable via interconversion of the correspondin alcohol), and a triple bond on the catalytic core. On the other side, an amino acid is needed in order to perform the final functionalization via “Prato reaction”.

Regarding the catalytic center, the idea was to develop a structure like the commercially available Jorgensen-Hayashi catalyst, capable to promote chirality using the extremely hindered group in the α -position respect to the nitrogen, a TMS-protected diarylmethanol, but avoiding the presence of the silyl ether, unstable under acid conditions. Furthermore, the catalyst should bring an alkyne functional group for the click functionalization reaction. Our choice was to synthesize a modification of a catalyst previously studied by Maruoka and coworkers, bearing a very stable trytil group as chirality promoter⁹⁸. The catalyst has been applied in α -functionalization reaction such as α -benzylation, and the reactivity has been extensively studied, revealing a high reactivity of the corresponding iminium ion respect to Jorgensen-Hayashi catalyst⁹⁹.

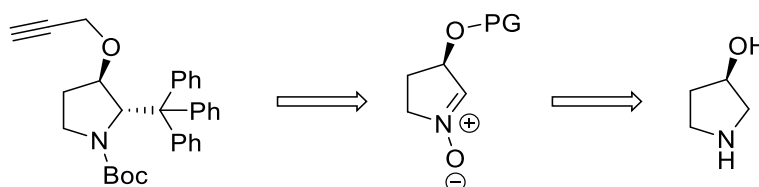
⁹⁸ T. Kano, H. Mii, K. Maruoka, *J. Am. Chem. Soc.*, **2009**, 131, 3450–3451

⁹⁹ H. Erdmann, F. An, P. Mayer, A. R. Ofial, S. Lakhdar, H. Mayr, *J. Am. Chem. Soc.* **2014**, 136, 14263–14269



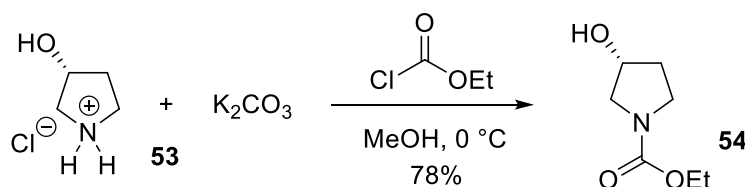
Scheme 60: Design of the catalyst

The catalyst should be synthesized converting the Pirrolydinol **32** into the corresponding nitron. After, addition of Trytyllithium should provide the *anti*-functionalized pyrrolidine as major product. Additions of organometallic compounds to pyrrolidine-derived nitrones have been already reported in literature.¹⁰⁰



Scheme 61: retrosynthetic analysis for the catalyst

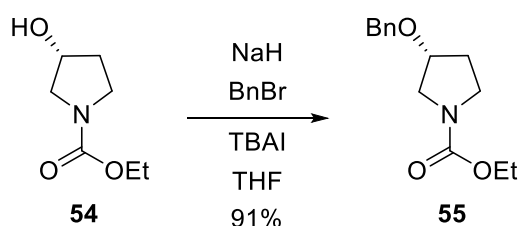
The synthesis of the catalyst started with the protection of the nitrogen of the 3-pyrrolidinol. This time, we decided to use the commercially available chlorohydrate **53**, and to use as protective group for the first part of the synthesis the cheaper ethyl chloroformiate. The reaction in presence of potassium carbonate as a base, gave the corresponding N-protected pyrrolidinol **54** with 78% yield.



Scheme 62: Nitrogen protection of compound **53**

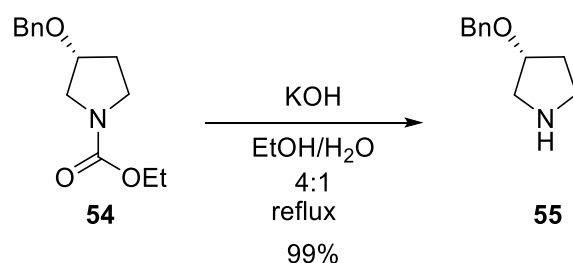
¹⁰⁰ a) P. Merino, T. Tejero, J. Revuelta, P. Romero, S. Cicchi, V. Mannucci, A. Brandi, A. Goti, *Tetrahedron: Asymmetry*, **2003**, *14*, 367–379; b) S. Wu, Y. Ruan, X. Zheng, P. Huang, *Tetrahedron*, **2010**, 1653-1660; c) P. Merino, I. Delso, T. Tejero, F. Cardona, M. Marradi, E. Faggi, C. Parmeggiani, A. Goti, *Eur. J. Org. Chem.* **2008**, 2929–2947; d) S. Cicchi, M. Bonanni, F. Cardona, J. Revuelta, A. Goti, *Org. Lett.*, **2003**, *5*, 1773–1776; e) S. Wu, X. Zheng, Y. Ruan, P. Huang, *Org. Biomol. Chem.*, **2009**, *7*, 2967–2975; f) R. Pulz, S. Cicchi, A. Brandi, H. Reißig, *Eur. J. Org. Chem.* **2003**, 1153-1156

After, also the oxygen needs a protective group orthogonal to the first. The benzyl group was chosen and the benzylation reaction proceeded with benzyl bromide in THF, with a catalytic amount of tetrabutyl ammonium bromide. The yield of the reaction is 83%.



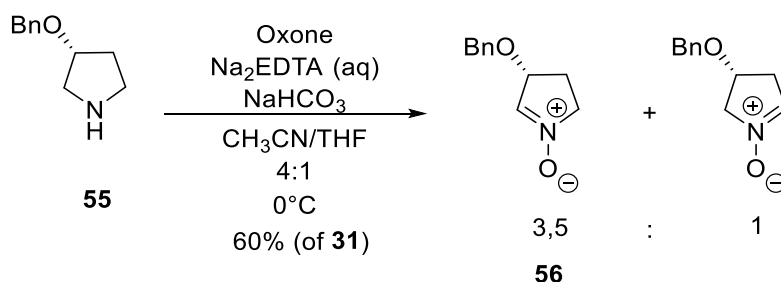
Scheme 63: Benzylation of compound **54**

Then, the nitrogen needs to be deprotected, using Potassium hydroxide and an Ethanol/Water mixture at reflux. The amine **56** was obtained in quantitative yield.



Scheme 64: Deprotection of compound **54**

The amine **56** is now ready for the oxidation with Oxone, EDTA and NaHCO_3 in $\text{CH}_3\text{CN}/\text{THF}$ at 0°C , following condition reported in literature¹⁰¹, to give nitron **56** in 60% yield after the separation of the minor regioisomer.

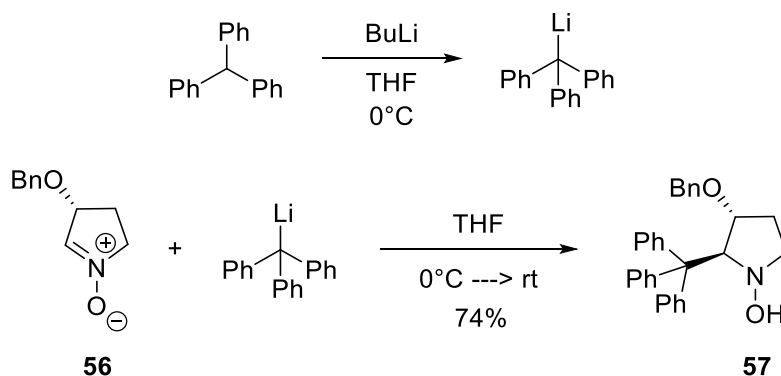


Scheme 65: oxidation of **56**

Nitron **56** is the major stereoisomer, and this is probably due to the proximity of the oxygen that stabilizes the double bond formation or the intermediate. It is good for our purposes, because the subsequent alkylation has got high chance to be totally *anti*-selective. The alkylation was carried out in THF at 0°C , and the first step is the lithiation of

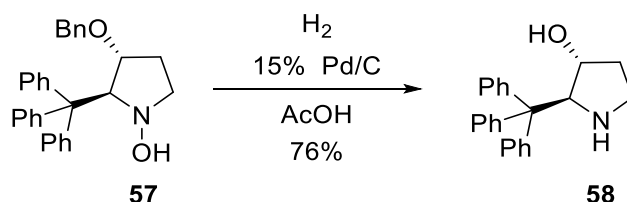
¹⁰¹ R. Alibés, C. Gella, P. De March, M. Figueredo, J. Font, E. Ferrer, F. Busquè, *J. Org. Chem.* **2009**, *74*, 6365–6367.

triphenylmethane using butyllithium as base. Then the corresponding Nitron **56** is added to the mixture, giving the corresponding hydroxylamine **57** in 74% yield.



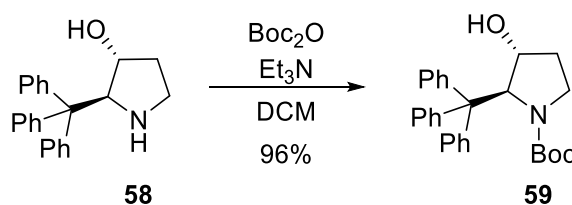
Scheme 66: alkylation of nitron 56

The hydroxylamine is not stable and undergoes to decomposition, then it has to be rapidly reduced. The reaction allows to reduce the hydroxylamine to the corresponding secondary amine, and in the same time to remove the benzyl group. This reaction is carried out using Pd/C as catalyst and atmosphere of hydrogen. The reaction in MeOH gave mixture of products, because the amine formation poisons the catalyst. Instead, the use of acetic acid as solvent for the reaction, following Maruoka's work¹⁰², gave only the product **58** in 76% yield.



Scheme 67: reduction of 57

The 2-trytyl-3-hydroxypyrrolidine **58** is now again protected on the nitrogen, this time with Boc₂O and TEA in DCM as solvent, obtaining the product **59** in 96% yield.

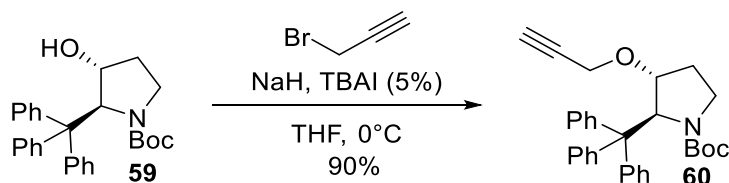


Scheme 68: Protection of compound 58

The protected catalyst can now be functionalized with the propargyl group for the click reaction with the spacer. The alcohol was subjected to metalation with sodium hydride, then

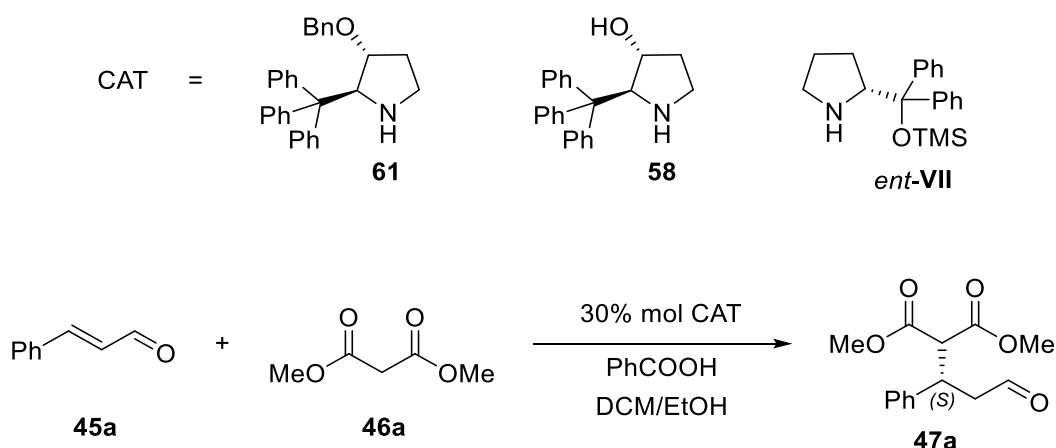
¹⁰² T. Kano, H. Mii, K. Maruoka, *J. Am. Chem. Soc.* **2009**, *131*, 3450–3451

to reaction with propargyl bromide and a catalytic amount of TBAI, in THF at 0°C. The reaction allowed to obtain compound **60** in 90% yield and to complete the first part of the synthesis.



Scheme 69: Propargylation of **59**

At this point, we decided to test the performance of the catalytic subunit in the Michael reaction in homogeneous phase. We compared three different molecules, the benzylated adduct **61**, obtained during the reduction trials, the amino alcohol **58** and the *R*-Hayashi catalyst *ent*-VII as a reference. The reactivity has been evaluated through the conversion, determined via ¹H-NMR, and the selectivity via Chiral HPLC after derivatization. The results are showed in **Table 19**:



Entry	Solvent	Concentration CAT	Loading CAT	Time	Conversion	ee
CAT OBn	DCM/EtOH 1:1	20 mg/mL	30% mol	18 h	79 %	90 %
CAT OH	DCM/EtOH 1:1	20 mg/mL	30% mol	18 h	85 %	92 %
Hayashi	DCM/EtOH 1:1	20 mg/mL	30% mol	18 h	99 %	74 %

Table 19: results for the test of catalyst in the homogeneous phase. Conversion determined by ¹H-NMR of the reaction mixture. d = days ee determined by CSP-HPLC of derivatized product

The results are quite interesting. The new catalysts are characterized by a low reactivity, compared to Hayashi catalyst, and can be explained with the presence of two substituent on the pyrrolidinic ring, that decrease the nitrogen's nucleophilicity. On the other side, these systems resulted to be more selective, probably due to the best stability of the trityl group during the reaction.

Now that the reactivity of the catalytic unity has been verified, the synthesis of the spacer is reported. The idea for the synthetic strategy is to have a quite long spacer, in order not to be too near to the fullerene, an amino acid on one side, that allows the fullerene functionalization, and an azide on the other side, to perform the click reaction with the propargylated catalytic unity. The amino acid needs to be protected for the cycloaddition.

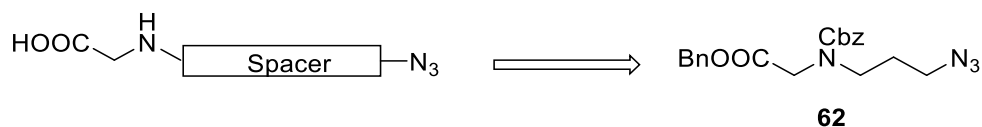
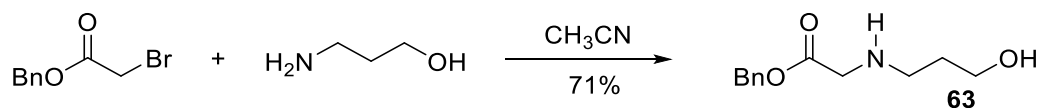


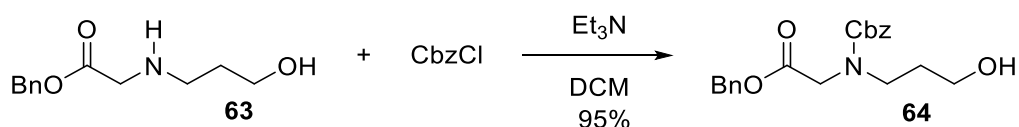
Figure 22: Strategy for the choice of the spacer

The first step is a nucleophilic substitution reaction between 2-Bromobenzyl acetate and 3-amino-1-propanol to give the amino alcohol **63**. Reaction time needs to be only two hours to avoid the double substitution, and allowed to obtain the product with 71% yield.



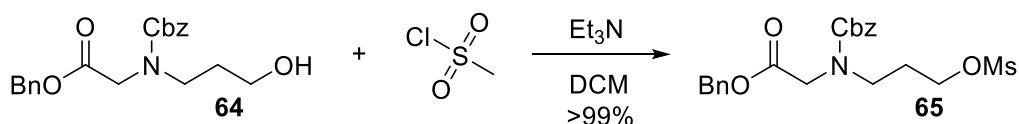
Scheme 70: Nucleophilic Substitution reaction to give product 9

The second step is the protection of the amine using CbzCl and TEA in DCM. The nitrogen needs to be protected in a way that allows the removal of both the benzyl ester and the Protective group. The reaction gave product **64** in 95% yield.



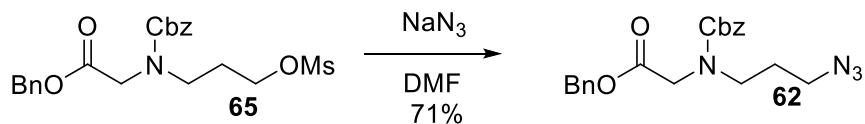
Scheme 71: Cbz Protection of **63** to afford compound **64**

The alcohol needs to be converted into an azide group. The first step is a mesylation reaction using mesyl chloride and TEA in DCM, to obtain the mesylated product **65** in quantitative yield. The mesyl group is a better leaving group compared to simple OH.



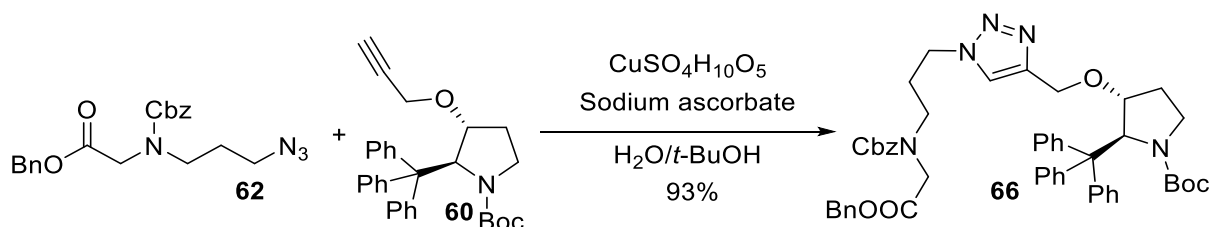
Scheme 72: Mesylation of **64** to give compound **65**

The final step for the spacer synthesis is the nucleophilic substitution using Sodium Azide in DMF. Is important to do the work up extraction using EtOAc and not DCM to avoid risk due to the presence of NaN₃. The product **62** was obtained in 71% yield.



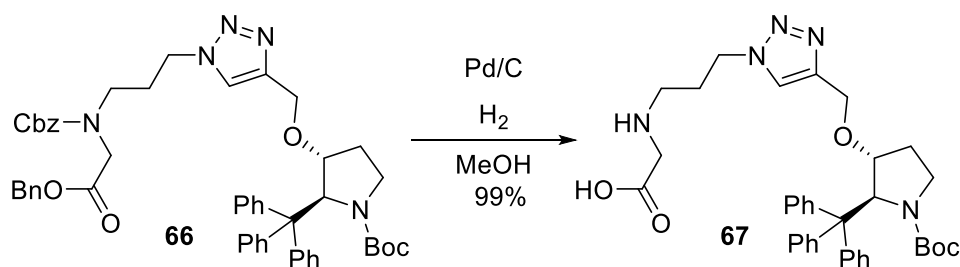
Scheme 73: Nucleophilic substitution of mesylated **65** with NaN_3

Once the synthesis of the spacer has been accomplished, the final part of the synthesis begins. In order to do as less steps possible using fullerene, we decided first to bind the spacer to the catalytic unit, and only after the subsequent deprotection of the amino acidic portion to functionalize the fullerene. The click reaction between the azide **62** and alkyne **60** took place in classic condition with a catalytic amount of copper sulphate and sodium ascorbate, in a mixture of water and tert-butanol. The reaction gave the product **66** in 93% yield.



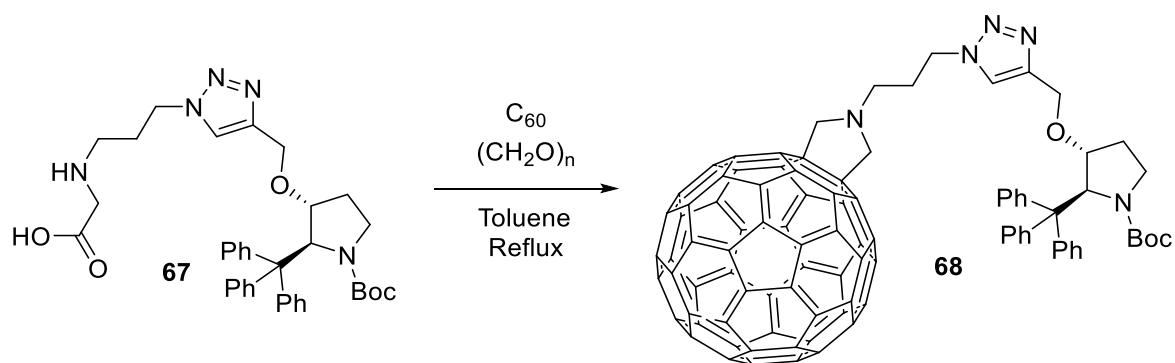
Scheme 74: click reaction between azide **62** and alkyne **60**

After, the aminoacidic portion need to be deprotected in order to functionalize the fullerene. With a hydrogenation with Pd/C in atmosphere of hydrogen in MeOH we were able to obtain the product **67** in a quantitative way.



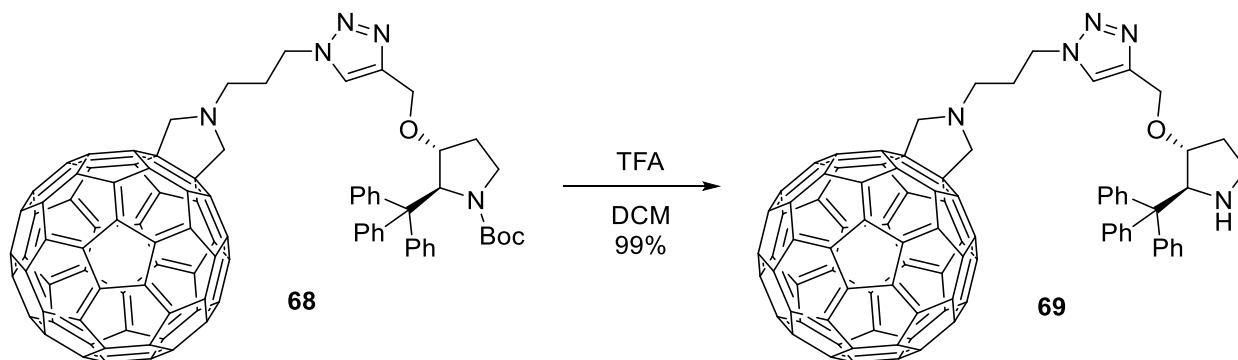
Scheme 75: deprotection of **66**

Now the substrate is ready for the “Prato reaction”. Since the substrate is very precious, we decided to modify the protocol using an excess of Pristine Fullerene and a higher concentration, among 3 mg for mL, paraformaldehyde and toluene heated to reflux. This time the mechanism is slightly different from the previous one, because the presence of a free carboxylic acid lead to a decarboxylation, and the fullerene pyrrolidine has no stereocenter. This factor simplified the synthesis and ensured the optical purity of the product. Despite of this changes the functionalization was accomplished with success, giving the product **68** with 50% yield.



Scheme 76: “Prato reaction” between **67** and Fullerene

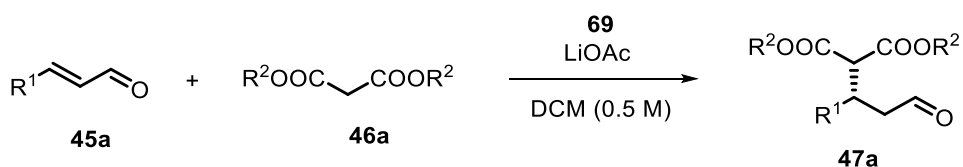
The final step of the reaction was the deprotection of the nitrogen of the catalyst, performed with trifluoroacetic acid in dichloromethane to obtain the final catalyst **69**, who was washed with saturated NaHCO_3 solution to free the ammonium salts giving the final catalyst in 99% yield, ready to be used.



Scheme 77: final deprotection for the synthesis of **69**

The synthesized catalyst has been fully characterized and their property has been explored. It seems to be stable if strictly stored under nitrogen to prevent any oxidation of the fullerene. The Michael reaction we used for the previous catalyst X unfortunately did not gave good results because catalyst 16 is not soluble in a mix of solvents that contains methanol or ethanol, while is completely soluble in dichloromethane. The problem is that the Michael reaction that use benzoic acid as a co-catalyst needs a polar protic solvent. Then, we looked in literature on a way to perform the reaction in DCM as solvent. As reported in a work by Pericas¹⁰³ the Michael addition of malonates to aldehydes give also good results in DCM if using a base like LiOAc as a co-catalyst instead of benzoic acid. In this way, the activation of the malonate passes through the formation of an enolate instead of an enol. Then we explored the reaction and the results are reported in **Table 20**:

¹⁰³ E. Alza, S. Sayalero, P. Kasaplar, D. Almas, M. A. Pericas, *Chem. Eur. J.* **2011**, *17*, 11585 – 11595



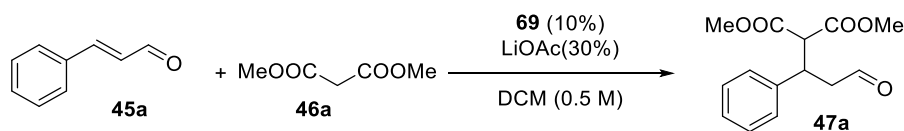
Entry ^a	R ¹	R ²	solvent	69(%)	LiOAc(%)	t(h)	Conv(%) ^b	ee(%) ^c
1	Ph 45a	Me 46a	DCM	10	30	8	85	92
2	Ph 45a	Me 46a	DCM/MeOH 9:1	10	30	5	97	80
3	Ph 45a	Me 46a	DCM/MeOH 95:5	10	30	5	96	84
4	Ph 45a	Me 46a	DCM	5	15	16	91	91
5	<i>p</i> NO ₂ -Ph 45b	Me 46a	DCM	5	15	24	83	85
6	<i>p</i> F-Ph 45c	Me 46a	DCM	5	15	24	89	85
7	<i>p</i> CH ₃ -Ph 45d	Me 46a	DCM	5	15	24	88	84
8	Et 45e	Me 46a	DCM	5	15	24	0	n.d.
9	Ph 45a	Et 46b	DCM	5	15	24 48	74 82	/ 93
10	Ph 45a	Bn 46c	DCM	5	15	24 48	79 80	/ 92
11	Ph 45a	t-Bu 46d	DCM	5	15	24	0	n.d.

Table 20: a) reaction conditions: Aldehyde **45**(1eq.), malonate **46**(3eq.), catalyst **69**, LiOAc and solvent 0.5M. b) determined via ¹H-NMR of the reaction mixture. c) determined via chiral HPLC after derivatization with Ph₃CHCOOEt **51**. h = hours n.d. = not determined.

The results of this trials are really interesting. As a starting point, the reaction between cinnamaldehyde and dimethyl malonate in only DCM as solvent with 10% catalyst (entry 1) gave a good conversion of 85% after 8 hours, and the enantiomeric excess was 92%, the same as the subunit in the homogeneous phase. This is an indication that the spacer length is enough to allow the reaction without interference due to fullerene. Then in entry 2-3 we explored the role of an amount of MeOH on the reaction. While the reaction rate is increased, there is a drop in ee. This can be related to the better solubility of lithium acetate in the reaction media, that allows a faster formation of the enolate, but probably also the increase of the background reaction. Then, the use of only DCM as solvent was chosen as the best condition. The catalyst loading was also reduced to 5% with good results, and the scope of the reaction was expanded on different aromatic α,β -unsaturated aldehydes, with quite good results in 24h. The limitations are related to aliphatic aldehydes (entry 8) which didn't show formation of the product. This is probably due to the formation of the corresponding dienamine, instead of the iminium. Also, different malonates were explored with good results. The only malonate which didn't show any reaction is the di tertbutyl malonate, for hindrance reason.

These results are quite satisfying, and the products were obtained in high conversion, short reaction time, low catalyst loading (5% is a quite low value for organocatalysts) and good enantiomeric excess. The reactions were very reproducible using different batches of catalyst. But the most important thing is that only very particular enamine-activated processes were reported with a Maruoka-like organocatalyst, like α -oxydation of aldehyde. This is the first example of an organocatalyst bearing a trityl group in an iminium-activated reaction.

Another important factor that need to be tested is the recycle of the catalyst. In order to check the recyclability of the catalyst we performed a cycle of reaction with 10% of catalyst, after 16 hours the reaction is diluted in a non-solvent like MTBE, that dissolves the reagents but not the catalyst, and the mixture is centrifuged. This protocol allowed to recover the supernatant and start a new reaction with recycled catalyst. The results are reported in **Table 21:**



Cycle ^a	t(h)	Conv (%) ^b	ee(%) ^c
1	16	99	91
2	16	95	90
3	16	87	90
4	16	41	90
5	16	10	n.d.

Table 21: a) reaction conditions: Aldehyde **45a**(1eq.), malonate **46a**(3eq.), catalyst **69**(10%), LiOAc (30%) and DCM 0.5M. Reaction mixture diluted in MTBE and centrifuged (5000 rpm, 5 minutes), solvent removed. b) determined via ¹H-NMR of the reaction mixture. c) determined via chiral HPLC after derivatization with Ph₃CHCOOEt **51**. h = hours. n.d. = not determined

Also in this case the results gave interesting indications. The first 3 cycle gave very good results in conversion, with only a slight but expected decrease (probably due to loss of little amount of material), while in the fourth and fifth cycles there is a strong drop in conversion. This can occur probably for the formation of molecular aggregates, that makes not available some of the catalytic units for the reaction. Since this feature seems strictly related to nature of fullerene, this can be seen as a limitation for this material. On the other side, the enantiomeric excess is not changed during all the cycles, indicating that the catalytic unity is always stable and is not affected by decomposition (like in Jorgensen-Hayashi supported catalysts).

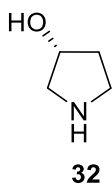
4.7 Conclusion

In conclusion, a deep study on functionalization of carbon-based nanomaterial has been accomplished. In particular, in collaboration with Prof. Prato and co-workers, we have successfully synthesized a fullerene-supported Trytyl pyrrolidine, able to perform enantioselective Michael addition of malonate to α,β -unsaturated aldehydes with results similar to literature. This is the first example of the use of a trityl Pyrrolidine organocatalyst in iminium ion activation mode. The catalyst has been recycled up to three times, and further studies will be done in order to build more stable catalysts, and to expand the number of reaction possible.

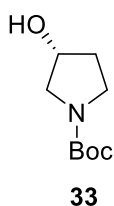
4.8 Synthetic Procedures and Product characterization

General Information. ^1H and ^{13}C NMR spectra were recorded on Varian Gemini 200 or Inova 400 NMR instruments with a 5 mm probe. Chemical shifts (δ) are reported in ppm, relative to the residual peaks of deuterated solvent signals. HPLC-MS analyses were performed on an Agilent Technologies HP1100 instrument coupled with an Agilent Technologies MSD1100 single-quadrupole mass spectrometer. A Phenomenex Gemini C18, 3 μm (100 x 3mm) column was employed for the chromatographic separation: mobile phase $\text{H}_2\text{O}/\text{CH}_3\text{CN}$, gradient from 30% to 80% of CH_3CN in 8 min, 80% of CH_3CN until 22 min, then up to 90% of CH_3CN in 2 min, flow rate 0.4 mL min^{-1} . Mass spectrometric detection was performed in full-scan mode from m/z 50 to 2500, scan time 0.1 s in positive ion mode, ESI spray voltage 4500 V, nitrogen gas 35 psi, drying gas flow rate 11.5 mL min^{-1} , fragmentor voltage 30 V. CSP-HPLC analyses were performed on an Agilent Technologies Series 1200 instrument using Daicel[®] chiral columns and n-hexane/2-propanol (n-Hex/IPA) mixtures. Optical rotation measurements were performed on a polarimeter Schmidt+Haensch UniPol L1000. Flash chromatography purifications were carried out using Merck silica gel 60 (230-400 mesh particle size). Thin layer chromatography was performed on Merck 60 F254 plates. Commercial reagents were used as received without additional purification. TGA analysis has been performed on the instrument TGA Q500 (TA Instruments) under nitrogen with equilibration at 100°C followed by a $10^\circ\text{C}/\text{min}$ gradient until 800°C . (T = working temperature, Δm = mass variation). Raman analysis have been performed with an Invia Renishaw (50x) microspectrometer and a laser source at 532, 633 e 785 nm. (RBM = *radial breathing mode*, D = D band, G = G band, 2D = D sovratone band).

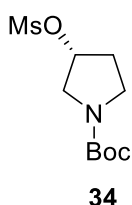
Synthesis and Product Characterization



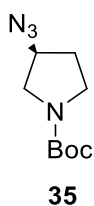
32: A suspension of trans-L-hydroxyproline (2,1 g, 16 mmol) in cyclohexanone (10 mL, 96 mmol) is heated 160°C using a Dean-Stark apparatus to remove water for 3h, until a yellow clear solution is formed. After, the mixture is cooled to room temperature and H_2O (8 mL, 444 mmol) is added. The reaction is stirred for 1 h. Finally, the aqueous layer is collected and the organic phase is extracted with additional H_2O . The combined aqueous layers are concentrated under vacuum and dried to obtain the crude product as a dark brown oil, that is used without further purification.



33: To a solution of **32** (1,4 g, 16 mmol) in DCM (40 mL) and Et₃N (6,7 mL, 48 mmol) at 0°C is added Boc₂O (4,2 g, 19,2 mmol). The mixture is stirred at room temperature overnight. After, the reaction is quenched with saturated NH₄Cl and extracted with DCM. The combined organic layers are dried over Na₂SO₄, filtered and concentrated under reduced pressure. The crude product is purified via flash chromatography (DCM/MeOH 9:1), giving the corresponding product **6** as a brown oil (2,1 g, 11,2 mmol, 70% over two steps). Compound characterized in literature.¹⁰⁴



34: To a solution of **33** (565 mg, 3 mmol) in DCM (6 mL) at 0°C is slowly added Et₃N (420 μL, 3 mmol) and MsCl (234 μL, 3 mmol). The mixture is stirred at room temperature overnight. After, the reaction is quenched with H₂O and extracted with DCM. The combined organic layers are washed with brine, dried over Na₂SO₄, filtered and concentrated under reduced pressure. The crude product is purified via flash chromatography (Cy/AcOEt 8:2), giving the corresponding product **34** as a brown oil (750 mg, 2,8 mmol, 94%). ¹H-NMR (400MHz, CDCl₃) δ = 1,46 (s, 9H), 2,14 (m, 1H), 2,26 (br, 1H), 3,04 (s, 3H), 3,47 (dd, J = 17,3; 10,2 Hz; 1H), 3,59 (dd, J = 13,1; 4,4 Hz; 1H), 3,66 (br, 2H), 5,26 (m, 1H). Compound characterized in literature.¹⁰⁵

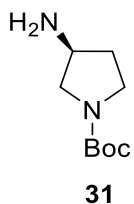


35: To a solution of **34** (295 mg, 1,1 mmol) in DMF (3 mL) at rt NaN₃ (145 mg, 2,2 mmol) is slowly added under stirring. The mixture is heated to 70°C and the reaction is stirred overnight. After, the mixture is cooled to room temperature, diluted with AcOEt (3 mL) and washed with aqueous 5% LiCl to remove the DMF. The organic layer is dried over Na₂SO₄,

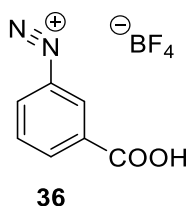
¹⁰⁴ F. Sternfeld, A. R. Guiblin, R. A. Jelley, V. G. Matassa, A. J. Reeve, P. A. Hunt, M. S. Beer, A. Heald, J. A. Stanton, B. Sohal, et al., *J. Med. Chem.* **1999**, *42*, 677–690.

¹⁰⁵ H. Zhang, Y. Chuan, Z. Li, Y. Peng, *Adv. Synth. Catal.* **2009**, *351*, 2288–2294.

filtered and concentrated under reduced pressure. The crude product **35** is obtained as a brown oil (210 mg, 991 μmol , 90%) $^1\text{H-NMR}$ (400MHz, CDCl_3) $\delta = 1,46$ (s, 9H), 2,01 (m, 2H), 3,44 (m, 4H), 4,11 (m, 1H). Compound characterized in literature.

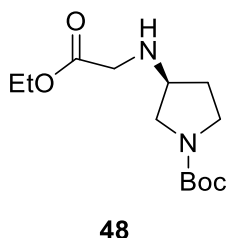


31: 10% Pd/C (121 mg, 114 μmol) is added to a solution of **35** (482 mg, 2,3 mmol) in MeOH (6 mL) and the reaction is stirred under H_2 atmosphere for 1h. After, the reaction mixture is filtered through celite and washed with MeOH. The solvent is removed under reduced pressure and the crude is purified via flash chromatography (DCM/MeOH 95:5), obtaining **31** as a dark brown oil (295 mg, 1,6 mmol, 70%). $^1\text{H-NMR}$ (400MHz, CDCl_3) $\delta = 1,46$ (s, 9H), 1,68 (bs, 1H), 2,05 (dt, $J = 12,7; 6,2$ Hz; 1H), 3,05 (m, 1H), 3,48 (m, 5H). Compound characterized in literature.



36: aqueous solution of NaNO_2 (2,1 g, 30 mmol) is slowly added over 30 min to a stirring solution of 3-aminobenzoic acid (4,8 g, 35 mmol) in 48% HBF_4 (7,8 mL, 60 mmol) at -5°C . After, the precipitate is filtered and washed with cold $\text{Et}_2\text{O}/\text{MeOH}$ 4:1 (2 x 10 mL), and dried under vacuum, affording **36** as a pale yellow solid without further purification (6,4 g, 27 mmol, 77%). $^{13}\text{C-NMR}$ (100 MHz, $\text{DMSO-}d_6$) $\delta = 117,6; 132,2; 133,8; 133,9; 136,3; 141,0; 164,4$.

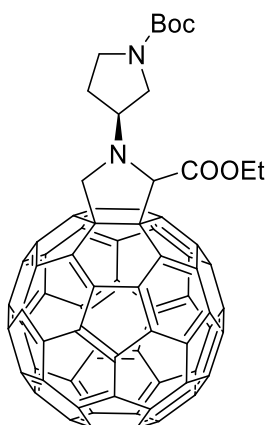
Compound already present in literature.¹⁰⁶



48: A solution of ethyl bromoacetate (357 μL , 3,22 mmol) in CH_3CN (3,7 mL) is added dropwise to a stirring solution of amine **31** (500 mg, 2,68 mmol) and Et_3N (748 μL , 5,37

¹⁰⁶ G. F. Kolar, *Zeitschrift für Naturforsch. - Sect. B J. Chem. Sci.* **1972**, 27, 1183–1185.

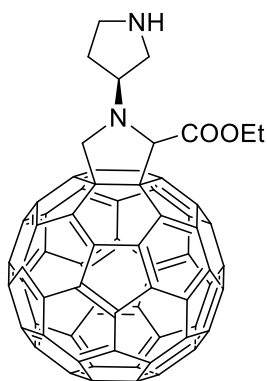
mmol) in CH₃CN (7,4 mL) at 0°C. The mixture is stirred at room temperature for 2 h. After, the solvent is removed under reduced pressure, water is added and is extracted with AcOEt. The organic phase is washed with brine, saturated NaHCO₃ and brine again, dried with Na₂SO₄, filtered and concentrated under reduced pressure. The crude product is purified with flash chromatography (DCM/MeOH 97:3) yielding product **48** as a yellow oil (349 mg, 1,28 mmol, 485). ¹H-NMR (400MHz, CDCl₃) δ = 1,28 (t, J = 7,1 Hz, 3H), 1,45 (s, 9H), 1,77 (m, 1H), 2,03 (dt, J = 13,4; 6,1 Hz; 1H), 3,15 (m, 1H), 3,35 (dt, J = 11,1; 5,7 Hz; 2H), 3,43 (s, 2H), 3,49 (m, 2H), 4,20 (q, J = 7,1 Hz; 2H). Compound already characterized in literature.¹⁰⁷



49

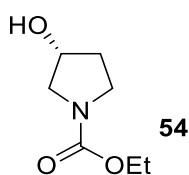
49: To a solution of C₆₀ (100 mg, 139 μmol) in toluene (100 mL) is added **48** (41,6 mg, 153 μmol) and paraformaldehyde (8,3 mg, 278 μmol). The mixture is heated to reflux for 4h. after TLC analysis (toluene/AcOEt 6:1, no double adduct formation), another aliquote of **48** and paraformaldehyde is added. The reaction is stirred at reflux another hour. After TLC analysis (toluene/AcOEt 6:1, double adduct formation) the heating is interrupted. The reaction mixture is directly purified by flash cromatography (gradient from only toluene to toluene/AcOEt 6:1). The product obtained is dissolved in CHCl₃, precipitated by adding MeOH, centrifugated (3000 rpm, 10 minutes), and the solidi s recollected. The product is dried under vacuum, obtaining a brown solid (71,2 mg, 71 μmol, 50%). ¹H-NMR (400MHz, CDCl₃) δ = 1,33 (t, J = 7,1 Hz; 3H), 1,53 (s, 9H), 2,39 (br, 2H), 3,53 (m, 1H), 3,72 (br, 2H), 3,94 (br, 2H), 4,41 (m, 2H), 4,63 (dd, J = 25; 8,9 Hz; 1H), 5,25 (d, J = 7 Hz; 1H), 5,34 (s; 0,5H), 5,44 (s; 0,5H). ¹³C-NMR (100 MHz, CDCl₃) δ = 14,4; 14,5; 28,6; 61,5; 63,2; 69,2; 69,4; 72,5; 72,7; 74,8; 77,2; 79,6; 136,4-159,9 (16 signals); 154,6; 155,6.

¹⁰⁷ A. Banerjee, V. A. Kumar, *Bioorg. Med. Chem.* **2013**, *21*, 4092–4101.



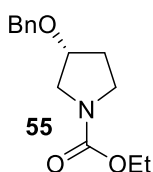
50

50: To a suspension of **49** (60 mg, 59,7 μmol) in DCM (10 mL) at 0°C is added trifluoroacetic acid (10 mL) and the mixture is stirred for 2h. After, after TLC analysis (DCM/acetone 9:1), the solvent is evaporated and the product is dissolved in DCM and washed with saturated NaHCO_3 and water. After, MeOH is added until complete precipitation of the product occurs, the suspension is centrifugated (3000 rpm, 10 minutes) and the solid is collected and dried under vacuum (39,9 mg, 44,1 μmol , 74%). $^1\text{H-NMR}$ interpretation is difficult because of poor solubility in CDCl_3 or CD_3OD . Presence of the free amine observed thanks to Michael reaction.



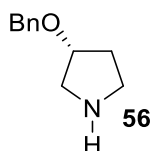
54

54: Ethyl chloroformate (4,13 mL, 42 mmol, 1.05 eq.) is added dropwise to a stirring suspension of (*R*)-3-hydroxypyrrolidin-1-ium chloride **53** (4,94 g, 40 mmol, 1 eq.) and K_2CO_3 (5,67 g, 41 mmol, 1.025 eq.) in dry MeOH (80 mL) at 0°C. The reaction is stirred at room temperature overnight. After, water is added and MeOH is removed under vacuum, and then is extracted with DCM, dried over Na_2SO_4 , dried and concentrated under vacuum. The crude product is purified by flash chromatography (AcOEt) to give the corresponding product **54** (4.98 g, 31.3 mmol, 78%) as a pale yellow oil. $^1\text{H NMR}$ (400 MHz, CDCl_3) δ = 4.46 (qt, J = 4.5, 2.3 Hz, 1H), 4.13 (q, J = 7.1 Hz, 2H), 3.60 – 3.34 (m, 4H), 2.07 – 1.87 (m, 3H), 1.25 (t, J = 7.1 Hz, 3H). $^{13}\text{C NMR}$ (100 MHz, CDCl_3) δ = 155.20, 69.72 (d, J = 80.0 Hz), 60.77 (d, J = 3.0 Hz), 53.82 (d, J = 40.6 Hz), 43.62 (d, J = 24.6 Hz), 33.28 (d, J = 57.7 Hz), 14.43 (d, J = 1.7 Hz).

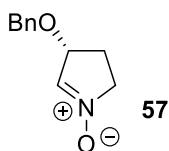


55

55: A solution of compound **54** (4.78 g, 30 mmol, 1 eq.) in THF (10 mL) is added dropwise to a stirring suspension of NaH (1.26 g, 60% w/w, 31,5 mmol, 1.05 eq.) in THF (20 mL) at 0°C and is kept stirring at 0°C for 30 minutes. After, a solution of benzyl Bromide (3.75 mL, 31.5 mmol, 1.05 eq.) in THF (10 mL) is added dropwise at 0°C and finally TBAI (554 mg, 1.5 mmol, 0.05 eq.) is added. The reaction is stirred at room temperature overnight. After, the reaction is quenched with saturated NH₄Cl and water. The aqueous phase is extracted with Et₂O, dried over Na₂SO₄, filtered and concentrated under vacuum. The crude product is purified by flash chromatography (Cy/AcOEt 75:25) to give the corresponding product **55** (6.81 g, 27.3 mmol, 91 %) as a colorless oil. ¹H NMR (400 MHz, CDCl₃) δ = 7.40 – 7.24 (m, 5H), 4.52 (d, *J* = 6.6 Hz, 2H), 4.13 (q, *J* = 7.1 Hz, 3H), 3.49 (s, 4H), 2.14 – 1.88 (m, 2H), 1.26 (t, *J* = 7.1 Hz, 3H). ¹³C NMR (100 MHz, CDCl₃) δ = 155.18 , 138.00 , 128.38 , 127.64 , 127.51 , 77.66 , 70.81 , 60.88 , 51.18 , 43.94 , 30.97 (d, *J* = 90.3 Hz), 14.80; HPLC-MS (ESI) tr = 8.8 min; [M+H]⁺ 250.0 m/z, [M+Na]⁺ 272.0 m/z.

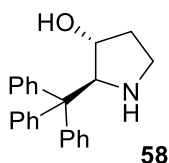


56: KOH (15,15 g, 270 mmol, 10 eq.) is added to a stirring solution of compound **55** (6,73 g, 27 mmol, 1 eq.) in EtOH/H₂O 4:1 (50 mL) and the reaction is refluxed for 72h. Finally, the reaction is cooled to room temperature, ethanol is removed under vacuum and the aqueous phase is extracted with DCM. The organic phase is dried over Na₂SO₄, filtered and concentrated under vacuum. The crude product is purified with flash chromatography (DCM/MeOH/NH₄OH 90:10:2) to give the corresponding compound **56** (4,73 g, 26,7 mmol, 99%) as a brown oil. ¹H NMR (400 MHz, CDCl₃) δ 7.39 – 7.20 (m, 5H), 4.47 (d, *J* = 1.3 Hz, 2H), 4.13 (ddd, *J* = 5.0, 3.4, 1.8 Hz, 1H), 3.97 (bs, 1H), 3.21 – 3.07 (m, 1H), 2.95 (tdd, *J* = 12.4, 5.9, 1.3 Hz, 1H), 1.98 – 1.85 (m, 2H). ¹³C NMR (100 MHz, CDCl₃) δ = 138.05, 128.08 , 127.30, 127.28 , 79.48 , 70.52 , 52.55 , 49.37 , 45.21 , 32.33.

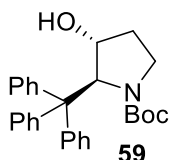


57: To a stirring solution of **56** (1,33 g, 7,5 mmol, 1 eq.), Na₂EDTA 0,01M (11,25 mL, 0,112 mmol, 0,01 eq.) and NaHCO₃ (3,15 g, 37,5 mmol, 5 eq.) in CH₃CN/THF 4:1 (15 mL) at 0°C, Oxone (4,84 g, 7,88 mmol, 1,05 eq.) is added in 4 portions over 1 hour. The mixture is kept stirring at 0°C for 1 hour. Finally, after TLC (DCM/MeOH 95:5), the reaction mixture is diluted AcOEt and extracted, then the aqueous phase is further extracted with DCM. The combined organic phases are dried over Na₂SO₄, filtered and concentrated under vacuum. The crude product is purified with flash chromatography (DCM/MeOH 98:2) to give the corresponding

nitronone **57** (0,86 g, 4,5 mmol, Y = 60%) as a brown oil. ^1H NMR (400 MHz, CDCl_3) δ = 7.42 – 7.28 (m, 5H), 7.11 (d, J = 3.7 Hz, 1H), 4.79 (d, J = 7.7 Hz, 1H), 4.63 – 4.52 (m, 1H), 4.26 – 4.13 (m, 2H), 3.92 (q, J = 11.0, 7.9 Hz, 1H), 2.65 – 2.50 (m, 1H), 2.25 (ddt, J = 13.6, 8.7, 3.9 Hz, 1H). ^{13}C NMR (100 MHz, CDCl_3) δ = 137.31, 134.26, 128.78, 128.33, 128.00, 78.38, 71.74, 61.44, 27.74.

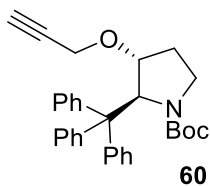


58: To a solution of triphenylmethane (4,89 g, 20 mmol, 2 eq.) in THF (40 mL) at 0°C is slowly added a BuLi solution 1,6M in Hexane (13,13 mL, 21 mmol, 2,1 eq.) under Ar. The solution became deeply red and the mixture is kept stirring at 0°C for 1 hour. After, a solution of nitronone **57** (1,91 g, 10 mmol, 1 eq.) in THF (10 mL) is added dropwise at 0°C. The reaction is stirred at room temperature for 2 h. Finally, the reaction is quenched with saturated NH_4Cl and THF is removed under reduced pressure. The aqueous suspension is extracted with DCM and the combined organic phases are dried over Na_2SO_4 , filtered and concentrated under vacuum. The crude product is purified with flash chromatography (CyHex/AcOEt 95:5). The pure hydroxilamine (3,2 g, 7,44 mmol, 74%) is directly dissolved in AcOH (80 mL), and Pd/C at 10% (1,05 g, 0,99 mmol, 0,1 eq.) is added. The mixture is kept stirring under H_2 (1 atm) atmosphere overnight. After, the suspension is removed by filtration on a celite pad, washing with MeOH, and the solvent is removed under reduced pressure. After, water is added and a solution of NaOH 5% is added until pH 9, then is extracted with DCM. the combined organic phases are dried over Na_2SO_4 , filtered and concentrated under vacuum. The crude product is purified with flash chromatography CyHex/AcOEt 1:1 to give the corresponding product **58** (2,49 g, 7,56 mmol, 76%) as a pale yellow solid. ^1H NMR (400 MHz, CDCl_3) δ = 7.40 (d, J = 7.8 Hz, 5H), 7.33 – 7.13 (m, 10H), 4.86 (d, J = 1.4 Hz, 1H), 4.19 (d, J = 5.3 Hz, 1H), 3.06 (ddd, J = 11.6, 9.6, 6.0 Hz, 1H), 2.75 (ddd, J = 9.5, 7.9, 1.4 Hz, 1H), 2.48 (bs, 2H), 1.39 (dd, J = 13.3, 5.9 Hz, 1H), 0.57 (dddd, J = 13.4, 11.7, 8.0, 5.4 Hz, 1H). ^{13}C NMR (100 MHz, CDCl_3) δ = 130.11, 127.97, 126.40, 75.36, 72.53, 60.79, 44.86, 35.53; HPLC-MS (ESI) tr = 26 min; $[\text{M}+\text{H}]^+$ 330.0 m/z; m.p.= 165-170°C.

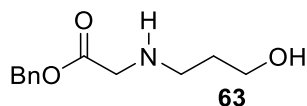


59: To a solution of compound **7** (2.1 g, 5 mmol, 1 eq.) in DCM (20 mL) and Et_3N (766 μL , 5,5 mmol, 1,1 eq.) at 0°C Boc_2O (1,15 g, 5,25 mmol, 1,05 eq.) is added. The reaction mixture is stirred overnight. After, the reaction is quenched with saturated NH_4Cl , the organic phase is

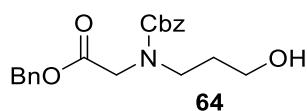
collected and the aqueous phase is extracted with DCM. The combined organic phases are dried over Na_2SO_4 , filtered and concentrated under vacuum. The crude product is purified with flash chromatography CyHex/AcOEt 1:1 to give the product **8** (2,5 g, 4,81 mmol, 96%) as a pale yellow solid. ^1H NMR (400 MHz, CDCl_3) δ = 7.45 – 7.41 (m, 6H), 7.28 – 7.09 (m, 9H), 5.75 (s, 1H), 4.35 (d, J = 5.2 Hz, 1H), 3.52 (q, J = 9.7 Hz, 1H), 2.95 (td, J = 10.7, 2.5 Hz, 1H), 1.33 (s, 9H), 1.29 – 1.18 (m, 1H), -0.01 (dtd, J = 14.8, 9.9, 5.2 Hz, 1H). ^{13}C NMR (100 MHz, CDCl_3) δ = 157.62, 144.80, 130.81, 127.46, 126.11, 80.03, 76.28, 72.45, 60.82, 49.46, 32.30, 28.33. HPLC-MS (ESI) t_r = 13.3 min; $[\text{M}-t\text{-Bu}]^+$ 372.0 m/z; m.p.= 85-90°C.



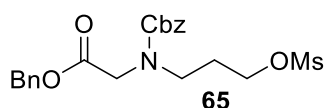
60: A solution of compound **59** (215 mg, 0,5 mmol, 1 eq.) in THF (2 mL) is added dropwise to a stirring suspension of NaH (22 mg, 60% w/w, 0,55 mmol, 1.1 eq.) in THF (2 mL) at 0°C and is kept stirring at 0°C for 1 hour. After, a solution of Propargyl Bromide (65 μL , 0,6 mmol, 1.2 eq.) in THF (2 mL) is added dropwise at 0°C. The reaction is stirred at room temperature overnight. After, the reaction is quenched with saturated NH_4Cl and water. The THF is removed under vacuum and the aqueous phase is extracted with AcOEt, dried over Na_2SO_4 , filtered and concentrated under vacuum. The crude product is purified by flash chromatography (Cy/AcOEt 80:20) to give the corresponding product **60** (210 mg, 0,45 mmol, Y = 90 %) as a yellow solid. ^1H NMR (400 MHz, CDCl_3) δ 7.48 – 7.10 (m, 15H), 5.79 (s, 1H), 4.27 – 4.16 (m, 2H), 3.95 (dd, J = 16.2, 2.3 Hz, 1H), 3.42 (q, J = 9.7 Hz, 1H), 2.93 (td, J = 10.6, 2.5 Hz, 1H), 2.34 (t, J = 2.4 Hz, 1H), 1.49 – 1.37 (m, 1H), 1.32 (s, 9H), -0.24 (dtd, J = 14.7, 9.8, 5.1 Hz, 1H). ^{13}C NMR (100 MHz, CDCl_3) δ = 157.22, 144.79, 130.96, 127.42, 126.08, 82.48, 80.03, 77.36, 74.50, 71.28, 61.16, 54.95, 49.50, 28.33, 26.37; HPLC-MS (ESI) t_r = 15.5 min; $[\text{M}-t\text{-Bu}]^+$ 412.0 m/z, m.p.=75-80°C.



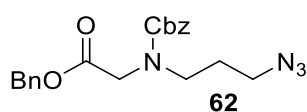
63: 2-Bromo-Benzyl acetate (1,58 mL, 10 mmol, 1 eq.) is slowly added to a stirring solution of 3-amino-1-propanol (1,90 mL, 25 mmol, 2.5 eq.) in CH_3CN (20 mL), and the mixture is stirred for 2h. After, the solvent is removed under vacuum. The crude product is purified with flash chromatography (AcOEt/MeOH 9:1) to give the corresponding product **63** (1,46 g, 6,54 mmol, 71%) as a colorless liquid. ^1H NMR (400 MHz, CDCl_3) δ = 7.40 – 7.27 (m, 5H), 4.69 (s, 2H), 4.00 (s, 2H), 3.56 (dt, J = 8.5, 6.0 Hz, 4H), 3.09 (s, 0H), 1.92 (bs, 1H), 1.85 – 1.71 (m, 2H). ^{13}C NMR (100 MHz, CDCl_3) δ = 164.33, 141.15, 128.39, 127.37, 126.92, 64.79, 58.65, 49.79, 43.12, 29.02; HPLC-MS (ESI) t_r = 3.4 min; $[\text{M}+\text{H}]^+$ 224.0 m/z



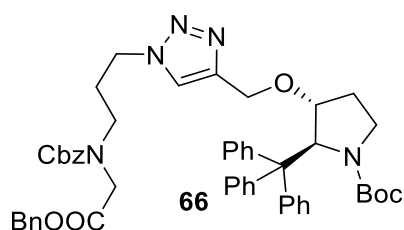
64: To a solution of **63** (1,12 g, 5 mmol, 1 eq.) in DCM (20 mL) and Et₃N (836 μL, 6 mmol, 1.2 eq.) is slowly added CbzCl (785 μL, 5,5 mmol, 1.1 eq.) at 0°C. The reaction mixture is stirred at room temperature overnight. After, the reaction is quenched with saturated NH₄Cl, the organic phase is collected and the aqueous phase is extracted with DCM. the combined organic phases are dried over Na₂SO₄, filtered and concentrated under vacuum. The crude product is purified with flash chromatography (AcOEt) to give the corresponding product **64** (1,7 g, 4,76 mmol, 95%) as a colorless liquid. ¹H NMR (400 MHz, CDCl₃) δ = 7.41 – 7.21 (m, 10H), 5.14 (dd, *J* = 29.6, 2.9 Hz, 4H), 4.04 (d, *J* = 35.3 Hz, 2H), 3.62 (t, *J* = 5.6 Hz, 2H), 3.49 (dt, *J* = 21.6, 6.5 Hz, 2H), 3.09 (bs, 1H), 1.70 (dq, *J* = 11.7, 6.3, 5.8 Hz, 2H). ¹³C NMR (100 MHz, CDCl₃) δ = 169.67 (d, *J* = 26.5 Hz), 156.77 (d, *J* = 39.4 Hz), 136.25 (d, *J* = 13.4 Hz), 135.34 (d, *J* = 16.9 Hz), 128.66 , 128.53 , 128.40 (d, *J* = 5.9 Hz), 128.18 (d, *J* = 6.1 Hz), 127.96 , 127.82 , 67.75 (d, *J* = 5.8 Hz), 67.04 , 59.08 (d, *J* = 94.2 Hz), 49.61 (d, *J* = 19.6 Hz), 45.45 (d, *J* = 18.5 Hz), 30.90 (d, *J* = 67.0 Hz); HPLC-MS (ESI) tr = 9 min; [M+H]⁺ 358.0 m/z, [M+Na]⁺ 380.0 m/z.



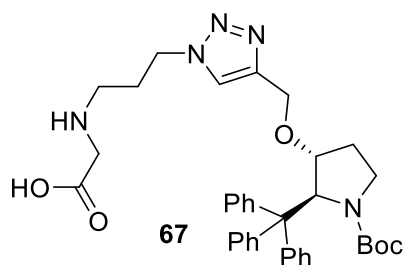
65: To a solution of **64** (1,61 g, 4,5 mmol, 1 eq.) in DCM (15 mL) and Et₃N (815 μL, 5,85 mmol, 1.3 eq.) is slowly added MsCl (435 μL, 5,63 mmol, 1.25 eq.) at 0°C. The reaction mixture is stirred at room temperature overnight. After, the reaction is quenched with saturated NH₄Cl, the organic phase is collected and the aqueous phase is extracted with DCM. the combined organic phases are dried over Na₂SO₄, filtered and concentrated under vacuum. The crude product is purified with flash chromatography (Cy/AcOEt 1:1) to give the corresponding product **65** (1,95 g , 4,48 mmol, >99%) as a pale yellow liquid. ¹H-NMR (400 MHz, CDCl₃) δ = 7.42 – 7.23 (m, 10H), 5.18 (d, *J* = 3.9 Hz, 2H), 5.09 (d, *J* = 10.9 Hz, 2H), 4.25 (dt, *J* = 21.5, 6.1 Hz, 2H), 4.05 (d, *J* = 24.8 Hz, 2H), 3.55 – 3.41 (m, 2H), 2.91 (d, *J* = 46.9 Hz, 3H), 2.00 (dp, *J* = 19.2, 6.4 Hz, 2H). ¹³C NMR (100 MHz, CDCl₃) δ 169.66 , 156.22 (d, *J* = 37.5 Hz), 136.29 (d, *J* = 2.3 Hz), 135.34 (d, *J* = 8.3 Hz), 128.69 (d, *J* = 2.7 Hz), 128.55 (t, *J* = 2.8 Hz), 128.39 , 128.30 , 128.13 (d, *J* = 2.3 Hz), 127.83 , 67.88 , 67.70 (d, *J* = 15.5 Hz), 67.35 – 67.04 (m), 49.99 , 45.55 (d, *J* = 66.8 Hz), 37.24 , 28.24 (d, *J* = 45.4 Hz), HPLC-MS (ESI) tr = 9.9 min; [M+H]⁺ 436.0 m/z, [M+H₂O]⁺ 453.0 m/z.



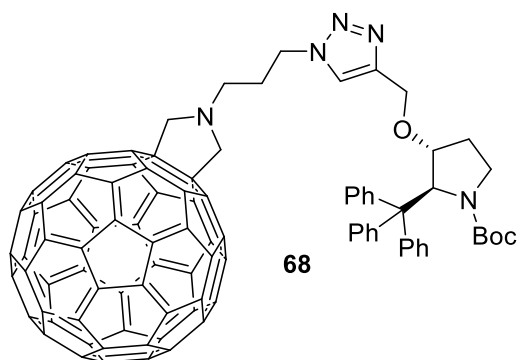
62: To a solution of **65** (1,74 g , 4 mmol, 1 eq.) in DMF (15 mL) at 0°C is slowly added NaN₃ (468 mg , 7.2 mmol, 1.8 eq.). The reaction is stirred at room temperature overnight. After, the reaction is diluted with AcOEt and washed with a solution of LiCl at 5%. Then the organic phase is dried over Na₂SO₄, filtered and concentrated under vacuum. The crude product is purified with flash chromatography (Cy/AcOEt 1:1) to give the corresponding product **62** (1,09 g, 2,85 mmol, 71%) as a colorless oil. ¹H NMR (400 MHz, CDCl₃) δ = 7.45 – 7.21 (m, 10H), 5.18 (d, *J* = 1.4 Hz, 2H), 5.10 (d, *J* = 7.4 Hz, 2H), 4.04 (d, *J* = 24.6 Hz, 2H), 3.44 (dt, *J* = 8.7, 6.9 Hz, 2H), 3.33 (dt, *J* = 26.5, 6.7 Hz, 2H), 1.81 (dp, *J* = 20.2, 6.8 Hz, 2H). ¹³C NMR (100 MHz, CDCl₃) δ = 169.43 (d, *J* = 4.6 Hz), 156.00 (d, *J* = 49.7 Hz), 136.24 , 135.24 (d, *J* = 8.3 Hz), 128.51 , 128.44 , 128.35 , 128.31 , 128.19 , 127.98 (d, *J* = 11.8 Hz), 127.74 (d, *J* = 14.7 Hz), 67.45 (d, *J* = 20.8 Hz), 66.86 (d, *J* = 3.5 Hz), 49.58 (d, *J* = 11.4 Hz), 48.65 (d, *J* = 21.0 Hz), 46.20 (d, *J* = 81.3 Hz), 27.59 (d, *J* = 30.5 Hz).



66: A solution of CuSO₄·5H₂O (10.7 mg, 0.043 mmol, 0.1 eq.) in H₂O (0.5 mL) and a solution of sodium ascorbate (17 mg, 0.086 mmol, 0.2 eq.) in H₂O (0.5 mL) are slowly added to a stirring solution of the corresponding azide **62** (164 mg, 0.43 mmol, 1 eq.) and alchine **60** (201 mg, 0.43 mmol, 1 eq.) in tert-butanol (1 mL) and the resulting suspension is stirred overnight at room temperature. After, the reaction is diluted with AcOEt and the aqueous phase is extracted. The organic phases are dried over Na₂SO₄, filtered and concentrated under vacuum. The crude product is purified by flash chromatography (Cy/AcOEt 80:20) to give the corresponding product **66** (340 mg, 0,4 mmol, 93 %) as a white solid. ¹H NMR (400 MHz, CDCl₃) δ 7.71 (s, 1H), 7.43 – 7.27 (m, 16H), 7.22 – 7.10 (m, 9H), 5.82 (s, 1H), 5.19 (s, 2H), 5.12 (d, *J* = 2.8 Hz, 2H), 4.61 (dd, *J* = 26.0, 12.3 Hz, 1H), 4.47 – 4.32 (m, 3H), 4.14 – 4.00 (m, 3H), 3.53 – 3.34 (m, 1H), 2.98 – 2.85 (m, 2H), 1.61 – 1.48 (m, 1H), 1.32 (s, 9H), -0.13 (dtd, *J* = 14.7, 9.7, 5.2 Hz, 1H). ¹³C NMR (100 MHz, CDCl₃) δ 169.66 , 157.08 , 156.22 (d, *J* = 9.1 Hz), 145.04 (d, *J* = 32.2 Hz), 144.65 (d, *J* = 1.6 Hz), 136.08 (d, *J* = 5.3 Hz), 135.16 (d, *J* = 8.5 Hz), 130.66, 128.64 (d, *J* = 3.7 Hz), 128.51 (d, *J* = 3.1 Hz), 128.31 (d, *J* = 2.6 Hz), 128.12, 127.78 , 127.26, 125.90 , 123.27 , 122.53 , 83.13 (d, *J* = 16.0 Hz), 79.67 , 71.08 , 67.77 (d, *J* = 23.6 Hz), 67.12 , 61.37 (d, *J* = 7.5 Hz), 60.96 , 49.87 (d, *J* = 26.2 Hz), 49.42 , 47.54 , 46.16 (d, *J* = 46.1 Hz), 29.29 (d, *J* = 22.7 Hz), 28.20, 26.63; HPLC-MS (ESI) tr = 17.3 min; [M+H]⁺ 850.0 m/z, [M+Na]⁺ 872.0 m/z.

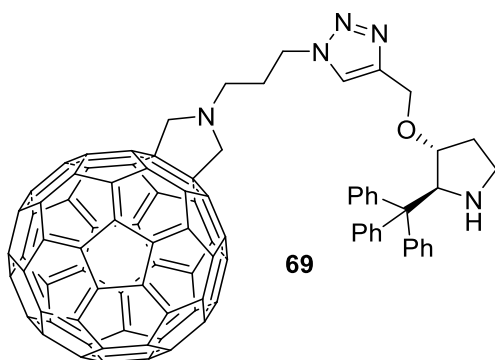


67: Compound **66** (239 mg, 0,28 mmol) is dissolved in MeOH (3 mL), and 10% Pd/C (30 mg, 28 μ mol, 0.1 eq.) is added. The mixture is kept stirring under H₂ (1 atm) atmosphere overnight. After, the suspension is removed by filtration on a celite pad, washing with MeOH, and the solvent is removed under reduced pressure. After, the product is dissolved in DCM and cold Pentane is added dropwise at 0°C, leading to the precipitation of a white solid. The solvent is removed by filtration and the product is dried under vacuum to give the product **67** (175 mg, 0,28 mmol, 99%) as a white solid. ¹H NMR (400 MHz, CDCl₃) δ = 7.72 (s, 1H), 7.35 (d, *J* = 7.7 Hz, 6H), 7.12 (dt, *J* = 13.8, 7.1 Hz, 9H), 5.76 (s, 1H), 4.58 – 4.42 (m, 3H), 4.30 (d, *J* = 12.2 Hz, 1H), 4.02 (d, *J* = 5.0 Hz, 1H), 3.74 (s, 2H), 3.46 – 3.31 (m, 1H), 3.12 (s, 2H), 2.91 – 2.79 (m, 1H), 2.47 (s, 2H), 1.49 (t, *J* = 12.0 Hz, 1H), 1.25 (s, 9H), -0.08 – -0.25 (m, 1H). ¹³C NMR (100 MHz, CDCl₃) δ = 171.06 , 157.00 , 144.99 , 144.60 , 130.60 , 127.28 , 125.98 , 123.58 , 83.40 , 79.63 , 70.99 , 61.41 , 60.98 , 53.44 , 50.36 , 49.37 , 47.46 , 44.58 , 28.20 , 26.86; HPLC-MS (ESI) *tr* = 8.9 min; [M+H]⁺ 626.0 m/z.



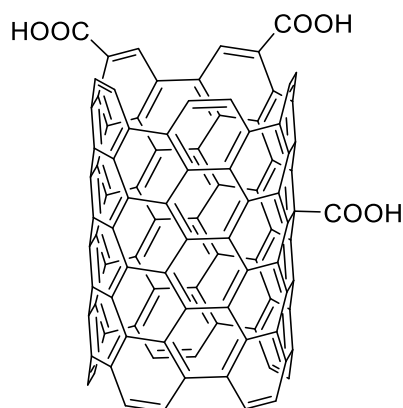
68: Pristine C₆₀ (168 mg, 0.23 mmol, 1.25 eq.) is dissolved in Toluene (60 mL) and is sonicated for 20 min under Ar. After, compound **67** (117 mg, 0.19 mmol, 1 eq.) and Paraformaldehyde (14 mg, 0.47 mmol, 2,5 eq.) are added and the reaction mixture is refluxed for 1 h. After, the reaction is cooled to room temperature and directly purified by flash chromatography (first Toluene to remove unreacted pristine C₆₀, after Toluene/Ethyl Acetate 7:3) giving the corresponding functionalized Fullerene **68** (122 mg, 0.93 mmol, 50%) as a Brown Powder. ¹H NMR (400 MHz, CDCl₃) δ = 7.79 (s, 1H), 7.48 – 7.35 (m, 5H), 7.22 – 7.10 (m, 10H), 5.85 (s, 1H), 4.86 – 4.76 (m, 1H), 4.68 (d, *J* = 12.2 Hz, 1H), 4.54 – 4.35 (m, 4H), 4.10 (s, 1H), 3.57 – 3.33 (m, 1H), 3.21 – 3.04 (m, 1H), 3.02 – 2.76 (m, 1H), 2.61 – 2.47 (m, 1H), 2.44 – 2.28 (m, 4H), 1.31 (s, 10H), -0.02 – -0.28 (m, 1H). ¹³C NMR (100 MHz, CDCl₃) δ = 157.12, 154.69, 147.31, 146.25, 146.07, 145.95, 145.63, 145.43, 145.29, 144.66, 144.53, 143.09, 142.63, 142.20,

142.05, 141.89, 140.19, 136.12, 130.65, 127.29, 125.95, 123.02, 83.25, 71.11, 70.56, 67.75, 61.59, 60.95, 51.04, 49.41, 48.26, 31.89, 29.67, 29.32, 29.20, 28.23, 26.78, 22.66, 14.07.



69: Compound **68** (140 mg, 0,11 mmol, 1 eq.) is dissolved in DMC (20 mL), and sonicated for 20 min. After, TFA (1 mL, 13,3 mmol, 250 eq.) is added dropwise at 0°C. The mixture is stirred at room temperature overnight. After, the mixture is concentrated under vacuum, the crude solid is dissolved in DCM and the organic phase is washed with saturated NaHCO₃ and Brine, dried over Na₂SO₄, filtered and concentrated under vacuum. The crude product is purified with flash chromatography DCM/MeOH 99:1 to give the corresponding product **69** (128 mg, 0.10 mmol, 99%) as brown powder. ¹H NMR (400 MHz, CDCl₃) δ = 7.77 (s, 1H), 7.35 (s, 6H), 7.26 – 7.11 (m, 9H), 4.85 – 4.78 (m, 3H), 4.67 (d, *J* = 12.0 Hz, 1H), 4.48 – 4.40 (m, 5H), 3.86 (d, *J* = 5.0 Hz, 1H), 3.13 (t, *J* = 6.6 Hz, 2H), 2.99 – 2.87 (m, 1H), 2.75 (t, *J* = 8.2 Hz, 1H), 2.56 (p, *J* = 6.8 Hz, 2H), 1.66 (dd, *J* = 13.3, 5.3 Hz, 1H), 0.43 (dp, *J* = 12.7, 6.4 Hz, 1H). ¹³C NMR (100 MHz, CDCl₃) δ = 154.67, 147.32, 146.25, 146.08, 145.92, 145.62, 145.42, 145.35, 145.30, 144.53, 143.09, 142.65, 142.20, 142.05, 141.88, 140.19, 136.11, 129.96, 127.55, 125.96, 123.05, 83.23, 77.29, 77.18, 76.97, 76.66, 70.92, 70.55, 67.67, 62.64, 61.00, 50.71, 48.05, 44.87, 30.47, 29.03.

General procedure for oxidation of pCNT **32** and **33**:



34 = SWCNT Ox
35 = MWCNT Ox

A suspension of pSWCNT **32** or pMWCNT **33** 4M Nitric Acid, after 20 min sonication, is heated to reflux for 8 h. After, the reaction is cooled to room temperature, diluted with water and filtered on a 0,45 μm filter under vacuum. The filtrate is suspended in water, sonicated for 20 min and filtered again. The operation is repeated until water does not reach pH of almost 6. After, the CNTs are washed with MeOH and Et₂O and dried under vacuum.

Synthesis of SWCNT Ox **34**:

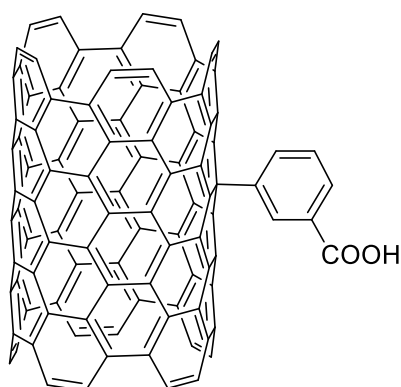
pSWCNT **32** (100 mg), HNO₃ 4M (100 mL). SWCNT Ox **34** are obtained (100 mg). TGA : T = 200 – 700 °C; $\Delta m = - 16,9 \%$; functionalization = 5,4 % \rightarrow 3,8 $\mu\text{mol}/\text{mg}$. Raman : RBM = 272,5 cm^{-1} ; D = 1366,6 cm^{-1} ; G = 1593,8 cm^{-1} ; 2D = 2673,1 cm^{-1} a 532 nm.

Synthesis of MWCNT Ox **35**:

pMWCNT **33** (100 mg), HNO₃ 4M (100 mL). MWCNT Ox **35** are obtained (99,6 mg). TGA : T = 200 – 700 °C; $\Delta m = - 1,77 \%$; functionalization = 0,5 % \rightarrow 0,4 $\mu\text{mol}/\text{mg}$. Raman : D = 1357,9 cm^{-1} ; G = 1582,8 cm^{-1} ; 2D = 2691,5 cm^{-1} a 532 nm.

Re-oxidation MWCNT Ox **35**: MWCNT Ox **35** (99,6 mg), HNO₃ 8M (100 mL). MWCNT Ox **35** more functionalized are obtained (78,1 mg). TGA: T = 200 – 700 °C; $\Delta m = - 3,6 \%$; funzionalizzazione = 1 % \rightarrow 0,8 $\mu\text{mol}/\text{mg}$.

General procedure for arylation of pCNT **32** and **33**



37 = SWCNT Ar
38 = MWCNT Ar

To a suspension of pSWCNT **32** or pMWCNT **33** in ODCB or NMP, after 20 minutes sonication, the diazonium salt is added and the mixture is heated to 60°C overnight. After, the mixture is cooled to room temperature, filtered using a 0,45 μm "JHWP" filter under vacuum, washing with the reaction solvent, H₂O and THF. The solid is suspended again in THF, sonicated for 20 minutes, and filtered again. The operation is repeated until the solvent after filtration is colorless. Finally. CNTs are washed with MeOH ed Et₂O and dried under vacuum.

Synthesis of SWCNT Ar **37** e MWCNT Ar **38**, according to the general procedure:

Entry 1: pSWCNT **32** (100 mg, 8,33 mmol), **36** (1,96 g, 8,33 mmol), ODCB (100 mL). SWCNT Ar **37** (141 mg) are obtained. TGA : T = 200 – 700 °C; $\Delta m = - 13,7 \%$; functionalization = 1,6 %

→ 1,1 $\mu\text{mol}/\text{mg}$.

Re-arylation SWCNT Ar **37**: SWCNT Ar **37** (90 mg, 7,5 mmol), **36** (1,77 g, 7,5 mmol), ODCB (90 mL). More functionalized SWCNT Ar **37** are obtained (88,4 mg). TGA : T = 200 – 700 °C; $\Delta m = - 21,9 \%$; Functionalization = 1,8 % → 1,2 $\mu\text{mol}/\text{mg}$.

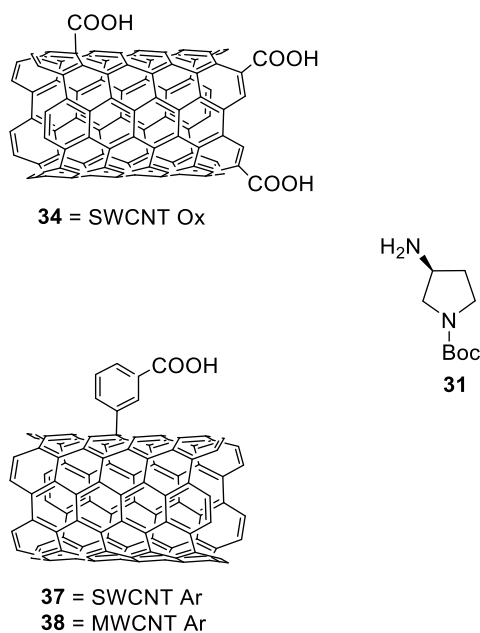
pSWCNT **32** (10 mg, 0,83 mmol), **36** (196 mg, 0,83 mmol), ODCB (10 mL). SWCNT Ar **37** are obtained (14 mg). TGA : T = 200 – 700 °C; $\Delta m = - 21,5 \%$; functionalization = 2,7 % → 1,8 $\mu\text{mol}/\text{mg}$. Raman : *RBM* = 197,8 cm^{-1} ; *D* = 1332,3 cm^{-1} ; *G* = 1595,2 cm^{-1} ; 2*D* = 2668,9 cm^{-1} a 532 nm.

Entry 2: pSWCNT **32** (10 mg, 0,83 mmol), **36** (196 mg, 0,83 mmol), NMP (10 mL). SWCNT Ar **37** are obtained (12,4 mg). TGA : T = 200 – 700 °C; $\Delta m = - 21,8 \%$; functionalization = 2,8 % → 1,8 $\mu\text{mol}/\text{mg}$. Raman : *RBM* = 270,9 cm^{-1} ; *D* = 1330,9 cm^{-1} ; *G* = 1592,5 cm^{-1} ; 2*D* = 2659,4 cm^{-1} a 532 nm.

Entry 3: pMWCNT **33** (100 mg, 8,33 mmol), **36** (1,96 g, 8,33 mmol), ODCB (100 mL). MWCNT Ar **38** are obtained (106,4 mg). TGA : T = 200 – 700 °C; $\Delta m = - 5,0 \%$; functionalization = 0,5 % $\rightarrow 0,4 \mu\text{mol/mg}$.

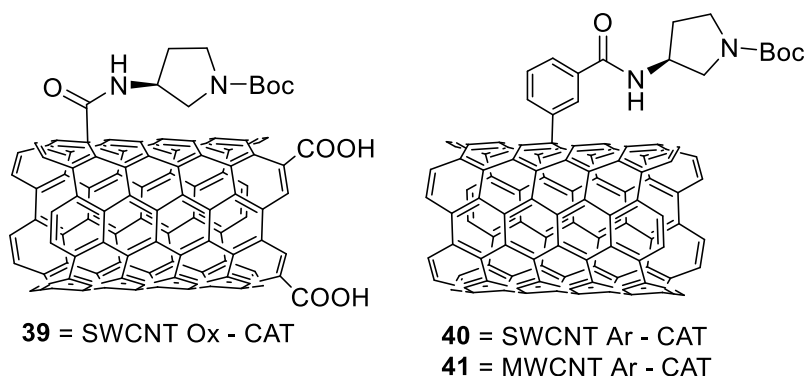
Re-arylation MWCNT Ar **38**: MWCNT Ar **38** (50 mg, 4,2 mmol), **36** (982 mg, 4,2 mmol), ODCB (50 mL). MWCNT Ar **38** are obtained (50 mg). TGA : T = 200 – 700 °C; $\Delta m = - 4,8 \%$; functionalization = 0,5 % $\rightarrow 0,4 \mu\text{mol/mg}$.

General procedure for amide coupling between CNT **34**, **37**, **38** and amine **31**



To a suspension of functionalized CNT in DMF, after 20 minutes sonication under argon, are added coupling reagents and DIPEA, and the reaction is stirred at room temperature for 24 hours. After, amine **31** in DMF is added, and the mixture is heated at 80°C for 48h (with HATU) or at room temperature for 48 hours (with EDC/NHS). Then, after cooling, the solids filtered on a 0,45 μm "JHWP" filter under vacuum, washing with solvent reaction, H₂O e THF. The solid is suspended again in THF, sonicated for 20 minutes, and filtered again. The operation is repeated until the solvent after filtration is colorless. Finally, CNTs are washed with MeOH ed Et₂O and dried under vacuum.

Synthesis of SWCNT Ox - CAT 39, SWCNT Ar - CAT 40 e MWCNT Ar - CAT 41, according to general procedure:



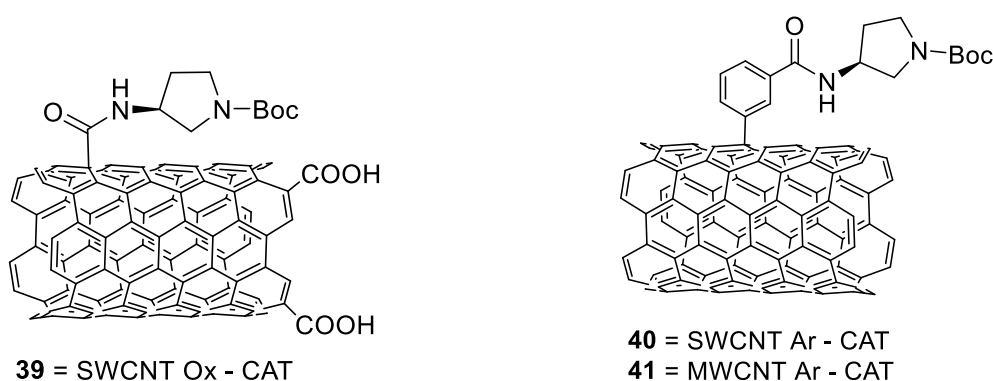
Entry 1: SWCNT Ox **34** (10 mg), DMF (100 mL), HATU (317 mg, 833 μmol), DIPEA (182 μL , 1,10 mmol), amine **31** (103 mg, 555 μmol). SWCNT Ox – CAT **39** are obtained (11,6 mg). TGA : T = 200 – 700 $^{\circ}\text{C}$; $\Delta m = - 24,4 \%$; functionalization = 1,8 % \rightarrow 1,1 $\mu\text{mol}/\text{mg}$. Raman : *RBM* = 272,5 cm^{-1} ; *D* = 1333,8 cm^{-1} ; *G* = 1593,8 cm^{-1} ; 2*D* = 2660,6 cm^{-1} a 532 nm.

Entry 2: SWCNT Ox **34** (10 mg), DMF (100 mL), EDC•HCl (160 mg, 833 μmol), DIPEA (136 μL , 833 μmol), NHS (96 mg, 833 μmol), amine **31** (103 mg, 555 μmol). SWCNT Ox – CAT **39** (12,6 mg) are obtained. TGA : T = 200 – 700 $^{\circ}\text{C}$; $\Delta m = - 16,2 \%$; functionalization = 1,1 % \rightarrow 0,8 $\mu\text{mol}/\text{mg}$. Raman: *RBM* = 270,9 cm^{-1} ; *D* = 1349,4 cm^{-1} ; *G* = 1593,8 cm^{-1} ; 2*D* = 2665,4 cm^{-1} a 532 nm.

Entry 3: SWCNT Ar **37** (50 mg), DMF (200 mL), HATU (1,6 mg, 4,2 mmol), DIPEA (908 μL , 5,6 mmol), amine **31** (517 mg, 2,8 mmol). SWCNT Ar – CAT **40** are obtained (48,2 mg). TGA : T = 200 – 700 $^{\circ}\text{C}$; $\Delta m = - 22,4 \%$; functionalization = 1,2 % \rightarrow 0,8 $\mu\text{mol}/\text{mg}$.

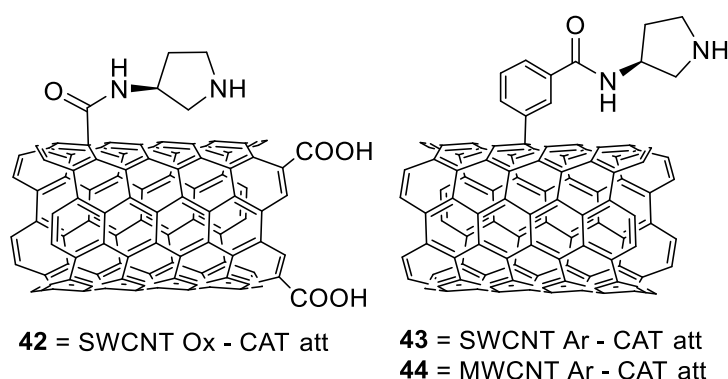
Entry 4: MWCNT Ar **38** (50 mg), DMF (200 mL), HATU (1,6 mg, 4,2mmol), DIPEA (908 μL , 5,6 mmol), amine **31** (517 mg, 2,8 mmol). MWCNT Ar – CAT **41** are obtained (49,8 mg). TGA : T = 200 – 700 $^{\circ}\text{C}$; $\Delta m = - 5,3 \%$; functionalization = 0,2 % \rightarrow 0,2 $\mu\text{mol}/\text{mg}$.

General procedure for deprotection of CNT 39, 40 e 41



To a suspension of functionalized CNTs in THF, after 20 minutes sonication, is added trifluoroacetic acid at 0°C and the mixture is stirred at room temperature overnight. Then, after cooling, the solids are filtered on a 0,45 µm "JHWP" filter under vacuum, washing with solvent reaction, H₂O e THF. The solid is suspended again in THF, sonicated for 20 minutes, and filtered again. The operation is repeated until the solvent after filtration is colorless. Finally, CNTs are washed with MeOH e Et₂O and dried under vacuum.

Synthesis of SWCNT Ox – CAT 42, SWCNT Ar – CAT 43 e MWCNT Ar – CAT 44 according to general procedure:

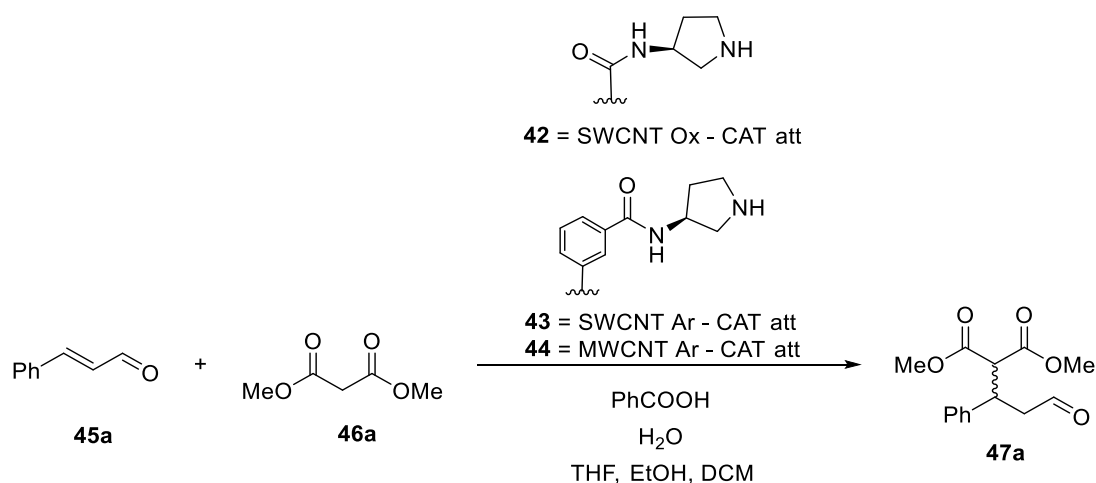


Entry 1: SWCNT Ox – CAT **39** (12,6 mg), TFA (2 mL), THF (10 mL). SWCNT Ox – CAT **42** are obtained (9 mg). TGA : T = 200 – 700°C; $\Delta m = - 20,4 \%$; functionalization = 2,7 % \rightarrow 1,8 µmol/mg.

Entry 2 SWCNT Ar – CAT **40** (48,0 mg), TFA (8 mL), THF (50 mL). SWCNT Ar – CA **43** are obtained (44,9 mg). TGA : T = 200 – 700°C; $\Delta m = - 20,5 \%$; functionalization = 1,6 % \rightarrow 1,1 µmol/mg.

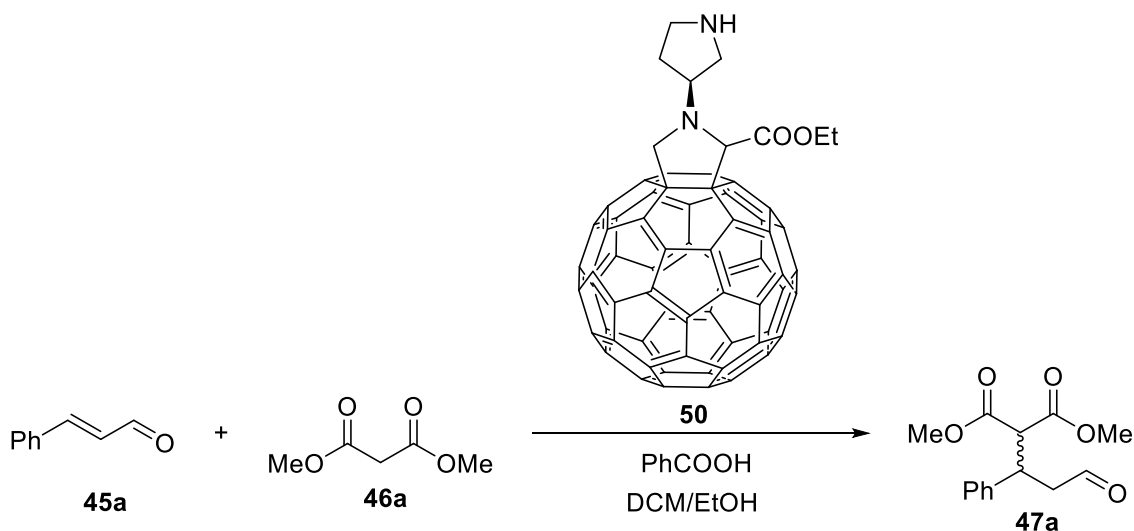
Entry 3: MWCNT Ar – CAT **41** (48,0 mg), TFA (8 mL), THF (50 mL). MWCNT Ar – CAT **44** are obtained (34,8 mg). TGA : T = 200 – 700°C; $\Delta m = - 5,6 \%$; functionalization = 0,4 % \rightarrow 0,3 µmol/mg.

General procedure for Michael reaction with catalysts **42,43** e **44**:



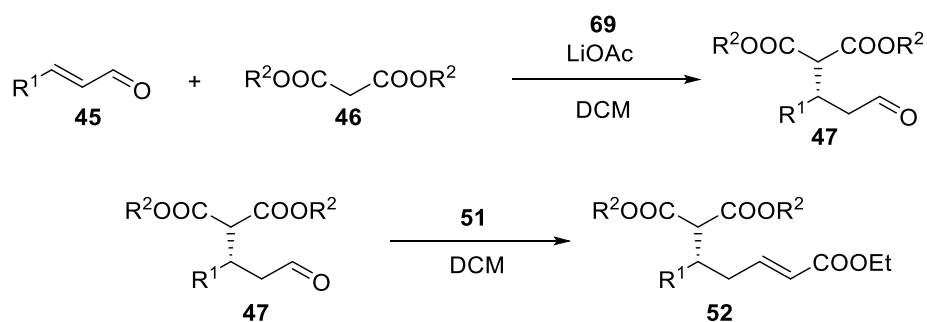
Dimethylmalonate **46a** (1 eq.) is added to a stirring suspension of supported catalyst (30%), cinnamaldehyde **45a** (1.5 eq.), PhCOOH (30%) and water in the selected reaction solvent. The reaction is left stirring for the desired time. Conversion is measured by ¹H-NMR spectroscopy of the reaction mixture.

Michael addition with catalyst **50**:



To a suspension of **50** (30 mg, 34,2 μmol), cinnamaldehyde **45a** (22 μL, 171 μmol), PhCOOH (4,2 mg, 34,2 μmol), in DCM/EtOH 1:1 (0,75 mL + 0,75 mL) at 0°C is added dimethylmalonate **46a** (13 μL, 113 μmol). The reaction is stirred for 3 days. The conversion is measured by ¹H-NMR spectroscopy on the reaction mixture. After, the solvent is removed under reduced pressure and the product is derivatized using witting reagent (43,2 mg, 124 μmol) in DCM (250 μL), and stirred overnight. Finally, water is added and extracted with DCM. The organic layer is concentrated and the crude derivatized product is purified by flash chromatography (CyHex/AcOEt 8:2). CSP-HPLC: IC, Hex/iPrOH 7:3, 0,5 mL min⁻¹, 40°C, rt= 13,1 min; 19,2 min.

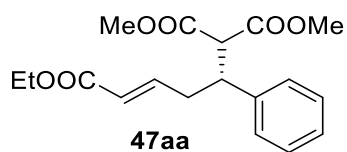
Procedures of catalysis, recycle and product characterization with catalyst 69



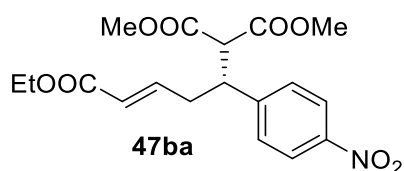
Standard Procedure for reaction of Malonates and Aldehydes catalyzed by catalyst 69: in a typical reaction catalyst **69** (5%) is charged in a centrifuge vial, dissolved in DCM (200 μ L, 0,5 M) and sonicated for 5 minutes. After, LiOAc (15%) and Aldehyde **45** (0,1 mmol, 1 eq.) are added to the solution. Finally, Malonate **46** (0,3 mmol, 3 eq.) is added and the solution is stirred for the desired time (20-48h). Finally, the reaction is diluted with MTBE (1 mL, 3 times) and centrifugated (5 min, 5000 rpm, 3 times). The organic layer is collected, concentrated under vacuum and the crude is analyzed with H-NMR. For e.e. determination the crude is diluted in MeOH and ylide **51** is added. The solution is stirred for 1h. After, the mixture is concentrated and purified by flash chromatography (Cy/AcOEt 80:20) to give the corresponding derivatized product **52** for analysis.

Standard Procedure for recycle of catalyst 69: in a typical reaction catalyst **16** (10%) is charged in a centrifuge vial, dissolved in DCM (200 μ L, 0,5M) and sonicated for 5 minutes. After, LiOAc (30%) and cinnamaldehyde **45a** (0,1 mmol, 1 eq.) are added to the solution. Finally, dimethylmalonate **46a** (0,3 mmol, 3 eq.) is added and the solution is stirred for 16h. Finally, the reaction is diluted with MTBE (1 mL, 3 times) and centrifugated (5 min, 5000 rpm, 3 times). The organic layer is collected, the catalyst is washed with H₂O, MTBE and concentrated under vacuum. After the solvent is recharged for a new reaction with recycled catalyst.

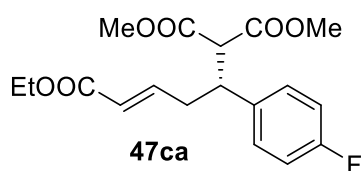
CSP-HPLC separation condition for adducts 47:



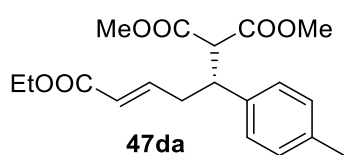
47aa: IC, Hexane : *i*-PrOH 80:20, 0.5 mL/min, 40°C, t^1 : 16,77 min, t^2 : 25.01 min



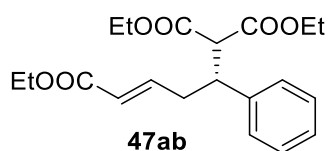
47ba: AD, Hexane : *i*-PrOH 80:20, 0.5 mL/min, 40°C, t^1 : 25,25 min, t^2 : 31.48 min



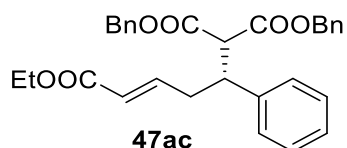
47ca: IC, Hexane : *i*-PrOH 80:20, 0.5 mL/min, 40°C, t^1 : 14,02 min, t^2 : 15.55 min



47da: IC, Hexane : *i*-PrOH 70:30, 0.5 mL/min, 40°C, t^1 : 12,83 min, t^2 : 15.06 min



47ab: IC, Hexane : *i*-PrOH 70:30, 0.5 mL/min, 40°C, t^1 : 11,49 min, t^2 : 16.99 min



47ac: IC, Hexane : *i*-PrOH 70:30, 0.5 mL/min, 40°C, t^1 : 12,75 min, t^2 : 16.92 min

